



**GEOSCIENCE BC  
SUMMARY OF ACTIVITIES 2014**



# **GEOSCIENCE BC SUMMARY OF ACTIVITIES 2014**



© 2015 by Geoscience BC.

All rights reserved. Electronic edition published 2015.

This publication is also available, free of charge, as colour digital files in Adobe Acrobat® PDF format from the Geoscience BC website: <http://www.geosciencebc.com/s/DataReleases.asp>.

Every reasonable effort is made to ensure the accuracy of the information contained in this report, but Geoscience BC does not assume any liability for errors that may occur. Source references are included in the report and the user should verify critical information.

When using information from this publication in other publications or presentations, due acknowledgment should be given to Geoscience BC. The recommended reference is included on the title page of each paper. The complete volume should be referenced as follows:

Geoscience BC (2015): Geoscience BC Summary of Activities 2014; Geoscience BC, Report 2015-1, 164 p.

ISSN 1916-2960 Summary of Activities (Geoscience BC)

**Cover photo:** M. Sánchez measuring structures and orogenic quartz veins near Barkerville, central British Columbia  
**Photo credit:** T. Bissig



## Acknowledgments

I would like to thank the government of British Columbia for its ongoing support of Geoscience BC and recognize the \$3 million investment made in 2014, allowing for our continued delivery of projects that generate new earth science information for everyone. I would also like to express appreciation for the leaders in British Columbia's mineral exploration, mining and energy sectors who support our organization through their guidance, use and recognition of the information that we collect and distribute.

Robin Archdekin  
President & CEO  
Geoscience BC  
[www.geosciencebc.com](http://www.geosciencebc.com)



## Foreword

Geoscience BC is pleased to present results from several of our ongoing geoscience projects in this, our eighth edition of the *Geoscience BC Summary of Activities*. The volume is divided into three sections, 'Minerals', 'Oil and Gas' and 'Scholarship Recipients', and contains a total of 21 papers.

The 'Minerals' section contains 12 papers from Geoscience BC minerals geoscience projects throughout BC. The first four papers highlight ongoing work in the TREK (Targeting Resources through Exploration and Knowledge) project area. Sacco and Jackaman summarize a second year of targeted geochemical and mineralogical studies in the region that focused on basal till sampling. Lett and Jackaman discuss tracing anomalous geochemical patterns in bog soils near the Nazko volcanic cone and their relationship to geothermal potential. This is a continuation of a study examining carbon dioxide seepages in the region, which was released in an initial report in 2014 (see below). Angen et al. and Kim et al. each summarize results from their first year of a three-year targeted bedrock geology mapping initiative in the TREK project area.

Two papers present advances in geochemistry in BC. Arne and Brown discuss using catchment basins to further the interpretation of geochemical data collected as part of Geoscience BC's Northern Vancouver Island Exploration Geoscience project. Yehia and Heberlein introduce a test of the use of a portable photometer for field-based rapid geochemical analysis of stream- and springwaters. Field photometer results will be compared to traditional laboratory analyses later in the project.

Two papers focus on the Quesnel terrane in central BC. Sánchez et al. are working toward improving the understanding of the Quesnel terrane geology beneath Quaternary cover by completing a structural interpretation of existing geophysical and geological datasets in the QUEST project area. Bouzari et al. discuss a new project that will examine field, mineralogical and geochemical characteristics of known porphyry-fertile plutons, and then develop exploration tools that will aid in future discovery.

Three papers focus on the mineral potential in southeastern BC. Höy and Jackaman introduce a new multiyear phase of mapping in the eastern half of the Penticton (NTS 082E) map area, which expands on their previous work for Geoscience BC in the Deer Park and Burrell Creek map areas. Seabrook and Höy and Kennedy and Höy present new initiatives within Geoscience BC's SEEK (Stimulating Exploration in the East Kootenays) project, examining structural controls on the Kimberley gold trend, and the relevance of mud volcanoes to massive-sulphide mineralization in the Purcell Basin, respectively.

Finally, Kilby and Fournier highlight a new Geoscience BC pilot project to extract analogue historical exploration data contained in the Assessment Report Indexing System (e.g., geochemical data, geology and geophysical maps) and convert it into a format that can be integrated into both a GIS and web mapping system. The pilot project focuses on the NTS 093L map area in central BC.

The 'Oil and Gas' section contains two papers from ongoing Geoscience BC projects. Hayes et al. describe detailed mapping and characterization of the Belloy, Kiskatinaw and Debolt deep saline aquifers to determine their potential as disposal zones in the Montney play fairway. Results will be publicly available in early 2015. Bustin et al. highlight continuing work quantifying the gas- and liquid-in-place and flow capacity of important shales in northeastern BC.

The new 'Scholarship Recipients' section presents papers from Geoscience BC's 2014 seven student scholarship winners. The scholarships are awarded annually to post-graduate students working on thesis topics relevant to supporting mineral or oil and gas exploration and development in BC.

Cook and Hart examine carbonate-hosted zinc-lead deposits in southeastern BC by applying carbon and oxygen isotopes. D'Souza and Canil focus on amphibole-cumulate rocks from the Bonanza Group on Vancouver Island, examining if amphibole is controlling magma evolution in the lower crust as well as contributing to the understanding of why select arcs are prospective for porphyry copper deposits.

MacKay et al. evaluate the use of a Mozley C800 laboratory mineral separator to produce heavy mineral concentrate for specialty metal exploration using indicator minerals, in this case examining Aley carbonatite stream sediments. This work is part of the larger Targeted Geoscience Initiative 4 to develop simpler, less expensive methods to explore for rare earth elements, niobium and possibly tantalum deposits.

Mak et al. examine historical geomechanical and hydrogeological data collected from the Mount Meager area to assess the natural fracture connectivity of the reservoir rocks that host the geothermal resource at the Meager Creek site. Mostaghimi et al. examine the structural geology of the Granite Lake pit at the Gibraltar copper-molybdenum mine, in part to determine the temporal relationship between mineralization and structural modification.

The use of magnetite as a porphyry copper indicator mineral in tills, with a focus on the Mount Polley deposits, is examined in Pisiak et al. Finally, Theny et al. discuss preliminary results of a study aimed at understanding the age, mineralization and structural history of the Ruddock Creek deposit and its relationship to the metallogenic evolution of the Canadian Cordillera.

Readers are encouraged to visit our website for additional information on all Geoscience BC-funded projects, including project descriptions, posters and presentations, previous *Summary of Activities* and *Geological Fieldwork* papers, and final datasets and reports. The website is launching an interactive web-mapping portal, which readers can use to explore all of Geoscience BC's public datasets, as well as select public geoscience databases.

All papers in this and past volumes are available for download through Geoscience BC's website ([www.geosciencebc.com](http://www.geosciencebc.com)). Limited print copies of past volumes are also available from the Geoscience BC office.

## Geoscience BC Publications 2014

In addition to this *Summary of Activities* volume, Geoscience BC releases interim and final products from our projects as Geoscience BC reports. All Geoscience BC data and reports can be accessed through our website at [www.geosciencebc.com/s/DataReleases.asp](http://www.geosciencebc.com/s/DataReleases.asp). Geoscience BC datasets and reports released in 2014 are:

- 14 technical papers in the *Geoscience BC Summary of Activities 2013* volume
- **Subsurface Aquifer Study to Support Unconventional Gas and Oil Development, Liard Basin, Northeastern British Columbia**, by Petrel Robertson Consulting Ltd. (Geoscience BC Report 2014-02)
- **Regional Stream Sediment Geochemical Data, Sample Reanalysis (INAA), Northern Vancouver Island, British Columbia**, by W. Jackaman (Geoscience BC Report 2014-03)
- **Fixed Wing Magnetic Geophysical Survey, TREK Project, Interior Plateau/Nechako Region, British Columbia, Canada**, by Aeroquest Airborne Ltd. (Geoscience BC Report 2014-04)
- **Acquired Heliborne High Resolution Aeromagnetic Surveys in the Blackwater District, TREK Project Area, British Columbia**, by Geoscience BC (Geoscience BC Report 2014-05)
- **Basal Till Potential Maps for the Interior Plateau, TREK Project, British Columbia**, by D. Sacco, T. Ferbey and W. Jackaman (Geoscience BC Maps 2014-06-01 to -10; British Columbia Geological Survey Open Files 2014-06 to -15)
- **Geology of the Mount Polley Intrusive Complex (Final Version)**, by C. Rees, G. Gillstrom, L. Ferreira, L. Bjornson and C. Taylor (Geoscience BC Report 2014-08)
- **Surficial Geology of the Nadina River Map Area (NTS 093E/15), British Columbia**, by T. Ferbey (Geoscience BC Map 2014-09-01 and British Columbia Geological Survey Geoscience Map 2014-01)
- **Surficial Geology of the Colleymount Map Area (NTS 093L/01), British Columbia**, by T. Ferbey (Geoscience BC Map 2014-09-02 and British Columbia Geological Survey Geoscience Map 2014-02)
- **Geochemical and Mineralogical Data, TREK Project, Interior Plateau, British Columbia**, by W. Jackaman and D. Sacco (Geoscience BC Report 2014-10)
- **Geochemical Expression in Soil and Water of Carbon Dioxide Seepages near the Nazko Volcanic Cone, Interior Plateau, Central BC, NTS 093B/13**, by R. Lett and W. Jackaman (Geoscience BC Report 2014-11)
- **Geologically-Constrained Gravity and Magnetic Earth Modelling of the Nechako-Chilcotin Plateau, British Columbia, Canada**, by Mira Geoscience Ltd. (Geoscience BC Report 2014-12)

All releases of Geoscience BC reports and data are announced through our website and e-mail list. If you are interested in receiving e-mail regarding these reports and other Geoscience BC news, please contact [info@geosciencebc.com](mailto:info@geosciencebc.com).

## Acknowledgments

Geoscience BC would like to thank all authors and reviewers of the *Summary of Activities* papers for their contributions to this volume. RnD Technical is also thanked for their work in editing and assembling this volume.

Christa Pellett  
Project Manager  
Geoscience BC  
[www.geosciencebc.com](http://www.geosciencebc.com)

## Contents

### Minerals Projects

- D.A. Sacco and W. Jackaman:** Targeted geochemical and mineralogical surveys in the TREK project area, central British Columbia: year two. . . . . 1
- R.E. Lett and W. Jackaman:** Tracing the source of anomalous geochemical patterns in carbonate-rich bog soils near the Nazko volcanic cone, central British Columbia . . . . . 13
- J.J. Angen, E. Westberg, C.J.R. Hart, R. Kim and C. Raley:** TREK geology project: recognizing Endako Group and Chilcotin Group basalts from airborne magnetic data in the Interior Plateau region, south-central British Columbia . . . . . 21
- R. Kim, C.J.R. Hart, J.J. Angen and E. Westberg:** Characterization of Late Cretaceous volcanic suites in the TREK project area, central British Columbia . . . 33
- D. Arne and O. Brown:** Catchment analysis applied to the interpretation of new stream sediment data from northern Vancouver Island, British Columbia . . . . . 41
- R. Yehia and D.R. Heberlein:** Use of a field portable photometer for rapid geochemical analysis of stream-water and springwater: a case history from Poison Mountain, southwestern British Columbia . . . . . 47
- M.G. Sánchez, T. Bissig and P. Kowalczyk:** Toward an improved basis for beneath-cover mineral exploration in the QUEST area: new structural interpretation of geophysical and geological datasets . . . . . 53
- F. Bouzari, C.J.R. Hart and T. Bissig:** Mineralogical characteristics of porphyry-fertile plutons: Guichon Creek, Takomkane and Granite Mountain batholiths, south-central British Columbia . . . . . 63
- T. Höy and W. Jackaman:** Geological mapping, compilation and mineral evaluation of the Almond Mountain map sheet, southern British Columbia . . . . . 69
- M. Seabrook and T. Höy:** Structural controls on the Kimberley gold trend, southeastern British Columbia . . . . . 73
- S. Kennedy and T. Höy:** Mud volcanoes in the Purcell Basin and their relevance to Middle Proterozoic massive-sulphide Ag-Pb-Zn deposits, Southeastern British Columbia . . . . . 77
- C.E. Kilby and M.A. Fournier:** Historical exploration data capture pilot project, northwestern British Columbia. . . . . 79

### Oil and Gas Projects

- B.J.R. Hayes, S. Macleod and J. Carey:** Characterization of Belloy, Kiskatinaw and Debolt water disposal zones in the Montney play area, northeastern British Columbia. . . . . 85
- R.M. Bustin, E. Munson, E. Letham and A.M.M. Bustin:** Quantification of the gas- and liquid-in-place and flow characteristics of shale and other fine-grained facies in northeastern British Columbia. . . . . 89

### Scholarship Recipients

- N.L. Cook and C.J.R. Hart:** Carbonate alteration footprints of carbonate-hosted zinc-lead deposits in southeastern British Columbia: applying carbon and oxygen isotopes . . . . . 95
- R.J. D'Souza and D. Canil:** Preliminary results from a trace-element study of amphibole-cumulate rocks from the Bonanza Arc, Vancouver Island, British Columbia. . . . . 103
- D.A.R. Mackay, G.J. Simandl, B. Grcic, C. Li, P. Luck, M. Redfearn and J. Gravel:** Evaluation of Mozley C800 laboratory mineral separator for heavy mineral concentration of stream sediments in exploration for carbonatite-hosted specialty metal deposits: case study at the Aley carbonatite, northeastern British Columbia . . . . . 111
- S.W. Mak, E. Eberhardt and J.A. Meech:** Assessing fracture network conductivity of prefeasibility-level high-temperature geothermal projects using discrete fracture network modelling at the Meager Creek site, southwestern British Columbia . . . . . 123
- N. Mostaghimi, L. Kennedy and J. Gabites:** Structural geology of the Granite Lake pit, Gibraltar copper-molybdenum mine, south-central British Columbia: preliminary observations. . . . . 129
- L.K. Pisiak, D. Canil, C. Grondahl, A. Plouffe, T. Ferbey and R.G. Anderson:** Magnetite as a porphyry copper indicator mineral in till: a test using the Mount Polley porphyry copper-gold deposit, south-central British Columbia. . . . . 141
- L.M. Theny, H.D. Gibson and J.L. Crowley:** Uranium-lead age constraints and structural analysis for the Ruddock Creek zinc-lead deposit: insight into the tectonic evolution of the Neoproterozoic metalliferous Windermere Supergroup, northern Monashee Mountains, southern British Columbia . . . . . 151



# Targeted Geochemical and Mineralogical Surveys in the TREK Project Area, Central British Columbia (Parts of NTS 093B, C, F, G): Year Two

D.A. Sacco, Consulting Quaternary Geologist, New Westminster, BC, [saccoda@gmail.com](mailto:saccoda@gmail.com)

W. Jackaman, Noble Exploration Services Ltd., Sooke, BC

---

Sacco, D.A. and Jackaman, W. (2015): Targeted geochemical and mineralogical surveys in the TREK project area, central British Columbia (parts of NTS 093B, C, F, G): year two; *in* Geoscience BC Summary of Activities 2014, Geoscience BC, Report 2015-1, p. 1–12.

## Introduction

The objective of the Targeting Resources through Exploration and Knowledge (TREK) project is to provide a better geological understanding of the central part of British Columbia's Interior Plateau through the integration of surficial geochemistry, airborne geophysics and geology data (Figure 1). The project is focused on an area of Stikine terrane that has the potential to host a variety of mineral deposit types, including porphyry Cu, porphyry Mo and epithermal Au deposits. Exploration in this region has been hindered by Neogene Chilcotin Group basalt flows and extensive glacial drift, which obscures underlying and prospective bedrock units.

The surficial geochemistry survey of the TREK project is currently underway and aims to provide a comprehensive geochemical database for the project area. Presented here are the program details and summary of the first two years' activities.

The TREK geochemistry program consists of three components:

- compilation of historical data from previous geochemical surveys;
- collection of new geochemical and mineralogical data; and
- reanalyses of archived till samples.

Various combinations of geochemical data from lake and stream sediment, water, till and biological material exists for different parts of the project area. Typically, geochemical data from these types of materials are not comparable due to different methods of transport and accumulation. Lake sediment and till geochemical data, however, have been shown to be correlative (Cook et al., 1995; Rencz et al., 2002). The present survey targets basal till, which is a common material throughout the region and well suited to

assessing the mineral potential of areas covered by glacial drift (Levson, 2001; McClenaghan et al., 2001; Lett et al., 2006). Basal till potential maps (BTPMs; Sacco et al., 2014a–j) were produced and used to assist in the planning and execution of this ambitious survey. Where basal till or access is limited, higher order bedrock derivatives that are comparable to the historical geochemical data are assessed for sampling. Till geochemical data from previous surveys is integrated with new data from this survey by reanalysis of available archived samples using modern laboratory techniques to produce a directly comparable, more comprehensive till geochemical dataset for the project area.

## Project Area

A summation of the known bedrock and surficial geology and references for the project area are provided in Sacco et al. (2014k). The project area is located in the Interior Plateau (Mathews, 1986), south of Vanderhoof and approximately 60 km west of Quesnel. It occupies parts of NTS 093B, C, F and G and covers more than twenty-eight 1:50 000 scale NTS map areas, approximately 25 000 km<sup>2</sup> (Figure 1). Access is through a network of forest service roads in the Vanderhoof, Quesnel, Chilcotin and Central Cariboo forest districts.

The project area includes parts of the Nechako Plateau, Fraser Plateau and the Fraser Basin physiographic regions (Holland, 1976; Figure 1). Thick surficial deposits composed dominantly of till and glacial lake sediments obscure most bedrock exposures. Higher relief features include the Nechako and Fawnie mountain ranges of the Nechako Plateau and the Ilgachuz and Itcha mountain ranges of the Fraser Plateau.

## Economic Geology

There are five developed prospects, seven prospects and 39 mineral showings in the TREK project area. Four developed prospects contain Au, Ag, Zn, Pb and Cu mineralization and include the Blackwater-Davidson intermediate sulphidation epithermal Au-Ag deposit (NTS 093F/02; MINFILE 093F 037; BC Geological Survey, 2013), the Capoose subvolcanic Cu-Ag-Au (As-Sb) and porphyry-related Au deposit (NTS 093F/06; MINFILE 093F 040), and

---

**Keywords:** TREK, mineral exploration, till geochemistry and mineralogy, regional geochemical data, basal till potential mapping  
*This publication is also available, free of charge, as colour digital files in Adobe Acrobat® PDF format from the Geoscience BC website: <http://www.geosciencebc.com/s/DataReleases.asp>.*

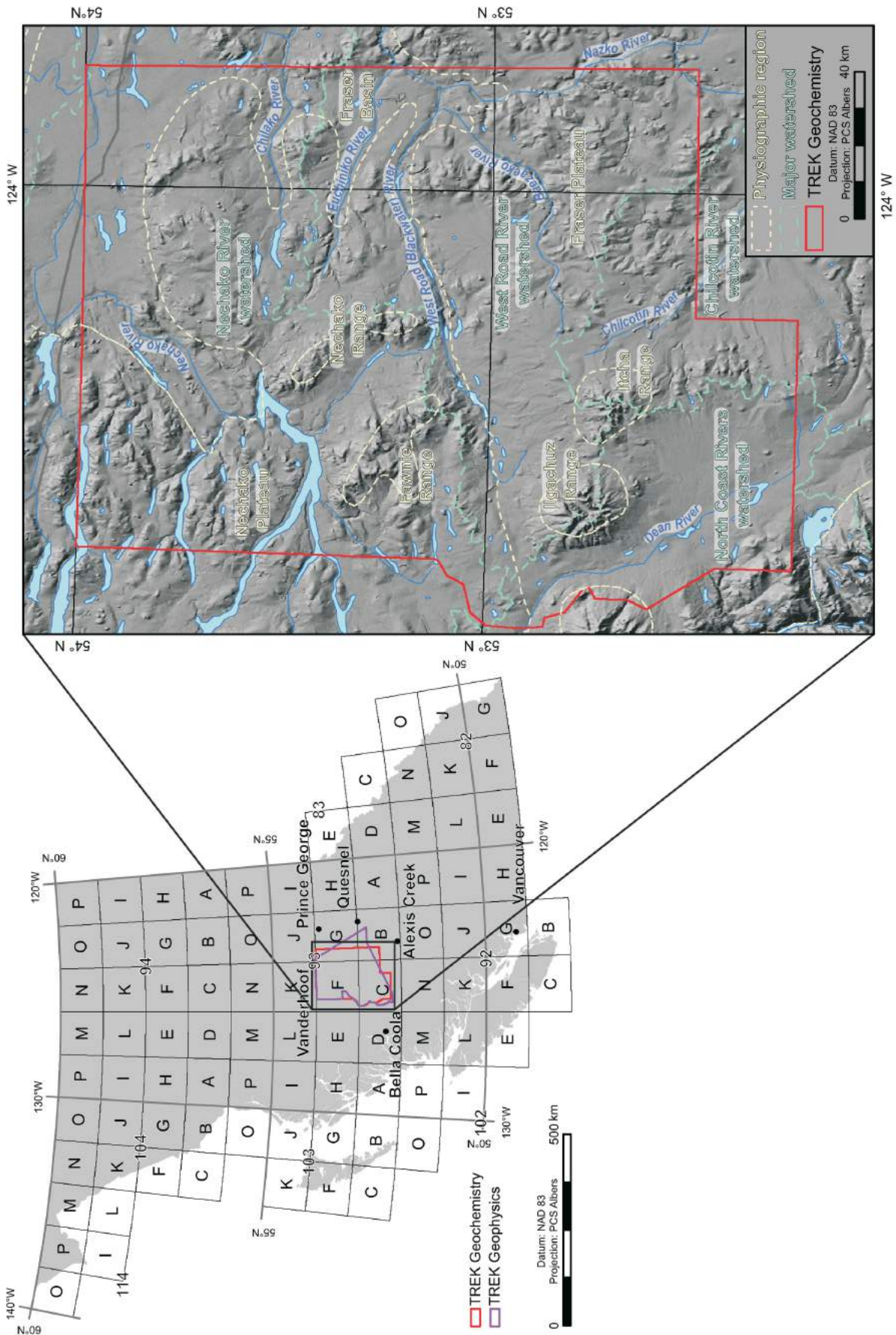


**Figure 1.** TREK project geochemistry and airborne geophysics boundaries in central British Columbia. Inset map illustrates physiographic regions (Holland, 1976) and major drainages of the geochemical survey area. Digital elevation model from Canadian digital elevation data (GeoBase®, 2007).

the 3Ts polymetallic Ag-Pb-Zn±Au veins (NTS 093F/03; MINFILE 093F 068) and low-sulphide epithermal Au-Ag-Cu deposit (NTS 093F/03; MINFILE 093F 055). The fifth developed prospect, the CHU deposit, hosts porphyry Mo (low F-type) mineralization (NTS 093F/07; MINFILE 93F 001).

The Baez (NTS 093C/16; MINFILE 093C 015), Clisbako (NTS 093C/09; MINFILE 093C 016), Trout (NTS 093F/10; MINFILE 093F 044) and Wolf (NTS 093F/03; MINFILE 093F 045) prospects all host low-sulphidation epithermal Au-Ag mineralization. In contrast, the April Au-Ag-Zn prospect has been classified as high-sulphidation epithermal Au-Ag-Cu mineralization (NTS 093F/07; MINFILE 093F 060). At Laidman prospect (NTS 093F/03; MINFILE 093F 067), Au, Ag, Pb and Zn occur within Au-quartz veins whereas at Bob prospect, Au, Ag, As, Sb and Hg occur within carbonate-hosted and disseminated Au-Ag mineralization (NTS 093B/13; MINFILE 093B 054).

## Historical Geochemical Data

Beginning in the early 1990s, several multimedia regional geochemical surveys have been conducted in the project area. This previously published biogeochemical, lake and stream sediment and till geochemical data are listed in Table 1 and depicted in Figure 2. Pine tree bark was targeted for biogeochemical sampling. The bark was reduced to ash and analyzed for multiple elements by instrumental neutron activation analysis (INAA) and inductively coupled plasma-emission spectrometry (ICP-ES) following an aqua-regia digestion (Dunn and Hastings, 1998, 1999, 2000). An abundance of lakes provided opportunity to conduct several lake sediment and water sampling programs. A

selection of archived sediment pulps from programs completed prior to 2000 were recently reanalyzed by Jackaman (2006, 2008a, b, 2009a, b). Reanalysis of lake sediments was by inductively coupled plasma-mass spectrometry (ICP-MS; 35 elements) following an aqua-regia digestion. Original geochemical analysis included INAA (25 elements), and analysis for fluoride using specific ion electrode (SIE). Till samples collected during previous surveys were originally analyzed by outdated ICP analytical techniques for various elements plus INAA for total gold determinations plus 34 elements. Samples have been re-analyzed for minor and trace elements by ICP-MS following aqua-regia digestion (53 elements), major and minor elements by ICP-ES following a lithium borate fusion and dilute acid digestion. The compilation of historical geochemical data will be released as a Geoscience BC report in 2015.

## Till Geochemical and Mineralogical Survey

Basal till is well suited to assessing mineral potential of an area because it is a first derivative of bedrock (Shilts, 1993) and therefore has a similar geochemical signature. It was eroded, transported and deposited under ice, thus its transport history is relatively simple and can be determined by reconstructing ice-flow histories. Furthermore, it produces a geochemical signature that is areally more extensive than the bedrock source and potentially easier to locate (Levson, 2001). Basal till in the project area is a massive, dense, dark brown, matrix-supported diamicton. In most exposures, it exhibits subhorizontal fissility and vertical jointing resulting in a blocky appearance (Figure 3a). The matrix composition varies; generally in the north it is silt to sandy silt and in the south it has a higher sand content. The matrix propor-

**Table 1.** Historical geochemical data reports for the TREK project area, central British Columbia.

Survey year	NTS map area	Type	Sample sites <sup>1</sup>	Reference
1996	093F/09, /10, /15, /16	Tree bark	224	Dunn and Hastings, 2000
1997	093F/13, /14, /12	Tree bark	100	Dunn and Hastings, 1998
1998	093K/02, /03	Tree bark	2	Dunn and Hastings, 1999
1980, 1985 <sup>2</sup>	093A, B, G, H, J, K, N, O	Stream	470	Jackaman, 2008a
2005	093C, F	Stream	66	Jackaman, 2006
2008	093E, F, G, J, K, L, M, N, O	Stream	32	Jackaman, 2009b
1993	093F	Lake	380	Jackaman, 2009a
2005	093C, F	Lake	1324	Jackaman, 2006
2007	093G, H, J, K, N, O	Lake	89	Jackaman, 2008b
1992	093C/09, /16	Till	176	Lett et al., 2006
1993	093F/03	Till	171	Levson et al., 1994; Plouffe et al., 2001
1994	093F/07	Till	143	Weary et al., 1997; Plouffe et al., 2001
1994, 1998	093F	Till	292	Plouffe et al., 2001
1996, 1997	093F	Till	314	Plouffe and Williams, 1998; Plouffe et al., 2001

<sup>1</sup>Only sample sites within the study area are listed

<sup>2</sup>Samples reanalyzed in 2007

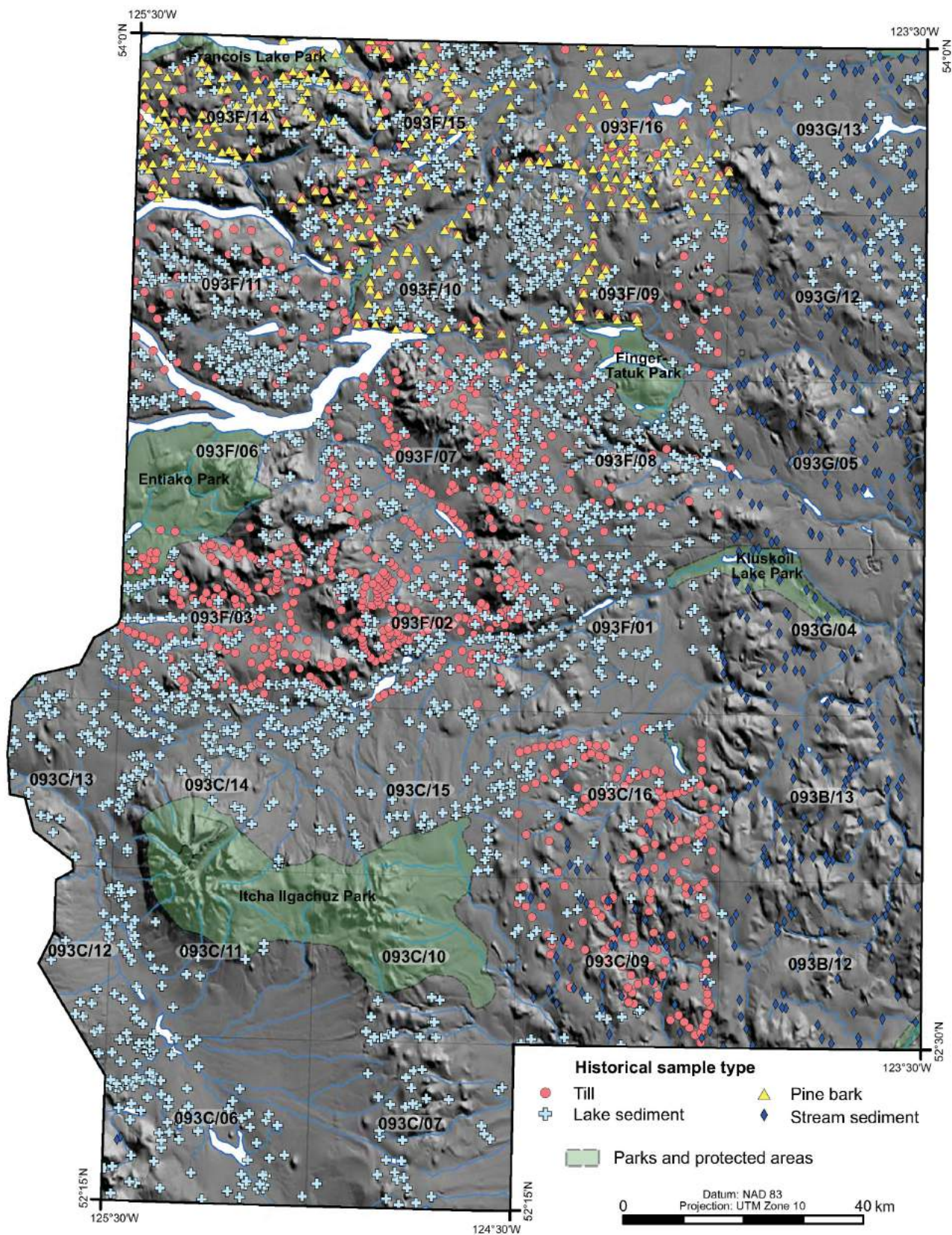


**Figure 2.** Distribution of archive till (red circle), lake (light blue cross) and stream (dark blue diamond) sediment geochemical data and biogeochemical (pine bark) data (green triangle), TREK project area, central British Columbia. See text for references. Digital elevation model from Canadian digital elevation data (GeoBase®, 2007).

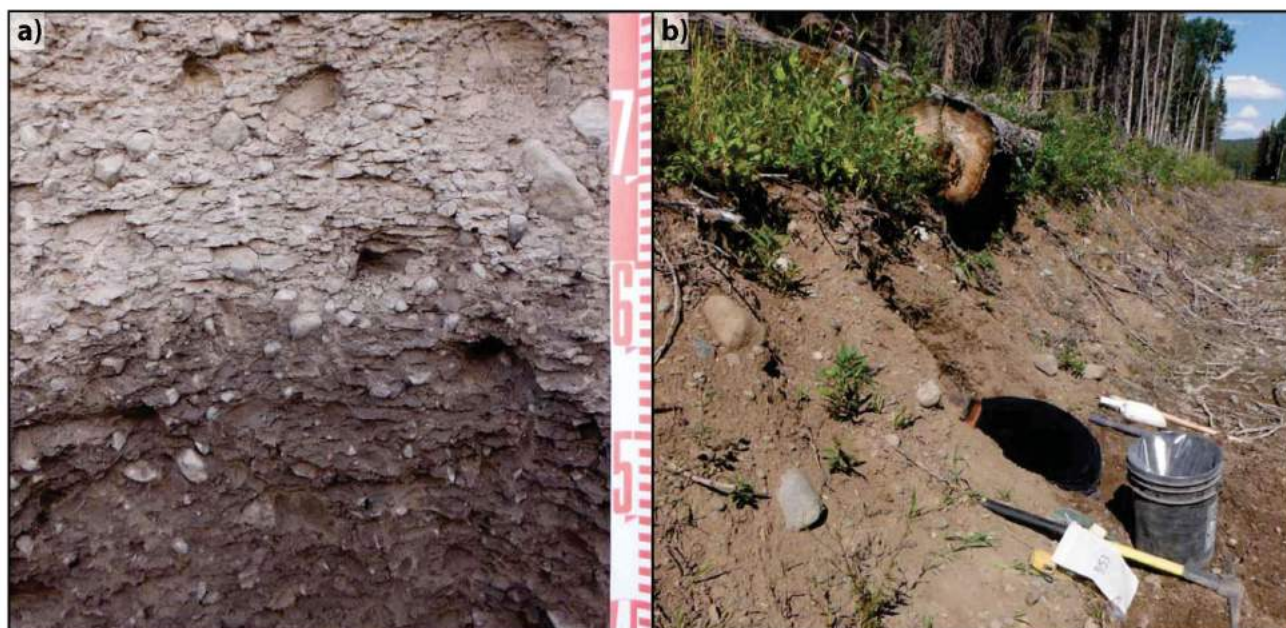


**Figure 3. a)** A basal till exposure displaying typical massive structure, fissility and jointing. In situ material targeted for sampling is highlighted by the darker colour. Scale in metres. **b)** Typical roadcut exposure used to access in situ basal till that is found below depths of 1 to 1.5 m, TREK project area, central British Columbia.

tion varies from 70 to 85% with a modal clast size of small to medium pebble and a range up to boulder.

Sediments that hinder the survey include ablation till and glaciolacustrine deposits. Ablation till is found in areally small deposits in depressions or basins throughout the project area, and is widespread to the north and west of the Ilgachuz and Itcha mountain ranges. Ablation till is differentiated from basal till by the lack of density, and high sand content in the matrix. It is generally matrix supported, shows some stratification, and contains sand or gravel lenses, but can also be clast supported or massive. Areally extensive glaciolacustrine deposits occur within the Fraser Basin in the northeastern part of the project area, and in the north coast river system watershed in the southwest. Diamictos deposited in a glaciolacustrine environment can be difficult to distinguish from basal till; however, they typically lack density and have a matrix composed almost entirely of silt.

### Basal Till Potential Mapping

Basal till potential maps (BTPMs) delineate areas where basal till is likely to occur and where it may be necessary to implement different geochemical sampling protocols. These maps are an extremely valuable tool for planning regional surveys and assisting exploration companies conduct detailed follow-up activities. The BTPMs are also an important tool in determining genesis of existing surface geochemistry samples. A comprehensive description of map protocols and production can be found in Sacco et al. (2014k). Aerial photographs were interpreted using

surficial geology mapping standards (Deblonde et al., 2012) that were modified to include additional information about basal till potential and till genesis. The BTPMs were instrumental in the planning and implementation of the survey. Ten 1:50 000 scale BTPMs have been published for the eastern portion of the TREK project area (Sacco et al., 2014a–j). In addition, eight complete and two partial map areas have been interpreted and ground truthed, and eight map areas are thus far unmapped (Figure 4). Unfortunately, the loss of the BC Geological Survey from the TREK project included access to digital resources and technology critical to the production of high quality maps. As a result, BTPMs will not be completed at this time for the remaining 16 complete and two partial map areas.

### Field Methods

Sampling locations are based on a 2 km, staggered grid, aligned with ice flow (see Levson, 2001). These locations, however, are restricted in some areas due to lack of material, access or exposure. Natural or anthropogenic exposures (>1 m) were typically required to obtain in situ basal till, which had not been altered by soil-forming processes or biological activity (Figure 3b). These exposures occurred predominantly as roadcuts and in some cases, borrow pits or river and lake cuts. Pits were hand dug in some situations. At each sample location 2–3 kg till samples were collected for major-, minor- and trace-element geochemical analyses and 50 stones, of large pebble to small cobble size, were collected for lithological studies. At approximately every other site, a 10–12 kg sample was collected

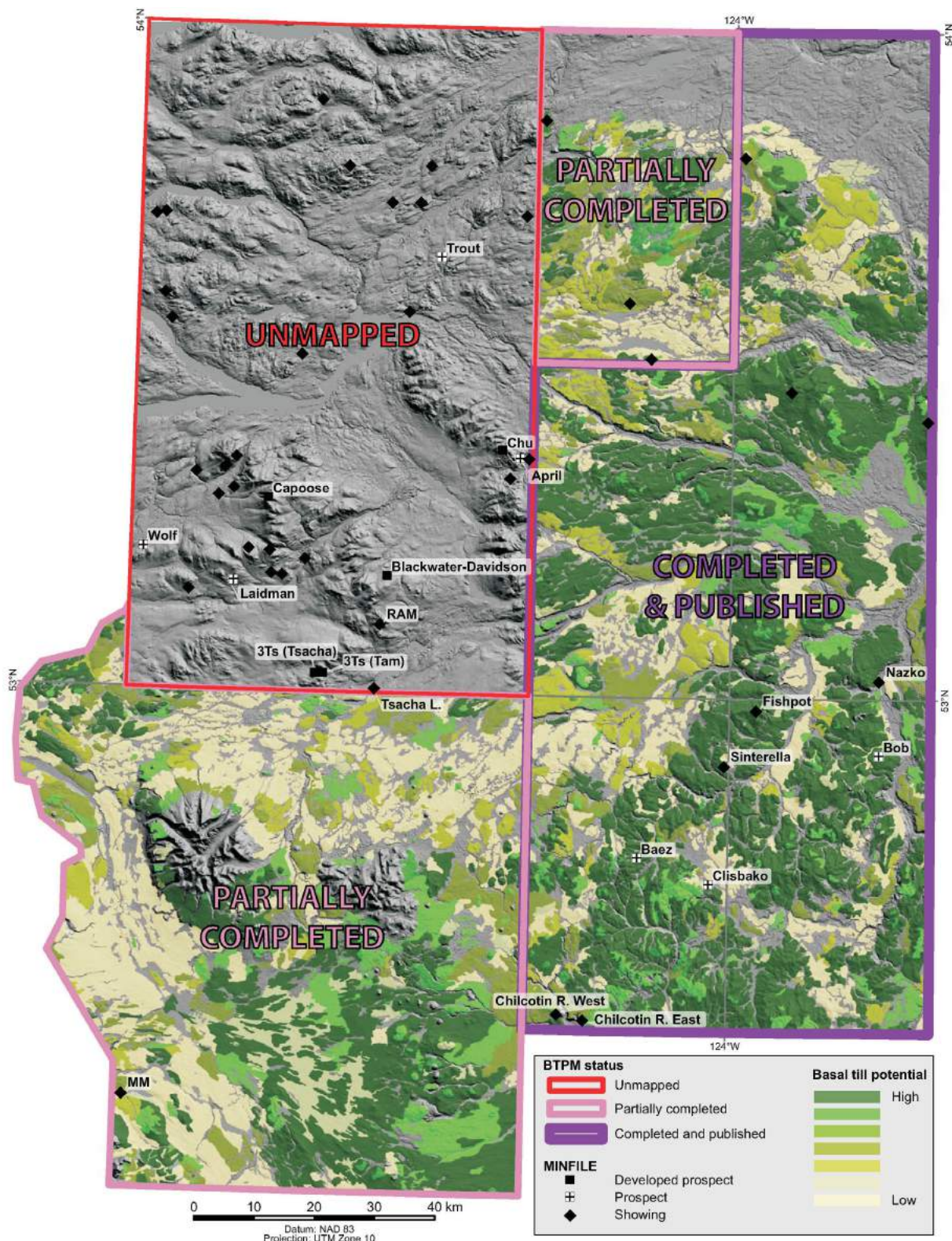


**Figure 4.** Basal till potential mapping (BTPM) coverage and completion status for the TREK project area. These BTPMs are a valuable asset to the planning and implementation of surface geochemical exploration projects. Ten, 1:50 000 scale map areas have been published (purple box; Sacco et al., 2014a–j). Eight complete and two partial map areas have been interpreted and ground truthed; however, the ground-truthing has not been applied to the initial interpretations (pink boxes). Mapping has not been conducted in eight map areas (red box). The loss of the BC Geological Survey from the TREK project has hindered map production, leaving areas with high potential for economic mineralization without this exploration tool. Digital elevation model from Canadian digital elevation data (GeoBase®, 2007).

for gold grain counts and heavyweight- and medium-weight-fraction mineral separations.

The 2013 field season focused on regions in the eastern part of the study area that had not previously been sampled. A total of 684 till samples of 2–3 kg each and 336 till samples of 10–12 kg each was collected (Figure 5). The 2014 field season focused on areas of NTS 093F, which were previously sampled at a low density (Levson et al., 1994; Weary et al., 1997; Plouffe and Williams, 1998; Plouffe et al., 2001), and NTS 093C, which have never been sampled for geochemical analysis. In this year, 582 till samples of 2–3 kg each and 277 till samples of 10–12 kg each were collected (Figure 5).

### Sample Analysis

Till samples collected for geochemistry and archived till samples were sent to Acme Analytical Laboratories Ltd. (Vancouver, BC) for preparation and major-, minor- and trace-element analyses. Tills were dried, an archive of the original till sample was generated, and the remaining material was sieved to produce splits of the silt plus clay-sized (<0.063 mm) fraction. The 10–12 kg till samples were sent to Overburden Drilling Management Limited (Nepean, Ontario) where samples were panned for gold, sulphides and platinum group minerals, concentrated by size (0.25–2.0 mm) and specific gravity (2.8–3.2 and  $\geq 3.2$ ) and picked for indicator minerals (Figure 6).

Samples were analyzed for minor- and trace-elements by ICP-MS following aqua-regia digestion (53 elements), major and minor elements by ICP-ES following a lithium borate fusion and dilute acid digestion, and total gold determinations plus 34 elements by INAA. All geochemical analyses were completed at Acme Analytical Laboratories Ltd. (Vancouver, BC), except INAA, which was conducted at Becquerel Laboratories Inc. (Mississauga, Ontario).

### Quality Control

In addition to contract labs in-house quality control procedures, additional quality control for analytical determinations includes the use of field duplicates, analytical duplicates, reference standards and blanks. For each block of 20 samples, one field duplicate (taken at a randomly selected sample site), one analytical duplicate (a sample split during the preparation process), and one reference standard is included in geochemical analyses. Reference standards are CANMET till 1 and 4, TREK till standards A and B, and NVI 1, 2, 3 and 4. Duplicate samples determine sampling and analytical variability and reference standards measure the accuracy and precision of the analytical methods. Blanks are introduced throughout the sample stream to determine if there is any cross-contamination between samples.

### Progress and Future Work

To date, 1546 new geochemical samples have been collected in the TREK project area. The geochemical, mineralogical and pebble data from the 684 till samples (e.g., Figure 7) and geochemical data from 280 lake sediment and water samples collected in 2013 have been released (Jackaman and Sacco, 2014). Data from the 582 till samples collected in 2014 and the reanalyzed archived till samples will be released in 2015. The TREK geochemistry program has provided adequate till geochemical sample density for the majority of the study area (see Figure 5). Low sample density still exists in the southwest, around the Itcha Ilgachuz Park, where thick units of ablation till and glaciolacustrine material overlie the basal till. Due to the limited access in these areas, a helicopter-supported biogeochemical treetop survey is the best option to attain useful geochemical data. Furthermore, the complex glacial history in the south needs to be resolved to allow for proper interpretation of the basal till geochemical data.

As a multiyear program, further TREK project geochemical activities will include the assembly of recently acquired survey data plus the further development of geoscience information required for additional field surveys in regions lacking the desired sample medium or access. The project action plan includes the following:

- evaluate and compile analytical results and field data for new basal till and pebble samples;
- evaluate and compile analytical data determined from the reanalysis of archived samples and provide additional information on sample media and genesis;
- complete BTPMs based on field survey ground-truthing exercises (if necessary resources can be acquired); and
- assess the use of treetop biogeochemical surveys to cover areas with challenging access or limited availability of other target media types.

Generating a comprehensive collection of regional, high quality, geochemical analytical data and field information is the primary objective of the geochemical component of the TREK project. This is being accomplished through the compilation of previous multimedia geochemical data, the collection of new samples, the reanalysis of archived samples using modern techniques, the collection of geological information necessary to successfully interpret the data, and the production of BTPMs, which provide a basis for the planning and implication of this and follow-up surveys. When packaged and released to the public, this dataset will be utilized in the exploration and discovery of new mineral occurrences.

### Acknowledgments

This program was funded by Geoscience BC. Contributions by A. Plouffe, A. Grenier and A. Therriault (Geological Survey of Canada) are appreciated. Comments from

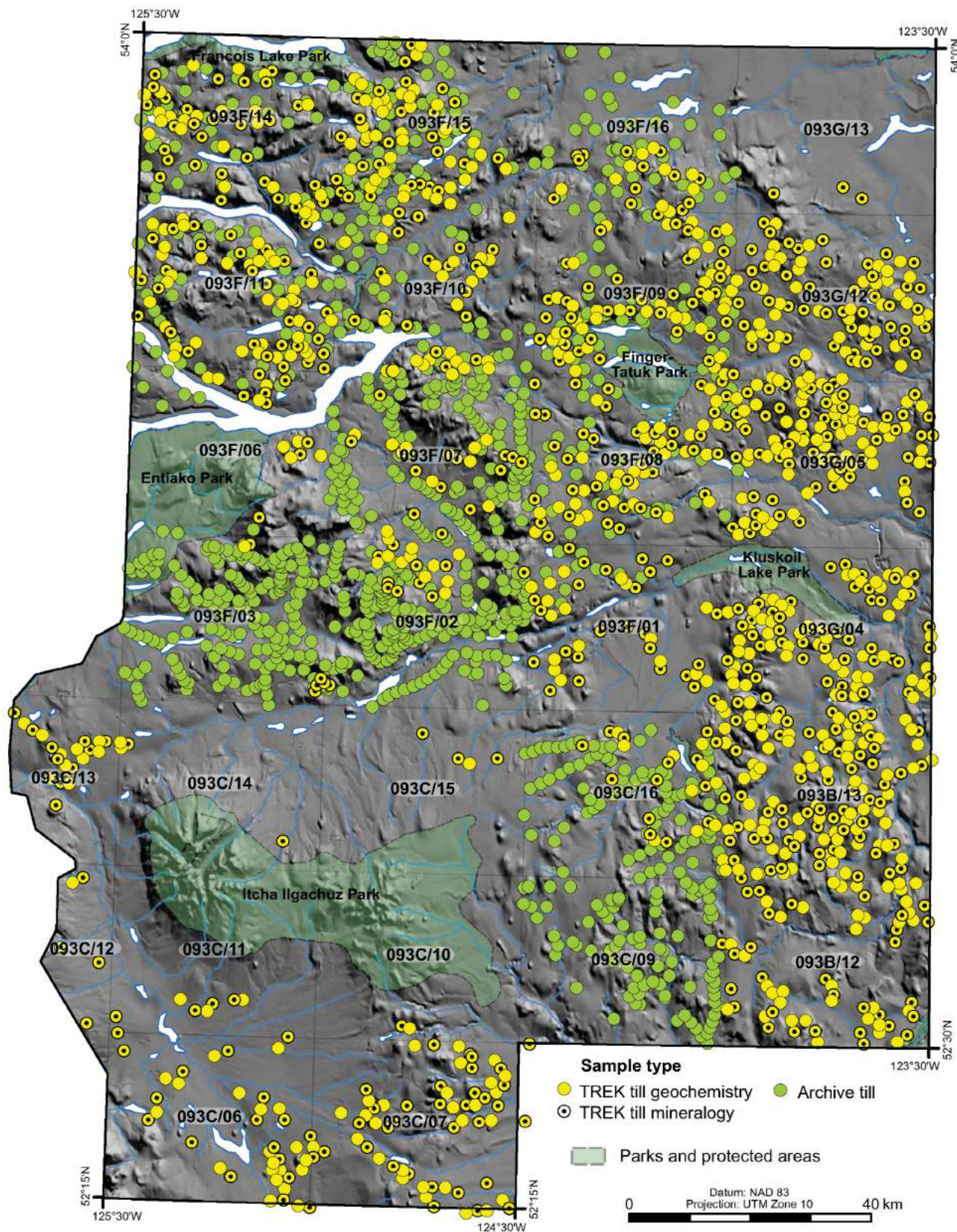


**Figure 5.** Distribution of previous and new sample locations in the TREK project area, central British Columbia. Digital elevation model from Canadian digital elevation data (GeoBase®, 2007).

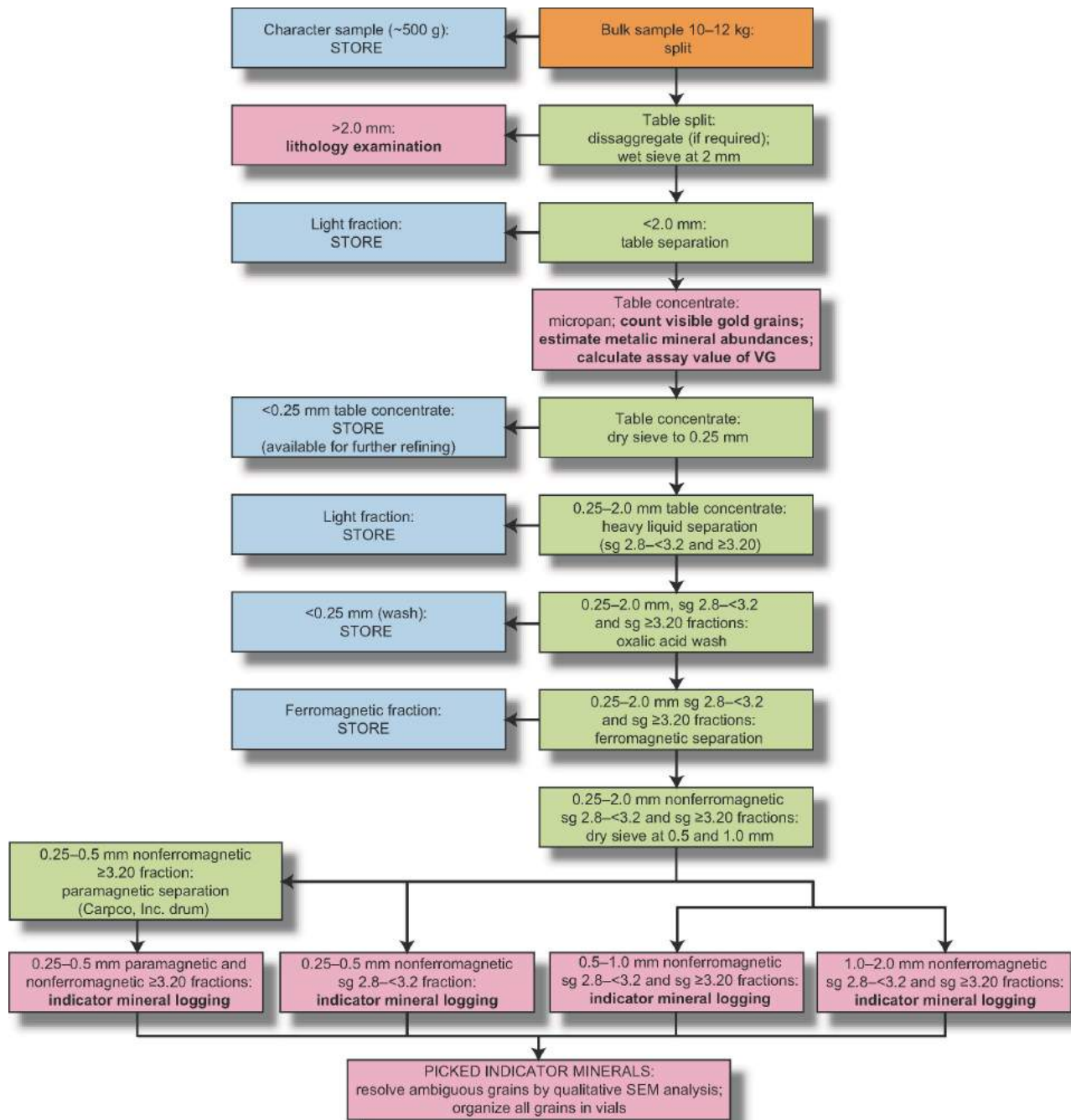


**Figure 6.** Processing flowsheet for indicator minerals and gold grains. Analysis conducted at Overburden Drilling Management Limited (Nepean, Ontario). Abbreviations: SEM, scanning electron microscope; sg, specific gravity; VG, visible gold.

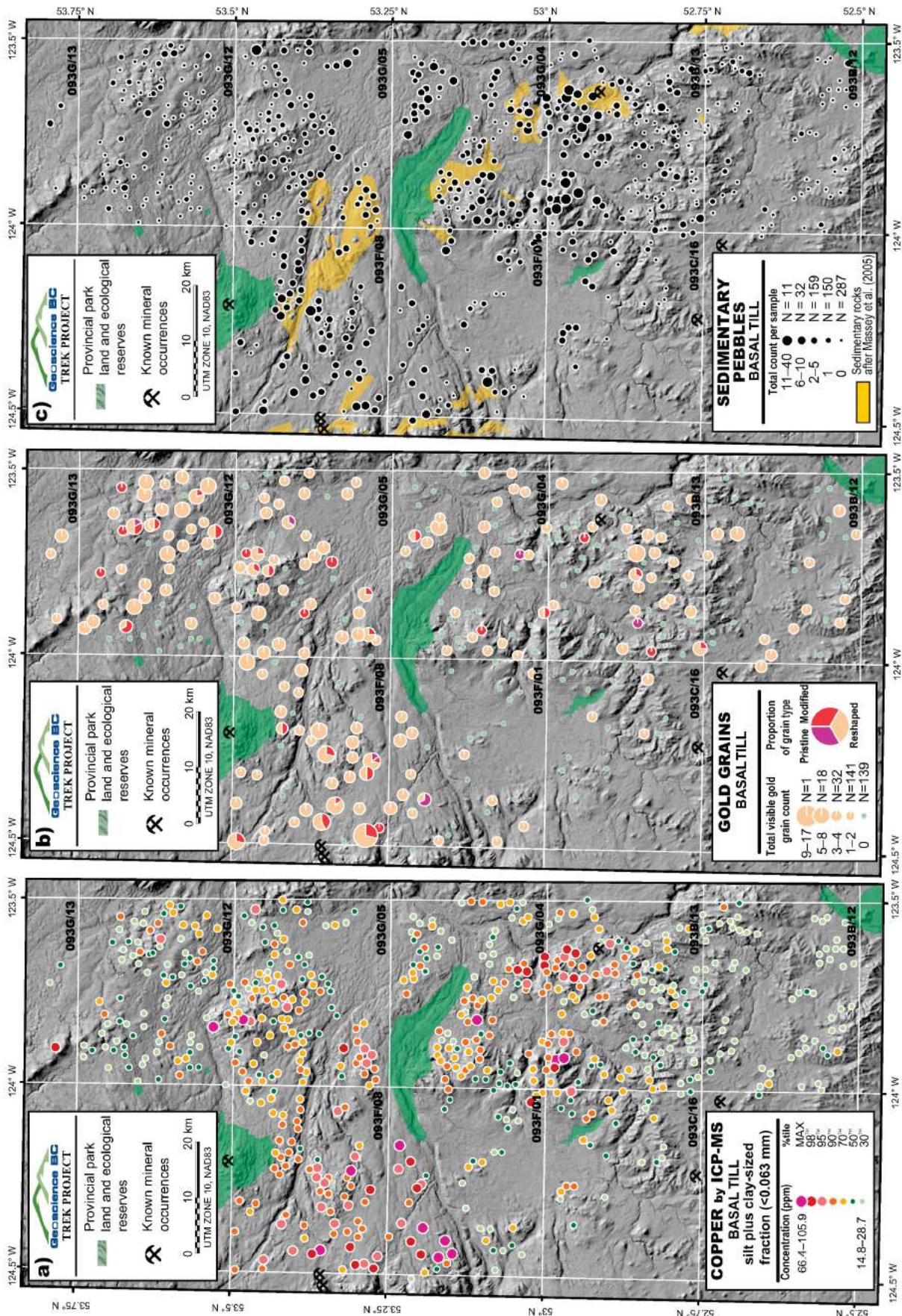


Figure 7. Examples of dot proportion plots from the TREK project 2013 basal till dataset: a) geochemistry: copper concentration by inductively coupled plasma–mass spectrometry (ICP-MS); b) mineralogy: gold grains; c) pebble lithologies: sedimentary pebbles plotted with known sedimentary bedrock sources (Massey et al., 2005). Glacial transport is generally to the northwest in the north, and slightly more northerly in the south. Digital elevation model from Canadian digital elevation data (GeoBase®, 2007).

T. Höy improved the quality of this manuscript. A special thanks to this year's field crew: E. Jackaman, B. Elder, B. Edgington, H. Bains, F. Bertoia and J. Dimock whose hard work, determination and unflinching sediment discriminations contributed greatly to the high quality dataset.

## References

- BC Geological Survey (2013): MINFILE BC mineral deposits database; BC Ministry of Energy and Mines, BC Geological Survey, URL <<http://minfile.ca/>> [October 2013].
- Cook, S.J., Levson, V.M., Giles, T.R. and Jackaman, W. (1995): A comparison of regional lake sediment and till geochemistry surveys: a case study from the Fawnie Creek area, central British Columbia; *Exploration Mining Geology*, v. 4, p. 93–101.
- Deblonde, C., Plouffe, A., Boisvert, É., Buller, G., Davenport, P., Everett, D., Huntley, D., Inglis, E., Kerr, D., Moore, A., Paradis, S.J., Parent, M., Smith, I.R., St. Onge, D. and Weatherston, A. (2012): Science language for an integrated Geological Survey of Canada data model for surficial geology maps, version 1.2; Geological Survey of Canada, Open File 7003, 224 p.
- Dunn, C.E. and Hastings, N.L. (1998): Biogeochemical survey of the Ootsa-Francois lakes using outer bark of lodgepole pine (NTS 93F13/14 and parts of 12 – north-central British Columbia): digital listings and summary notes; Geological Survey of Canada, Open File 3587d, 1 diskette, URL <<http://geoscan.nrcan.gc.ca/starweb/geoscan/servlet.starweb?path=geoscan/download.web&search1=R=209916>> [October 2013].
- Dunn, C.E. and Hastings, N.L. (1999): Biogeochemical survey of the Fraser Lake area using outer bark of lodgepole pine (NTS 93K/2 and parts of 93K/3 – north-central British Columbia): digital data listings and summary notes; Geological Survey of Canada, Open File 3696d, 1 diskette, URL <<http://geoscan.nrcan.gc.ca/starweb/geoscan/servlet.starweb?path=geoscan/download.web&search1=R=210377>> [October 2013].
- Dunn, C.E. and Hastings, N.L. (2000): Biogeochemical survey of the Nechako River area using outer bark of lodgepole pine (NTS 93 F/9, 93 F/10, 93 F/15, 93 F/16 and parts of 93 F/11, 93 F/14, 93 K/1 and 93 K/2), central British Columbia: digital data release for Open Files 3594a-c; Geological Survey of Canada, Open File 3594, 1 diskette, URL <<http://geoscan.nrcan.gc.ca/starweb/geoscan/servlet.starweb?path=geoscan/download.web&search1=R=211478>> [October 2013].
- GeoBase<sup>®</sup> (2007): Canadian digital elevation data, edition 3.0; Natural Resources Canada, URL <<http://www.geobase.ca/geobase/en/find.do?produit=cded>> [October 2012].
- Holland, S.S. (1976): Landforms of British Columbia: a physiographic outline; BC Ministry of Energy and Mines, Bulletin 48, 138 p.
- Jackaman, W. (2006): Regional drainage sediment and water geochemical data Anahim Lake & Nechako River, central British Columbia (NTS 93C & 93F); BC Ministry of Energy and Mines, BC Geological Survey, GeoFile 2006-11, 463 p., URL <<http://www.empr.gov.bc.ca/Mining/Geoscience/PublicationsCatalogue/GeoFiles/Pages/2006-11.aspx>> [October 2013].
- Jackaman, W. (2008a): QUEST project sample reanalysis; Geoscience BC, Report 2008-3, 4 p., URL <<http://www.geosciencebc.com/s/2008-03.asp>> [October 2013].
- Jackaman, W. (2008b): Regional lake sediment and water geochemical data, northern Fraser Basin, central British Columbia (parts of NTS 093G, H, J, K, N & O); Geoscience BC, Report 2008-5, 446 p., URL <<http://www.geosciencebc.com/s/2008-05.asp>> [October 2013].
- Jackaman, W. (2009a): QUEST-West project sample reanalysis; Geoscience BC, Report 2009-5, 4 p., URL <<http://www.geosciencebc.com/s/2009-05.asp>> [October 2013].
- Jackaman, W. (2009b): Regional drainage sediment and water geochemical data, central British Columbia (parts of NTS 93E, F, G, J, K, L, M, N & O); Geoscience BC, Report 2009-11, 347 p., URL <<http://www.geosciencebc.com/s/2009-11.asp>> [October 2013].
- Jackaman, W. and Sacco, D. (2014): Geochemical and mineralogical data, TREK project, Interior Plateau, British Columbia; Geoscience BC, Report 2014-10, 13 p.
- Lett, R.E., Cook, S.J. and Levson, V.M. (2006): Till geochemistry of the Chilanko Forks, Chezacut, Clusko River and Toil Mountain map areas, British Columbia (NTS 93C/1, 8, 9 & 16); BC Ministry of Energy and Mines, BC Geological Survey, GeoFile 2006-1, 272 p., URL <<http://www.empr.gov.bc.ca/Mining/Geoscience/PublicationsCatalogue/GeoFiles/Pages/2006-1.aspx>> [October 2013].
- Levson, V.M. (2001). Regional till geochemical surveys in the Canadian Cordillera: sample media, methods, and anomaly evaluation; *in* Drift Exploration in Glaciated Terrain, M.B. McClenaghan, P.T. Bobrowsky, G.E.M. Hall and S.J. Cook (ed.), Geological Society, Special Publication, no. 185, p. 45–68.
- Levson, V.M., Giles, T.R., Cook, S.J. and Jackaman, W. (1994): Till geochemistry of the Fawnie Creek map area (93F/03); BC Ministry of Energy and Mines, BC Geological Survey, Open File 1994-18, 40 p., URL <<http://www.empr.gov.bc.ca/Mining/Geoscience/PublicationsCatalogue/OpenFiles/1994/Pages/1994-18.aspx>> [October 2013].
- Massey, N.W.D., MacIntyre, D.G., Desjardins, P.J. and Cooney, R.T. (2005): Digital geology map of British Columbia: whole province; BC Ministry of Energy and Mines, BC Geological Survey, GeoFile 2005-1, 1:250 000 scale, URL <<http://www.empr.gov.bc.ca/Mining/Geoscience/PublicationsCatalogue/GeoFiles/Pages/2005-1.aspx>> [October 2013].
- Mathews, W.H. (1986): Physiographic map of the Canadian Cordillera; Geological Survey of Canada, "A" Series Map 1710A, scale 1:5 000 000, URL <<http://geoscan.nrcan.gc.ca/starweb/geoscan/servlet.starweb?path=geoscan/download.web&search1=R=122821>> [October 2013].
- McClenaghan, M.B., Bobrowsky, P.T., Hall, G.E.M. and Cook, S.J., editors (2001): Drift exploration in glaciated terrain; Geological Society, Special Publication, no. 185, p. 45–68.
- Plouffe, A. and Williams, S.P. (1998): Regional till geochemistry, gold and pathfinder elements, northern Nechako River, British Columbia; Geological Survey of Canada, Open File 3687, 3 p., scale 1:400 000, URL <<http://geoscan.nrcan.gc.ca/starweb/geoscan/servlet.starweb>>

- eb? path=geoscan/download.web&search1=R=210023> [October 2013].
- Plouffe, A., Levson, V.M. and Mate, D.J. (2001): Till geochemistry of the Nechako River map area (NTS 93F), central British Columbia; Geological Survey of Canada, Open File 4166, 66 p., URL <<http://geoscan.nrcan.gc.ca/starweb/geoscan/servlet.starweb?path=geoscan/download.web&search1=R=212986>> [October 2013].
- Rencz, A.N., Klassen, R.A. and Moore, A. (2002): Comparison of geochemical data derived from till and lake sediment samples, Labrador, Canada; Geochemistry: Exploration, Environment, Analysis, v. 2, p. 27–35.
- Sacco, D., Ferbey, T. and Jackaman, W. (2014a): Basal till potential of the Clusko River map area (NTS093C/09), British Columbia; BC Ministry of Energy and Mines, BC Geological Survey, Open File 2014-06, Geoscience BC Map 2014-06-01, scale 1:50 000, URL <<http://www.geosciencebc.com/s/Report2014-06.asp>> [December 2014].
- Sacco, D., Ferbey, T. and Jackaman, W. (2014b): Basal till potential of the Clisbako River map area (NTS093B/12), British Columbia; BC Ministry of Energy and Mines, BC Geological Survey, Open File 2014-07, Geoscience BC Map 2014-06-02, scale 1:50 000, URL <<http://www.geosciencebc.com/s/Report2014-06.asp>> [December 2014].
- Sacco, D., Ferbey, T. and Jackaman, W. (2014c): Basal till potential of the Marmot Lake map area (NTS093B/13), British Columbia; BC Ministry of Energy and Mines, BC Geological Survey, Open File 2014-08, Geoscience BC Map 2014-06-03, scale 1:50 000, URL <<http://www.geosciencebc.com/s/Report2014-06.asp>> [December 2014].
- Sacco, D., Ferbey, T. and Jackaman, W. (2014d): Basal till potential of the Toil Mountain map area (NTS093B/16), British Columbia; BC Ministry of Energy and Mines, BC Geological Survey, Open File 2014-09, Geoscience BC Map 2014-06-04, scale 1:50 000, URL <<http://www.geosciencebc.com/s/Report2014-06.asp>> [December 2014].
- Sacco, D., Ferbey, T. and Jackaman, W. (2014e): Basal till potential of the Suscha Creek map area (NTS093F/01), British Columbia; BC Ministry of Energy and Mines, BC Geological Survey, Open File 2014-10, Geoscience BC Map 2014-06-05, scale 1:50 000, URL <<http://www.geosciencebc.com/s/Report2014-06.asp>> [December 2014].
- Sacco, D., Ferbey, T. and Jackaman, W. (2014f): Basal till potential of the Coglistiko River map area (NTS093G/04), British Columbia; BC Ministry of Energy and Mines, BC Geological Survey, Open File 2014-11, Geoscience BC Map 2014-06-06, scale 1:50 000, URL <<http://www.geosciencebc.com/s/Report2014-06.asp>> [December 2014].
- Sacco, D., Ferbey, T. and Jackaman, W. (2014g): Basal till potential of the Pelican Lake map area (NTS093G/05), British Columbia; BC Ministry of Energy and Mines, BC Geological Survey, Open File 2014-12, Geoscience BC Map 2014-06-07, scale 1:50 000, URL <<http://www.geosciencebc.com/s/Report2014-06.asp>> [December 2014].
- Sacco, D., Ferbey, T. and Jackaman, W. (2014h): Basal till potential of the Euchiniko River map area (NTS093F/08), British Columbia; BC Ministry of Energy and Mines, BC Geological Survey, Open File 2014-13, Geoscience BC Map 2014-06-08, scale 1:50 000, URL <<http://www.geosciencebc.com/s/Report2014-06.asp>> [December 2014].
- Sacco, D., Ferbey, T. and Jackaman, W. (2014i): Basal till potential of the Chilako River map area (NTS093G/12), British Columbia; BC Ministry of Energy and Mines, BC Geological Survey, Open File 2014-14, Geoscience BC Map 2014-06-09, scale 1:50 000, URL <<http://www.geosciencebc.com/s/Report2014-06.asp>> [December 2014].
- Sacco, D., Ferbey, T. and Jackaman, W. (2014j): Basal till potential of the Hulatt map area (NTS093G/13), British Columbia; BC Ministry of Energy and Mines, BC Geological Survey, Open File 2014-15, Geoscience BC Map 2014-06-10, scale 1:50 000, URL <<http://www.geosciencebc.com/s/Report2014-06.asp>> [December 2014].
- Sacco, D.A., Jackaman, W. and Ferbey, T. (2014k): Targeted geochemical and mineralogical surveys in the TREK project area, central British Columbia (parts of NTS 093B, C, F, G); *in* Geoscience BC Summary of Activities 2013, Geoscience BC, Report 2014-1, p. 19–34, URL <<http://www.geosciencebc.com/s/SummaryofActivities.asp?ReportID=619756>> [December 2014].
- Shilts, W. (1993): Geological Survey of Canada's contributions to understanding the composition of glacial sediments; Canadian Journal of Earth Sciences, v. 30, p. 333–353.
- Weary, G.F., Levson, V.M. and Broster, B.E. (1997): Till geochemistry of the Chedakuz Creek map area (93F/7), British Columbia; BC Ministry of Energy and Mines, BC Geological Survey, Open File 1997-11, 97 p., URL <<http://www.empr.gov.bc.ca/Mining/Geoscience/PublicationsCatalogue/OpenFiles/1997/Pages/1997-11.aspx>> [October 2013].

# Tracing the Source of Anomalous Geochemical Patterns in Carbonate-Rich Bog Soils near the Nazko Volcanic Cone, Central British Columbia (NTS 093B/13)

R.E. Lett, Consultant, Victoria, BC, raylett@shaw.ca

W. Jackaman, Noble Exploration Services Ltd., Sooke, BC

Lett, R.E. and Jackaman, W. (2015): Tracing the source of anomalous geochemical patterns in carbonate-rich bog soils near the Nazko volcanic cone, central British Columbia (NTS 93B/13); *in* Geoscience BC Summary of Activities 2014, Geoscience BC, Report 2015-1, p. 13–20.

## Introduction

Two wetlands, informally named the North and South bogs, near the Nazko volcanic cone in central British Columbia have CO<sub>2</sub> gas seepages, travertine deposits and organic soil mixed with abundant CaCO<sub>3</sub> (Figure 1). In 2013, soil, water and rock samples were collected in the bogs and in the surrounding area to identify the possible surface geochemical expression of concealed geothermal activity (Lett and Jackaman, 2014). Previous sampling by Alterra Power Corp. of seepage gas in the bogs revealed that CO<sub>2</sub> had negative δ<sup>13</sup>C values in addition to traces of CH<sub>4</sub> and He, suggesting a magmatic and possibly geothermal source for the gas (Hickson, pers. comm., 2013; Vigouroux, pers. comm., 2013). However, median bog-water temperatures of 14.5°C, measured in 2013, suggested that surface upwelling of thermal water from depth is unlikely. Sampling in 2013 found that bog water is typically alkaline and has high concentrations of dissolved Ca and CO<sub>2</sub>. Trace-element analysis of samples also measured higher dissolved Li and B in bog surface water and groundwater compared to levels in wetland streams, but concentrations of these elements are lower than those reported in springs sampled at known geothermal fields. The source of the Li and B in the Nazko bog water is unknown, but it may be in the soil and rock surrounding the bogs. Concentrations of Si and Sr in bog waters, two other potential geothermal indicators, are less than 18 ppm. Calcium carbonate mixed with organic soil and travertine deposits on the surface of the North and South bogs is likely the result of mineral precipitation when dissolved Ca in streamwater mixes with CO<sub>2</sub> seeping through the bog water. During the 2013 fieldwork, a vigorous CO<sub>2</sub> flow from the base of a small travertine cone was discovered on the edge of the North bog. A probable source for up to 44 ppb Ni and 2.4 ppb As dissolved in the water in the bottom of the travertine cone is the groundwater solution

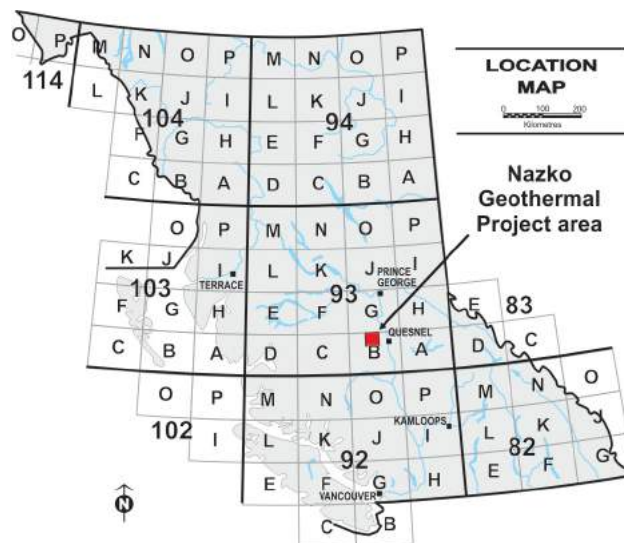


Figure 1. Location of the Nazko geothermal project area.

draining soil and glacial sediment surrounding the bog, rather than upwelling deeper thermal water.

Boron and Li levels are less than 65 ppm in soil and show little variability along profiles extending from well-drained mineral-rich soils developed on glacial deposits surrounding the bogs to CaCO<sub>3</sub>-rich organic soil. However, As, Ni, Ag, Cu and Hg increase sharply at the bog margin, where well-drained soils give way to water-saturated organic soil. The highest Hg values measured during the 2013 study are in the water-saturated organic soil near the travertine cone-CO<sub>2</sub> vent. Cinnabar grains have been identified in a till heavy-mineral concentrate at a TREK regional till-survey site 2 km from the vent, so the cinnabar could be a source for the high Hg found in the soil (Jackaman and Sacco, 2014). Other trace metals (e.g., Cu, Ni, Ag) weathered from the surrounding glacial sediments and transported in solution by groundwater could be concentrated in the organic soil or precipitated in the alkaline (pH >8) CaCO<sub>3</sub> deposits.

Travertine samples were found to have an average 48.34% CaO, equivalent to more than 88% calcite assuming that the travertine is mainly calcite and aragonite. The remaining 12% of the mineral content is most likely to be MgCO<sub>3</sub>, Fe-

**Keywords:** geochemistry, soil, water, geothermal, carbon dioxide, mercury

This publication is also available, free of charge, as colour digital files in Adobe Acrobat® PDF format from the Geoscience BC website: <http://www.geosciencebc.com/s/DataReleases.asp>.

carbonates, strontianite and trace elements. Most travertine samples have low trace-element concentrations, except for a sample from the wall of the travertine cone in the North bog that has anomalously high Fe, As, Hg and Ni.

This paper reports the results of resampling and analysis of groundwater and streamwater in the North bog to confirm results of the 2013 study. Also described here are the soil and tree-bark sampling around the travertine cone–CO<sub>2</sub> vent in the North bog to better establish the size of the geochemical patterns. Proposed collection of CO<sub>2</sub> seepage gas for <sup>3</sup>He:<sup>4</sup>He isotope analysis, to identify if there is a possible magmatic source for the gas, and the analysis of water samples for stable isotopes are also mentioned in the paper.

## Geology and Surface Environment

The North and South bogs lie in the Anahim volcanic belt, an east-trending cluster of Pleistocene–Holocene volcanoes, the most easterly of which is the Nazko cone. Much of the surrounding area is underlain by Eocene Ootsa Lake Group, Miocene Endako Group and Pleistocene–Holocene volcanic rocks, and by clastic sedimentary rocks of the Cretaceous Taylor Creek formation (Riddell, 2011; Talinga and Calvert, 2014). Glacial deposits covering the bedrock are till and glaciofluvial sediments.

Souther et al. (1987) estimated that Nazko volcanism began during the Fraser Glaciation. Later, in the Holocene, ejection of red pyroclastic ash, lapilli and volcanic bombs formed the cone. An ash layer, found in a bog near the cone, was interpreted by these authors to have been the result of an eruption around 7200 years BP when, in addition to the ash fall, olivine basalt lava flowed from the volcano to the south and west. Although there has been no volcanic activity since the original eruption, an earthquake swarm in 2007 near the Nazko cone (Cassidy et al., 2011) and an interpretation of seismic data by Kim et al. (2014) suggest that there is magma in the lower crust at a depth of 22–36 km.

Sedge and scattered wetland shrubs, CaCO<sub>3</sub>-rich mud, stagnant pools or slow moving streams, small isolated areas of travertine, forest-dominated bog, small ponds and meandering streams are characteristic of the North and South bogs. Vegetation ranges from scattered willow and spruce stands in the wetland to a second-growth pine canopy on the surrounding upland. Luvisolic and brunisolic soils have formed on the hill slope above the wetland and gleysolic soil has formed along the poorly drained bog margin. Peat mixed with a CaCO<sub>3</sub>-rich mud is the most common bog deposit. Travertine, typically a rust- to white-coloured rubble, forms small isolated mounds on the bog surface. The small (35 cm high) inverted cone-shaped travertine deposit discovered in 2013 on the northern edge of the North bog has a partially submerged vent from which there is a steady flow of CO<sub>2</sub> though water filling the bottom of the cone.

## Fieldwork

In August 2014, fieldwork in the Nazko bogs and surrounding area included

- sampling water from the travertine cone–CO<sub>2</sub> vent, shallow dug pits and the stream flowing through the North bog. An Oakton PCSTestr 35 meter was used to measure the pH, temperature, salinity and conductivity of the water at each site. Water flow, water-table depth and other site features were recorded. Eight water samples were collected.
- sampling Ah (humus), B and C soil horizons and pine-tree bark at intervals along several profiles extending from the edge of the North bog into the surrounding upland. A total of 20 bark and 67 soil samples was collected. At each site, the pH of a –2 mm fraction of the mineral soil beneath the humus was measured on a slurry of soil and distilled water (1:1 vol:vol) with an Oakton PCSTestr 35 meter. The slurry pH was measured again after addition of 0.1 ml of 10% HCl.
- sampling travertine deposits in the North and South bogs (five samples).
- resampling bulk till at seven sites where TREK regional till samples had been taken in 2013 (Jackaman and Sacco, 2014). Soil profiles and tree bark were also sampled in addition to the bulk till collected for later heavy-mineral preparation.

The water, soil, bark and bulk-till sample locations are shown on Figures 2 and 3.

## Sample Preparation and Analysis

Four water samples were collected in high-density polyethylene (HDPE) bottles at each site for the following analysis:

- Within 6 hours of collection, one of the water samples was analyzed using Hach portable test kits for total alkalinity and dissolved CO<sub>2</sub>.
- A second sample was stored at 4°C for later analysis by ALS Environmental (Vancouver) for hardness; total alkalinity by titration; and F<sup>-</sup>, Cl<sup>-</sup>, Br<sup>-</sup>, NO<sub>3</sub><sup>-</sup>, NO<sub>2</sub><sup>-</sup> and SO<sub>4</sub><sup>-2</sup> by ion chromatography.
- A third sample was filtered through a Phenex™ polyethersulfone 0.45 μm membrane filter, acidified with ultrapure HNO<sub>3</sub> to pH 1 and later analyzed by ALS Environmental for Ag, Al, As, B, Ba, Be, Bi, Ca, Cd, Co, Cr, Cs, Cu, Fe, Ga, K, Li, Mn, Mo, Na, Ni, P, Pb, Rb, Rh, Sb, Se, Si, Sn, Sr, Te, Th, Ti, Tl, U, V, Y, Zn and Zr by mass spectrometry. One blank sample of distilled–deionized water and one sample of the National Research Council Canada (NRCC) riverwater standard SLRS 3 were analyzed with the field samples.
- A fourth sample, filtered through a Phenex™ polyethersulfone 0.45 μm membrane filter and acidified with ultrapure HCl to pH 1, was stored in a glass vial for later

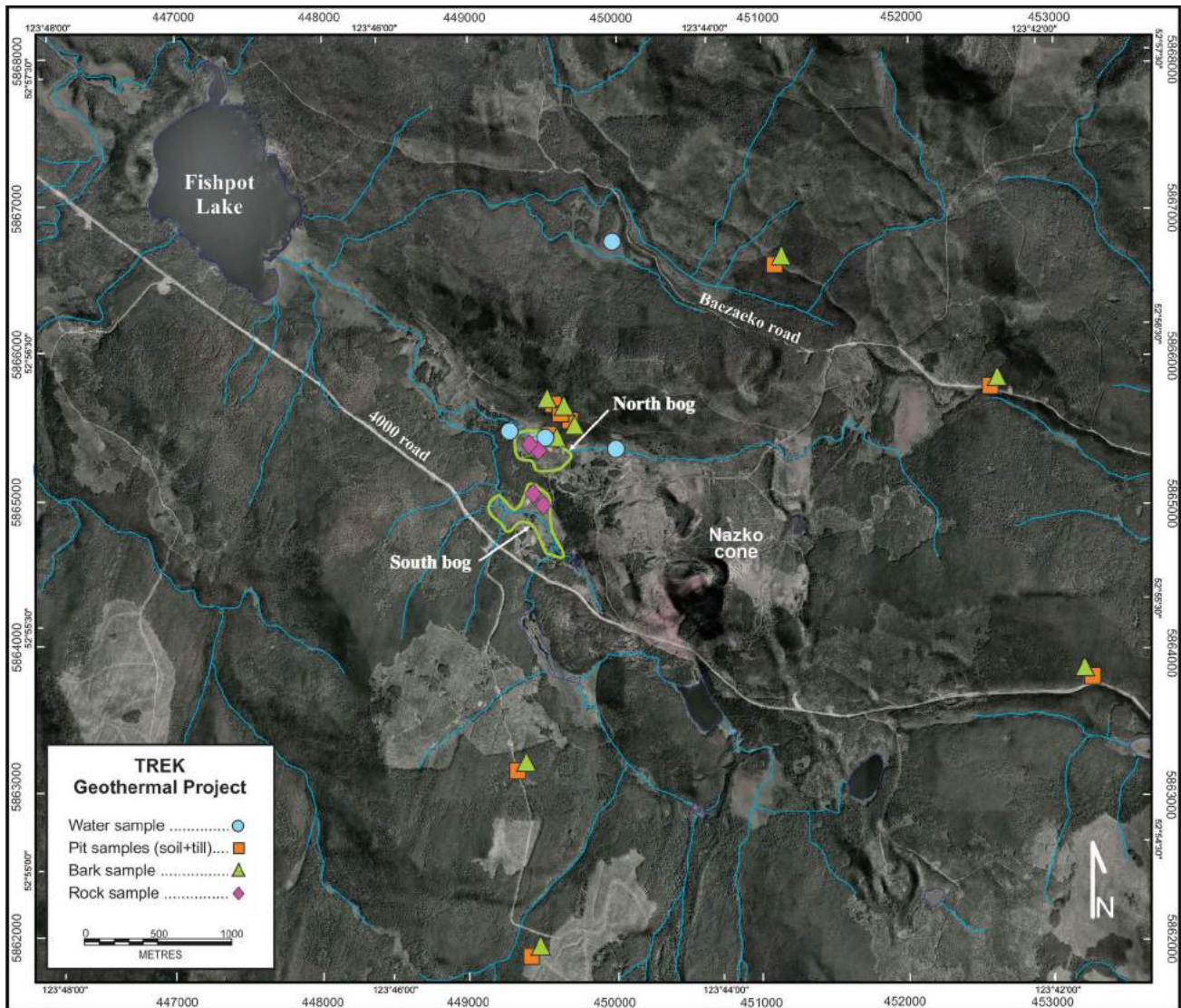


**Figure 2.** Soil, till, rock, water and tree-bark sample sites in the area surrounding the Nazko cone. Digital elevation model from Canadian Digital Elevation Data (CDED; GeoBase®, 2007).

analysis for dissolved Hg by ALS Environmental (Vancouver).

Soil and tree-bark samples were air dried at <math>30^{\circ}\text{C}</math> and sieved to -80 mesh (<math>0.177\text{ mm}</math>). Travertine samples were also air dried and milled to -150 mesh (<math>0.050\text{ mm}</math>). The -80 mesh fraction of the soil and the -150 mesh fraction of the travertine were analyzed at Bureau Veritas Commodities Canada Limited (Vancouver; formerly Acme Analytical Laboratories Ltd.) for the trace and minor elements Ag, Al, As, Au, B, Ba, Be, Bi, Ca, Cd, Co, Cr, Cs, Cu, Fe, Ga, K, Li, Mn, Mo, Na, Ni, P, Pb, Rb, Rh, Sb, Se, Sn, Sr, Te, Th, Ti, Tl, U, V, Y, Zn and Zr by aqua-regia digestion and inductively coupled plasma-mass spectrometry (ICP-MS); for the major oxides ( $\text{Al}_2\text{O}_3$ ,  $\text{SiO}_2$ ,  $\text{Fe}_2\text{O}_3$ ,  $\text{CaO}$ ,  $\text{MgO}$ ,  $\text{MnO}$ ,  $\text{P}_2\text{O}_5$ ) and minor elements Ba, Ce, Co, Cu, Nb, Ni, Sc, Sr, Y, Zn and Zr by lithium borate-ICP-MS; for loss-on-ignition at  $1100^{\circ}\text{C}$ ; and for C and S by LECO combustion.

## Preliminary Geochemistry Results

Table 1 lists element detection limits, reported values for the distilled-de-ionized water blank, the reported values for water standard SLRS 3 and the NRCC-reported element values for SLRS 3. No element concentrations were found to be above the instrument detection limits in the filtered water blank. Where the NRCC reported a value for an element in SLRS 3, the detected concentration is within 20% of the recommended value. Table 2 lists the pH, temperature, total alkalinity (mg  $\text{CaCO}_3$ ), dissolved  $\text{CO}_2$  and element concentrations measured in water samples collected from the North bog, including data for water from the bottom of the travertine cone- $\text{CO}_2$  vent sampled in August 2013, June 2014 and August 2014. Also listed in Table 2 are analyses of groundwater samples from pits within 3 m of the  $\text{CO}_2$  vent and surface water from the stream flowing through the North bog.

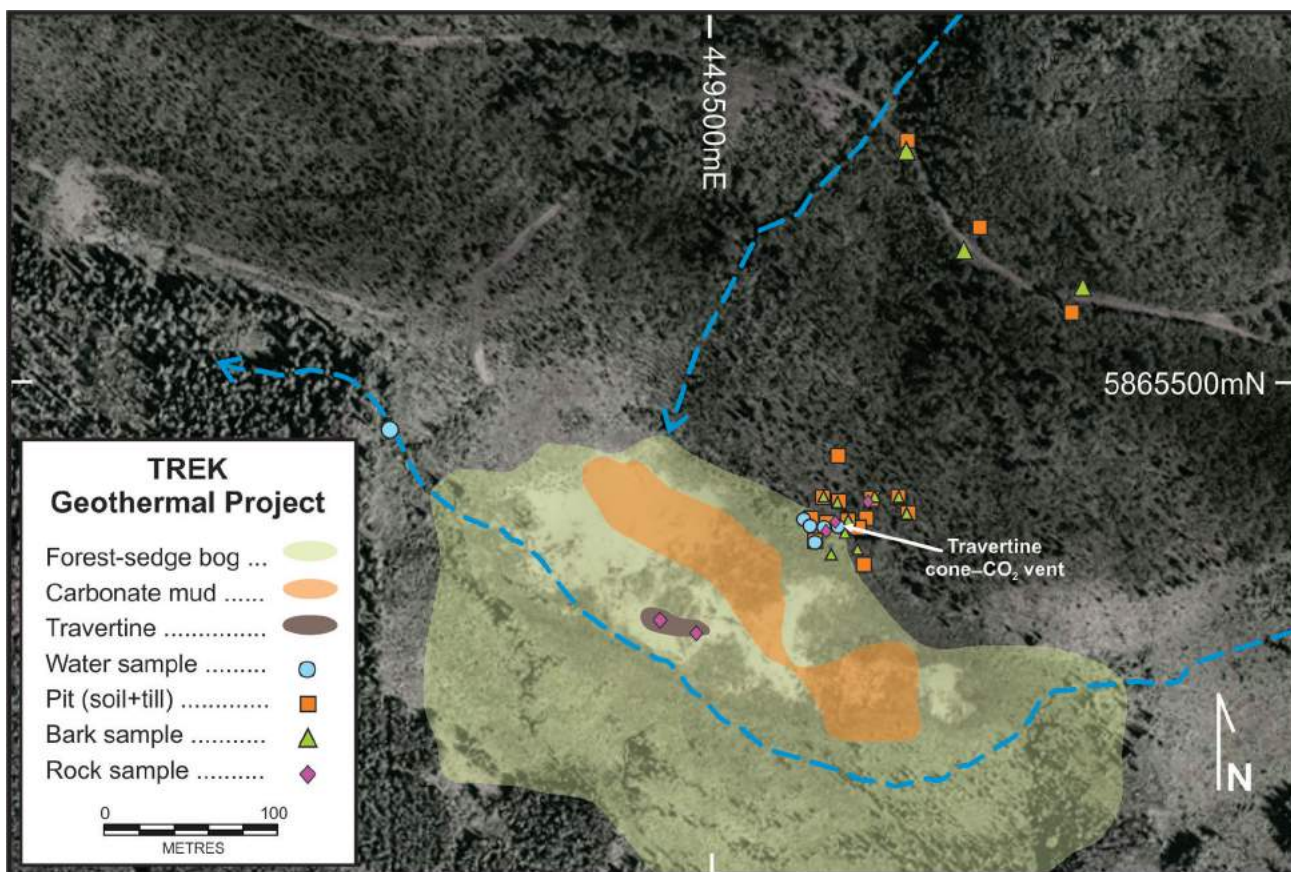


**Figure 3.** Soil, till, rock, water and tree-bark sample sites in the North bog. Digital elevation model from Canadian Digital Elevation Data (CDED; GeoBase®, 2007).

Table 2 reveals that temperature, pH, sulphate and most element concentrations in the water from the travertine cone-CO<sub>2</sub> vent sampled in August 2013 are very similar to those of water collected in June 2014 and in August 2014. There are, however, large differences in alkalinity, dissolved CO<sub>2</sub> and dissolved Fe concentrations measured in this water sampled on the three dates. Alkalinity and dissolved CO<sub>2</sub> differences may reflect a change in the CO<sub>2</sub> flux through the water over the vent. A large difference in the dissolved Fe could be explained by changes in the deeper groundwater circulation through different bedrock. Boron (343–369 ppb), Li (323–346 ppb), Ni (37–44 ppb) and As (1.71–2.56 ppb) are elevated in the travertine cone-CO<sub>2</sub> vent water compared to levels in surface water, and the concentrations are similar in samples collected on the three dates. However, B, Li, Ni, As, dissolved Fe and Ca are much lower in the groundwater from a pit that is 3 m north of the vent, suggesting a nearby source for the mineralized water. Table 2 also shows that there are differences in the chemistry of the streamwater flowing into the bog compared to that of the water draining the bog. For example, water pH increases from 7 to 8 along the stream, but As, Fe and Ca concentrations decrease. No dissolved Hg was detected in any of the water samples.

The geochemical analyses of the soil, tree-bark and travertine samples are still in progress. Soil pH was measured during sampling, and soil pH variation is shown in Figure 4 as inverse difference hydrogen ion (IDH) values, calculated by a method developed by Smee (2009). The IDH is calculated from the difference between the pH of the initial soil-distilled water slurry and that of the soil-distilled water slurry measured after addition of 1 drop of 10% HCl. Inverse difference hydrogen ion values compensate for the buffering effect on pH of high CaCO<sub>3</sub> in the soil and allow the display of a wider range of values compared to the conventional pH units. Although the IDH results for the North bog soils show no clear trends in soil pH, the integration of IDH values with the results of the geochemical analysis may reveal more significant relationships among the trace elements.

### Future Work

Completion of this project will involve

- preparation and geochemical analysis of the soil, bark and travertine samples;
- analysis of the travertine samples by X-ray diffraction for amounts of calcite and aragonite;

**Table 1.** Analytical detection limits, results of National Research Council Canada (NRCC) riverwater standard SLRS 3, and NRCC-reported SLRS 3 'best values'.

Analyte	Detection limit	201493B2010 (SLRS 3)	NRCC SLRS 3 best values
Total alkalinity (ppm)	0.5	nd	
Br (ppm)	0.05	nd	
Cl (ppm)	0.5	nd	
F (ppm)	0.02	nd	
NO <sub>3</sub> (ppm)	0.005	nd	
NO <sub>2</sub> (ppm)	0.001	nd	
SO <sub>4</sub> (ppm)	0.5	nd	
Al (ppb)	1	30.6	31
Ag (ppb)	0.005	-0.005	
As (ppb)	0.05	0.97	0.72
B (ppb)	5.00	13.10	
Ba (ppb)	0.1	15.6	13.4
Be (ppb)	0.005	0.0077	0.005
Bi (ppb)	0.05	-0.05	
Ca (ppm)	0.050	6.28	6
Cd (ppb)	0.005	0.0152	0.013
Co (ppm)	0.05	-0.05	0.027
Cr (ppb)	0.5	-0.5	0.3
Cs (ppb)	0.005	0.0065	
Cu (ppb)	0.2	1.55	1.35
Fe (ppb)	30.0	104.0	100
Ga (ppb)	0.05	-0.05	
Hg (ppb)		-0.05	
K (ppm)	2	-2	0.7
Li (ppb)	0.2	0.85	
Mg (ppm)	0.1	1.69	1.6
Mn (ppb)	0.2	4.05	3.9
Mo (ppb)	0.05	0.188	0.19
Na (ppm)	2	2.6	2.3
Ni (ppb)	0.2	0.77	0.83
P (ppm)	0.3	-0.3	
Pb (ppb)	0.05	0.070	0.068
Rb (ppb)	0.02	1.72	
Re (ppb)	0.005	-0.005	
Sb (ppb)	0.01	0.17	0.12
Se (ppb)	0.2	-0.2	
Si (ppm)	0.05	1.80	
Sn (ppb)	0.2	-0.2	
Sr (ppm)	0.001	0.0325	0.028
Te (ppb)	0.010	-0.01	
Th (ppb)	0.005	0.037	
Ti (ppb)	0.2	0.68	
Tl (ppb)	0.002	0.007	
U (ppb)	0.002	0.044	0.045
V (ppb)	0.05	0.301	0.3
W (ppb)	0.01	-0.01	
Y (ppb)	0.005	0.122	
Zn (ppb)	1.00	1.70	1.04
Zr (ppb)	0.05	0.118	

- analysis of the travertine samples for <sup>16</sup>O/<sup>18</sup>O and <sup>13</sup>C/<sup>12</sup>C isotopes;
- preparation of heavy-mineral concentrates of the till samples and identification of indicator minerals, including cinnabar, in the concentrates;
- sampling of groundwater and surface water for stable isotopes (<sup>1</sup>H, <sup>2</sup>D, <sup>16</sup>O, <sup>18</sup>O);
- analysis of soil samples for Hg using selective extractions and aqua regia-cold vapour atomic absorption spectroscopy;
- sampling of soil gas from CO<sub>2</sub> seepage sites and analysis for <sup>3</sup>He and <sup>4</sup>He isotopes;
- interpretation of the water, soil and sediment data; and
- final reporting, scheduled for the spring of 2015.

## Summary

Geology, seismic-data analysis, travertine-deposit analysis, numerous CO<sub>2</sub> seepages and anecdotal evidence (e.g., snow-free wetland areas) of a thermal anomaly beneath the Nazko bogs and the results of seepage-gas analysis all suggest the existence of a geothermal resource. However, there is only tenuous evidence for geothermal activity from water and soil geochemistry, and the absence of thermal springs may reflect capping of the upwelling water by the wetland sediments. Additional field studies to detect other signs of geothermal activity will include resampling of groundwater in the bogs near a travertine cone-CO<sub>2</sub> seep, analysis of the water for O and C isotopes, and analysis of the seepage gas for He isotopes. High Hg levels in soil near the North bog travertine cone-CO<sub>2</sub> vent may reflect the presence of glacially transported cinnabar in till from a mineralized bedrock source rather than migration of Hg vapour to the surface with the escaping CO<sub>2</sub>. A practical application of this study to support future exploration for geothermal resources is the development of baseline geochemical data for such indicator elements as B and Li in soils, vegetation, water and rock. The study also aims to improve existing methods for sampling and isotope analysis of seepage-gas samples, and techniques designed to distinguish surface geochemical patterns caused by a geothermal source from those that reflect sulphide mineralization in bedrock.

## Acknowledgments

Assistance from F. Bertoia with fieldwork during August 2014 was very much appreciated. N. Vigouroux-Callibot (Douglas College, Vancouver) and G. Williams-Jones (Simon Fraser University, Vancouver) are thanked for their generous advice on the Nazko wetland study. A critical review of this paper by N. Massey was most welcome and greatly improved the quality of the paper. This study is funded by Geoscience BC as part of the 2014 TREK Project.

**Table 2.** Analytical results for North bog travertine cone–CO<sub>2</sub> vent water sampled in 2013 and 2014, and groundwater from pits close to the vent and streamwater. Chloride, bromide, Cr, Ga, P, Th, Sn and Pb are not reported because values in all samples were below detection limit. Abbreviation: nd, not determined.

Sample	2013-1038	2014-1003	2014-2002	2014-2003	2014-2004	2014-2006	2014-2007
Date	6-Aug-13	23-Jun-14	24-Aug-14	24-Aug-14	26-Aug-14	26-Aug-14	26-Aug-14
UTM easting	449580	449580	449569	449881	449580	449328	450046
UTM northing	5865428	5865428	5865420	5865428	5865428	5865493	5865431
Notes	CO <sub>2</sub> vent water	CO <sub>2</sub> vent water	3 m south of CO <sub>2</sub> vent	3 m north of CO <sub>2</sub> vent	CO <sub>2</sub> vent water	Stream into North bog	Stream leaving North bog
Temp	5.9	5.80	14.1	11.26	5.5	14.3	11.2
pH	6.37	6.31	6.46	5.76	6.44	7.14	8.12
CO <sub>2</sub>	600	1450	990	660	1210	80	30
Total alkalinity (ppm)	2410	4600	2670	249	2720	375	123
F (ppm)	0.45	nd	0.57	0.159	0.57	0.240	0.194
NO <sub>3</sub> (ppm)	-0.1	nd	-0.1	-0.005	-0.1	0.0058	0.0212
SO <sub>4</sub> (ppm)	18	nd	19	10.3	19	-0.5	3.98
Ag (ppb)	-0.005	-0.005	-0.005	-0.005	-0.005	0.027	-0.005
Al (ppb)	-1	-30	1.1	30.7	2.4	8.5	2.2
As (ppb)	2.56	1.79	1.17	0.21	2.51	4.73	0.66
B (ppb)	343	369	429	34	353	44	21
Ba (ppb)	187	159.0	241.0	29.2	232.0	99.9	61.5
Be (ppb)	0.044	0.054	-0.005	0.025	0.059	0.006	-0.005
Ca (ppm)	235	207	231	47.1	231	65.1	25.2
Cd (ppb)	0.0376	0.044	0.007	0.219	0.025	-0.005	-0.005
Co (ppb)	2.24	1.95	5.16	1.03	2.07	2.51	-0.05
Cs (ppb)	1.73	1.73	2.58	0.01	2.18	0.08	0.01
Cu (ppb)	-0.2	0.50	0.47	2.79	-0.2	-0.2	0.23
Fe (ppb)	3920	1330	1750	-30	5240	6390	-30
Hg (ppb)	nd	nd	-0.05	-0.05	-0.05	-0.05	-0.05
K (ppm)	31.5	30	31.8	3.9	32.1	4.2	3.0
Li (ppb)	323	378	450	9	436	26	2
Mg (ppm)	239	267	306	26.3	295	42.6	11.9
Mn (ppb)	193	142	471	60	194	1400	1
Mo (ppb)	0.459	0.38	0.0990	0.6310	0.4210	1.7500	1.2600
Na (ppm)	307	275	303	8.0	304	18.9	7.2
Ni (ppb)	44	36.5	37.3000	12.0000	40.8000	2.6200	0.2600
Rb (ppb)	39.3	37.1	42.7000	3.9300	39.1000	4.3700	2.0800
Re (ppb)	0.0064	0.007	-0.005	0.0152	-0.005	-0.005	0.0308
Sb (ppb)	0.039	0.05	0.0280	0.4900	0.0320	0.0420	0.0640
Se (ppb)	-0.2	-0.2	-0.2	0.5500	-0.2	0.7200	3.2200
Si (ppm)	9.63	9.3	9.26	21.3	8.54	21.6	14.0
Sr (ppm)	7.68	7.16	8.05	0.278	9.37	1.05	0.149
Te (ppb)	-0.01	-0.01	0.014	-0.01	0.013	-0.01	-0.01
Ti (ppb)	0.23	0.3	2.3200	1.3700	0.3700	0.5400	-0.2
Tl (ppb)	0.323	0.36	0.3180	0.5940	0.3400	0.0028	-0.002
U (ppb)	0.12	0.125	0.2200	0.2550	0.1590	0.1240	0.1500
V (ppb)	1.08	0.81	0.1190	0.3740	1.5600	1.4500	1.6900
Y (ppb)	0.358	0.185	0.0167	0.8390	0.4780	0.0514	0.0103
Zn (ppb)	10.5	12	5	10	11	-1	-1
Zr (ppb)	1.73	0.38	0.9600	0.5150	1.7300	0.2270	-0.05

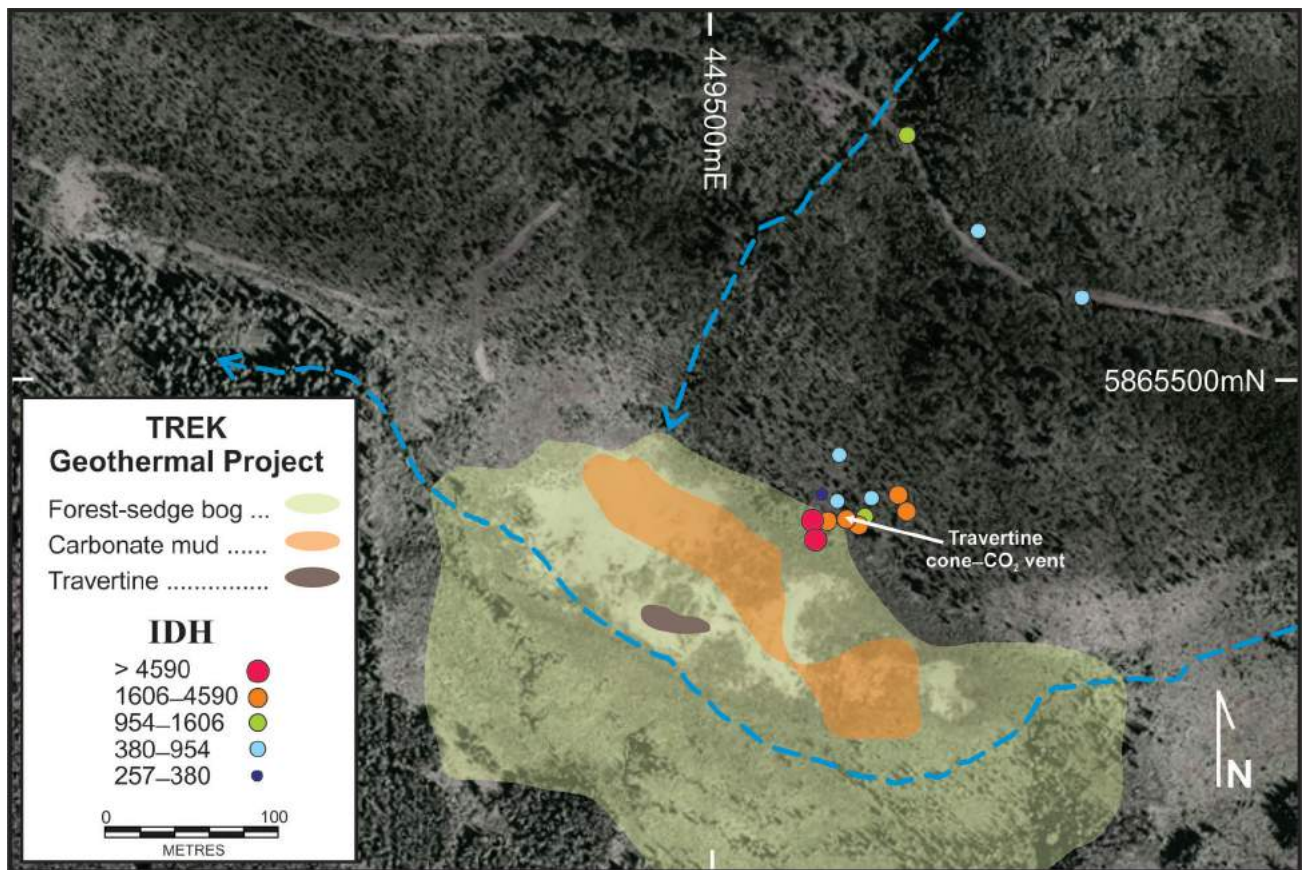


**Figure 4.** Inverse difference hydrogen ion (IDH) values for soil samples taken around the North bog. Digital elevation model from Canadian Digital Elevation Data (CDED; GeoBase®, 2007).

## References

- Cassidy, J.F., Balfour, N., Hickson, C., Kao, H., White, R., Caplan-Auerbach, J., Mazzotti, S., Rogers, G.C., Al-Khoubbi, I., Bird, A.L., Esteban, L., Kelman, M., Hutchinson, J. and McCormack, D. (2011): The 2007 Nazko, British Columbia, earthquake sequence: injection of magma deep in the crust beneath the Anahim volcanic belt; *Bulletin of the Geological Society of America*, v. 101, no. 4, p. 1732–1741.
- GeoBase® 2013: Canadian digital elevation data; Natural Resources Canada, URL <<http://www.geobase.ca/geobase/en/data/cded/>> [November 2014].
- Jackaman, W. and Sacco, D.A. (2014): Regional geochemical and mineralogical data, TREK Project, Interior Plateau, British Columbia; Geoscience BC, Report 2014-10, 13 p.
- Kim, H.S., Cassidy, J.F., Dosso, S.E. and Kao, H. (2014): Mapping crustal structure of the Nechako-Chilcotin plateau using teleseismic receiver function analysis; *Canadian Journal of Earth Sciences*, v. 51, p. 407–417.
- Lett, R.E. and Jackaman, W. (2014): Geochemical expression in soil and water of carbon dioxide seepages near the Nazko volcanic cone, Interior Plateau, BC, NTS 93B/13; Geoscience BC, Report 2014-11, 88 p.
- Riddell, J. (2011): Lithostratigraphic and tectonic framework of Jurassic and Cretaceous intermountain sedimentary basins of south-central British Columbia; *Canadian Journal of Earth Sciences*, v. 48, p. 870–896.
- Smee, B.W. (2009): Soil micro-layer airborne particles and pH: the Govett connection; *in Proceedings of the 24th International Applied Geochemistry Symposium*, v. 1, p. 91–95.
- Souther, J.G. Clague, J.J. and Mathews, R.W. (1987): Nazko cone: a Quaternary volcano in eastern Anahim Belt; *Canadian Journal of Earth Sciences*, v. 24, p. 2477–2485.
- Talinga, D. and Calvert, A.J. (2014): Distribution of Paleogene and Cretaceous rocks around the Nazko River belt of central British Columbia from 3-D long-offset first-arrival seismic tomography; *Canadian Journal of Earth Sciences*, v. 51, p. 358–372.



# TREK Geology Project: Recognizing Endako Group and Chilcotin Group Basalts from Airborne Magnetic Data in the Interior Plateau Region, South-Central British Columbia (NTS 093B, C, F, G)

J.J. Angen, Mineral Deposit Research Unit, University of British Columbia, Vancouver, BC, joelangen@eos.ubc.ca

E. Westberg, Consulting Geologist, Calgary, AB

C.J.R. Hart, Mineral Deposit Research Unit, University of British Columbia, Vancouver, BC

R. Kim, Mineral Deposit Research Unit, University of British Columbia, Vancouver, BC

C. Raley, Consulting Geologist, Vancouver, BC

Angen, J.J., Westberg, E., Hart, C.J.R., Kim, R. and Raley, C. (2015): TREK geology project: recognizing Endako Group and Chilcotin Group basalts from airborne magnetic data in the Interior Plateau region, south-central British Columbia (NTS 093B, C, F, G); in Geoscience BC Summary of Activities 2014, Geoscience BC, Report 2015-1, p. 21–32.

## Introduction

The Targeting Resources through Exploration and Knowledge (TREK) project is a multidisciplinary Geoscience BC initiative to facilitate more successful mineral exploration in a portion of the Interior Plateau (Figure 1) in south-central BC (Clifford and Hart, 2014). The study area is bounded to the west by Tweedsmuir and Entiako provincial parks, extends easterly to Quesnel, as far north as Vanderhoof and Fraser Lake, and south to include Anahim Lake (Figure 1). This region hosts several significant epithermal and porphyry deposits (Figure 1) including the Blackwater epithermal Au-Ag deposit at approximately 270 million g (9.5 million oz. contained Au, total measured and inferred, Christie et al., 2014) and is therefore considered to have high exploration potential.

However, the Early Jurassic to Eocene stratigraphy and associated intrusions, which are known to host mineralization, have limited exposure at surface. This is partially due to the masking effects of extensive Eocene Endako Group and Neogene Chilcotin Group basalt flows, as well as ubiquitous glacial till cover. This has resulted in uncertain distributions and relationships for the prospective units. Consequently, exploration activity and success is considered to have been muted by this lack of confident geological knowledge. A more detailed understanding of the distribution of these basaltic sequences will aid in future investigations of the controls on mineralization within underlying units.

**Keywords:** northern Interior Plateau, Endako Group, Chilcotin Group, TREK, magnetic susceptibility

This publication is also available, free of charge, as colour digital files in Adobe Acrobat® PDF format from the Geoscience BC website: <http://www.geosciencebc.com/s/DataReleases.asp>.

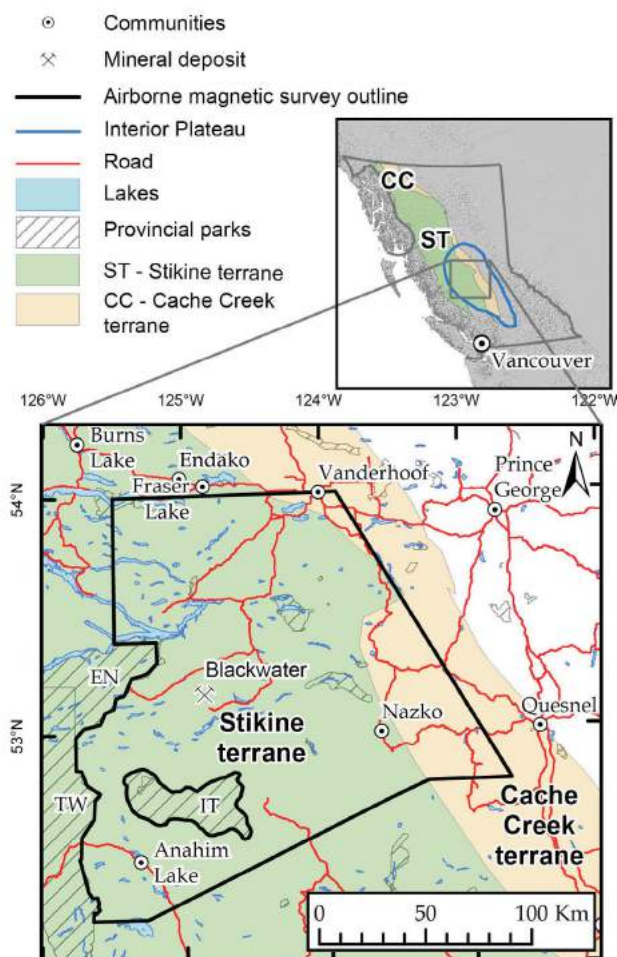


**Figure 1.** Location of TREK study area outlined in black (south-central British Columbia), excluding the Itcha Ilgachuz Provincial Park (modified after Mihalynuk et al., 2008; Colpron and Nelson, 2011; BC Geological Survey, 2014; DataBC, 2014). Abbreviations: EN, Entiako Provincial Park; IT, Itcha Ilgachuz Provincial Park; TW, Tweedsmuir Provincial Park.

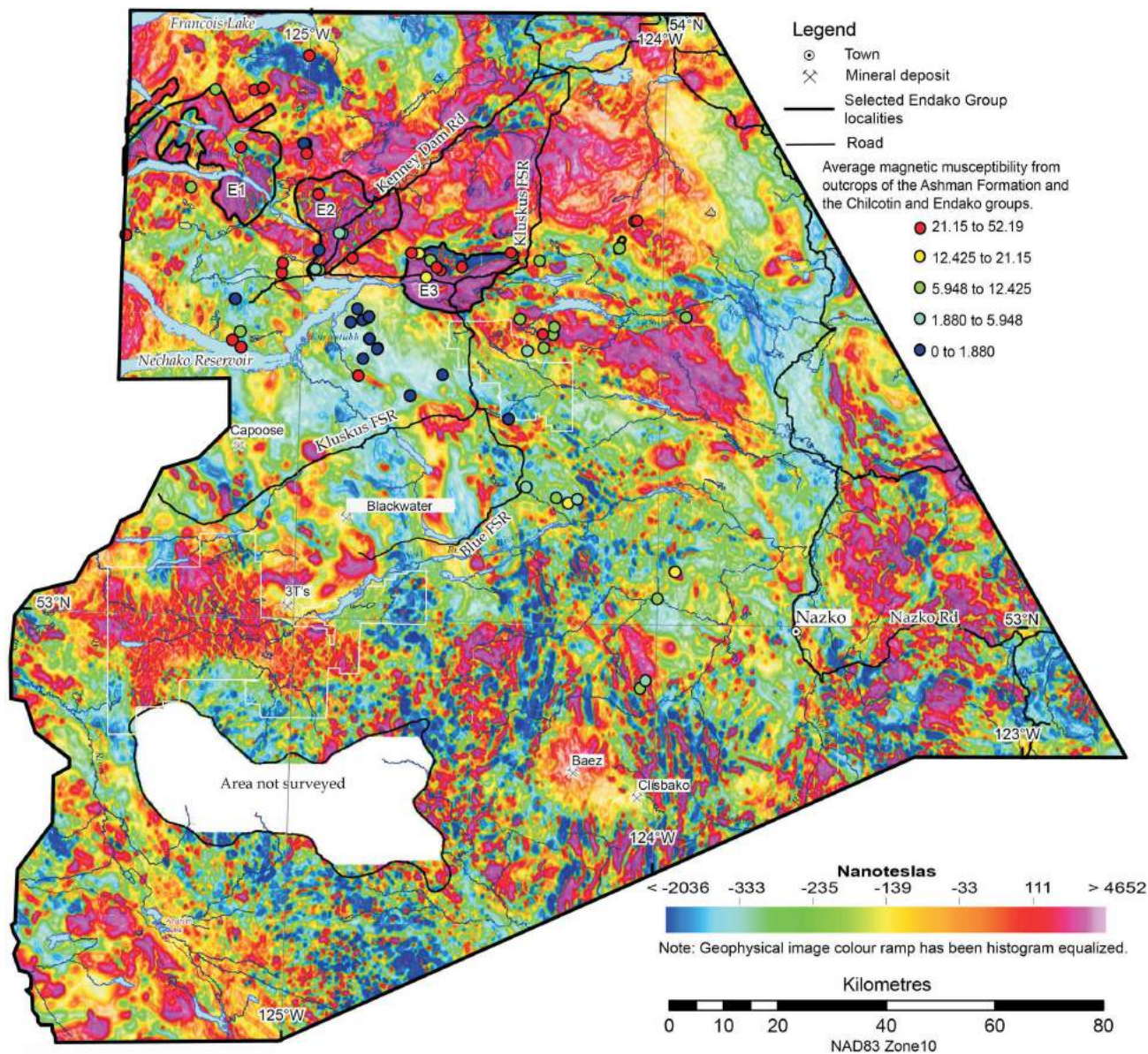


**Figure 2.** Airborne magnetic data (residual magnetic intensity) for the TREK study area, south-central British Columbia (modified after Geoscience BC, 2014); E1, E2 and E3 indicate three distinct high-magnetic-intensity polygons that correlate to exposures of Endako Group. The average magnetic susceptibilities are plotted for stations in the three units discussed within the text. Selected mineral occurrences are located as well to serve as reference points (BC Geological Survey, 2014).

The TREK geology project utilizes recently acquired airborne magnetic data (Figure 2; Aeroquest Airborne, 2014; Geoscience BC, 2014) to support improved interpretations of the regional geology, geochronology and structure, and to update the regional geological map of this portion of the Interior Plateau. In order to correlate features observed in the airborne magnetic data to rock types and unit distributions, ground-truthing is supported with magnetic susceptibility readings that were routinely carried out in conjunction with 1:50 000 scale regional mapping. Among the most obvious features in the airborne magnetic data and maps are a linear, northwest-trending belt of

three regions, each roughly 20 km across, of predominantly high magnetic responses as well as a widespread mottled texture (Figure 2). Field observations indicate that these regions are mostly underlain by rocks of the Endako and Chilcotin groups. To better understand the character and distribution of these rock units, their magnetic and lithological properties were evaluated. This study provides one of many examples where rock petrophysical characteristics can be used to develop a better geological understanding from the newly collected TREK airborne magnetic data, and subsequently improve geological maps to guide mineral exploration efforts.

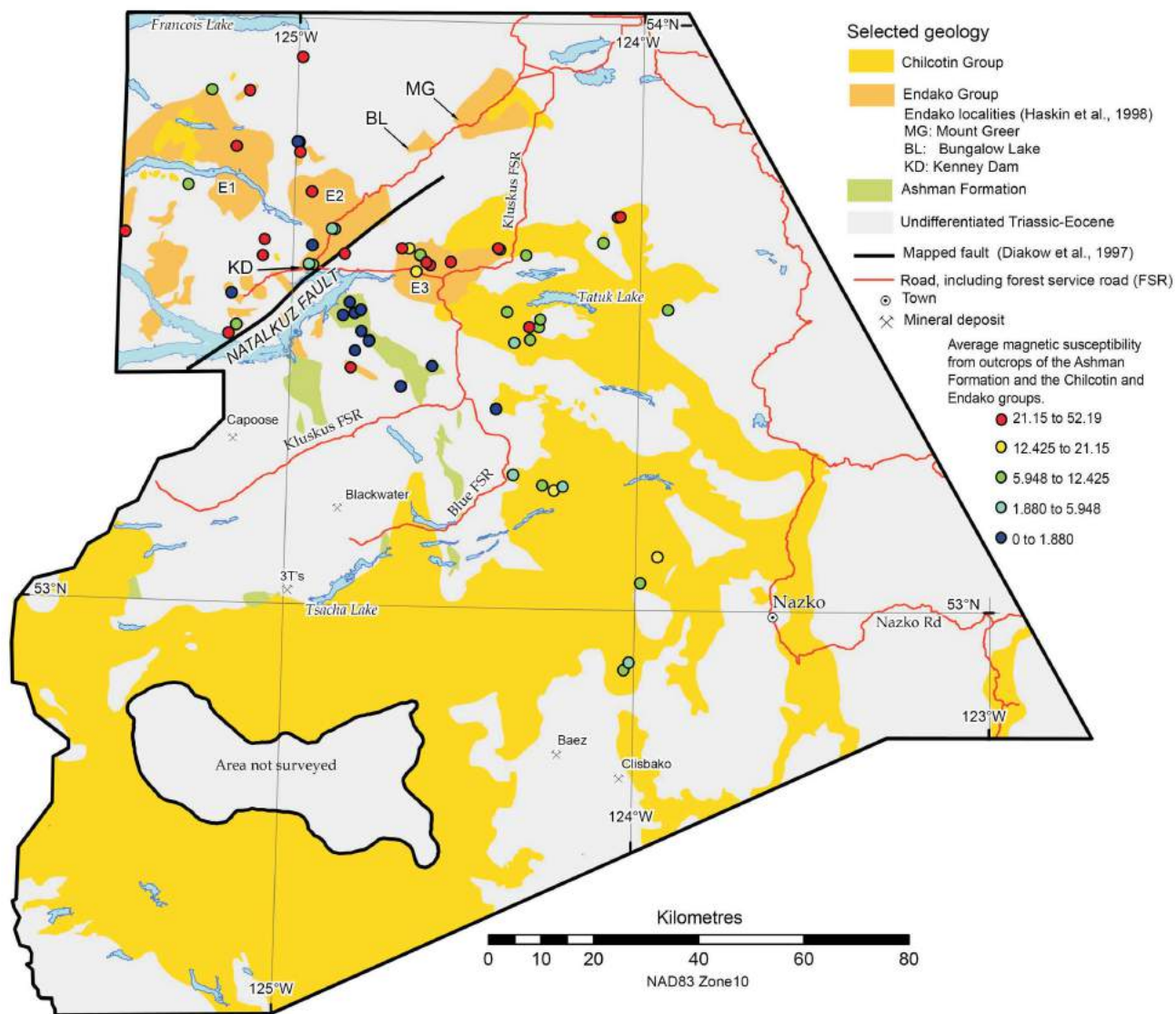


**Figure 3.** Simplified geological map showing the distribution of the Ashman Formation and the Endako and Chilcotin groups in the TREK study area, south-central British Columbia. Produced from new observations, interpolation of magnetic data, and previous mapping by Diakow and Levson, 1997; Anderson et al., 1998, 1999, 2000; Struik et al., 1999. The average magnetic susceptibilities are plotted for stations in the three units discussed within the text; E1, E2 and E3 indicate three distinct high-magnetic-intensity polygons that correlate to exposures of Endako Group. Selected mineral occurrences are located as well to serve as reference points (BC Geological Survey, 2014).

### Geological Setting

The TREK study area is predominantly underlain by rocks of Stikine terrane, with minor exposure of Cache Creek terrane rocks in the east (Figure 1). The Stikine terrane comprises Middle Devonian to Middle Jurassic island-arc volcanic and sedimentary strata with associated plutonic rocks (Gabrielse and Yorath, 1991). In the TREK study area, the oldest Stikine terrane rocks with significant exposure are island arc volcanic rocks of the Lower to Middle Jurassic Hazelton Group (Tipper 1963, 1969; Tipper and Richards, 1976; Diakow and Levson, 1997; Diakow et al., 1997). These are overlain by Middle to Upper Jurassic marine to nonmarine sedimentary stratigraphy of the Bowser Lake Group, including the Ashman Formation (Tipper and Richards, 1976; Diakow et al., 1997; Riddell, 2011). A sig-

nificant unconformity, interpreted as a period of uplift and deformation, marks the Late Jurassic to Early Cretaceous (Tipper and Richards, 1976). This unconformity is overlain by similar marine to nonmarine strata of the Lower Cretaceous Skeena Group (Tipper and Richards, 1976; Riddell, 2011). The Skeena Group is in turn overlain by felsic to intermediate continental-arc-related volcanic rocks of the Late Cretaceous Kasalka Group (Diakow et al., 1997; Kim et al., 2015).

Eocene volcanic strata in central BC include the Ootsa Lake Group and Endako Group. The Ootsa Lake Group is composed predominantly of rhyolite to dacite flows and minor associated volcanoclastic rocks (Duffel, 1959) and is geochronologically constrained from 55 to 46 Ma (Grainger et al., 2001; Bordet et al., 2014). The Endako Group was

originally defined north of Francois Lake (Figure 3) by Armstrong (1949) as a 600 m thick sequence of Oligocene basalt flows. It comprises andesitic to basaltic flows that conformably overlie the Ootsa Lake Group at Bungalow Lake and Mount Greer (Figure 2; Haskin et al., 1998). It has yielded K-Ar whole rock ages ranging from 50 to 31 Ma (Mathews 1964; Stevens et al., 1982; Diakow and Koyanagi, 1988; Rouse and Mathews 1988), but the more reliable Ar-Ar dates constrain it to between 51 and 45 Ma (M.E. Villeneuve, unpublished data, reported in Grainger et al., 2001). This indicates that the Endako Group is, at least in part, coeval with the Ootsa Lake Group (Grainger et al., 2001; Bordet, 2014). In the southeastern portion of the map area, basalt and basaltic andesite are observed interfingering with felsic volcanic rocks of the Ootsa Lake Group leading to the conclusion that they should be included in the Ootsa Lake Group in this area (Bordet, 2014). The tectonic setting for Eocene volcanism in this region is northwest-directed extension associated with movement on faults with dextral transtensional offsets (Struik, 1993; Struik and MacIntyre, 2001).

The Chilcotin Group is a sequence of Neogene flood basalts that cover much of south-central BC (Bevier, 1983). They are estimated to cover roughly 30 000 km<sup>2</sup> of south-central BC and unconformably overlie Eocene and older rocks (Andrews and Russell, 2007, 2008). Exposures of the Chilcotin Group generally occur in areas of low topography, with older units occupying adjacent higher topography, suggesting that it was deposited within paleovalleys (Mihalynuk, 2007). Analysis of well data supports this, and also indicates that the flood basalts rarely exceed 50 m in thickness (Andrews and Russell, 2008).

## Methodology

Airborne magnetic data were collected for the TREK study area during the summer of 2013 (Aeroquest Airborne, 2014). The residual magnetic-intensity (RMI) map is reproduced as Figure 2 (Geoscience BC, 2014). The RMI is the remaining signal after primary data have been modified to remove the Earth's current magnetic field and large scale trends. Features of interest were identified from the airborne data and evaluated during regional ground-truthing and geological mapping between July and September of 2014.

Magnetic susceptibility measurements were collected using either a KT-9 (Exploranium Radiation Detection Systems, 1997) or KT-10 (Terraplus Inc., 2013) Kappameter. These hand-held field meters are designed for measurements on outcrops, and drillcore and rock samples, but the large induction coil on these instruments makes them most appropriate for collecting data at the outcrop scale (Lee and Morris 2013). They both have an inductive coil diameter of 65 mm and utilize an operating frequency of 10 kHz. The

KT-9 has a reported sensitivity of  $1 \times 10^{-5}$  SI units (Exploranium Radiation Detection Systems, 1997) while the KT-10 has a sensitivity of  $1 \times 10^{-6}$  SI units (Terraplus Inc., 2013). However, these values are for when the Kappameters are used in standard mode on a flat surface. All measurements were collected in pin mode, where a pin holds the measuring coil a fixed distance above the surface of the rock, and a correction factor is applied for this separation. This is deemed to provide the most accurate value for rough surfaces if a minimum of five measurements are averaged (Exploranium Radiation Detection Systems, 1997). A typical accuracy of  $\pm 10\%$  compared to laboratory measured values is estimated for the KT-9 when operating in pin mode (Exploranium Radiation Detection Systems, 1997). Given that this is predominantly a result of surface roughness, not the measurement capability of the Kappameter, the same accuracy is implied for the KT-10 model as well. Periodically, a single rock was measured using both models to check for consistency. These measurements were well within the cumulative measurement error.

A total of ten measurements were collected within a single rock type at each outcrop. These data can be used to indicate within-site variability, as well as to determine an average value for each station. The average value for each station is interpreted as the most likely value to correlate with readings obtained from the airborne data, and is therefore the value chosen for presentation within the simplified geological map (Figure 3).

## Field Observations

### Endako Group

Outcrops of Endako Group are resistant to weathering, often forming steep cliffs composed of distinct flows (1–5 m) that are rarely columnar jointed. These vary from subhorizontal to dipping as much as 20° (Figure 4a). Flow tops frequently exhibit pahoehoe textures (Figure 4b). They have variable hematization ranging from a thin veneer on otherwise dark grey basalt (Figure 4b) to pervasively oxidized and red to orange throughout (Figure 4c). They weather dark grey to dark reddish-brown. Fresh surfaces are dark green-grey to black, aphanitic to porphyritic with 1 to 3% (and rarely up to 20%) plagioclase phenocrysts that range in size from 1 to 5 mm. The size and abundance of plagioclase phenocrysts helps to distinguish it from the Chilcotin Group. Several localities were observed to contain from 1 to 2% olivine and pyroxene phenocrysts up to 2 mm. Amygdules are often filled with opalescent silica (Figure 4d), and less commonly with quartz, calcite, chlorite and/or limonite. These range in size and shape from 3 mm and spherical to 10 cm and elongate. The abundant vesicle infill, particularly with opalescent silica, aids in distinguishing the Endako Group from the Chilcotin Group.



**Figure 4.** Distinctive features of Endako Group volcanic rocks, south-central British Columbia: **a)** Endako Group basalt flows dipping 10° to the east, photograph taken looking downdip; **b)** weakly hematized flow top exhibiting pahoehoe texture; **c)** strongly hematized flow top; **d)** opaline silica and clay minerals filling vesicles.

Haskin et al. (1998) report pillow lava and hyaloclastite within the Endako Group.

### Chilcotin Group

The Chilcotin Group generally forms dun brown weathering outcrops in low topography. At some localities, it produces a distinctive bright red soil (Figure 5a). Where cliff exposures were observed, they exhibit subhorizontal flows with both colonnade and entablature (Figure 5b) style columnar jointing, as well as minor pillow basalt. They are characteristically olivine-phyric, with as much as 20% olivine up to 2 mm. Sparse plagioclase (up to 3%) and pyroxene (up to 10%) phenocrysts up to 2 mm were also observed. Flow tops are vesicular with little to no infill of vesicles (Figure 5c). Bevier et al. (1983) report rare chabazite amygdules. Dark green, coarse-grained, dunite to lherzolite xenoliths are far from ubiquitous, but where they are observed they are an excellent diagnostic feature when trying to distinguish the Chilcotin Group from the Endako Group (Figure 5d). Resnick et al. (1999) report these xenoliths as containing olivine, chromian diopside, orthopyrox-

ene and magnetite. Rare hyaloclastite and felsic tephra have been documented previously but were not observed during this study (Bevier et al., 1983; Andrews and Russell, 2007; Farrell et al., 2007; Gordee et al., 2007).

### Magnetic Data

#### Endako Group

In the study area, three domains identified from the RMI data, each covering >100 km<sup>2</sup> with exceptionally high magnetic responses, predominantly >400 nanoteslas (nT) and as high as 1500 nT, correlate with large mapped exposures of Endako Group basalt (Figures 2, 3). These domains also contain local (5–25 km<sup>2</sup>) subdomains with magnetic responses as low as –1000 nT, see discussion below. Outcrop magnetic susceptibilities for Endako Group outcrops exhibit a wide range of values, as low as  $0.309 \times 10^{-3}$  and as high as  $52.2 \times 10^{-3}$ , with a mean of  $19.2 \times 10^{-3}$  (Figure 6). The lowest magnetic susceptibility value for the Endako Group (Figure 6) corresponds to an intensely hematized flow top such as the one represented in Figure 4c. The high



**Figure 5.** Distinctive features of Chilcotin Group volcanic rocks, south-central British Columbia: **a)** red soil and weathering colour; **b)** road outcrop exhibiting entablature columnar jointing; **c)** flow top without infill of vesicles; **d)** dunite xenolith.

magnetic response recorded for Endako Group rocks, generally  $>400$  nT, in the RMI data (Figure 2) corresponds well with the predominantly high magnetic susceptibilities, with a mean value of  $19.2 \times 10^{-3}$  recorded for Endako Group outcrops (Figure 6).

### Chilcotin Group

Extensive exposures of Chilcotin Group basalts generally correspond to regions in the airborne magnetic data with a distinctive mottled appearance including relatively small (approximately 1 km in diameter) highs in the range of 400 to 800 nT and lows in the range of  $-400$  to  $-800$  nT (Figures 2, 3). This texture has been observed elsewhere for the Chilcotin Group including in the Bonaparte Lake region to the southeast of the current study area (Thomas and Pilkington, 2008; Thomas et al., 2011). Magnetic susceptibilities recorded for rocks of the Chilcotin Group during this study exhibit values with a range from  $2.82 \times 10^{-3}$  to  $39.1 \times 10^{-3}$ , and an average of  $10.9 \times 10^{-3}$  (Figure 6).

### Ashman Formation

The Ashman Formation is included as a reference to compare the basaltic sequences to. Within the study area it is composed predominantly of chert pebble conglomerate with lesser siltstone and sandstone. Ashman Formation outcrops identified in the field correspond to regions in the airborne magnetic data with limited variability, exhibiting magnetic intensities consistently between  $-300$  nT and  $-200$  nT. Magnetic susceptibilities measurements record similarly limited variability, from  $0.00 \times 10^{-3}$  to  $0.249 \times 10^{-3}$ , with a mean value of  $0.102 \times 10^{-3}$  (Figure 6).

### Data Comparison

The magnetic susceptibility data for the Endako Group (Figure 6) would fall along the ‘magnetite trend’ of Henkel (1991). The highest density of data that define this trend are centred around  $30 \times 10^{-3}$  (Enkin, 2014). In contrast, the magnetic susceptibility for the Ashman Formation (Figure 6) falls near the ‘paramagnetic trend’ of Henkel (1991), centred around  $0.3 \times 10^{-3}$  (Enkin, 2014). This suggests that the magnetic intensity for the Endako Group is controlled

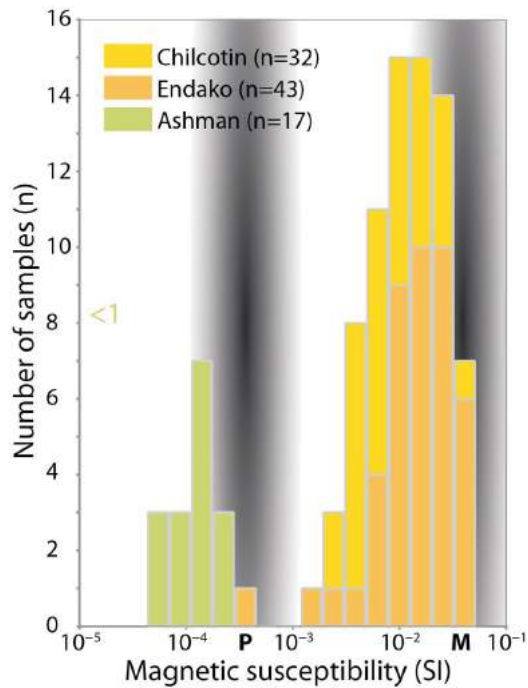


**Figure 6.** Magnetic susceptibility data: histogram plot of mean magnetic susceptibilities from confidently identified outcrops of Chilcotin Group, Endako Group and Ashman Formation, south-central British Columbia. The <1 indicates a single data point for Ashman Formation that plots below the limit of this diagram. The approximate location of the magnetite (M) and paramagnetic (P) trends of Henkel (1991) as reported by Enkin (2014) are indicated by shading. The Endako Group data best fit the magnetite trend, the Ashman Formation data best fit the paramagnetic trend, and the Chilcotin Group data largely fit between them.

by magnetite, whereas the magnetic intensity for the Ashman Formation is controlled by paramagnetic minerals (e.g., biotite, clays). Magnetic susceptibilities recorded for rocks of the Chilcotin Group during this study exhibit similar variability to those of the Endako Group, but tend toward slightly lower values (Figure 6). This is in agreement with previous observations by Enkin (2014) who noted that magnetic susceptibilities for Chilcotin Group samples generally fall in the gap between the magnetite and paramagnetic trends.

## Discussion

### Distribution of Endako Group and Eocene Extension

The high magnetic signature of the Endako Group was combined with field observations to reinterpret some of the map boundaries for this unit (Figure 3). These new map patterns provide additional insight into adjacent structures within the region. The linear southeastern boundary of the E2 Endako Group polygon in the vicinity of Kenney Dam suggests a fault contact (Figures 2, 3). Furthermore, the Endako Group outcrops to the west of this feature are ex-

posed to the bottom of the Nechako River canyon below Kenney Dam, approximately 100 m below adjacent older volcanic rocks (Figure 3). This supports the inferred north-west-side-down movement along the Nataalkuz normal fault (Figure 3; Diakow et al., 1997). It also fits the currently accepted model where Eocene volcanism in central BC is coeval with normal faulting related to extensional tectonics, leading to the deposition of these rocks in extensional basins (Struik, 1993; Struik and MacIntyre, 2001; Grainger et al., 2001; Bordet, 2014). The up to 20° dip of Endako Group basalts reported by Haskin et al. (1998) supports syn- to postdepositional faulting as opposed to pre-existing faults that controlled deposition of Eocene volcanic strata as previously proposed (Diakow et al., 1997; Anderson et al., 1999).

The E1 and E2 polygons exhibit some high (1500 nT) to low (–1000 nT) magnetic response striping whereas the E3 polygon exhibits only one zone of low magnetic intensity to the north (Figure 2). It may be that the high-low magnetic striping observed for E1 and E2 is the result of faulting and associated fluid flow that destroys magnetic minerals. If this is the case, the more uniform high magnetic signature of E3 (Figure 2) could reflect a slightly younger age than the Endako domains with striping.

### Mottled Texture of Chilcotin Group

The extremely low magnetic responses recorded within the airborne magnetic data for the Chilcotin Group (–800 nT) are lower than those recorded for regions of known sedimentary rocks (–300 nT to –200 nT) belonging to the Ashman Formation (Figures 2, 3). Magnetic susceptibilities for the Ashman Formation are consistently at least an order of magnitude lower than those of the Chilcotin Group (Figure 6). This indicates that there is not a direct correlation between magnetic response in airborne data and magnetic susceptibility. Enkin (2014) reported exceptionally high Koenigsberger ratios ( $K_N = \text{remnant magnetism/induced magnetization in a } 50\,000 \text{ nT field}$ ) for Chilcotin Group samples, with 96% of samples having  $K_N > 1$  and 45% having  $K_N > 10$ . Therefore, the remnant component will dominate the RMI signature for Chilcotin Group rocks (Enkin, 2014).

Bevier et al. (1983) reported normal and reverse polarity for differing flows within the Chilcotin Group. Locally, two reversals were documented in a single cliff exposure. If each flow has varying magnetic susceptibility, the combined inputs from a series of normal polarity flows overlain by a series of reverse polarity flows will have a different value at each location. Regions dominated by normal polarity flows will exhibit extremely high magnetic responses while those dominated by reverse polarity flows will exhibit extremely low magnetic responses in airborne data as the magnetic intensity of the flows either adds to or

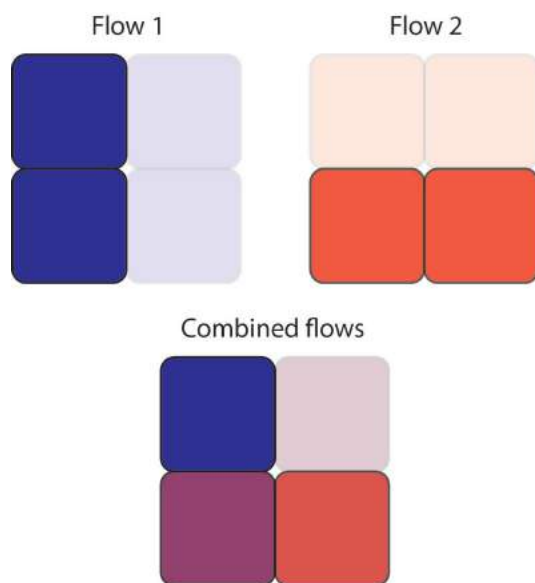


**Figure 7.** Schematic showing possible cause of mottled aeromagnetic signature of Chilcotin Group basalts, south-central British Columbia. The blue solid fill in flow one indicates strong reverse polarity remnant magnetization, while the translucent fill indicates weak remnant magnetization. Similarly, the solid and translucent red fill in flow two indicates strong and weak normal polarity remnant magnetization. When flow two is overlain on flow one, a variable signature is recorded where red indicates strong normal polarity, blue indicates strong reverse polarity, and purple indicates zones where equal and opposite remnant magnetizations have cancelled one another out.

subtracts from the overall field (Enkin, 2014). In outcrop, many of the high magnetic susceptibility Chilcotin Group stations contained dunite to lherzolite xenoliths. Resnick et al. (1999) reported that such xenoliths are proximal to eruptive centres. Analogous studies documented lateral variations in magnetic intensity associated with variable cooling rates, with the region in close proximity to the eruptive centre exhibiting a magnetic susceptibility twice that of distal regions of the same flow (Kolofíková, 1976).

Consider a simple model with only two flows; a lower flow of reverse polarity that has high magnetic susceptibility in the west and low in the east (flow 1, Figure 7), while an upper flow of normal polarity has high magnetic intensity in the south and low in the north (flow 2, Figure 7). The south-west quadrant will be neutral, the southeast quadrant will have strong normal polarity, the northeast quadrant will be neutral, and the northwest quadrant will have strong reversed polarity (Figure 7). If this model was extended to include flows of various shapes, each with varying magnetic intensity, a mottled texture with extreme highs and lows (or rather, inverse polarity highs) as observed in the airborne dataset would be conceivable.

## Limitations

The magnetic datasets have limitations with respect to bed-rock mapping. There are several localities where exposures of both Endako and Chilcotin group basalts outcrop but do not correspond to their distinctive magnetic signatures (Figures 2, 3). This may result from the basaltic strata being relatively thin in these locations. Airborne magnetic surveys represent an averaged value in the uppermost part of the crust. Therefore, thin exposures of Chilcotin basalt will not yield the distinctive magnetic signature since the data will more accurately reflect the underlying or surrounding rock type. This will prove valuable in future efforts to develop thickness models. There are also regions that exhibit magnetic intensities up to 1500 nT that were underlain by rocks not belonging to the Endako Group. This emphasizes the need to ground-truth airborne magnetic data.

## Conclusion

Regional geological mapping during the summer of 2014 revealed that several large regions of high magnetic response that cumulatively form a northwesterly trend on the TREK airborne magnetic survey RMI (Geoscience BC, 2014) correspond to thick successions of Eocene Endako Group basalts. Outcrops of these rocks yield high magnetic susceptibilities, averaging  $19.2 \times 10^{-3}$ . The Neogene Chilcotin Group basalts exhibit a distinctive mottled signature on airborne magnetic maps reflecting exceptionally strong remnant magnetism with normal and reversed polarity variations between flows. The evaluation and recognition of magnetic signatures for thick sequences of these two basaltic units will aid in developing improved geological and structural maps as well as three dimensional models for the TREK region. Now that these distinct magnetic signatures are identified, future efforts to interpret the TREK airborne magnetic data can be focused on more subtle features that may provide insight into the controls on mineralization.

## Acknowledgments

This research was made possible by a grant from Geoscience BC. The authors thank E. Bordet for a thoughtful review of an earlier draft of this manuscript.

## References

- Aeroquest Airborne Ltd. (2014): Report on a fixed wing and magnetic geophysical survey, TREK Project, Interior Plateau/Nechako Region, British Columbia, Canada; Geoscience BC, Report 2014-04, 40 p., URL <[http://www.geosciencebc.com/i/project\\_data/GBCReport2014-04/GBCReport2014-04\\_AQ130250\\_Logistics\\_Report.zip](http://www.geosciencebc.com/i/project_data/GBCReport2014-04/GBCReport2014-04_AQ130250_Logistics_Report.zip)> [November, 2014].
- Anderson, R.G., Snyder, L.D., Grainger, N.C., Resnick, J. and Barnes, E.M. (2000): Tertiary geology of the Takysie Lake and Marilla map areas, central British Columbia; Geological Survey of Canada, Current Research 2000-A13, 11 p., URL

- <[http://ftp2.cits.rncan.gc.ca/pub/geott/ess\\_pubs/211/211183/cr\\_2000\\_a13.pdf](http://ftp2.cits.rncan.gc.ca/pub/geott/ess_pubs/211/211183/cr_2000_a13.pdf)> [November 2014].
- Anderson, R.G., Snyder, L.D., Resnick, J. and Barnes, E. (1998): Geology of the Big Bend Creek map area, central British Columbia; in *Current Research 1998-A*, Geological Survey of Canada, p. 145–154, URL <[http://ftp2.cits.rncan.gc.ca/pub/geott/ess\\_pubs/209/209427/cr\\_1998\\_ab.pdf](http://ftp2.cits.rncan.gc.ca/pub/geott/ess_pubs/209/209427/cr_1998_ab.pdf)> [November 2014].
- Anderson, R.G., Snyder, L.D., Resnick, J., Grainger, N. C. and Barnes, E.M. (1999): Bedrock geology of the Knapp Lake map area, central British Columbia; in *Current Research 1999-A*, Geological Survey of Canada, p. 109-118, URL <[http://ftp2.cits.rncan.gc.ca/pub/geott/ess\\_pubs/210/210136/cr\\_1999\\_ab.pdf](http://ftp2.cits.rncan.gc.ca/pub/geott/ess_pubs/210/210136/cr_1999_ab.pdf)> [November 2014].
- Andrews, G.D.M. and Russell, J.K. (2007): Mineral exploration potential beneath the Chilcotin Group, south-central BC: preliminary insights from volcanic facies analysis; in *Geological Fieldwork 2006*, Geoscience BC, Report 2007-1, p. 229–238, URL <<http://www.empr.gov.bc.ca/Mining/Geoscience/PublicationsCatalogue/Fieldwork/Documents/2006/22-Andrews.pdf>> [November 2014].
- Andrews, G.D.M. and Russell, J.K. (2008): Cover thickness across the southern Interior Plateau, British Columbia (NTS 0920, P; 093A, B, C, F): constraints from water-well records; in *Geoscience BC Summary of Activities 2007*, Geoscience BC, Report 2008-1, p. 11–20, URL <[http://www.geosciencebc.com/i/pdf/SummaryofActivities2007/SoA2007-Andrews\\_original.pdf](http://www.geosciencebc.com/i/pdf/SummaryofActivities2007/SoA2007-Andrews_original.pdf)> [November 2014].
- Armstrong, J.E. (1949): Fort St. James map-area, Cassiar and Coast districts, British Columbia; Geological Survey of Canada, Memoir 252, 210 p.
- BC Geological Survey (2014): MINFILE BC mineral deposits database; BC Ministry of Energy and Mines, BC Geological Survey, URL <<http://minfile.ca/>> [November 2014].
- Bevier, M.L. (1983): Regional stratigraphy and age of the Chilcotin Group basalts, south-central British Columbia; *Canadian Journal of Earth Sciences*, v. 20, p. 515–524, URL <<http://www.nrcresearchpress.com/doi/pdf/10.1139/e83-049>> [November 2014].
- Bordet, E. (2014): Eocene volcanic response to the tectonic evolution of the Canadian Cordillera; Ph.D. thesis, University of British Columbia, 220 p., URL <[https://circle.ubc.ca/bitstream/handle/2429/46271/ubc\\_2014\\_spring\\_bordet\\_esther.pdf?sequence=1](https://circle.ubc.ca/bitstream/handle/2429/46271/ubc_2014_spring_bordet_esther.pdf?sequence=1)> [November 2014].
- Bordet, E., Mihalyuk, M.G., Hart, C.J.R., Mortensen, J.K., Friedman, R.J. and Gabites, J. (2014): Chronostratigraphy of Eocene volcanism, central British Columbia; in *Canadian Journal of Earth Sciences*, v. 51, p. 56–103, doi.org/10.1139/cjes-2013-0073, URL <<http://www.nrcresearchpress.com/doi/pdf/10.1139/cjes-2013-0073>> [November 2014].
- Christie, G., Lipiec, I., Simpson, R.G., Horton, J. and Borntreager, B. (2014): Blackwater gold project British Columbia, NI 43-101: technical report on feasibility study; AMEC Americas Limited, report prepared for New Gold Inc., 336 p., URL <[http://www.newgold.com/files/documents\\_properties/blackwater/Blackwater%20Gold%20Project%20Technical%20Report%20January%2014%202014.pdf](http://www.newgold.com/files/documents_properties/blackwater/Blackwater%20Gold%20Project%20Technical%20Report%20January%2014%202014.pdf)> [November 2014].
- Clifford, A. and Hart, C.J.R. (2014): Targeting Resources through Exploration and Knowledge (TREK): Geoscience BC's newest minerals project, Interior Plateau region, central British Columbia (NTS 093B, C, F, G); in *Geoscience BC Summary of Activities 2013*, Geoscience BC, Report 2014-1, p. 13–18, URL <<http://www.geosciencebc.com/i/pdf/SummaryofActivities2013/SoA2013-CliffordHart.pdf>> [November 2014].
- Colpron, M. and Nelson, J.L. (2011): A digital atlas of terranes for the Northern Cordillera; BC Ministry of Energy and Mines, BC Geological Survey, GeoFile 2011-11, URL <<http://www.empr.gov.bc.ca/Mining/Geoscience/PublicationsCatalogue/GeoFiles/Pages/2011-11.aspx>> [November 2014].
- DataBC (2014): BC parks, ecological reserves, and protected areas; Province of British Columbia website, URL <<http://www.data.gov.bc.ca/dbc/catalogue/detail.page?config=dbc&P110=recorduid:173844&recorduid=173844&title=BC Parks, Ecological Reserves, and Protected Areas>> [November 2014].
- Diakow, L.J. and Koyanagi, V. (1988): Stratigraphy and mineral occurrences of Chikamin Mountain and Whitesail Reach map areas; in *Geological Fieldwork 1987*, BC Ministry of Energy and Mines, BC Geological Survey, Paper 1988-1, p. 155–168, URL <<http://www.empr.gov.bc.ca/Mining/Geoscience/PublicationsCatalogue/Fieldwork/Documents/1987/155-168-diakow.pdf>> [November 2014].
- Diakow, L.J. and Levson, V.M. (1997): Bedrock and surficial geology of the southern Nechako plateau, central British Columbia; BC Ministry of Energy and Mines, BC Geological Survey, Geoscience Map 1997-2, scale 1:100 000, URL <<http://www.empr.gov.bc.ca/Mining/Geoscience/PublicationsCatalogue/Maps/GeoscienceMaps/Documents/GM1997-02.pdf>> [November 2014].
- Diakow, L.J., Webster, I.C.L., Richards, T.A. and Tipper, H.W. (1997): Geology of the Fawnie and Nechako ranges, southern Nechako Plateau, central British Columbia (93F/2, 3, 6, 7); in *Interior Plateau Geoscience Project: Summary of Geological, Geochemical and Geophysical Studies*, L.J. Diakow, J.M. Newell and P. Metcalfe (ed.); BC Ministry of Energy and Mines, BC Geological Survey, Open File 1997-2 and Geological Survey of Canada, Open File 3448, p. 7–30, URL <[http://www.empr.gov.bc.ca/mining/geoscience/publicationscatalogue/papers/documents/p1997-02\\_02.pdf](http://www.empr.gov.bc.ca/mining/geoscience/publicationscatalogue/papers/documents/p1997-02_02.pdf)> [November 2014].
- Duffell, S. (1959): Whitesail Lake map-area, British Columbia; Geological Survey of Canada, Memoir 299, 119 p.
- Enkin, R.J. (2014): The rock physical property database of British Columbia, and the distinct petrophysical signature of the Chilcotin basalts; *Canadian Journal of Earth Sciences*, v. 51, p. 327–338, dx.doi.org/10.1139/cjes-2013-0159, URL <<http://nrcresearchpress.com/doi/pdfplus/10.1139/cjes-2013-0159>> [November 2014].
- Exploranium Radiation Detection Systems (1997): User's Guide KT-9 Kappameter, Rev. 1; Exploranium G.S. Limited, p. 1–80, URL <[http://users.monash.edu.au/~rjarmit/Mag\\_sus\\_meter\\_instructions/KappaMeter\\_KT9/KT9\\_manual.pdf](http://users.monash.edu.au/~rjarmit/Mag_sus_meter_instructions/KappaMeter_KT9/KT9_manual.pdf)> [November 2014].
- Farrell, R.E., Andrews, G.D.M., Anderson, B. and Russell, J.K. (2007): Chasm and Dog Creek lithofacies, internal architecture of the Chilcotin Group basalt, Bonaparte Lake map area, British Columbia; Geological Survey of Canada, *Current Research 2007-A5*, 11 p., URL <<http://bibvir1.uqac.ca/archivage/25033021.pdf>> [November 2014].
- Gabrielse, J. and Yorath, C.J. (1991): Tectonic synthesis; Chapter 18 in *Geology of the Cordilleran Orogen in Canada*, J. Gabrielse and C.J. Yorath (ed.), *Geology of Canada*, v. 4, (also Geological Society of America, *Geology of North America*, v. G-2),

- p. 677–705, URL <[http://ftp2.cits.rncan.gc.ca/pub/geott/ess\\_pubs/134/134069/dnag\\_04.zip](http://ftp2.cits.rncan.gc.ca/pub/geott/ess_pubs/134/134069/dnag_04.zip)> [November 2014].
- Geoscience BC (2014): TREK project: airborne geophysics, residual magnetic intensity map (NTS 092E, F, K, L and parts of 092B, C, G, J and 102I); Geoscience BC, Map TREK-1-4, scale 1:500 000, accompanies Geoscience BC Report 2014-04, URL <[www.geosciencebc.com/i/project\\_data/GBCReport2014-04/Maps\\_by\\_GBC/TREK-1-4\\_500K\\_RMI.pdf](http://www.geosciencebc.com/i/project_data/GBCReport2014-04/Maps_by_GBC/TREK-1-4_500K_RMI.pdf)> [November 2014].
- Gordee, S.M., Andrews, G.D.M., Simpson, K. and Russell, J.K. (2007): Sub-aqueous, channel-confined volcanism: Bull Canyon Provincial Park, BC; *in* Geological Fieldwork 2006, BC Ministry of Energy and Mines, BC Geological Survey, Paper 2007-1 and Geoscience BC, Report 2007-1, p. 285–290, URL <<http://www.empr.gov.bc.ca/Mining/Geoscience/PublicationsCatalogue/Fieldwork/Documents/2006/28-Gordee.pdf>> [November 2014].
- Grainger, N.C., Villeneuve, M.E., Heaman, L.M. and Anderson, R.G. (2001): New U-Pb and Ar-Ar isotopic age constraints on the timing of Eocene magmatism, Fort Fraser and Nechako River map areas, central BC; *Canadian Journal of Earth Sciences*, v. 38, p. 679–696, URL <<http://www.nrcresearchpress.com/doi/pdf/10.1139/e00-093>> [November 2014].
- Haskin, M.L., Snyder, L.D. and Anderson, R.G. (1998): Tertiary Endako Group volcanic and sedimentary rocks at four sites in the Nechako River and Fort Fraser map area, central British Columbia; *in* Current Research 1998-A, Geological Survey of Canada, p. 155–164, URL <[http://ftp2.cits.rncan.gc.ca/pub/geott/ess\\_pubs/209/209427/cr\\_1998\\_ab.pdf](http://ftp2.cits.rncan.gc.ca/pub/geott/ess_pubs/209/209427/cr_1998_ab.pdf)> [November 2014].
- Henkel, H. (1991): Petrophysical properties (density and magnetization) of rocks from the northern part of the Baltic Shield; *Tectonophysics*, v. 192, p. 1–19, doi: 10.1016/0040-1951(91)90242-K [November 2014].
- Kim, R., Hart, C.J.R., Angen, J.J. and Westberg, E. (2015): Characterization of Late Cretaceous volcanic suites in the TREK Project Area, central British Columbia (NTS 093F, K); *in* Geoscience BC Summary of Activities 2014, Geoscience BC, Report 2015-1, p. 33–40.
- Kolofíková, O. (1976): Geological interpretation of measurements of magnetic properties of basalts on example of the Chřibský les lava flow of the Velký Roudný volcano (Nížký Jeseník, Mts.); *Časopis pro mineralogii a geologii*, v. 21, p. 387–396.
- Lee, M.D. and Morris, W.A. (2013): Comparison of magnetic-susceptibility meters using rocks samples from the Wopmay Orogen, Northwest Territories, Canada; *in* Geological Survey of Canada, Technical Note 5, 7 p., doi:10.4095/292739, URL <[http://publications.gc.ca/collections/collection\\_2013/rncan-rncan/M41-10-5-2013-eng.pdf](http://publications.gc.ca/collections/collection_2013/rncan-rncan/M41-10-5-2013-eng.pdf)> [November 2014].
- Mathews, W.H. (1964): Potassium–argon age determinations of Cenozoic volcanic rocks from British Columbia; *Geological Society of America Bulletin*, v. 75, p. 465–468, URL <<http://bulletin.geoscienceworld.org/content/75/5/465.full.pdf>> [November 2014].
- Mihalynuk, M.G. (2007): Neogene and Quaternary Chilcotin Group cover rocks in the Interior Plateau, south-central British Columbia: a preliminary 3-D thickness model; *in* Geological Fieldwork 2006, BC Ministry of Energy and Mines, BC Geological Survey, Paper 2007-1 and Geoscience BC, Report 2007-1, p. 143–148, URL <<http://www.em.gov.bc.ca/Mining/Geoscience/PublicationsCatalogue/Fieldwork/Documents/2006/15-Mihalynuk.pdf>> [November 2014].
- Mihalynuk, M.G., Peat, C.R., Terhune, K. and Orovan, E.A. (2008): Regional geology and resource potential of the Chezacut map area, central British Columbia (NTS 093C/08); *in* Geological Fieldwork 2007, BC Ministry of Energy and Mines, BC Geological Survey, Paper 2008-1 and Geoscience BC, Report 2008-1, p. 117–134, URL <<http://www.empr.gov.bc.ca/Mining/Geoscience/PublicationsCatalogue/Fieldwork/Documents/2007/13-Mihalynuk-Chezacut34526.pdf>> [November 2014].
- Resnick, J., Anderson, R.G., Russell, J.K., Edwards, B.R. and Grainger, N.C. (1999): Neogene basaltic flow rocks, xenoliths, and related diabase, northern Nechako River map area, central British Columbia; *in* Current Research 1999-A, Geological Survey of Canada, p. 157–167, URL <[http://ftp2.cits.rncan.gc.ca/pub/geott/ess\\_pubs/210/210136/cr\\_1999\\_ab.pdf](http://ftp2.cits.rncan.gc.ca/pub/geott/ess_pubs/210/210136/cr_1999_ab.pdf)> [November 2014].
- Riddell, J.M. (2011): Lithostratigraphic and tectonic framework of Jurassic and Cretaceous Intermontane sedimentary basins of south-central British Columbia; *Canadian Journal of Earth Sciences*, v. 48, p. 870–896, URL <<http://www.nrcresearchpress.com/doi/pdf/10.1139/e11-034>> [November 2014].
- Rouse, G.E. and Mathews, W.H. (1988): Palynology and geochronology of Eocene beds from Cheslatta Falls and Nazko areas, central British Columbia; *Canadian Journal of Earth Sciences*, v. 25, p. 1268–1276, URL <<http://www.nrcresearchpress.com/doi/pdf/10.1139/e88-122>> [November 2014].
- Stevens, R.D., Delabio, R.N. and Lachance, G.R. (1982): Age determinations and geological studies, K–Ar isotopic ages: Report 15; Geological Survey of Canada, Paper 81-2, 56 p.
- Struik, L.C. (1993): Intersecting intracontinental Tertiary transform fault systems in the North American Cordillera; *Canadian Journal of Earth Sciences*, v. 30, p. 1262–1274, URL <<http://www.nrcresearchpress.com/doi/pdf/10.1139/e93-108>> [November 2014].
- Struik, L.C. and MacIntyre, G. (2001): Introduction to the special issue of *Canadian Journal of Earth Sciences*: the Nechako NATMAP project of the central Canadian Cordillera; *Canadian Journal of Earth Sciences*, v. 38, p. 485–494, URL <<http://www.nrcresearchpress.com/doi/pdf/10.1139/e01-019>> [November 2014].
- Struik, L.C., Anderson, R.G. and Plouffe, A. (1999): Geology of the Eucheniko map area, central British Columbia; *in* Current Research 1999-A, Geological Survey of Canada, p. 119–128, URL <[http://ftp2.cits.rncan.gc.ca/pub/geott/ess\\_pubs/210/210136/cr\\_1999\\_ab.pdf](http://ftp2.cits.rncan.gc.ca/pub/geott/ess_pubs/210/210136/cr_1999_ab.pdf)> [November 2014].
- Terraplus Inc. (2013): KT-10 v2 and KT-10R v2 magnetic susceptibility meters; Terraplus Inc., website, URL <<http://www.terraplus.ca/products/pdf/KT-10.pdf>> [November 2014].
- Thomas, M.D. and Pilkington, M. (2008): New high-resolution aeromagnetic data: a new perspective on geology of the Bonaparte Lake map area, British Columbia; Geological Survey of Canada, Open File 5743, 3 Sheets, URL <<http://geoscan.rncan.gc.ca/starweb/geoscan/servlet.starweb?path=geoscan/download.web&search1=R=224676>> [November 2014].
- Thomas, M.D., Pilkington, M. and Anderson, R.G. (2011): Geological significance of high resolution magnetic data in the

- Quesnel terrane, Central British Columbia; Canadian Journal of Earth Sciences, v. 48, p. 1065–1089, doi:10.1139/e10-109, URL <<http://www.nrcresearchpress.com/doi/pdf/10.1139/e10-109>> [November 2014].
- Tipper, H.W. (1963): Nechako River map area, British Columbia; Geological Survey of Canada, Memoir 324, 59 p.
- Tipper, H.W. (1969): Anahim Lake, British Columbia; Geological Survey of Canada, Map 1202A, scale 1:253 440 <[http://ftp2.cits.rncan.gc.ca/pub/geott/ess\\_pubs/109/109116/gscmap-a\\_1202a\\_e\\_1969\\_mn01.pdf](http://ftp2.cits.rncan.gc.ca/pub/geott/ess_pubs/109/109116/gscmap-a_1202a_e_1969_mn01.pdf)> [November 2014].
- Tipper, H.W. and Richards, T.A. (1976): Jurassic stratigraphy and history of north-central British Columbia; Geological Survey of Canada, Bulletin 270, 73 p., URL <[http://ftp2.cits.rncan.gc.ca/pub/geott/ess\\_pubs/103/103065/bu\\_270.zip](http://ftp2.cits.rncan.gc.ca/pub/geott/ess_pubs/103/103065/bu_270.zip)> [November 2014].



## Characterization of Late Cretaceous Volcanic Suites in the TREK Project Area, Central British Columbia (NTS 093F, K)

**R. Kim**, Mineral Deposit Research Unit, University of British Columbia, Vancouver, BC, [rsykim@eos.ubc.ca](mailto:rsykim@eos.ubc.ca)

**C.J.R. Hart**, Mineral Deposit Research Unit, University of British Columbia, Vancouver, BC

**J.J. Angen**, Mineral Deposit Research Unit, University of British Columbia, Vancouver, BC

**E. Westberg**, Consulting Geologist, Calgary, AB

---

Kim, R., Hart, C.J.R., Angen, J.J. and Westberg, E. (2015): Characterization of Late Cretaceous volcanic suites in the TREK project area, central British Columbia (NTS 093F, K); *in* Geoscience BC Summary of Activities 2014, Geoscience BC, Report 2015-1, p. 33–40.

### Introduction

With the discovery of the large gold resource at the Blackwater deposit of 344 Mt grading 0.74 g/t Au, 5.5 g/t Ag (10 million oz., Christie et al., 2014), volcanic rocks of the associated Kasalka Group have increasingly been recognized as an important exploration target. However, these rocks are not well understood or represented on geological maps as they are poorly exposed over much of the northern Interior Plateau region in central BC. Moreover, they share similar lithological features to older Jurassic and younger Eocene volcanic rocks, making them difficult to confidently identify.

In order to provide increased knowledge about these important rocks, Geoscience BC, in partnership with the Mineral Deposit Research Unit at the University of British Columbia, is undertaking the TREK (Targeting Resources for Exploration and Knowledge) project. The TREK project was developed to increase the geological knowledge about controls on mineralization in this important area, and as an initiative to promote exploration in central BC, by combining surficial, bedrock and geophysical data (Clifford and Hart, 2014).

The focus of this research subproject is to characterize the Kasalka Group, and to identify those features that allow for differentiation of Late Cretaceous volcanic rocks from similar looking Jurassic and Eocene volcanic suites in and around the TREK project area. Previous workers have, for example, indicated that the presence of hornblende is a defining feature of Kasalka Group rocks (Anderson et al., 1999). As such, distinguishing stratigraphic and lithological features, textures and mineralogical components in these volcanic rocks is a goal, in addition to providing constraints from geochronology, geochemistry and physical

properties. Because the region benefits from excellent aeromagnetic coverage (Aeroquest Airborne Ltd. 2014), the project will also utilize the magnetic characteristics of the various volcanic rock packages.

Fieldwork was conducted in the northern half of the TREK project area and also the surrounding area during July and August 2014. Bedrock mapping at the 1:50 000 scale and sample collection were facilitated by logging road and foot access, and concentrated on the area covered by NTS 093F, K map sheets. Field observations and data presented here are primarily from the area south of Vanderhoof, Fraser Lake and Burns Lake and around eastern François Lake (Figure 1). Hand specimens were collected from outcrops for the purpose of geochemical and petrographic analysis. Large rock samples (~20 kg) were collected for geochronology analysis; U-Pb zircon, Ar-Ar hornblende and biotite dating methods will be used on these samples. Selected MINFILE (BC Geological Survey, 2014) locations within the study area were also investigated, and assay samples were taken from these localities.

### Previous Work

The wider region benefits from the extensive ongoing regional bedrock mapping as well as the more focused topical studies conducted in the TREK area. The Interior Plateau project, which was initiated in 1992, was conducted under the auspices of the Canada–British Columbia Mineral Development Agreement (1991–1995), and involved geoscientists from the BC Geological Survey and Geological Survey of Canada (Diakow and Levson 1997). More recent regional mapping projects were conducted in the northern part of the TREK area from 1995 to 2000 as part of the Nechako NATMAP project, which was initiated to further improve bedrock and surficial data for central BC (MacIntyre and Struik, 2000). Regional 1:50 000 scale bedrock mapping of the Fawnie and Nechako ranges, now the central area of the TREK project, was conducted between 1992 and 1994 and compiled at the 1:100 000 scale (Diakow and Levson, 1997).

---

**Keywords:** *Kasalka Group, volcanic suites, geochronology, TREK*

*This publication is also available, free of charge, as colour digital files in Adobe Acrobat® PDF format from the Geoscience BC website: <http://www.geosciencebc.com/s/DataReleases.asp>.*

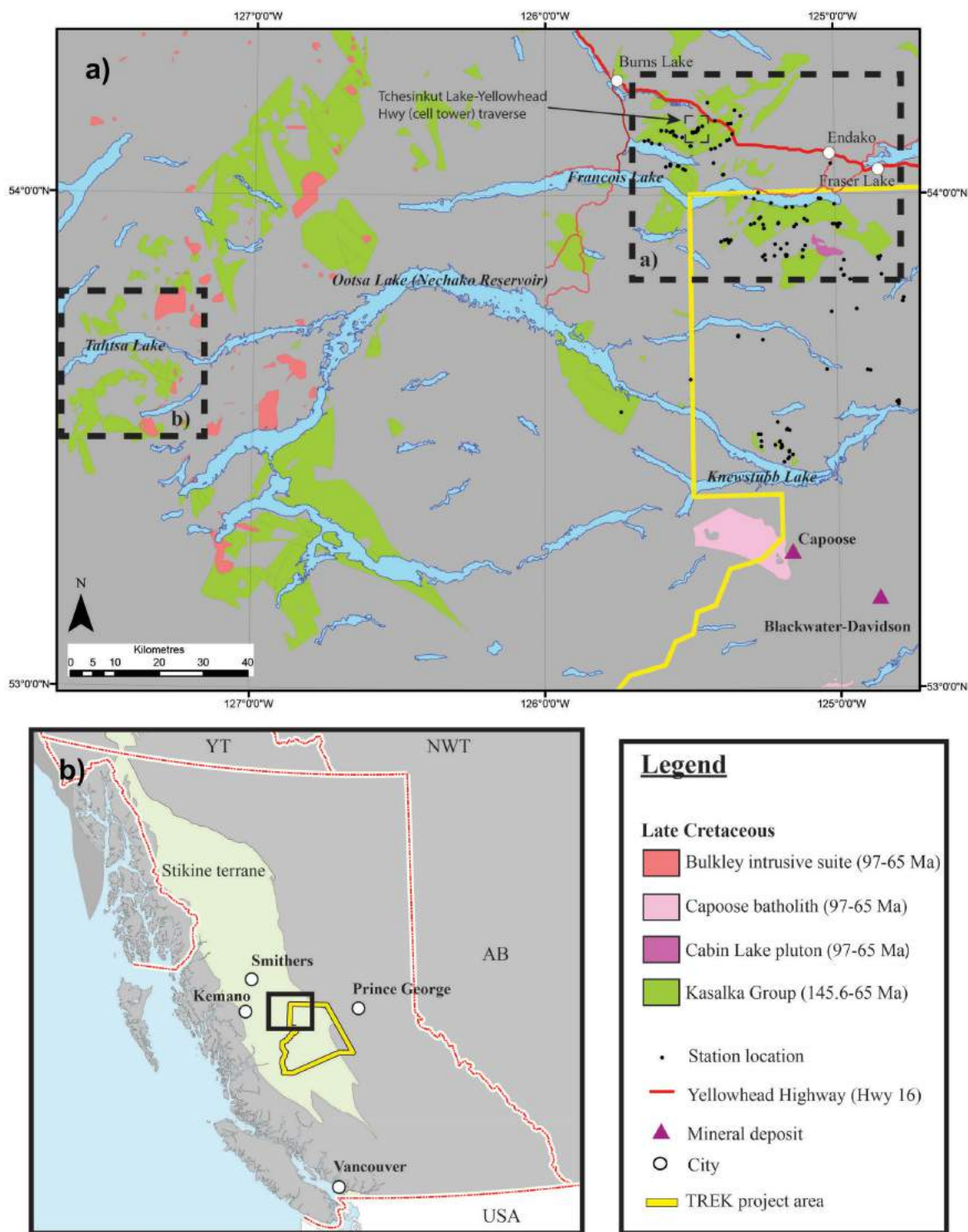


**Figure 1.** Location map for study area with respect to local communities and the Targeting Resources for Exploration and Knowledge (TREK) project area, central British Columbia: **a)** 2014 study area; station localities from field visits are shown as small black dots; **b)** Tahtsa Lake map area, locality for the Kasalka Group type section (MacIntyre, 1977).

## Regional Geology

### Tectonic Framework

British Columbia is dominantly composed of tectonic blocks that were accreted onto the western margin of the ancestral North America continent through the Mesozoic. Much of central BC is underlain by the Intermontane terrane, which is composed of the amalgamated Stikine, Cache Creek and Quesnel terranes (Monger and Price, 2002). The Stikine and Quesnel terranes formed as oceanic island volcanic arcs, with similar compositions and stratigraphy. The two terranes may have been part of the same Late Triassic arc that enclosed the Cache Creek terrane during accretion onto the continental margin (Mihalynuk et al., 1994). The Mesozoic volcano-sedimentary packages of Stikinia form the basement rocks in the study area, and are composed of Late Triassic to Middle Jurassic arc volcanic rocks and their erosional products. Overlapping basinal assemblages of the Bowser Lake Group record marine deposition from Upper Jurassic until the mid-Cretaceous, with subsequent deposition of the Skeena Group in the Early Cretaceous (Riddell, 2011). Postdeformation, continental margin arcs were unconformably deposited episodically during the Late Cretaceous to the Eocene and produced the Kasalka, Ootsa Lake and Endako groups of volcanic strata (Evenchick, 1991). Miocene volcanism produced the Chilcotin flood basalts, which overlie older units (Mathews, 1989).

### Kasalka Group

Rocks attributed to the Late Cretaceous Kasalka Group have a wide distribution from Kemano, in coastal BC, and as far north as Smithers, BC. The Kasalka Group was first described by MacIntyre (1977), west of the TREK project area, in the Whitesail Lake map area (NTS 093E) of west-central BC; a generalized stratigraphic section is shown in Figure 2. Previously, these rocks have been interpreted to be either Jurassic andesite or younger Eocene felsic rocks. The Kasalka Group is described to have an angular unconformity of basal conglomerate overlying deformed older rocks. The conglomerate is unconformably overlain by thick packages of andesite flows and volcanoclastic rocks. The youngest members of the Kasalka Group consist of rhyolitic flows that unconformably overlie the andesite and volcanic rocks (MacIntyre, 1977, 1985).

Other volcanic rock units with Late Cretaceous age constraints are variably considered to be equivalent to the Kasalka Group. Most notably, the Tip Top Hill volcanic suite located near Smithers, northwest of the study area, has been interpreted to be part of a similar Late Cretaceous package (Church and Barakso, 1990).

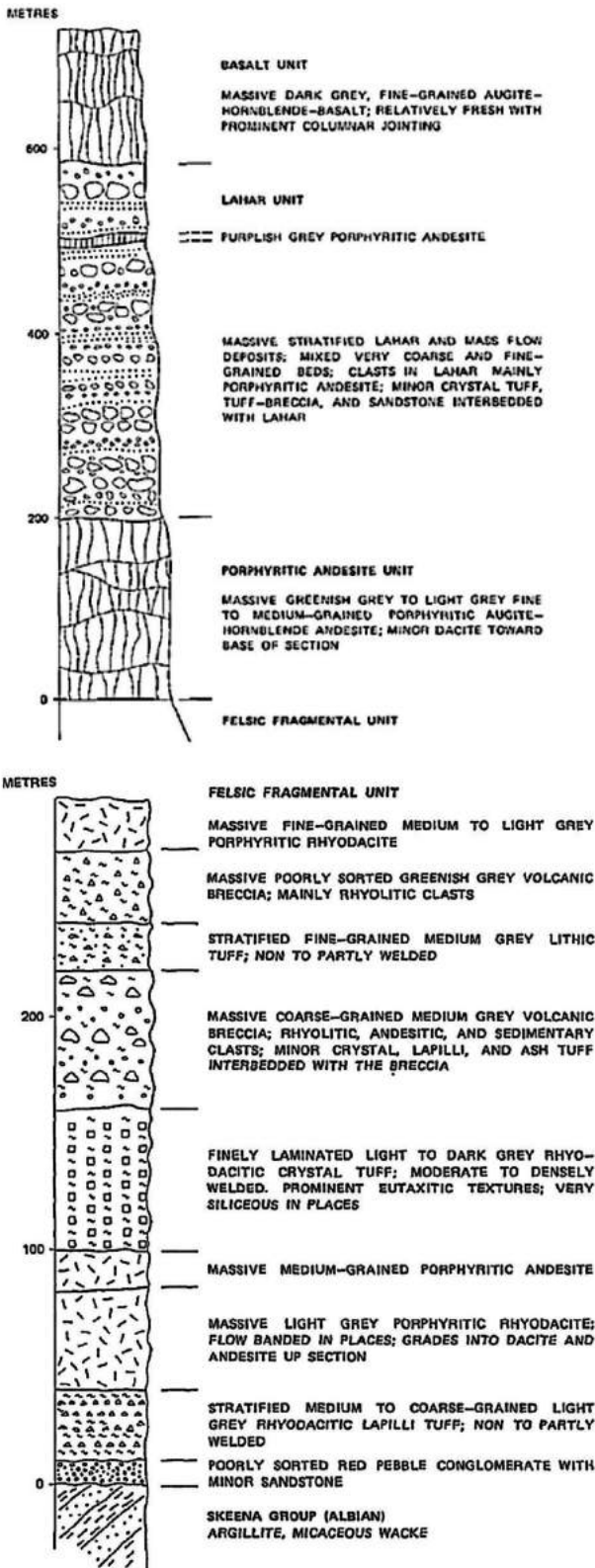


Figure 2. Stratigraphic type section of the Kasalka Group, central British Columbia (from MacIntyre, 1977, 1985).

Kasalka Group volcanic rocks host or are directly associated with several mineral deposits, including the large Blackwater epithermal style Au-Ag deposit (Christie, et al., 2014). The Capoose Au-Ag deposit ~100 km south of Fraser Lake is hosted in similar rock types of comparable age (Diakow et al., 1997). The Newton deposit, located ~175 km southeast of the Blackwater deposit, is also hosted in Late Cretaceous felsic fragmental volcanic rocks (McClenaghan, 2013) and likely represents the most southerly occurrence. Lithologically similar rocks also host the Silver Queen epithermal Au-Ag-Zn-Pb deposit (Leitch et al., 1991).

From field observations, contacts between the various Kasalka Group units described across the study area are inferred to follow a generally northwest trend. The map patterns these interpretations are based on are from past British Columbia Geological Survey (BCGS) publications of the region. Field observations incorporated with data from previous studies are included in the following descriptions of stratigraphic units of the Kasalka Group.

### **Conglomerate**

The conglomerate is composed of a polymictic, poorly sorted, boulder-to-cobble, clast-supported package (Figure 3a). Exposures are found north and south of François Lake and trend northwest over approximately 28 km. Outcrops have an overall low profile, with greater topographic relief observed toward the northwest. This unit is readily identified by the weathering contrast between the clasts and matrix. Cobble-sized clasts (5–10 cm diameter) are well rounded, with the majority of clasts consisting of fine-grained green and maroon volcanic suites and flow-banded rhyolite. Less common are pebble-sized clasts (0.5–5 cm diameter) of black to dark grey chert and siltstone, granite to granodiorite/monzonite, and polymictic pebble conglomerate.

Two matrix compositions are observed in the conglomerate. The first is volcanic in origin, similar in composition to the green and maroon clasts. The second type is sedimentary, dominantly dark red quartz-feldspar sand matrix (MacIntyre, 1977) with green-grey silica. At one locality a dark red quartz-feldspar sandstone lens is found to be interleaved within the conglomerate. This sandstone is the same composition as the sedimentary matrix. The conglomerate is described as forming the base of the Kasalka Group, which unconformably overlies the Jurassic Hazelton and Middle Cretaceous Skeena groups (Leitch et al., 1991; Diakow et al., 1997). Contacts with other units were not observed; however, outcrops are located stratigraphically and topographically lower than andesite and rhyolite outcrops. Detrital zircon ages will further constrain the ages of this unit.

### **Andesite Flows**

Andesite flows are the largest unit of the Kasalka Group, and unconformably overlie the basal conglomerate (MacIntyre, 1977). Outcrops are found along a similar north-northwest trend from Burns Lake to Knewstubb Lake, a distance of ~83 km. The andesite to dacite flows are similar in appearance to U-Pb and K-Ar dated Late Cretaceous samples (Friedman et al., 2001). The weathering profile ranges from pale grey-brown to grey-purple. The fresh surfaces of these andesite flows are variable, generally green or grey to maroon/purple (Figure 3b). The plagioclase and hornblende phenocrysts (overall 10–20% each, 1–3 mm in length) are ubiquitous, and can give the unit a porphyritic texture.

The andesite flows are largely coherent, but fragmental assemblages are also observed where segments of the flow are suspended in a matrix of the same andesite flow. The uniformity of these fragmented sections suggests they are either volcanic debris or reworked sections of these flows (MacIntyre, 1977).

### **Rhyolite**

Outcrops of rhyolitic ash to crystal tuff of the Kasalka Group are located south of the eastern half of François Lake, within the François Lake Provincial Park. This unit consists of whitish-pink to grey weathering surfaces, on low profile outcrops and rubble piles. Fresh surfaces are light pink-grey to bright pink, with a fine-grained matrix, and chalky green lithic fragments of altered green pumice (0.3–2 cm) making up ~15% of the unit (Figure 3c).

### **Tchesinkut Lake–Yellowhead Highway (Cell Tower) Traverse**

A traverse was carried out approximately 8 km southeast of the town of Burns Lake (Figure 1), along a forest service road (accessible from the Yellowhead Highway) that leads to a radio reception tower. Along this road there are a number of outcrops that show a stratigraphic succession moving uphill. This traverse consists of a relatively undeformed, subhorizontal to gently northwest-dipping succession of units, beginning with a basal conglomerate that is subsequently overlain by andesite and rhyolite flows, and lahar deposits. The succession is capped by dark black basalt that is lithologically similar to the Chilcotin Group. Given that the stratigraphy is intact, this traverse crosses through at the lowermost stratigraphy of the Kasalka Group. A plagioclase dacite sample previously taken for geochronology near the tower location returned an igneous crystallization age of  $74.2 \pm 0.3$  Ma (Grainger, 2000). Lithological similarities from these outcrops can be correlated to the Kasalka Group type section described by MacIntyre (1985) and shown in Figure 2.



**Figure 3.** Kasalka(?) Group members, central British Columbia: **a)** basal conglomerate; **b)** andesite flows; **c)** pink rhyolite tuff with altered pumice clasts; **d)** flow-banded rhyolite.

### Previous Geochronology

Previous geochronological studies of Cretaceous and Jurassic rocks were conducted in conjunction with the Nechako National Geoscience Mapping Program (NATMAP) project (Friedman et al., 2001; Grainger et al., 2001). These studies were constrained to the Ootsa Lake, western François Lake and Fawnie Range areas. Rocks from the Blackwater-Davidson deposit returned ca. 70 Ma mineralization ages (K-Ar whole rock), which are similar to those from the Capoose prospect and suggest that mineralization was Late Cretaceous and related to continental-arc magmatism (Friedman et al., 2001). Late Cretaceous U-Pb dates (75–67 Ma; 72–70 Ma) were more recently reported near Ootsa Lake and François Lake (Ferbey and Diakow, 2012) on rocks previously mapped as Eocene. At the Blackwater-Davidson deposit, U-Pb ages between 74 and 72 Ma are reported for the host Kasalka Group (Christie et al., 2014). At the Silver Queen deposit, 75 km northeast of Tahtsa Lake, the Kasalka Group rocks returned K-Ar whole rock ages from 105 Ma to 78 Ma (Leitch et al., 1991). The Newton deposit in the Chilcotin Plateau is also hosted in

similar Late Cretaceous rocks with U-Pb ages between 72 and 70 Ma (McClenaghan, 2013).

### Discussion

The characteristics of volcanic rocks and suites in the northern TREK project area that are presented herein were documented by field observations. Geochemical, petrographic and geochronological analysis will be used to understand similarities and differences between these similar-looking units of Eocene, Cretaceous and Jurassic age. Late Cretaceous Kasalka Group rocks have been found proximal to, and hosting, the Blackwater-Davidson deposit and Capoose prospect (Friedman et al., 2001; Diakow, 2012 and Christie et al., 2014). Exposures of Kasalka Group rocks near Ootsa and François Lake (Ferbey and Diakow, 2012) have been dated using U-Pb geochronology; however, the distribution of these Late Cretaceous rocks in the TREK area is otherwise poorly constrained due to the lack of defining characteristics to distinguish them from other volcanic packages. Kasalka Group exposures are interpreted

dominantly as andesite to rhyolite, with sparse basal conglomerate exposures.

The stratigraphic succession at the Tchesinkut Lake radio tower from this study utilizes the Kasalka Group type-sections developed by MacIntyre (1985). Compared to the type-section, the radio tower traverse consists of the lower and uppermost portions of the type-section, similar to those described at Mont Baptiste (MacIntyre, 1985). A large portion of the type-section is composed of rhyodacite, lahar deposits and volcanic breccia, and was not observed along this traverse. In other parts of the study area, rhyodacite and rhyolitic volcanic breccia units are observed, but with little stratigraphic context.

The presence of hornblende phenocrysts was suggested by Anderson et al. (1999) as a common feature in Late Cretaceous fragmental volcanic rocks of the Knapp Lake area, 20 km south of François Lake. Hornblende phenocrysts were observed in this study, mainly in the andesitic volcanic rocks and intrusive suites and as such, are tentatively interpreted to be Late Cretaceous. However, the presence of hornblende phenocrysts is not pervasive across previously mapped Kasalka Group rocks, and as such this mineral may not be entirely reliable as a distinguishing feature. Hornblende phenocrysts also appear as components in the late Jurassic Bowser Lake Group (Nechako) volcanic rocks (Diakow et al., 1997) and are lithologically difficult to differentiate from Kasalka Group volcanic rocks. Evaluation of these rock types and hornblende phenocrysts by petrographic and geochemical methods may provide further constraints on the characteristics of the Kasalka Group volcanic rocks.

Furthermore, the age distribution of the Kasalka Group is broad and variable. Reported ages ranging from 105 to 75 Ma (MacIntyre, 1988) suggest that the Kasalka Group ranges from mid to latest Cretaceous in age, while Late Cretaceous ages have been reported for rocks that were previously mapped as Jurassic and Eocene (Friedman et al., 2001). Improved lithological and age constraints on the Late Cretaceous volcanic suites will provide improved regional context and discriminate potential regions that may be more prospective for precious-metal mineralization. Further work will include detailed characterization of samples using geochronology, petrology and geochemical analyses. Correlations between geochemical and petrographic observations will be made in order to determine characterizing features at the macro and microscopic scales. The age and stratigraphy of the Kasalka Group units will also be constrained with U-Pb and Ar-Ar dating.

## Acknowledgments

Geoscience BC is thanked for funding, and for making this project possible. The authors would also like to thank A. Toma, S. Jenkins and C. Marr, Mineral Deposit Research

Unit, for their patience and for providing logistical support for various parts of the project. The thoughtful review of this manuscript provided by L. Bickerton is gratefully acknowledged.

## References

- Aeroquest Airborne Ltd.(2014): Fixed wing magnetic geophysical survey, TREK project, Interior Plateau/Nechako Region, British Columbia; Geoscience BC, Report 2014-04, 40 p., URL <<http://www.geosciencebc.com/s/Report2014-04.asp>> [November 2014].
- Anderson, R.G., Snyder, L.D., Grainger, N.C., Resnick, J., Barnes, E.M. and Pint, C.D. (2000): Mesozoic geology of the Takysie Lake and Marilla map areas, central British Columbia; Geological Survey of Canada, Current Research 2000-A12, 11 p., URL <[http://ftp2.cits.mcan.gc.ca/pub/geot/ess\\_pubs/211/211182/cr\\_2000\\_a12.pdf](http://ftp2.cits.mcan.gc.ca/pub/geot/ess_pubs/211/211182/cr_2000_a12.pdf)> [November 2014].
- Anderson, R.G., Snyder, L.D., Resnik, J., Grainger, N.C. and Barnes, E.M. (1999): Bedrock geology of the Knapp Lake map area, central British Columbia; *in* Geological Survey of Canada, Current Research 1999-A, p. 109–118., URL <<http://www.em.gov.bc.ca/MINING/GEOSCIENCE/PUBLICATIONSCATALOGUE/OPENFILES/2007/2007-10/PAPERS/CURRENTRESEARCH/Pages/ar991.aspx>> [November 2014].
- BC Geological Survey (2014): MINFILE BC mineral deposits database; BC Ministry of Energy and Mines, BC Geological Survey, URL <<http://www.minfile.ca/>> [August 2014].
- Christie, G., Lipiec, I., Simpson, R.G., Horton, J. and Bromtraeger B. (2014): Blackwater gold project British Columbia: NI 43-101 technical report on feasibility study; New Gold Inc., 2014, 336 p., URL <[http://www.newgold.com/files/documents\\_properties/blackwater/Blackwater%20Gold%20Project%20Technical%20Report%20January%2014%202014.pdf](http://www.newgold.com/files/documents_properties/blackwater/Blackwater%20Gold%20Project%20Technical%20Report%20January%2014%202014.pdf)> [November 2014].
- Church, B.N. and Barakso, J.J. (1990): Geology, litho-geochemistry and mineralization in the Buck Creek area, British Columbia (93L); *in* Paper 1990-2, BC Ministry of Energy and Mines, BC Geological Survey, 81 p., URL <[http://www.empr.gov.bc.ca/Mining/Geoscience/Publications/Catalogue/Papers/Documents/P1990-02\\_Buck\\_Ck.pdf](http://www.empr.gov.bc.ca/Mining/Geoscience/Publications/Catalogue/Papers/Documents/P1990-02_Buck_Ck.pdf)> [October 2014].
- Clifford, A. and Hart, C.J.R. (2014): Targeting Resources through Exploration and Knowledge (TREK): Geoscience BC's newest minerals project, Interior Plateau region, central British Columbia (NTS 093B, C, F, G); *in* Geoscience BC Summary of Activities 2013, Geoscience BC, Report 2014-1, p. 13–18, URL <[http://www.geosciencebc.com/i/pdf/SummaryofActivities2013/SoA2013\\_CliffordHart.pdf](http://www.geosciencebc.com/i/pdf/SummaryofActivities2013/SoA2013_CliffordHart.pdf)> [November 2014].
- Diakow, L.J. and V.M. Levson (1997): Bedrock and surficial geology of the southern Nechako Plateau, central British Columbia; BC Ministry of Energy and Mines, BC Geological Survey, Geoscience Map 1997-2, scale 1:100 000, URL <<http://www.empr.gov.bc.ca/Mining/Geoscience/PublicationsCatalogue/Maps/GeoscienceMaps/Documents/GM1997-02.pdf>> [November 2014].
- Diakow, L.J., Webster, I.C.L., Richards, T.A. and Tipper H.W. (1997): Geology of the Fawnie and Nechako ranges, southern Nechako Plateau, central British Columbia (98F/2, 3, 6, 7); *in* Interior Plateau Geoscience Project: Summary of Geo-

- logical, Geochemical and Geophysical Studies, L.J. Diakow, J.M. Newell and P. Metcalfe (ed.), BC Ministry of Energy and Mines, BC Geological Survey, Paper 1997-2, p. 7–3, URL <[http://ftp2.cits.rncan.gc.ca/pub/geott/ess\\_pubs/208/208972/of\\_3448.pdf](http://ftp2.cits.rncan.gc.ca/pub/geott/ess_pubs/208/208972/of_3448.pdf)> [November 2014].
- Evenchick, C.A. (1991): Geometry, evolution and tectonic framework of the Skeena fold belt, north central British Columbia; *Tectonics*, v. 10, p. 527–546, URL <<http://onlinelibrary.wiley.com/doi/10.1029/90TC02680/pdf>> [October 2014].
- Ferbey, T. and Diakow, L.D. (2012): U-Pb Isotopic ages from volcanic rocks near Ootsa Lake and François Lake, west-central British Columbia; *in* Geological Fieldwork 2011, BC Ministry of Energy and Mines, BC Geological Survey, Paper 2012-1, p. 149–156, URL <[http://www.empr.gov.bc.ca/Mining/Geoscience/PublicationsCatalogue/Fieldwork/Documents/2011/11\\_Ferbey\\_2011.pdf](http://www.empr.gov.bc.ca/Mining/Geoscience/PublicationsCatalogue/Fieldwork/Documents/2011/11_Ferbey_2011.pdf)> [October 2014].
- Friedman, R.M., Diakow, L.J., Lane, R.A. and Mortensen, J.K. (2001): New U-Pb age constraints on latest Cretaceous magmatism and associated mineralization in the Fawnie Range, Nechako Plateau, central British Columbia; *Canadian Journal of Earth Sciences*, v. 38, p. 619–637, URL <<http://www.nrcresearchpress.com/doi/pdf/10.1139/e00-122>> [November 2014].
- Grainger, N. (2000): Petrogenesis of Middle Jurassic to Miocene magmatism within the Nechako Plateau, central British Columbia: insight from petrography, geochemistry, geochronology and tracer isotope studies; University of Alberta, M.Sc. thesis, 138 p.
- Grainger, N.C., Villeneuve, M.E., Heaman, L.M. and Anderson, R.G. (2001): New U-Pb and Ar/Ar isotopic age constraints on the timing of Eocene magmatism, Fort Fraser and Nechako River map areas, central British Columbia; *Canadian Journal of Earth Sciences*, v. 38, p. 679–696, URL <<http://www.nrcresearchpress.com/doi/pdf/10.1139/e00-093>> [October 2014].
- Leitch, C.H.B., Hood, C.T., Cheng, X.-L. and Sinclair, A.J. (1991): Tip Top Hill volcanics: Late Cretaceous Kasalka Group rocks hosting Eocene epithermal base- and precious-metal veins at Owen Lake, west-central British Columbia; *in* *Canadian Journal of Earth Sciences*, v. 29, p. 854–864, URL <<http://www.nrcresearchpress.com/doi/citedby/10.1139/e92-073#.VFgHQvnF9DA>> [October 2014].
- MacIntyre, D.G. (1977): Evolution of upper Cretaceous volcanic and plutonic centres and associated porphyry copper occurrences Tahtsa Lake area, British Columbia; University of Western Ontario, Ph.D. thesis, 216 p.
- MacIntyre, D.G. (1985): Geology and mineral deposits of the Tahtsa Lake District, west-central British Columbia; BC Ministry of Energy and Mines, BC Geological Survey, Bulletin 75, URL <<http://www.empr.gov.bc.ca/Mining/Geoscience/PublicationsCatalogue/BulletinInformation/BulletinsAfter1940/Documents/Bull75.pdf>> [November 2014].
- Mathews, W.H. (1989): Neogene Chilcotin basalts in south-central British Columbia: geology, ages and geomorphic history; *Canadian Journal of Earth Sciences*, v. 26, p. 969–982, URL <<http://www.nrcresearchpress.com/doi/pdf/10.1139/e89-078>> [October 2014].
- McClenaghan, L. (2013): Geology and genesis of the Newton bulk-tonnage gold-silver deposit, central British Columbia; University of British Columbia, M.Sc. thesis, 205 p., URL <[https://circle.ubc.ca/bitstream/handle/2429/44008/ubc\\_2013\\_spring\\_mcclenaghan\\_lindsay.pdf?sequence=1](https://circle.ubc.ca/bitstream/handle/2429/44008/ubc_2013_spring_mcclenaghan_lindsay.pdf?sequence=1)> [November 2014].
- Mihalnyuk, M.G., Nelson, J. and Diakow, L.J. (1994): Cache Creek terrane entrapment: oroclinal paradox within the Canadian Cordillera; *Tectonics*, v. 13, no. 2, p. 575–595, URL <<http://www.empr.gov.bc.ca/Mining/Geoscience/Staff/Documents/MihalynuketAll1994.pdf>> [November 2014].
- Monger, J. and Price, R. (2002): The Canadian Cordillera: geology and tectonic evolution; *Canadian Society of Exploration Geophysicists Recorder* v. 27, no. 2, p. 17–36, URL <[http://geosolutionsauthority.com/download/esfs\\_educator\\_resource\\_compilation/from\\_kamloops\\_exploration\\_group\\_-\\_keg/geology/feb02\\_02-cordillera.pdf](http://geosolutionsauthority.com/download/esfs_educator_resource_compilation/from_kamloops_exploration_group_-_keg/geology/feb02_02-cordillera.pdf)> [November 2014].
- Pint, C.D., Anderson, R.G. and Mahoney, J.B. (2000): Stratigraphy and structures within the Lower to Middle Jurassic Hazelton Group, Takysie Lake and Marilla map areas, central British Columbia; Geological Survey of Canada, Current Research 2000-A11, 9 p., URL <[http://ftp2.cits.rncan.gc.ca/pub/geott/ess\\_pubs/211/211137/cr\\_2000\\_a11.pdf](http://ftp2.cits.rncan.gc.ca/pub/geott/ess_pubs/211/211137/cr_2000_a11.pdf)> [October 2014].
- Riddell, J. (2011): Lithostratigraphic and tectonic framework of Jurassic and Cretaceous Intermontane sedimentary basins of south-central British Columbia; *Canadian Journal of Earth Sciences*, v. 48, p. 870–896, URL <<http://www.nrcresearchpress.com/doi/pdf/10.1139/e11-034>> [October 2014].
- Struik, L.C. and MacIntyre, D.G. (2000): Nechako NATMAP project overview, year five, central British Columbia; Geological Survey of Canada, Current Research 2000-A10, 10 p., URL <<http://www.empr.gov.bc.ca/MINING/GEOSCIENCE/PUBLICATIONSCATALOGUE/OPENFILES/2007/2007-10/PAPERS/CURRENTRESEARCH/Pages/sl001.aspx>> [November 2014].
- Struik, L.C. and MacIntyre, D.G. (2001): Introduction to the special issue of *Canadian Journal of Earth Sciences*: the Nechako NATMAP project of the central Canadian Cordillera; *Canadian Journal of Earth Sciences*, v. 38, p. 485–494, URL <<http://cjes.geoscienceworld.org/content/38/4/485.full.pdf+html>> [November 2014].
- Tipper, H.W. and Richards, T.A. (1976): Jurassic stratigraphy and history of north-central British Columbia; Geological Survey of Canada, Bulletin 270, 73 p., URL <<http://geoscan.nrcan.gc.ca/starweb/geoscan/servlet.starweb?path=geoscan/download.web&search1=R=103065>> [November 2014].



# Catchment Analysis Applied to the Interpretation of New Stream Sediment Data from Northern Vancouver Island, British Columbia (NTS 102I, 092L)

D.C. Arne, CSA Global, Vancouver, BC, dennis.arne@csaglobal.com

O. Brown, CSA Global, Vancouver, BC

---

Arne, D.C. and Brown, O. (2015): Catchment analysis applied to the interpretation of new stream sediment data from northern Vancouver Island, British Columbia (NTS 102I, 092L); in Geoscience BC Summary of Activities 2014, Geoscience BC, Report 2015-1, p. 41–46.

## Introduction

For many years, Geoscience BC has been engaged in the reanalysis of archived Regional Geochemical Survey (RGS) sample material, as well as in the collection of new samples to cover areas where historical sample coverage was not adequate. A number of projects in the past have examined ways to add value to these new regional geochemistry datasets, including the use of catchment analysis to level the geochemical data for dominant bedrock types in the catchments, and to assess whether the catchment areas used for sampling were appropriate. Arne and Bluemel (2011) is an example of a project using a catchment analysis approach previously sponsored by Geoscience BC with the then newly acquired QUEST-South stream sediment geochemical data. A summary of the approach used can be found in that paper. Such approaches are designed to identify second- and third-order geochemical anomalies often overlooked during a routine analysis of the data by accounting for the effects of metal scavenging by secondary Fe and Mn oxides, as well as variable background levels for important pathfinder elements due to the exposure of different bedrock types in catchment basins. In this way, the analysis adds value to the existing datasets by providing additional information not readily available to most prospectors and geologists working for small exploration companies.

The approach to catchment analysis proposed herein is aligned with the concept of productivity described by Hawkes (1976) and further expanded on by Pan and Harris (1990) and Moon (1999). Bonham-Carter and Goodfellow (1986) demonstrated that catchment lithology was the main control on observed variation in stream sediment data from the Nahanni region, Yukon. Other effects, such as catchment area, possible adsorption of some elements onto secondary Fe or Mn oxides, or onto organic material, and water pH were considered to be minor by comparison. A similar conclusion was reached by Carranza and Hale (1997) in a

study of the main controls on stream sediment geochemistry in the Philippines. Bonham-Carter et al. (1987) applied a similar approach to stream sediment data from the Cobequid Highlands of Nova Scotia and further concluded that use of the dominant rock type in the catchment basins was not as effective as taking into account the areal extent of all rock types in the catchment. One of the fundamental assumptions of these approaches is that similar erosion rates affect all lithological units, although this is unlikely to be the case in many instances, particularly in areas of variable relief.

The moss-mat stream sediment dataset selected for evaluation was assembled as part of the Northern Vancouver Island Exploration Geoscience project by Geoscience BC in co-operation with the Island Coastal Economic Trust. This project consisted of collecting new samples (Jackaman, 2013a) and reanalyzing historical RGS samples from the same area (Jackaman, 2011, 2014). The location of the study area, along with the distribution of sample points, is illustrated in Figure 1. Data from this terrain should be ideal for the automated generation of catchment basins. Raw Cu in the historical RGS dataset from Vancouver Island has previously been demonstrated to be a poor predictor of Cu mineralization within individual catchment basins due to the widespread distribution of mafic volcanic rocks in the region contributing to high background Cu levels (Sibbick, 1994).

This project will assess the impact of various approaches to estimating background geochemical levels for stream sediment (moss mat) samples from the northern Vancouver Island study area. New Cu anomalies should be apparent in the map products to be generated for this study once the effects of elevated background Cu have been addressed. Data for other elements important for mineral exploration that also show variable background levels related to bedrock geology (e.g., Ni and Ba), or tend to be easily adsorbed onto the surfaces of secondary Fe and Mn oxides in the stream sediments (e.g., Zn and As), will also be easier to interpret in terms of anomalies that might be related to unrecognized mineralization within the catchment basins. It is hoped that the release of these new map products will stimulate further mineral exploration in the study area.

---

**Keywords:** geochemistry, regional geochemical survey, RGS, catchment analysis

This publication is also available, free of charge, as colour digital files in Adobe Acrobat® PDF format from the Geoscience BC website: <http://www.geosciencebc.com/s/DataReleases.asp>.

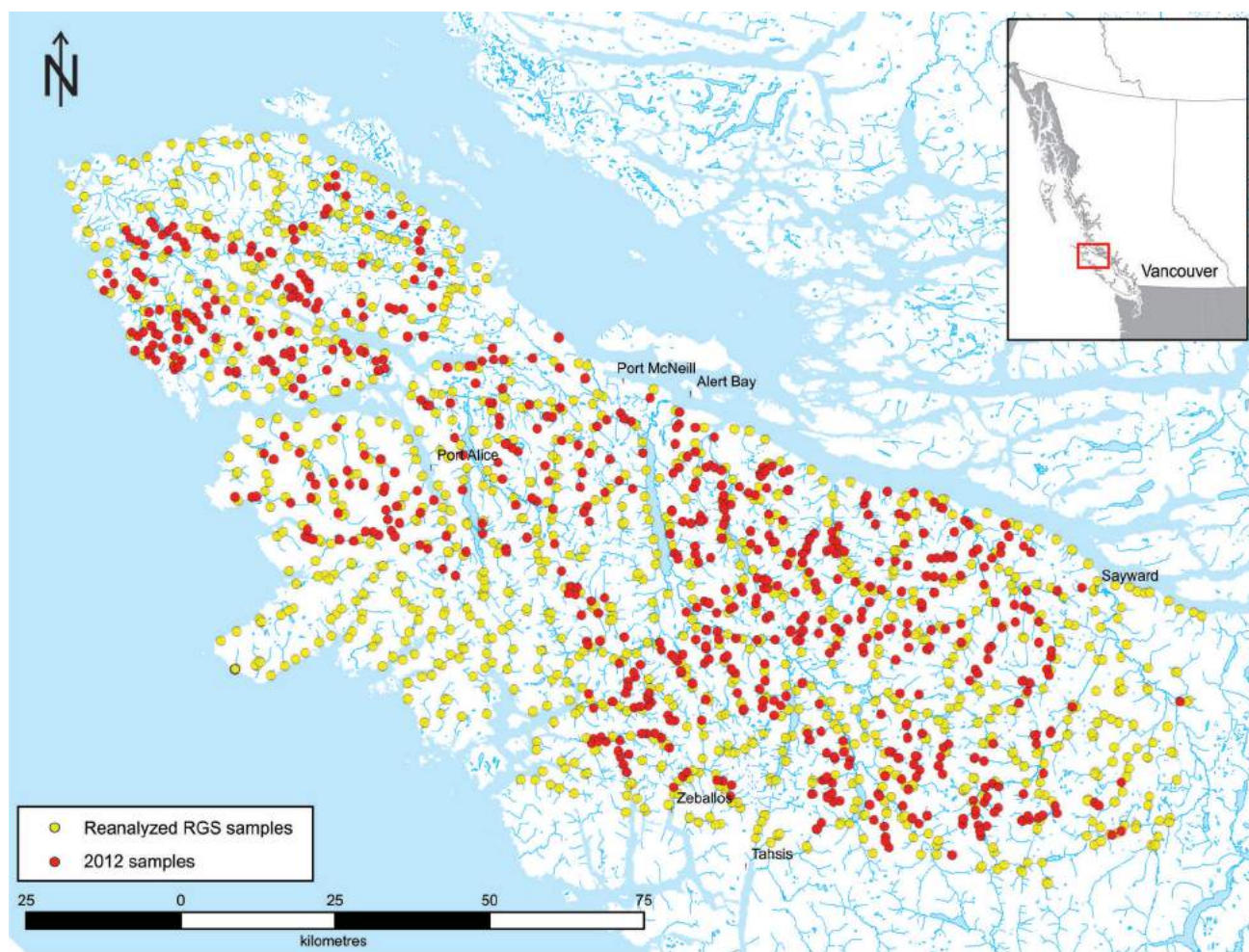


**Figure 1.** Location of study area showing the distribution of moss-mat stream sediment samples reanalyzed and collected as part of the Northern Vancouver Island Exploration Geoscience project.

Validation of historical RGS sample location points against the terrain resource information management (TRIM) hydrology for the area is nearly completed. Catchment basins will be defined for these samples shortly, followed by attribution with bedrock geology and interpretation of the geochemical data by the end of the year. The catchment basins will be made available as digital geographic information system (GIS) files along with the compiled geochemical data and the bedrock geology for each catchment. A series of map products in both portable document format (PDF) and as GIS data files will also be supplied. Completion of this project is anticipated in early 2015.

### Method

Historical and recent moss-mat sediment geochemical data and sample location metadata were obtained from previous Geoscience BC papers. Original field and analytical data obtained by Gravel and Matysek (1989) were taken from Jackaman (2013a). Data from the reanalyses of the original samples by inductively coupled plasma–mass spectrometry (ICP-MS) following an aqua-regia digestion at ALS Min-

erals (North Vancouver, British Columbia) were also obtained from Jackaman (2013a). These data were supplemented by the addition of Pt and Pd data by lead-collection fire assay from the reanalysis of the original RGS samples in Jackaman (2011). A total of 721 new moss-mat samples were collected for the Northern Vancouver Island Exploration Geoscience project area in 2012 (Jackaman, 2013). These samples were analyzed using both ICP-MS following an aqua-regia digestion at ALS Minerals and by instrumental neutron activation analysis (INAA) at Becquerel Laboratories Ltd. (Mississauga, Ontario). Data on water F contents, pH and conductivity, as well as sediment loss-on-ignition (LOI) and F were also obtained for these new samples. The archived RGS samples were also reanalyzed by INAA at Becquerel Laboratories Ltd. and the results are reported in Jackaman (2014). The sources of data compiled for this study are summarized in Table 1.

The stream sediment samples from the northern Vancouver Island study area were obtained from moss mats. The high flow velocities of many streams in this region meant that very little fine-grained material could be recovered through

**Table 1.** Summary of data sources and type compiled for this project, northern Vancouver Island. Abbreviations: ICP-MS, inductively coupled plasma–mass spectrometry; INAA, instrumental neutron activation analysis; LOI, loss-on-ignition.

Source	Data type	Number	Data
Geoscience BC Report 2013-11 Appendix B (MEMPR RGS 21-25)	Original analyses	1120	original field metadata; Au by fire assay with charge weights; LOI, F in sediment and water, U in water, pH
Geoscience BC Report 2011-04	Reanalyses	1120	aqua-regia ICP-MS: Pt and Pd by fire assay with charge weights
Geoscience BC Report 2013-11 Appendix A	New samples	721	aqua-regia ICP-MS: INAA with charge weights; LOI, F in sediment and water, pH, conductivity
Geoscience BC Report 2014-03	Reanalyses	1107	INAA with charge weights
		1841	Total number of samples

the collection of traditional stream sediment samples from local traps (Gravel and Matysek, 1989). Moss mats, however, contained abundant fine-grained sediment and preferentially trapped heavy minerals, and so were the preferred sampling material for both the 1988 and 2012 surveys. The samples were disaggregated after drying to remove the organic material and then the sediment was sieved to  $-177\ \mu\text{m}$ .

Cui (2010) emphasized the necessity of validating the historical RGS sample locations, which were manually located on NTS 1:50 000 topographic map sheets, against the hydrology layer using the current 1:20 000 scale TRIM topographic and hydrological data available in British Columbia, as the entire approach is predicated on the attribution of sample data to the correct watershed. Catchment basins for the validated sample locations are provided by Y. Cui of the British Columbia Geological Survey using the automated methodology described in Cui et al. (2009). This approach involves a three-stage computation:

- 1) identify the root watershed for each stream sediment sample site
- 2) retrieve all watersheds upstream of the root watershed
- 3) dissolve the upstream watershed boundaries to yield a single catchment for each sample

This approach differs from that used by Sibbick (1994). The catchments defined for that analysis were digitized manually from NTS 1:50 000 topographic maps; however, the catchment basins for samples with nested catchments were truncated at the next upstream sample, meaning that the catchment area for some RGS samples in that study will be underestimated compared to this study's approach. In addition, the contribution of bedrock types to the geochemistry of the stream sediment samples from areas located upstream from other samples on the same drainage system would not be taken into account using these root catchments only. A previous comparison of catchment areas derived using the two methods indicates good agreement for the bulk of the catchments, but reveals considerable scatter between a significant number of catchments determined manually and those derived using the automated procedure described by Cui et al. (2009). In some instances, the differ-

ences are on the order of several orders of magnitude. These differences either reflect the different approaches to evaluating nested catchments or differences in placement of the samples on the different hydrology layers (NTS 1:50 000 versus TRIM).

The investigation by Arne and Bluemel (2011) used a simple approach to leveling stream sediment data for catchment geology by using the dominant bedrock type. The dominant bedrock type was identified in a GIS query of published bedrock geology and catchments derived using an automated analysis of TRIM terrain data by the British Columbia Geological Survey, as previously described. Considerable effort on the QUEST-South project was expended in manually validating the locations of 8536 historical RGS samples using archived field maps. In the case of the 721 newly acquired northern Vancouver Island stream sediment samples available for this study, the locations are assumed to have been well positioned using modern satellite technology. The locations of 1120 historical samples collected in 1988, however, need to be validated against the TRIM hydrology layer.

The approach used by Arne and Bluemel (2011) will not always be appropriate in large catchment basins where multiple rock types are to be anticipated, nor does it account for variable erosion rates within the catchment. A spatially insignificant rock unit may contribute disproportionately to the geochemistry of a stream sediment sample from the catchment if it is relatively enriched in a particular element. A more accurate approach would be to estimate a background value for each catchment and element of interest using background values for individual lithological units and then apply a weighting to these values based on the proportion of each unit exposed within the catchment. Such weightings assume a constant supply of sediment from each rock type and may require adjustment to account for local variations in relief and erosion weights. Topography and variable weathering effects for different rock types are no doubt important factors in controlling the geochemical input from each rock type in a catchment basin, but such a detailed study is beyond the scope of this investigation. An intermediate approach that is computationally efficient is to

use the presence of a particular lithological unit or units to assess catchment basins in a pass/fail approach. This may be as effective as using the entire catchment geology (Bonham-Carter et al., 1987).

The approach used in this study is to estimate background stream sediment values for as many lithological units in the study area as possible in catchments underlain by a single lithological unit but not known to contain mineralization enriched in the elements of interest. Where insufficient catchments meet these criteria, it may be necessary to include catchment basins outside the study area to obtain sufficient data or to statistically filter anomalous data from mineralized catchments from the entire dataset. Geochemical values from till in the study area (Jackaman, 2013b) may also be used where a significant amount of till occurs within the catchment. A theoretical background value for key elements will be calculated for each catchment using the estimated proportion of various lithological units and a weighted average calculated from the background geochemical values for the units (weighted background value, WBV; or catchment background values), a procedure that inherently assumes constant sediment supply from all areas of the catchment.

Observed stream sediment data will be compared to the WBV and the differences recorded in terms of the number of standard deviations above the WBV in order to level the data and define anomalous catchments. In practice, these calculations can be performed using robust multiple regression following the approach recommended by Rose et al. (1970), Bonham-Carter and Goodfellow (1986), and Carranza and Hale (1997). Unlike the traditional approach to productivity, there will be no attempt to estimate the size or element enrichment associated with a theoretical mineral deposit within the catchment, as this approach is also influenced by the position of the deposit within the catchment relative to the stream sediment sample location. The approach will be validated by comparing the results to known mineral occurrences and deposits to see if there is an improvement in predictive capability compared to more traditional and less computationally intensive approaches.

An additional factor to be considered is the possibility of scavenging cations by secondary iron oxides in the samples. This is known to be an important influence on stream sediment data in areas of low relief (Bonham-Carter and Goodfellow, 1986) and is suggested by a positive association of Fe and elements such as V in the original 1988 mossmat dataset from northern Vancouver Island. Elements affected by suspected scavenging effects will have to be treated through principal component analysis that includes the variables Fe and/or Mn, or by the generation of residuals to indicate the presence of anomalous metals within particular catchments.

Principal component analysis will be used to assess a variety of influences on the raw geochemical data (lithological control, possible scavenging effects by secondary Fe and Mn oxides or organic matter, commodity element associations related to mineral deposits). Regression analysis of the data against the most important principal components will highlight samples that are anomalous and allow an independent validation of the weighted background values.

The effectiveness of current sampling coverage will be assessed through the evaluation of plots of metal concentration versus catchment area sampled to identify the catchment area at which the effects of dilution appear to reduce most stream sediment samples to regional background levels. This represents the maximum catchment area that should be sampled. Samples that capture sediment from larger catchments than this value can be considered to have been undersampled and these areas provide opportunities for follow-up sampling at a higher density to assess mineral potential. Regional background values for individual elements can also be compared to catchment background values to assess the influence of particular lithological units on the stream sediment data.

### Comments on Data Quality

The issue of data precision for the original RGS Au data has previously been noted, most recently by Arne and MacFarlane (2014). Gold was originally determined on the RGS samples from northern Vancouver Island using a lead collection fire assay with a 10 g (and occasionally a 5 g) charge. Data for 656 duplicate pairs were obtained from all RGS samples collected on Vancouver Island in 1988 and 1989. The data for 383 duplicate pairs having average values in excess of 10 ppb (i.e., an order of magnitude above the 1 ppb lower limit of detection for a 10 g charge) are presented in Figure 2. The data clearly suffer from poor reproducibility with an indication of a negative bias in the duplicate analyses. The average coefficient of variation for these duplicate pairs is 102%, calculated using the root-mean-squared (RMS) method described by Stanley and Lawrie (2007).

Gold data obtained from the more recent ICP-MS reanalyses are likely to have even greater variance given the 0.5 g aliquot analyzed. The INAA Au analyses are based on an average charge weight of 37.3 g for the new sample analyses and 27.41 for the reanalyses by INAA. The latter includes a wide range of aliquot weights, from just over 50 g to less than 1 g, so the precision of individual values will be variable. The INAA Au data are assumed to be superior to the original RGS Au data given average aliquots three times what was originally analyzed. Only 8% of the archived samples analyzed by INAA had sample weights less than 10 g; therefore, the INAA data will be used to provide the Au values for this study.

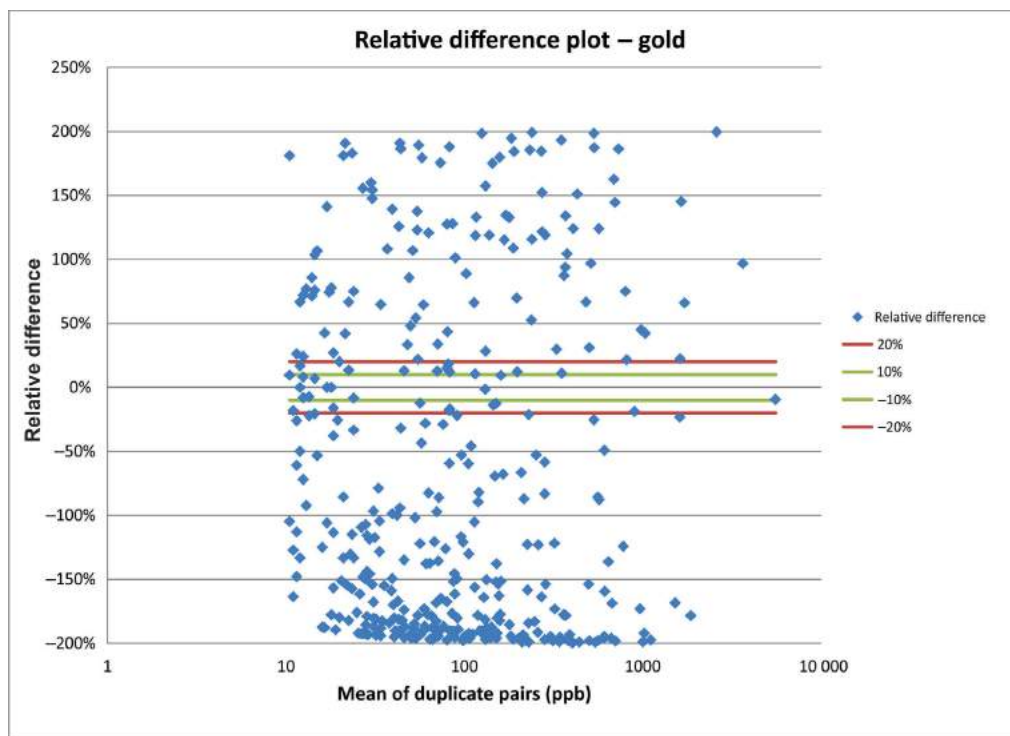


**Figure 2.** Comparison of historical RGS Au data from analytical duplicates analyzed by fire assay in 1988 and 1989, Vancouver Island.

The quality of the PGE data is also variable depending on which dataset is examined. The archived RGS samples for all of Vancouver Island were analyzed for Pt and Pd by fire assay using an average charge weight of 22.7 g and lower limits of detection for Pd and Pt of 0.5 and 0.1 ppb, respectively. The PGE data for the new samples collected on northern Vancouver Island in 2012 have been analyzed by ICP-MS using a 0.5 g aliquot with lower limits of detection for Pd and Pt of 1 and 2 ppb, respectively. The fire assay PGE data from the archived samples are therefore considered to be superior. Equal weighting should not be given to all Pd and Pt results from the project area given the possible physical transport of PGE grains in the streams sampled due to their high velocities and therefore it is likely the data were obtained from nonrepresentative samples.

Although data quality for the reanalysis of historical RGS samples and the analysis of new samples collected in 2012 have previously been assessed, the quality-control data were not made publicly available. The final report on this project will include a brief assessment of the quality-control samples associated with the new data acquired by Geoscience BC.

### Acknowledgments

The authors thank Geoscience BC for financial support to undertake this work. In particular, the authors thank D. Heberlein for helpful suggestions at an early stage of project development and W. Jackaman for providing qual-

ity-control data from the new survey and reanalysis of RGS data undertaken on northern Vancouver Island. Y. Cui of the British Columbia Geological Survey is thanked for agreeing to provide catchment outlines based on the current TRIM data. E. Grunsky of the Geological Survey of Canada reviewed the manuscript and provided several helpful recommendations regarding data analysis approaches.

### References

- Arne, D.C. and Bluemel, E.B. (2011): Catchment analysis and interpretation of stream sediment data from QUEST South, British Columbia; Geoscience BC Report 2011-5, 24 p., URL <<http://www.geosciencebc.com/s/2009-023.asp>> [October 2014].
- Arne, D.C. and MacFarlane, B. (2014): Reproducibility of gold analyses in stream sediment samples from the White Gold districts and Dawson Range, Yukon Territory, Canada; *Explore*, v. 164, p. 1–11, URL <<http://www.appliedgeochemists.org/index.php/publications/explore-newsletter>> [October 2014].
- Bonham-Carter, G.F and Goodfellow, W.D. (1986): Background corrections to stream geochemical data using digitized drainage and geological maps: application to Selwyn Basin, Yukon and Northwest Territories; *Journal of Geochemical Exploration*, v. 25, p. 139–155.
- Bonham-Carter, G.F., Rogers, P.J. and Ellwood, D.J. (1987): Catchment basin analysis applied to surficial geochemical data, Cobequid Highlands, Nova Scotia; *Journal of Geochemical Exploration*, v. 29, p. 259–278.
- Carranza, E.J.M. and Hale, M. (1997): A catchment basin approach to the analysis of reconnaissance geochemical-geo-

- logical data from Albay Province, Philippines; *Journal of Geochemical Exploration*, v. 60, p. 157–171.
- Cui, Y. (2010): Regional geochemical survey: validation and refitting of stream sample locations; *in* Geological Fieldwork 2010, BC Ministry of Energy and Mines, BC Geological Survey, Paper 2011-1, p. 169–179, URL <[http://www.empr.gov.bc.ca/Mining/Geoscience/PublicationsCatalogue/Fieldwork/Documents/2010/12\\_Cui\\_2010\\_hr.pdf](http://www.empr.gov.bc.ca/Mining/Geoscience/PublicationsCatalogue/Fieldwork/Documents/2010/12_Cui_2010_hr.pdf)> [October 2014].
- Cui, Y., Eckstrand, H. and Lett, R.E. (2009): Regional geochemical survey: delineation of catchment basins for sample sites in British Columbia; *in* Geological Fieldwork 2008, BC Ministry of Energy and Mines, BC Geological Survey, Paper 2009-1, p. 231–238, URL <[http://www.empr.gov.bc.ca/Mining/Geoscience/PublicationsCatalogue/Fieldwork/Documents/2008/19\\_Cui.pdf](http://www.empr.gov.bc.ca/Mining/Geoscience/PublicationsCatalogue/Fieldwork/Documents/2008/19_Cui.pdf)> [October 2014].
- Gravel, J.L. and Matysek, P.F. (1989): 1988 regional geochemical survey, northern Vancouver Island and adjacent mainland (92E, 92K, 92L, 102I); *in* Geological Fieldwork 1988, BC Ministry of Energy and Mines, BC Geological Survey, Paper 1989-1, p. 585–591, URL <<http://www.empr.gov.bc.ca/Mining/Geoscience/PublicationsCatalogue/Fieldwork/Documents/1988/585-592-gravel.pdf>> [October 2014].
- Hawkes, H.E. (1976): The downstream dilution of stream sediment anomalies; *Journal of Geochemical Exploration*, v. 6, p. 345–358.
- Jackaman, W. (2011): Regional stream sediment and water geochemical data, Vancouver Island, British Columbia (NTS 92B, C, E, F, G, K, L & 102I); Geoscience BC Report 2011-4, 5 p., URL <<http://www.geosciencebc.com/s/2011-04.asp>> [October 2014].
- Jackaman, W. (2013a): Regional stream sediment and water geochemical data, northern Vancouver Island, British Columbia; Geoscience BC Report 2013-11, 7 p., <<http://www.geosciencebc.com/s/Report2013-11.asp>> [October 2014].
- Jackaman, W. (2013b): Northern Vancouver Island till sample reanalysis (ICP-MS); Geoscience BC Report 2013-12, 3 p., URL <<http://www.geosciencebc.com/s/Report2013-12.asp>> [October 2014].
- Jackaman, W. (2014): Regional stream sediment geochemical data, sample reanalysis (INAA), northern Vancouver Island, British Columbia; Geoscience BC Report 2014-03, 4 p., URL <<http://www.geosciencebc.com/s/Report2014-03.asp>> [October 2014].
- Moon, C.J. (1999): Towards a quantitative model of downstream dilution of point source geochemical anomalies; *Journal of Geochemical Exploration*, v. 65, p. 111–132.
- Pan, G. and Harris, D.P. (1990): Quantitative analysis of anomalous sources and geochemical signatures in the Walker Lake quadrangle of Nevada and California; *Journal of Geochemical Exploration*, v. 38, p. 299–321.
- Rose, A.W., Dahlberg, E.C. and Keith, M.L. (1970): A multiple regression technique for adjusting background values in stream sediment geochemistry; *Economic Geology*, v. 65, p. 156–165.
- Sibbick, S.J. (1994): Preliminary report on the application of catchment basin analysis to regional geochemical survey data, northern Vancouver Island (NTS 92L/03,04,05 and 06); *in* Geological Fieldwork 1993, BC Ministry of Energy and Mines, BC Geological Survey, Paper 1994-1, p. 111–117, URL <<http://www.empr.gov.bc.ca/Mining/Geoscience/PublicationsCatalogue/Fieldwork/Documents/1993/111-118-sibbick.pdf>> [October 2014].
- Stanley, C.R. and Lawie, D. (2007): Average relative error in geochemical determinations: clarification, calculations and a plea for consistency; *Exploration and Mining Geology*, v. 16, p. 267–275.

# Use of a Field Portable Photometer for Rapid Geochemical Analysis of Streamwater and Springwater: a Case History from Poison Mountain, Southwestern British Columbia (NTS 0920/02)

R. Yehia, MYAR Consulting, Vancouver, BC, myar@telus.net

D.R. Heberlein, Heberlein Geoconsulting, North Vancouver, BC

---

Yehia, R. and Heberlein, D.R. (2015): Use of a field portable photometer for rapid geochemical analysis of streamwater and springwater: a case history from Poison Mountain, southwestern British Columbia (NTS 0920/02); *in* Geoscience BC Summary of Activities 2014, Geoscience BC, Report 2015-1, p. 47–52.

## Introduction

Mineral exploration traditionally focuses on the analysis of rock, soil and stream sediment sampling for the detection of primary and secondary dispersion anomalies derived from outcropping mineralization. In the past, the analysis of surficial water samples for this purpose has been underutilized by the mineral exploration community because of the perceived difficulty of sampling and the relatively high cost of analysis at commercial laboratories. Now, alternative techniques are available that can provide rapid field analysis of waters at a relatively low cost and, hence, can significantly improve the ability to make exploration decisions by providing near real-time analyses.

Hydrogeochemistry, or aqueous geochemistry, is used extensively for exploration of geothermal resources (Zehner et al., 2006), but has not seen widespread use in mineral exploration. The application of hydrogeochemistry to mineral exploration is well documented by Taufen (1997). Lett, Sibbick and Runnells (1998) and Leybourne and Cameron (2007). It has been shown to be an excellent technique for identifying commodity and pathfinder element dispersion patterns from both outcropping and concealed mineralization. In addition, it is a good technique for exploring areas with difficult access, such as the coastal mountain ranges of British Columbia. Large areas can be sampled at a low sample density to identify hydrological basins containing anomalous metal sources. When water sampling is used in conjunction with stream sediment geochemistry and water pH, it can be an effective tool for both regional- and property-scale exploration.

A range of analytical instruments called portable spectrophotometers, or photometers, is available for field-based water testing. They can determine ion concentration by

measuring the colour and light transmittance of a solution after the addition of metal-sensitive colour dyes; a technique called visible light reflectance photometry. These devices can measure concentrations of a diverse suite of dissolved anions and cations to relatively low detection limits. The tests can be completed on location; providing almost real-time (i.e., within 48 hours) results. Cost of analysis, including photometer reagents, is a fraction of the cost of analysis at a commercial laboratory. For example, photometer analysis is \$5 to 12 per sample suite (depending on reagent selection) compared to up to \$200 for commercial water analysis. Operating costs for photometer analysis in this study was \$31.25/sample with two operators. Additional savings are realized by other aspects of real-time exploration, such as faster target identification, reduced field and overall exploration time, and a smaller environmental impact footprint than other sampling methods. This innovative technique could have far reaching consequences for exploration and large-scale environmental background testing and monitoring.

This proof of concept study was carried out at the previously drilled porphyry copper-gold-molybdenum deposit at Poison Mountain, southwestern BC (Seraphim and Rainboth, 1976; Raven, 1994; Brown, 1995). The study aims to test the reliability of the Palintest® Photometer 8000 by comparing the results from water samples analyzed using this instrument with the results of identical samples analyzed at ALS Environmental laboratory (Burnaby, BC). The study also partially tests for repeatability over time by comparing analyses of the water samples collected in late summer and fall. It also includes a comparison of the results of water sample analysis with stream sediment sample analysis, where applicable.

Interpretation of the results includes an examination of the accuracy and precision of the photometer readings based on replicate readings, the analysis of the manufacturers' standard colour solutions and the results of field duplicate samples. The interpretation also addresses the dispersion distances of key anions and cations from the exposed porphyry mineralization and discusses the advantages of using

---

**Keywords:** hydrogeochemistry, photometer, rapid field analysis, water sampling, pathfinders

*This publication is also available, free of charge, as colour digital files in Adobe Acrobat® PDF format from the Geoscience BC website: <http://www.geosciencebc.com/s/DataReleases.asp>.*

this technique for mineral exploration throughout BC and elsewhere.

## Background

The photometer field survey technique was conceived by the lead author and field tested on a geothermal exploration program carried out in 2012 by Alterra Power Corp. (Yehia et al., 2013). The geothermal industry relies heavily on water analysis in early stage exploration. To accelerate exploration at reduced cost, new types of devices designed for rapid water testing were investigated. After comparing the devices available at the time, it was decided that the Palintest Photometer 8000 was the most suitable and cost-effective instrument for use in the field. It was chosen mainly for its portability, ease of use, reagent selection (Table 1) and overall cost. Early results from the geothermal project at three main locations around the Coast Mountains of southwestern BC demonstrated the photometer's reliability and showed that meaningful results could be achieved rapidly in the field (Yehia et al., 2013). MYAR Consulting subsequently received cost-sharing funding from Canada's National Research Council (NRC), under the Industrial Research Assistance Program (IRAP), to test the technique's potential for mineral exploration. Results of that study demonstrated that the photometer can produce rapid meaningful field data at relatively low cost (Yehia, 2013).

## Project Area

### Location and Access

The project area is located approximately 95 km northwest of Lillooet and is accessible via the Yalakom River Forest Service road (FSR). It is bounded by the headwaters of the Yalakom River to the east, and Churn Creek and Buck Mountain to the west (Figure 1). Elevations in the area range from 1600 m in the Yalakom River to 2250 m at the Poison Mountain peak. Above the treeline are bare alpine slopes at approximately at 2075 m and below this level the vegetation is mostly naturally occurring and replanted stands of lodgepole pine. The latter vegetation is located on the eastern slopes of Poison Mountain. The drainage divide south of the mountain between the Yalakom River and Churn Creek is occupied by a large swamp with beaver dams.

### Geology

The Poison Mountain porphyry copper-gold-molybdenum deposit consists of disseminated and stockwork mineralization associated with small stocks that intrude sandstone, shale and conglomerate of the Lower Cretaceous Jackass Mountain Group (Seraphim and Rainboth, 1976; Raven, 1994; Brown, 1995). The three main porphyry intrusions are biotite diorite, hornblende diorite and granodiorite. Pri-

mary sulphide mineralization consists of pyrite, chalcopyrite, molybdenite and bornite. Weathering of bedrock extends to about 5 m in the sedimentary units, and is undeveloped in the quartz diorite porphyry. Supergene enrichment is intense along fractures and joints to a depth of about 80 m. Oxidation of copper sulphide minerals occurs to depths of about 10 m from the surface (Brown, 1995).

## Sample Collection and Analysis

A first round of field sample collection was performed in late August 2014 (Figure 1). Water samples were collected directly from midstream sites, and from springs as close as possible to source. Samples were stored in #2 high density polyethylene (HDPE) bottles. Photometer sample bottles were reused and rinsed thoroughly at least twice with the sample waters with the cap on before sample collection. If a sample bottle displayed any type of discolouration, it was not used for sample collection and was recycled appropriately. Filtration and acid preservation were not carried out because the majority of samples were clear with very little fines, and analysis was carried out within 48 hours of collection. As well, filtration was not carried out to simulate expedited sampling and processing, as filtration adds a significant amount of time to overall procedures. Sample location sites were tested for temperature, pH, conductivity, total dissolved solids (TDS) and salinity, using an OAKTON Instruments PCS Testr 35 meter.

**Table 1.** Listing of photometer available reagents selected for this project and their published detection limits.

Type	Palintest published detection range (mg/l)
Aluminum	0–0.5
Boron	0–2.5
Bromine	0–10.0
Calcium hardness (calcol)	0–500
Chloride (chloridol, NaCl)	0–50 000
Copper (coppercol, free and total)	0–5.0
Fluoride	0–1.5
Hardness (hardicol, total)	0–500
Iron	0–10
Magnesium	0–100
Manganese	0–5.0
Molybdate (MoO <sub>4</sub> )	0–100
Nickel	0–10
Potassium	0–12
Silica (SiO <sub>2</sub> )	0–150
Sulphate (SO <sub>4</sub> )	0–200
Zinc	0–4.0

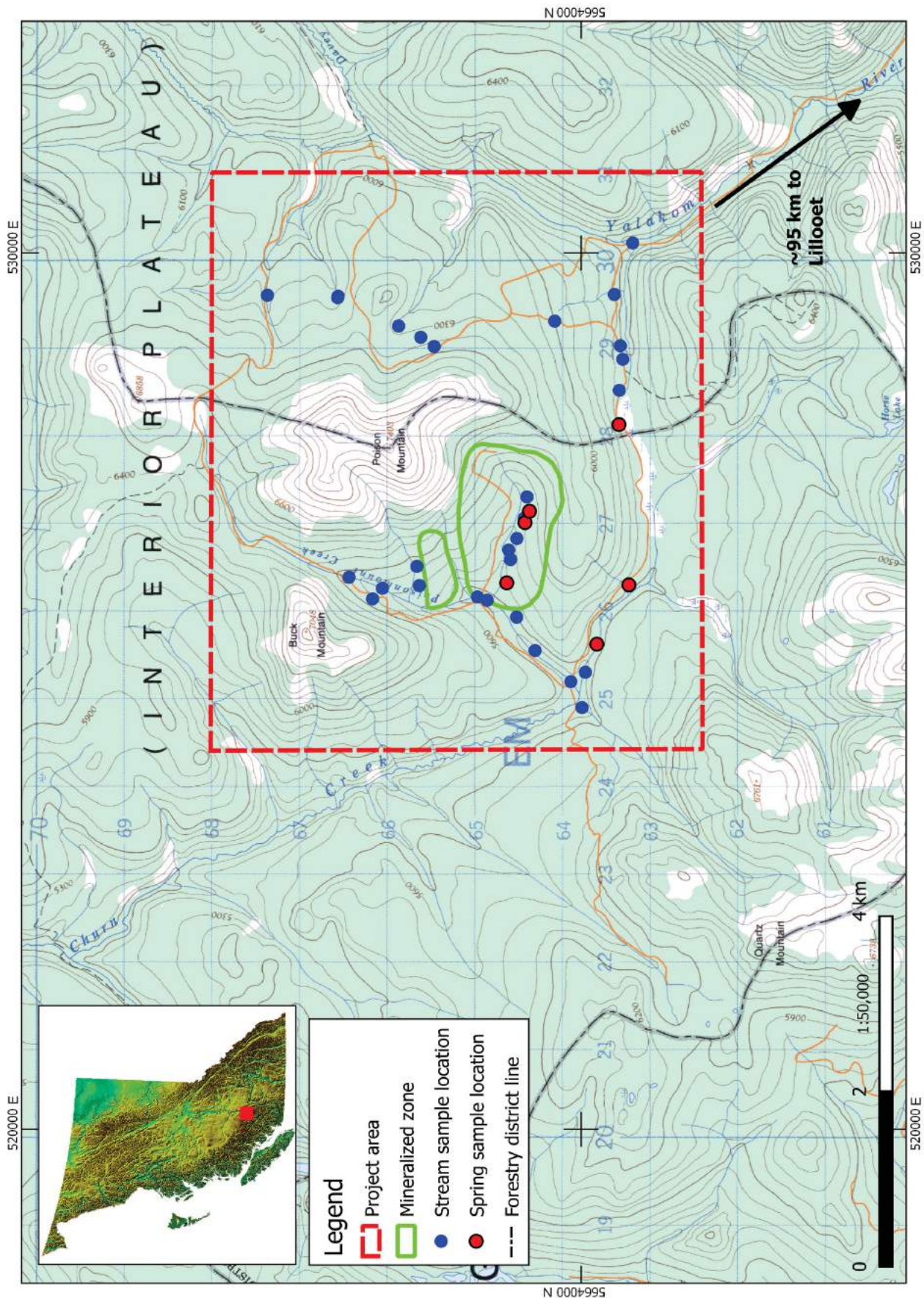


Figure 1. Poison Mountain project area and sample location map, southwestern British Columbia (background raster image from Natural Resources Canada, 1992). UTM Zone 10.

The same sample bottles as above were used for analysis at ALS Environmental laboratory. They were rinsed twice and the water was not filtered to match the photometer sample collection procedure and to prevent data disparity. The water samples were collected in 1 L and 250 mL bottles, and 3 mL of ultrapure nitric acid was added to the 250 mL bottle for sample preservation. Water in the 250 mL bottle is intended for cations analysis and the water in the 1 L bottle is required by the laboratory for TDS analysis, quality control–quality assurance (QA-QC) monitoring of results and possible repeatability tests for various reasons.

Stream sediment samples were wet sieved to –20 mesh and collected in Hubco Inc.’s New Sentry 5 by 8 in. (13 by 20 cm) sample bags. The bags were allowed to stand to drain excess water and then stored in Ziploc® sealed freezer bags to prevent cross-contamination between samples. All sampling equipment was rinsed thoroughly before and after each sample collection.

The following samples were analyzed in August:

- 1) forty water samples for photometer analysis, four of which were field duplicates, and one QC deionized water,
- 2) twenty water samples submitted to ALS Environmental laboratory, including four field duplicates and a fifth duplicate for the deionized water sample, and
- 3) thirty-three stream sediment samples, including four field duplicates.

During the survey, all of the samples above were stored inside coolers at room temperature. Water samples were transported in coolers to the ALS Environmental laboratory and sediments delivered to the ALS Mineral laboratory (North Vancouver, BC).

Samples collected for photometer analysis were tested within 48 hours. The reagents listed in Table 1 were used for each sample.

Quality control measures used for the project included

- 1) collection of field duplicates for each sample type,
- 2) photometer calibration tests every eight samples using manufacturer’s standard solutions,
- 3) triplicate photometer readings were taken for each reagent for each sample to measure instrument precision, and
- 4) deionized water blanks were used to monitor contamination and instrument drift.

MYAR returned to the project site in October to repeat the sampling as part of testing for differences in geochemical responses resulting from repeatability over time; in this case summer and fall. Details of this work will be presented in a future publication.

## Future Work

Now that all of the data has been collected, the following analysis and reporting is planned:

- 1) estimation of photometer analytical precision by replicate readings,
- 2) estimation of photometer accuracy by comparing photometer and laboratory results,
- 3) comparison between the summer and fall results,
- 4) comparison of stream sediment laboratory results and photometer results,
- 5) evaluation of the relative costs of photometer and laboratory analysis, and
- 6) commentary on the validity of the photometer technique.

The project is expected to be completed in early 2015, and a final report will be released by Geoscience BC.

## Acknowledgments

The authors would like to thank P. Winterburn, R. Lett and C. Pellett for their valuable feedback. Warm thanks to S. Hashmi for field assistance and advice.

## References

- Brown, R. (1995): Poison Mountain porphyry copper-gold-molybdenum deposit, south-central British Columbia; *in* Porphyry Deposits of the Northwestern Cordillera of North America, T.G. Schroeter (ed.), Canadian Institute of Mining, Metallurgy and Petroleum, Special Volume 46, pt. B, Paper 20, p. 343–351.
- Lett, R.E., Sibbick, S. and Runnells, J. (1998): Regional stream water geochemistry of the Adams Lake – North Barriere Lake Area, British Columbia (NTS 82M/4 and 82M/5); BC Ministry of Energy and Mines, BC Geological Survey, Open File 1998-9, 238 p.
- Leybourne, M.I. and Cameron, E.M. (2007): Groundwaters in geochemical exploration: methods, applications, and future directions; *in* Proceedings of Exploration 07: Fifth Decennial International Conference on Mineral Exploration, B. Milkereit (ed.), Prospectors and Developers Association of Canada, Toronto, Ontario, p. 201–221.
- Natural Resources Canada (1992): Noaxe Creek NTS 0920/02; Natural Resources Canada, National Topographic System map sheet, 0920/02, scale 1:50 000, raster image.
- Raven, W. (1994): Assessment report of diamond drilling and soil geochemistry Poison Mountain Project for Bethlehem Resources Corp.; BC Ministry of Energy and Mines, Assessment Report 23243, 238 p., URL <<http://aris.empr.gov.bc.ca/ArisReports/23243.PDF>> [September 2014].
- Seraphim, R.H. and Rainboth, W. (1976): Poison Mountain; *in* Porphyry Deposits of the Canadian Cordillera, A. Sutherland Brown (ed.), Canadian Institute of Mining, Metallurgy and Petroleum, Special Volume 15, pt. B, Paper 22, p. 323–328.
- Taufen, P.M. (1997): Ground waters and surface waters in exploration geochemical surveys; *in* Proceedings of Exploration 97: Fourth Decennial International Conference on Mineral Ex-

- ploration, A. Gubins (ed.), Prospectors and Developers Association of Canada, Toronto, Canada, p. 271–284.
- Yehia, R. (2013): Final project report; MYAR Enterprises Inc., unpublished report for Industrial Research Assistance Program, National Research Council, 57 p.
- Yehia, R., Vigouroux, N. and Hickson, C. (2013): Use of a portable photometer for accelerated exploration: testing for geothermal indicators in surface waters; GRC Transactions, v. 37, p. 375–381.
- Zehner, R.E., Coolbaugh, M.F. and Shevenell, L. (2006): Regional ground water geochemical trends in the Great Basin: implications for geothermal exploration; GRC Transactions, v. 30, p. 117–124.



# Toward an Improved Basis for Beneath-Cover Mineral Exploration in the QUEST Area, Central British Columbia: New Structural Interpretation of Geophysical and Geological Datasets (NTS 093A, B, G, H, J, K, N)

M.G. Sánchez, Fault Rocks Consulting, Vancouver, BC, msanchez@faultrocks.com

T. Bissig, Mineral Deposit Research Unit, University of British Columbia, Vancouver, BC

P. Kowalczyk, Consulting Geophysicist, Vancouver, BC

---

Sánchez, M.G., Bissig, T. and Kowalczyk, P. (2015): Toward an improved basis for beneath-cover mineral exploration in the QUEST area, central British Columbia: new structural interpretation of geophysical and geological datasets (NTS 093A, B, G, H, J, K, N); *in* Geoscience BC Summary of Activities 2014, Geoscience BC, Report 2015-1, p. 53–62.

## Introduction

Geoscience BC's QUEST survey area in central British Columbia (Figure 1) has a large amount of regional geophysical and geochemical data available to the exploration industry; however, despite the wealth of data, the bedrock geology remains poorly constrained, especially in the extensive areas covered by glacial drift in the Prince George area. The area is generally prospective for porphyry Cu-Au mineralization beneath covering glacial drift. Previous attempts to integrate geophysical, geochemical and geological information to constrain the geology beneath cover (Logan et al., 2010) provided results that were heavily biased toward interpolation between known outcrops and failed to take into consideration much of the geophysical and geochemical evidence. Moreover, this bedrock geology interpretation could only be poorly reconciled with new outcrops documented recently (Bissig et al., 2011) during ground-truthing of maps based on neural-network processing of stream and lake-sediment geochemical data (Barnett and Williams, 2009). The existing map interpretations from Logan et al. (2010) and Barnett and Williams (2009) are vastly different and neither considers the structural fabric evident from magnetic data. This project aims to improve previous geological maps by using a new and systematic multi-dataset 'stacking' methodology (Sánchez et al., 2014) for the interpretation of Geoscience BC's Bouguer and isostatic residual (IR) gravity grids, Natural Resources Canada's (NRCAN) regional reduced-to-pole (RTP) aeromagnetic data (Figure 1b, c) and the satellite-derived Shuttle Radar Topography Mission (SRTM) digital elevation model. The new structural and geological interpretation will provide a fresh look at the bedrock geology in this

highly prospective terrain and will contribute to the generation of new exploration targets.

## Geological and Metallogenic Framework

The QUEST project area is focused on the Quesnel and Cache Creek terranes, which are part of the Intermontane (or Peri-Laurentian) tectonic realm (Monger et al., 1982; Nelson et al., 2013) and the western part of ancestral North America (Laurentian realm; Nelson et al., 2013; Figure 1). The latter contains orogenic and placer Au mineralization that, in the QUEST area, is concentrated most importantly in the historical Wells-Barkerville camp (Figure 2b). The Quesnel terrane is composed largely of Triassic volcanic and volcano-sedimentary rocks of basaltic composition assigned to the Nicola Group and along-strike equivalent Takla Group (Mortimer, 1987; Nelson et al., 2013; Figure 2c). These rocks represent an oceanic-arc assemblage and vary from alkalic to calcalkalic and tholeiitic. The Nicola and Takla groups host late Triassic to early Jurassic alkalic Cu-Au porphyry deposits, such as Mount Polley and Mount Milligan (Jago et al., 2014; Pass et al., 2014; Figure 2c). Located west of the Quesnel terrane, the oceanic Cache Creek terrane includes shale and deep water limestone, basalt and ultramafic complexes (e.g., Massey et al., 2005; Nelson et al., 2013; Figure 2d). The Peri-Laurentian terranes were accreted to the North American continent during the early Jurassic, during which time the alkalic Cu-Au porphyry deposits of Mount Milligan and Lorraine were emplaced (e.g., Devine et al., 2014; Figure 1). The southwestern part of the QUEST area includes some of the Nechako Plateau, a domain containing thick sequences of late Cretaceous to Eocene volcanic deposits that are prospective for epithermal mineralization (Bordet et al., 2014; Figure 1a).

## Datasets

The structural and geological interpretation in this study uses Geoscience BC's airborne gravity grid, NRCAN's aeromagnetic grids (Geoscience BC, 2009a) and the SRTM90v3

---

**Keywords:** *QUEST, structure, geophysics, magnetometry, gravity, mineral exploration*

*This publication is also available, free of charge, as colour digital files in Adobe Acrobat® PDF format from the Geoscience BC website: <http://www.geosciencebc.com/s/DataReleases.asp>.*

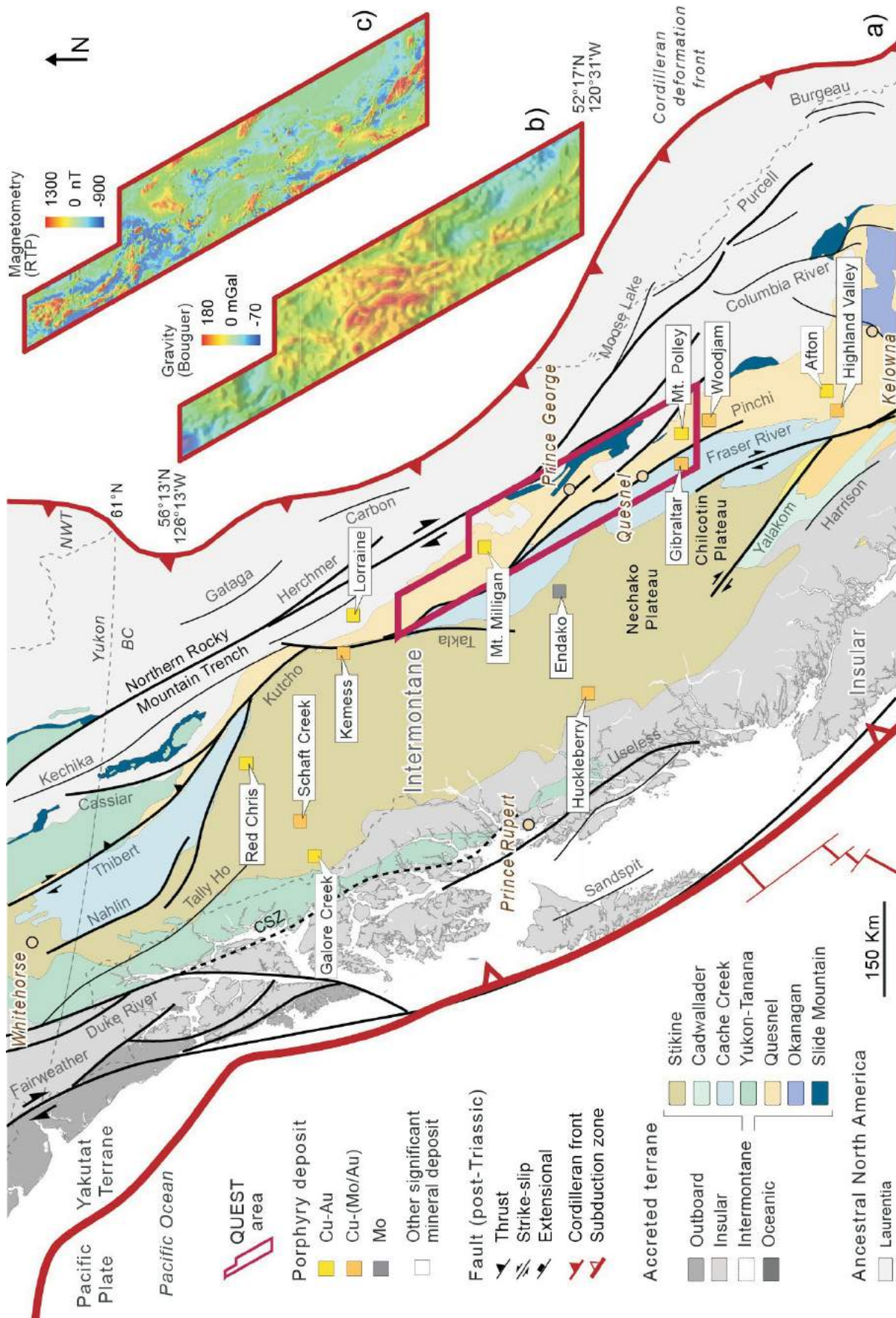


**Figure 1. a)** Tectonic map of the North American Cordillera of British Columbia, showing major tectonic boundaries (after Colpron and Nelson, 2011), Mesozoic and Cenozoic faults, and main porphyry-style mineral deposits. **b)** Geoscience BC's airborne gravity grid. **c)** Natural Resources Canada's aeromagnetic grids (Geoscience BC, 2009a). Location of (b) and (c) shown by red outline in (a). Abbreviations: RTP, reduced-to-pole.

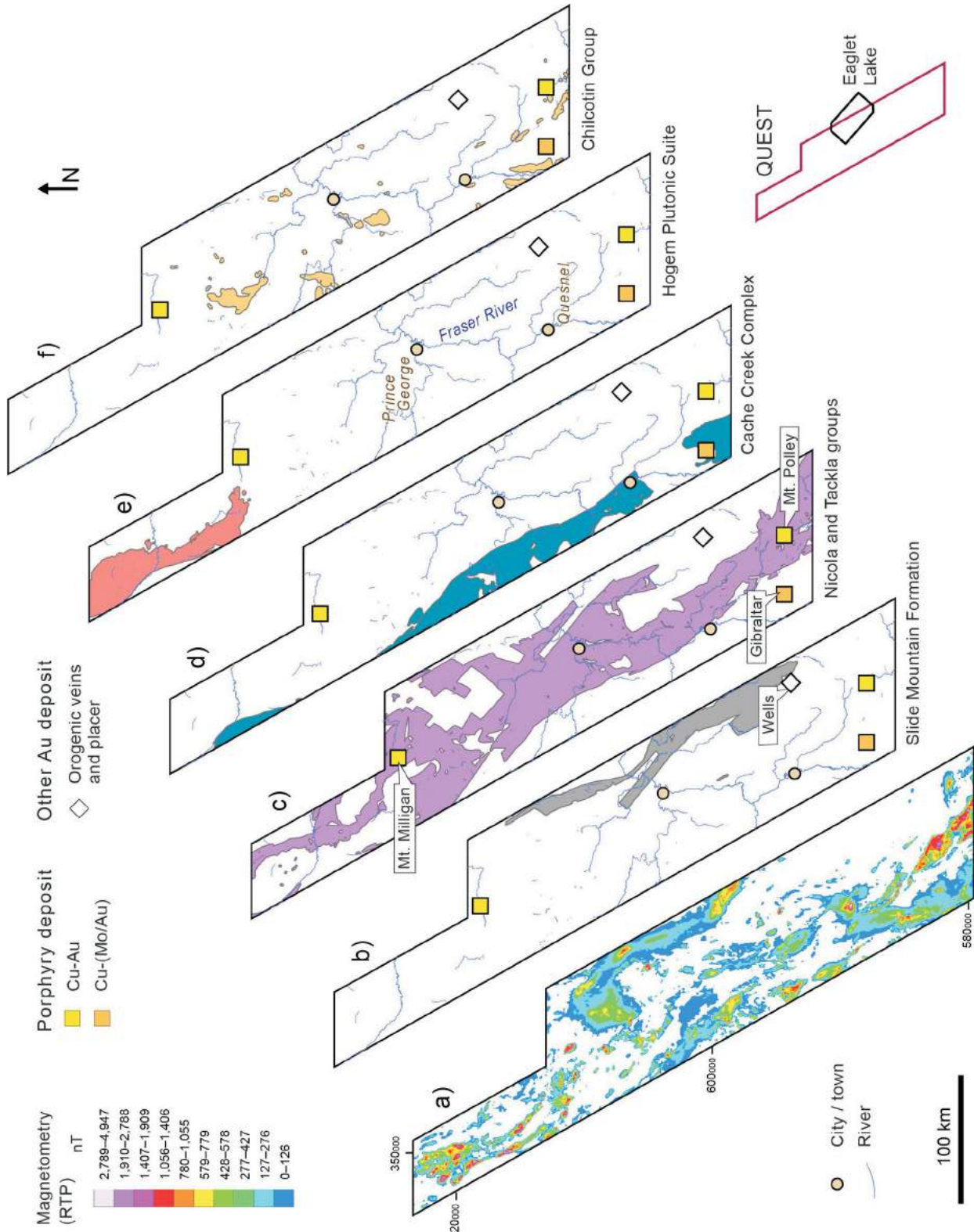


**Figure 2.** Reduced-to-pole (RTP) aeromagnetic anomalies and their correlation with principal geological units of the QUEST project area (Geoscience BC, 2009b), showing also the spatial distribution of porphyry deposits: **a)** positive-intensity RTP aeromagnetic grid; **b) to f)** major geological units with a magnetic response.

digital elevation model (Farr et al., 2007). All remotely sensed datasets have been jointly interpreted with the 1:1 000 000 surface geology map published by the BC Geological Survey (Massey et al., 2005) and the 1:500 000 scale QUEST project geology map (Geoscience BC, 2009b; Figure 2b–f). Geophysical acquisition for Geoscience BC’s QUEST project began in 2007 and included an airborne electromagnetic (EM) survey (not used in this study) and an airborne gravity survey, which covered an area of approximately 150 000 km<sup>2</sup> between Williams Lake and Mackenzie in northeastern BC (Figure 1; Barnett and Kowalczyk, 2008). The high-resolution airborne gravity survey was conducted by Sander Geophysics Ltd. (SGL) in 2007 and 2008 (Sander Geophysics Ltd., 2008). It consisted of 27 480 line-km, with traverse lines spaced at 2000 and 1000 m intervals oriented at 090° and control lines at 20 km spacing and oriented at 150.5°. The survey was flown using SGL’s Airborne Inertially Referenced Gravimeter (AIRGrav) system at a nominal terrain clearance of 200 m. Three final airborne gravity grids were released by Geoscience BC (Geoscience BC, 2009a): a Bouguer anomaly map, an isostatic residual (IR) map and a first vertical derivative (1VD) map. The aeromagnetic data used in this project consist of a seamless mosaic assembled by Geoscience BC using data from NRCan (Geoscience BC, 2009a). Most airborne magnetic surveys in this unified grid were flown on east-trending flight lines at a line spacing of 805 m and gridded at an interval of 250 m (Barnett and Kowalczyk, 2008). Three final aeromagnetic grids were released by Geoscience BC (Geoscience BC, 2009a): a total magnetic intensity map, a reduced-to-pole (RTP) grid and a potential map grid.

## Upward Continued Residual Filters

In order to represent depth surfaces in potential-field data, upward-continued datasets were produced following a methodology similar to the one proposed by Jacobsen (1987), whereby a band-pass filter is used to separate causative sources at various depths. The method implies that, in order to isolate a regional field at a given depth ( $z_0$ ), the observed field is upward-continued to a height above the land surface equivalent to twice its depth ( $2 \times z_0$ ). For the definition of upward-continued residual levels, the authors followed the recommendations of Gunn (1997), which emphasize the use of geological constraints at the expense of spectral information (Spector, 1985). Three upward-continuation levels were selected for brittle crustal conditions of less than ~10 km depth. In accordance with a typical geothermal gradient of 30°C/km (Dragoni, 1993), these levels are located well below the Curie temperature of magnetite (585°C) and have the potential to generate a magnetic response. Previously known geological constraints, such as maximum thickness of Quaternary drift cover and of the Chilcotin Group volcanic rocks (Andrews and Russell,

2010), were essential for the definition of shallower depth slices (Figure 2).

The selection of three upward-continued levels is based on the following geological criteria:

- 500 m to 0 m (depth slice from surface to ~250 m):** This range includes the maximum thickness of Quaternary drift cover (~200 m; Andrews and Russell, 2010), as well as Miocene–Pleistocene Chilcotin Group basalts ( $\leq 200$  m; Andrews and Russell, 2010; Figure 2f). This residual range is proposed to assist in the interpretation of very shallow and lowermost order structures. However, the signal’s very short wavelength is highly sensitive to linear artifacts, which need to be carefully assessed throughout the interpretation process.
- 1000 m to 500 m (depth slice from ~250 m to ~500 m):** This residual depth range is intended to suppress the magnetic signal of the Chilcotin Group volcanic rocks and Quaternary drift. It highlights the magnetic fabric of metamorphic foliation, as well as magnetic lineaments of near-surface, lower order, steeply dipping faults.
- 5000 m to 1000 m (equivalent to a ~500 m to ~2500 m depth slice):** This is the depth range for shallow upper crust with Mesozoic plutons and Mesozoic and Paleozoic metamorphic assemblages that commonly occur below unmetamorphosed Cenozoic volcanic and sedimentary rocks. This residual slice is intended to provide valuable information on the magnetic signal of principal northwest- to north-northwest-trending faults that occur subparallel to the main Cordilleran tectonic fabric and principal plutonic belts. It also has the potential to depict the distribution and edges of major gravity and magnetic domains.

## Interpretation Method

The current methodologies for structural and geological interpretation focus primarily on high-frequency and variable-intensity aeromagnetic lineaments that correspond to discontinuities with an aeromagnetic domain change (Sanchez et al., 2014). The interpretation of magnetic- and gravity-domain boundaries was further corroborated by their correlation with major geological units. Aeromagnetic lineaments and domain boundaries were first manually traced by using two pairs of high-pass filters: 1) analytic signal (AS) in combination with the horizontal-gradient magnitude (HGM) grid, and 2) 1VD grid in addition to the tilt-derivative (TD) filter. All four filters suppress deep, long-wavelength signals and accentuate or sharpen the near-surface responses that are useful for structural interpretation in drift- and/or basalt-covered areas (Gunn et al., 1997; Milligan and Gunn, 1997). The AS filter and the HGM grid help detect magnetic- and gravity-anomaly boundaries because both filters place their ‘peak’ amplitude signal over edges or geological contacts. Furthermore, as the amplitude of the AS signal is always positive, it

works as an effective antiremanence tool (Gunn, 1997). The 1VD grid and the TD filter are effective in accentuating the high-frequency signals that commonly arise from linear features such as faults, fractures, stratification, foliation and dikes. All four high-pass filters are valuable tools for the textural characterization of magnetic and gravity domains.

For the delineation of gravity and magnetic domains, and their correlation to geological units, the study focused on the interpretation of the previously described upward-continued residual levels. These low-pass filters were used in addition to a series of pseudogravity (PG) grids for non- and upward-continued RTP magnetic residuals. The PG transformation implies an approximate conversion of magnetic to gravity data by changing its rate of decay from the inverse cube of the distance to source to the inverse square of the distance to source (Hildenbrand, 1983).

The structural interpretation in this study is based on a systematic, multi-dataset ‘stacking’ methodology, in which lineaments are compared against various data layers to provide a measure of geological confidence. In order to evaluate the reliability of the lineament interpretation, individual magnetic lineaments were classified by assigning binary numeric values, depending upon whether they can be traced in each individual grid (Sánchez et al., 2014). The summation of these values results in a reliability scale with which most probable structures were detected. Values were then evaluated against other spatial parameters, such as fault orientations, lineament length, normalized length and line densities. Offsets across magnetic lineaments were then inspected in map-view and cross-section. Finally, results were assessed against known local structural types and the regional structural and tectonic framework for the classification of magnetic lineaments into fault types and systems (Sánchez et al., 2014).

### **Preliminary Regional Observations**

The Nicola Group and laterally equivalent Takla Group, the most widely occurring mafic rocks in the QUEST area, are accurately depicted by the unfiltered RTP grid (Figure 2a, c) and by the longer wavelength, ~500 m to ~2500 m depth-equivalent residual. This residual slice provides valuable information on principal northwest- to north-northwest-trending faults that run subparallel to the main Cordilleran tectonic fabric and the distribution of Mesozoic and Early Cenozoic intrusive rocks. Early Jurassic intrusive rocks from the Hogem Plutonic Suite are the most significant magnetic sources across the northernmost part of the QUEST area (Figure 2a, e). In the central and southern parts, northwest-trending linear magnetic anomalies from Cache Creek’s serpentinite sources, as well as scattered magnetic anomalies sourced from basalts, gabbro and diorite from the Slide Mountain Complex, are evident from the RTP grid (Figure 2a, b, d). Ongoing interpretations indi-

cate that northwest- to north-northwest-trending structures and metamorphic fabrics linked to principal fault systems are well represented in all depth-equivalent slices. A series of younger, north- and northeast-trending, steeply dipping faults, which commonly displace orogen-parallel north-northwest-trending structures, is also highlighted.

### **Structural and Geophysical Interpretation of the Eaglet Lake Area**

The Eaglet Lake area, located 30 km northeast of Prince George, serves as a case study for the work discussed herein. This area offers reliable field evidence of northwest- and northeast-trending, steeply dipping brittle faults and fractures (Figure 2). Remotely sensed data interpretation indicates that regional-scale, northwest-trending aeromagnetic lineaments bound a 40 km long aeromagnetic anomaly that is cut and offset by northeast- to east-northeast-oriented, normal to oblique sinistral-normal faults (Figure 3). The aeromagnetic high is overlapped by Cretaceous and Eocene plutons that crop out mainly as northeast-trending, elongated (in plan-view) bodies.

Field observations at a quarry located immediately west of Eaglet Lake (Figure 3) show at least two northwest-trending, plagioclase- and K-feldspar–phyric felsic dikes with disseminated pyrite intruding nonfoliated basaltic rocks of the Slide Mountain Complex (Figure 4a). These approximately 5 m thick dikes occupy subparallel dilational joints with dextral strike-slip reactivation (Figure 3, location 2; Figure 4b). Along the northwestern flank of Eaglet Lake, a series of subparallel, northwest-dipping, dilational quartz veins with epidote and chlorite haloes occupies northeast-trending dilational fractures that are oriented nearly orthogonal to the felsic dikes and dextral strike-slip faults (Figure 3, location 3; Figure 4c). Both dikes and quartz veins occur in the vicinity of a major granodiorite pluton of Eocene age that shows a dense arrangement of planar, southeast-dipping dilational fractures conjugate to the quartz veins and fault/fracture sets (Figure 3, location 3; Figure 4d; Geoscience BC, 2009b).

The authors infer that the Eaglet Lake basin is bounded by a southeast-dipping, normal to oblique sinistral-normal master fault that, in combination with an antithetic, northwest-dipping normal fault, accommodates a 40 km long, northeast- to east-northeast-trending half graben (Figure 3). The most prominent Eocene pluton of the Eaglet Lake area crops out within the Eaglet Lake graben and along its master faults, suggesting syn- to postemplacement control by extensional to oblique-sinistral faults.

### **Future Work**

In order to fully integrate airborne magnetic and gravity datasets, as well as structural-geomorphology interpreta-

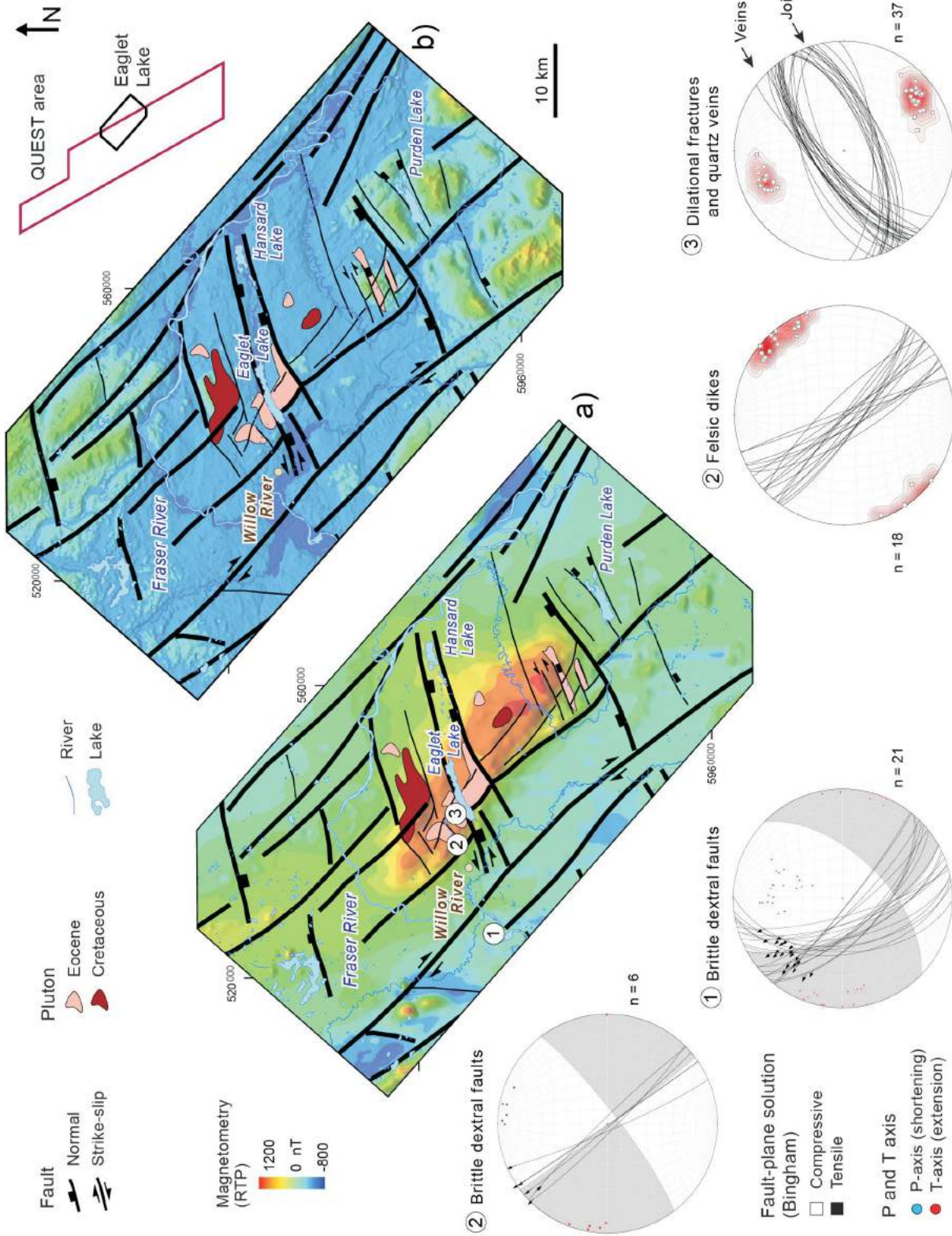


**Figure 3.** Structural interpretation of aeromagnetic (a) and geomorphology (b) datasets of the Eaglet Lake area, east of Prince George. Principal northwest-trending, strike-slip faults bound a 40 km long aeromagnetic anomaly that is cut and offset by northeast- to east-northeast-oriented, oblique sinistral-extensional faults that accommodate the Eaglet Lake basin. Field-based structural measurements are shown as stereoplots, the locations of which are indicated by numbers in map (a). Plutons modified after Massey et al. (2005).

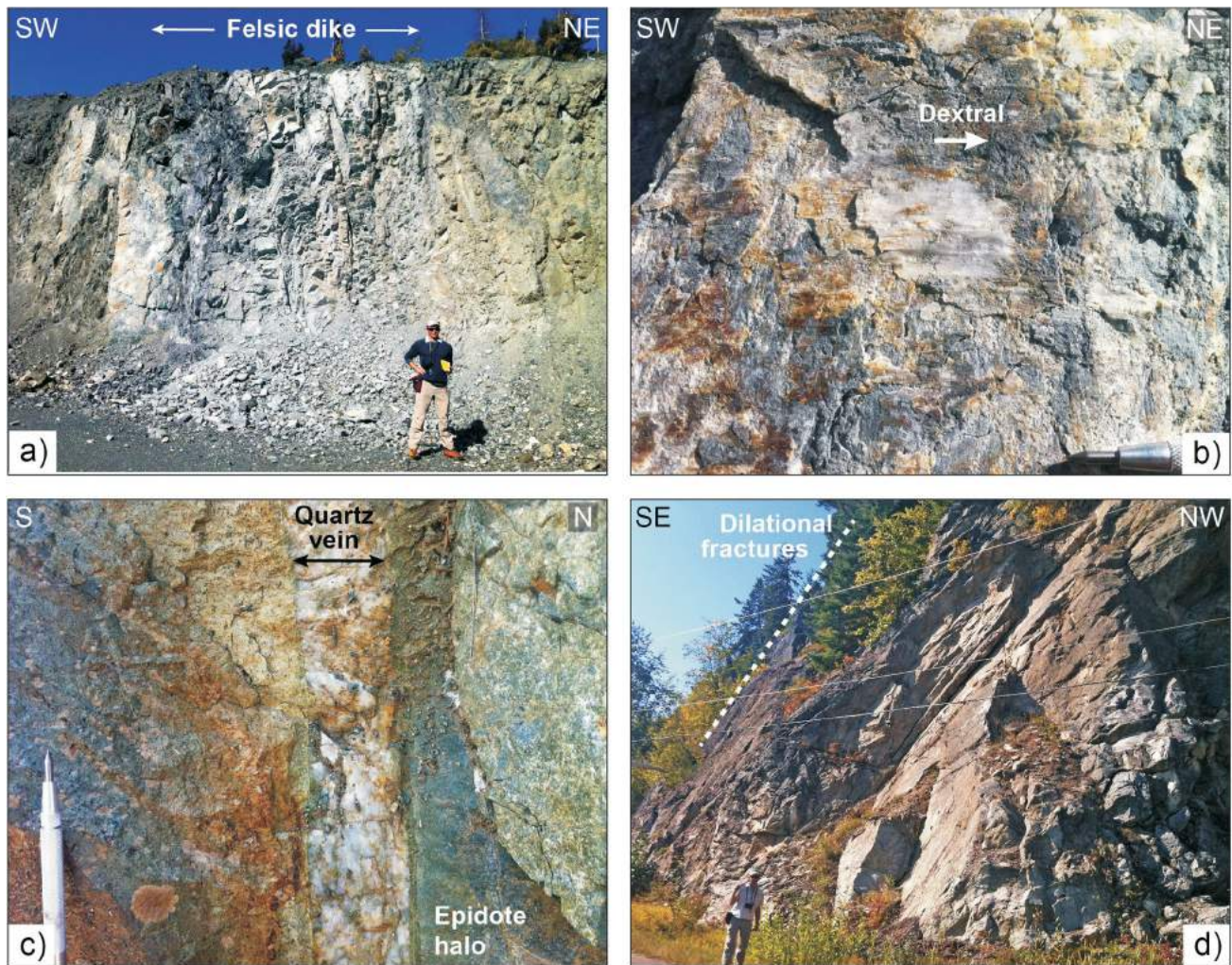


**Figure 4.** Northwest- and northeast-trending, steeply dipping brittle structures of the Eaglet Lake area: **a)** northwest-trending, plagioclase- and K-feldspar–phyric felsic dike intruding highly magnetic and nonfoliated basaltic rocks of the Slide Mountain Complex; **b)** northwest-trending, dextral strike-slip fault plane along the contact of felsic dikes and basaltic hostrocks; **c)** series of subparallel, northeast-trending, dilational quartz veins with epidote-chlorite haloes; **d)** subparallel, northeast-trending joints in granodiorite of Eocene age. Refer to Figure 3 for stereonet graphics.

tion, this project will focus on the multi-dataset ‘stacking’ methodology (Sánchez et al., 2014). Deliverables will include

- an aeromagnetic-lineament map, including magnetite-destructive and magnetite-additive discontinuities;
- map of lineaments defining magnetic-anomaly axes;
- a multi-dataset attribute database, including airborne magnetic and gravity interpretation, and structural geomorphology for lineament reliability index; and
- airborne magnetic- and gravity-domain maps.

The goal is to generate an updated 1:400 000 scale geological map for the QUEST project area. This final phase of the project will consider

- multilayer correlation of airborne magnetic and gravity domains with known geological units; and

- interpretation of aeromagnetic lineaments as faults, sedimentary and metamorphic fabric, dikes or other geological structures.

All maps and digital files, including the new set of geophysical filters, will be delivered with the final technical report in April 2015. The goal is that this new geological and geophysical dataset will contribute considerably to a better understanding of BC’s geology and can be used as a base layer for the exploration for porphyry-style deposits across the QUEST project area. Airborne magnetic surveys constitute one of the most widely used geophysical techniques for mineral exploration, and their structural interpretation has long been used as a guide to regional structural controls on mineralization. The outcomes of this study will enhance mineral exploration decision-making by providing the structural framework required for porphyry and related deposits. Both the structural setting for porphyry emplace-

ment and the subsequent structural disruption may be elucidated.

## Acknowledgments

The authors thank Geoscience BC for funding this project. Special thanks go to C. Barnett for providing valuable editorial comments.

## References

- Andrews, G.D.M. and Russell, J.K. (2010): Distribution and thickness of volcanic and glacial cover on the interior plateaus; *in* Geological Association of Canada, Cordilleran Section 2010, Program and Abstracts, p. 45–48, URL <[http://www.gac-cs.ca/workshops/TGI3/abstracts/12\\_GAC\\_TGI3\\_Andrews\\_distrib\\_thickness\\_cover.pdf](http://www.gac-cs.ca/workshops/TGI3/abstracts/12_GAC_TGI3_Andrews_distrib_thickness_cover.pdf)> [November 2014].
- Barnett, C.T. and Kowalczyk, P.L. (2008): Airborne electromagnetics and airborne gravity in the QUEST project area, Williams Lake to Mackenzie, British Columbia (parts of NTS 093A, B, G, H, J, K, N, O; 094C, D); *in* Geoscience BC Summary of Activities 2007, Geoscience BC, Report 2008-1, p. 1–6, URL <[http://www.geosciencebc.com/i/pdf/SummaryofActivities2007/SoA2007-Barnett\\_original.pdf](http://www.geosciencebc.com/i/pdf/SummaryofActivities2007/SoA2007-Barnett_original.pdf)> [November 2014].
- Barnett, C.T. and Williams, P.M. (2009): Using geochemistry and neural networks to map geology under glacial cover; *in* Geoscience BC, Report 2009-03 (updated 2011), URL <<http://www.geosciencebc.com/s/2009-03.asp>> [November 2014].
- Bissig, T., Logan, J., Heberlein, D.R. and Ma, F. (2011): Ground testing of predicted geology based on stream and lake sediment geochemistry in the QUEST area, using previously undocumented bedrock exposures; Geoscience BC, Report 2011-06, 34 p., URL <<http://www.geosciencebc.com/s/2011-06.asp>> [November 2014].
- Bordet, E., Mihalynuk, M.G., Hart, C.J.R. and Sanchez, M. (2014): Three-dimensional thickness model for the Eocene volcanic sequence, Chilcotin and Nechako plateaus, central British Columbia (NTS 0920, P, 093A, B, C, E, F, G, K, L); *in* Geoscience BC Summary of Activities 2013, Geoscience BC, Report 2014-1, p. 43–52, URL <[http://www.geosciencebc.com/i/pdf/SummaryofActivities2013/SoA2013\\_Bordet.pdf](http://www.geosciencebc.com/i/pdf/SummaryofActivities2013/SoA2013_Bordet.pdf)> [November 2014].
- Colpron, M., and Nelson, J.L. (2011): A digital atlas of terranes for the northern Cordillera; BC Ministry of Energy and Mines, BC Geological Survey, GeoFile 2011-11, URL <http://www.empr.gov.bc.ca/Mining/Geoscience/PublicationsCatalogue/GeoFiles/Pages/2011-11.aspx> [November 2014].
- Devine, F.A., Chamberlain, C.M., Davies, A.G., Friedman, R. and Baxter, P. (2014). Geology and district-scale setting of tilted alkalic porphyry Cu-Au mineralization at the Lorraine deposit, British Columbia; *Economic Geology*, v. 109, p. 939–977.
- Dragoni, M. (1993): The brittle-ductile transition in tectonic boundary zones; *Annals of Geophysics*, v. 36, p. 37–44.
- Farr, T.G., Rosen, P.A., Caro, E., Crippen, R., Duren, R., Hensley, S., Kobrick, M., Paller, M., Rodriguez, E., Roth, L., Seal, D., Shaffer, S., Shimada, J. and Umland, J. (2007): The Shuttle Radar Topography Mission; *Reviews of Geophysics*, v. 45, no. 2.
- Geoscience BC (2009a): QUEST project compilation maps; Geoscience BC, Report 2009-4, URL <<http://www.geosciencebc.com/s/2009-04.asp>> [November 2014].
- Geoscience BC (2009b): QUEST project – geology; Geoscience BC, Map 2009-4-1, scale 1:500 000, URL <[http://www.geosciencebc.com/i/project\\_data/QUESTdata/GBCReport2009-4/map\\_2009\\_4\\_1\\_geo.pdf](http://www.geosciencebc.com/i/project_data/QUESTdata/GBCReport2009-4/map_2009_4_1_geo.pdf)> [November 2014].
- Gunn, P.J. (1997): Quantitative methods for interpreting aeromagnetic data: a subjective review; *AGSO Journal of Australian Geology and Geophysics*, v. 17, p. 105–114.
- Gunn, P.J., Maidment, D. and Milligan, P.R. (1997): Interpreting aeromagnetic data in areas of limited outcrop; *AGSO Journal of Australian Geology and Geophysics*, v. 17, p. 175–186.
- Hildenbrand, T.G. (1983): FFTFIL: a filtering program based on two-dimensional Fourier analysis; United States Geological Survey, Open-File Report 83–237, 54 p., URL <<http://pubs.usgs.gov/of/1983/0237/report.pdf>> [November 2014].
- Jacobsen, B.H. (1987): A case for upward continuation as a standard separation filter for potential-field maps; *Geophysics*, v. 52, p. 1138–1148, doi:10.1190/1.1442378.
- Jago, C.P., Tosdal, R.M., Cooke, D.R. and Harris, A.C. (2014): Vertical and lateral variation of mineralogy and chemistry in the Early Jurassic Mt. Milligan alkalic porphyry Au-Cu deposit, British Columbia, Canada; *Economic Geology*, v. 109, no. 4, p. 1005–1033.
- Logan, J.M., Schiarizza, P., Struik, L.C., Barnett, C., Nelson, J.L., Kowalczyk, P., Ferri, F., Mihalynuk, M.G., Thomas, M.D., Gammon, P., Lett, R., Jackaman, W. and Ferbey, T. (2010): Bedrock geology of the QUEST map area, central British Columbia; Geoscience BC, Report 2010-5, British Columbia Geological Survey, Geoscience Map 2010-1 and Geological Survey of Canada, Open File 6476, URL <<http://www.geosciencebc.com/s/2010-005.asp>> [November 2014].
- Massey, N.W.D., MacIntyre, D.G., Desjardins, P.J. and Cooney, R.T. (2005): Geology of British Columbia; British Columbia Geological Survey, Geoscience Map 2005-3, scale 1:1 000 000, URL <<http://www.empr.gov.bc.ca/Mining/Geoscience/PublicationsCatalogue/Maps/GeoscienceMaps/Pages/2005-3.aspx>> [November 2014].
- Milligan, P.R., and Gunn, P.J. (1997): Enhancement and presentation of airborne geophysical data; *AGSO Journal of Australian Geology and Geophysics*, v. 17, p. 63–75.
- Monger, J.W.H., Price, R.A. and Tempelman-Kluit, D.J. (1982): Tectonic accretion and the origin of the two major metamorphic and tectonic belts in the Canadian Cordillera; *Geology*, v. 10, p. 70–75.
- Mortimer, N. (1987) The Nicola Group: Late Triassic and Early Jurassic subduction-related volcanism in British Columbia; *Canadian Journal of Earth Sciences*, v. 24, p. 2521–2536.
- Nelson, J.L., Colpron, M. and Israel, S. (2013): The Cordillera of British Columbia, Yukon and Alaska: tectonics and metallogeny; *in* *Tectonics, Metallogeny, and Discovery: The North American Cordillera and Similar Accretionary Settings*, M. Colpron, T. Bissig, B.G. Rusk and J.F.H. Thompson (ed.), Society of Economic Geologists, Special Publication 17, p. 53–110.
- Pass, H.E., Cooke D.R., Davidson G., Maas R., Dipple G., Rees C., Ferreira L., Taylor C. and Deyell C.L. (2014): Isotope geochemistry of the Northeast zone, Mount Polley alkalic Cu-

- Au-Ag porphyry deposit, British Columbia: a case for carbonate assimilation; *Economic Geology*, v. 109, no. 4, p. 859–890.
- Sánchez, M.G., Allan, M.M., Hart, C.J.R. and Mortensen J.K. (2014): Extracting ore-deposit–controlling structures from aeromagnetic, gravimetric, topographic, and regional geologic data in western Yukon and eastern Alaska; *Interpretation*, v. 2, no. 4, p. 1–28.
- Sander Geophysics Ltd. (2008): Airborne gravity survey, Quesnellia region, British Columbia; Geoscience BC, Report 2008-8, 121 p., URL <<http://www.geosciencebc.com/s/2008-08.asp>> [November 2014].
- Spector, A. (1985): Comment on “Statistical methods for interpreting aeromagnetic data”, by A. Spector and F.S. Grant; *Geophysics*, v. 50, p. 2278.



# Mineralogical Characteristics of Porphyry-Fertile Plutons: Guichon Creek, Takomkane and Granite Mountain Batholiths, South-Central British Columbia

F. Bouzari, Mineral Deposit Research Unit, University of British Columbia, Vancouver, BC, fbouzari@eos.ubc.ca

C.J.R. Hart, Mineral Deposit Research Unit, University of British Columbia, Vancouver, BC

T. Bissig, Mineral Deposit Research Unit, University of British Columbia, Vancouver, BC

---

Bouzari, F., Hart, C.J.R. and Bissig, T. (2015): Mineralogical characteristics of porphyry-fertile plutons: Guichon Creek, Takomkane and Granite Mountain batholiths, south-central British Columbia; *in* Geoscience BC Summary of Activities 2014, Geoscience BC, Report 2015-1, p. 63–68.

## Introduction

Distinguishing metal-fertile from barren plutons continues to be a significant challenge for geologists exploring for porphyry Cu (Au, Mo) deposits. Information that contributes such a priori knowledge provides guidance early in the exploration process to make decisions more effectively and efficiently on focusing exploration resources on more prospective targets. However, geologists do not have access to such tools that can effectively identify features of enhanced fertility and prospectivity. This research project, therefore, provides tools and strategies that emphasize porphyry fertility in the BC context (see Figure 2 below for project location).

The most fundamental process in the formation of porphyry copper deposits is the exsolution of metal-rich magmatic hydrothermal fluids in large crystallizing batholiths below the site of the deposit (Dilles and Einaudi, 1992). These buoyant fluids stream through the crust to form perched porphyry copper deposits, but in many districts large deposits are hosted directly within or adjacent to the large causative plutons. In all cases, these plutons will host evidence that record porphyry fertility characteristics. The relationship between magmatic processes and ore deposits has long been the focus of ore deposit research, but past studies have generally concentrated on the deposit scale. The purpose of this project is to look at the district to batholith scale, which will provide a level of assessment not previously documented in BC.

The characterization of fertility features is of particular importance for BC porphyry exploration. In BC, many porphyry systems occur within or around the edges of large batholiths, or are in systems that have been tilted such that

the deeper plutonic parts of the system are well exposed. These combined features make BC an exceptional locality to test and utilize such porphyry fertility indicators. In addition to the evaluation of such plutons on the basis of rock characteristics, fertility can also be assessed using mineral concentrates from stream sediments and glacial till.

## Mineral Recorders of Fertility

Previous studies have indicated a range of preferable melt characteristics and ore-forming processes that influence the porphyry fertility of a crystallizing magma. Information about these features and processes, such as oxidation state, fractionation, magma mixing and the amount and saturation of water, metal, chlorine and sulphur and so forth, are variably recorded in crystallizing accessory minerals of the parent pluton. Evidence of these features may be recorded as particular mineral assemblages or as minerals having particular characteristics or chemical composition. The most apparent features would include zoning, mineral or fluid inclusions, or resorbed zones or margins. Examples include the following:

- Apatite crystals from fertile systems can be zoned with sulphur-rich cores and sulphur-poor rims, indicating early sulphate saturation and the crystallization of anhydrite (Figure 1a, b). Such observations have been made at the Yerington batholith, Nevada (Streck and Dilles, 1998) and Galore Creek porphyry Cu-Au deposit, BC (Liaghat and Tosdal, 2008).
- Apatite trace-element compositions can record the degree of fractionation and oxidation state of the magma (Belousova et al., 2002).
- Zircons from porphyry fertile intrusions in northern Chile have Ce and Eu compositions with significantly higher oxidation states than barren intrusions (Ballard et al., 2002).
- Co-existing hornblende and magnetite is a diagnostic feature of mineralized silica-undersaturated igneous complexes in BC (Lueck and Russell, 1994).

---

**Keywords:** *fertile plutons, porphyry copper, British Columbia*

*This publication is also available, free of charge, as colour digital files in Adobe Acrobat® PDF format from the Geoscience BC website: <http://www.geosciencebc.com/s/DataReleases.asp>.*

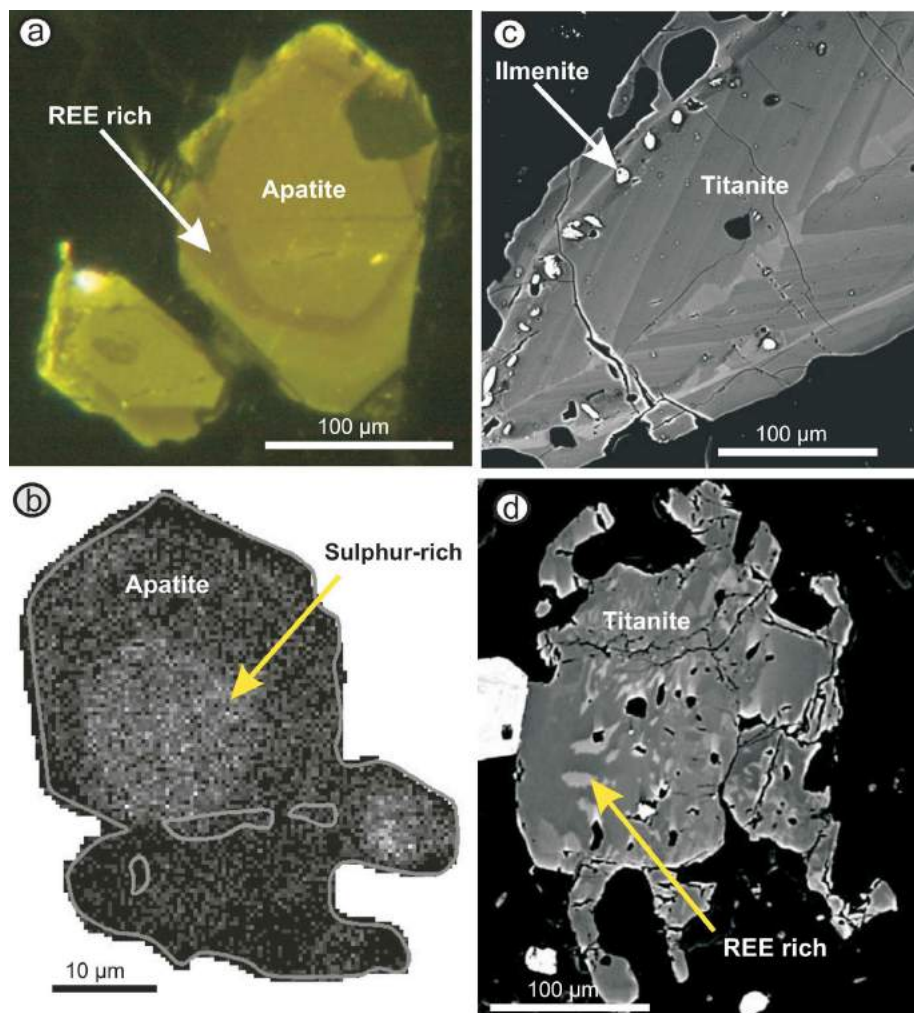


**Figure 1.** Examples of mineralogical features that can be used to characterize porphyry fertility of igneous bodies: **a)** apatite grain from Bethlehem granodiorite (Highland Valley) of the Guichon Greek batholith displays zoning reflecting changing magma compositions and enrichment, in this case recorded by rare-earth element (REE) and probably sulphur content (Bouzari et al., 2011); **b)** X-ray intensity of apatite from Yerington batholith showing a sulphur-poor rim indicating sulphur extraction from the magma (Streck and Dilles, 1998); **c)** titanite with concentric oscillatory and sector zoning, which records redox changes and instability in the melt, particularly a distinctly reducing event that deposited ilmenite grains near the margin (Russ of Mull granite, Scotland; McLeod et al., 2011); **d)** patchy zoning in titanite with interstitial and marginal growth indicating the introduction of late fluids and modification of REE compositions (McLeod et al., 2011).

- Titanite displays concentric oscillatory zoning and rare-earth element-rich patches that represent changes in melt composition from magma mixing and late subsolidus modification by fluids (Figure 1c, d; McLeod et al., 2011).

Therefore, mineralogical characteristics observed in the plutonic rocks hosting porphyry stocks can record processes that led to the generation of porphyry copper-gold mineralization.

### Objectives

This project identifies field, mineralogical and geochemical characteristics of known porphyry-fertile plutons and develops exploration tools for the subsequent identifica-

tion of new fertile plutonic terrains of BC. Physical and chemical features in common accessory minerals, (e.g., apatite, titanite, zircon) that show evidence of magmatic processes such as high oxidation state, evidence of fluid saturation, magma fertilization by mafic melt injection, and sulphate saturation and depletion in the melt will be characterized. Specific objectives of this project are to

- determine the mineralogical features of common accessory minerals that characterize and distinguish porphyry-fertile intrusions;
- assess geochemical features of common accessory minerals that indicate fertility;
- document fertility evidence over time and space in an evolving composite zoned pluton;

- assess the utilization of rapid mineralogical characterization tools; and
- construct a toolkit to provide a predictive decision-making framework to assess fertility in rocks, stream sediment and till-heavy mineral concentrates.

Porphyry copper-gold deposits in BC provide an excellent opportunity to study the relationship between ore deposits and hosting plutons and batholiths. This is because many of the BC porphyry deposits are hosted in stocks within a composite zoned batholith of similar age (Lang et al., 1995; McMillan et al., 1995). Various phases of the batholith and mineralized stock are exposed at or near surface and accessory minerals such as apatite, titanite, zircon, magnetite and garnet (melanite) occur in various proportions in different plutons and associated alteration zones.

### Methods

Field and laboratory work will focus on characterization of accessory minerals in various intrusive bodies of three well-documented and mapped batholiths, the Guichon Creek, Takomkane and the Granite Mountain batholiths, located in southern and central BC (Figure 2).

#### Guichon Creek Batholith

The Late Triassic Guichon Creek batholith (65 by 20 km) is a composite batholith that ranges from diorite and quartz diorite compositions at the border, to younger granodiorite in the centre (Casselmann et al., 1995), which hosts most of the several Highland Valley porphyry Cu-Mo deposits (Valley, Lornex, Highmont, Alwin, Bethlehem and JA). The geology of the footprint regions surrounding the mineral deposits is currently being evaluated through a project funded by the Canadian Mining Innovation Council (CMIC), and the alteration mineralogy and geochemistry of Valley, Bethlehem and Alwin deposits were the subject of past Mineral Deposit Research Unit (MDRU) projects on alteration footprints and porphyry indicator mineral projects. These studies provide an excellent basis for this project.

#### Takomkane Batholith

The Takomkane batholith is a large (40 by 50 km) Late Triassic–Early Jurassic composite intrusive body that hosts several mineralized centres including the Woodjam porphyry camp (Megabuck, Takom, Southeast and Dehorn). Previous investigations of these rocks (e.g., Schiarizza et al., 2009), and a recent MDRU study (Bouzari et al., 2011; del Real et al., 2014) provide a strong foundation for the geology, geochronology and mineralization of this region. The Takomkane batholith records a magmatic evolution lasting 11 m.y., with three separate mineralizing events at Woodjam. Moreover, the presence of Cu-Au and Cu-Mo deposits together with the regional northwest tilting of geological units provides an insight into different levels of exposure

and potentially subtle geochemical variations within the intrusive bodies.

#### Granite Mountain Batholith

The Granite Mountain batholith (18 by 10 km) occurs near McLeese Lake in south-central BC and hosts the Gibraltar porphyry Cu-Mo mine. The Late Triassic Granite Mountain batholith is subdivided into three main units, namely from southwest to northeast: Border phase diorite to quartz diorite; Mine phase tonalite; and Granite Mountain phase leucocratic tonalite. It was originally thought that the Granite Mountain batholith had intruded into the Cache Creek terrane (Bysouth et al., 1995). But recent study by Schiarizza (2014) recognized Nicola Group strata occurring on the northeastern margin of the batholith and suggested that it is more likely a part of the Quesnel terrane, and correlative with the Late Triassic, calcalkaline Guichon Creek batholith, host to the Highland Valley porphyry Cu-Mo deposits, 250 km to the south-southeast.

Rock samples from different intrusive units will be examined to characterize each unit. Minerals will be examined in situ but also extracted initially using nondestructive crushing. The focus of this work will be on examining the physical and chemical features of accessory minerals such as apatite, titanite, zircon, magnetite or garnet.

Techniques used to study these samples will emphasize observational methods such as binocular microscopy, petrography, cathodoluminescence, infrared/ultraviolet light and scanning electron microscopy (SEM). In cases where features are observed, trace-element–geochemical analysis of these minerals will be performed using electron microprobe and laser-ablation, multiple-collector, inductively coupled plasma–mass spectrometry (LA-MC-ICP-MS) methods. Automated SEM techniques such as mineral liberation analysis (MLA) will be tested to provide a fast method to record textural and chemical characteristics. In addition, all other aspects such as physical properties, whole rock litho-geochemistry, redox state and age of crystallization (for unknown units) will be determined. Relative and absolute timing is also an important factor. Thus, characterizing the evolution and differences between intrusive phases within a single mineralizing system that form slightly before and after mineralization (which is common in porphyry deposits) is important.

#### Current Work

Sampling was initiated in late August 2014 and will continue in summer 2015. Archived sample material in MDRU’s rock collection from previous projects as well as current mapping projects in Granite Mountain batholith by the British Columbia Geological Survey (BCGS) will also be utilized to complement this year’s fieldwork.

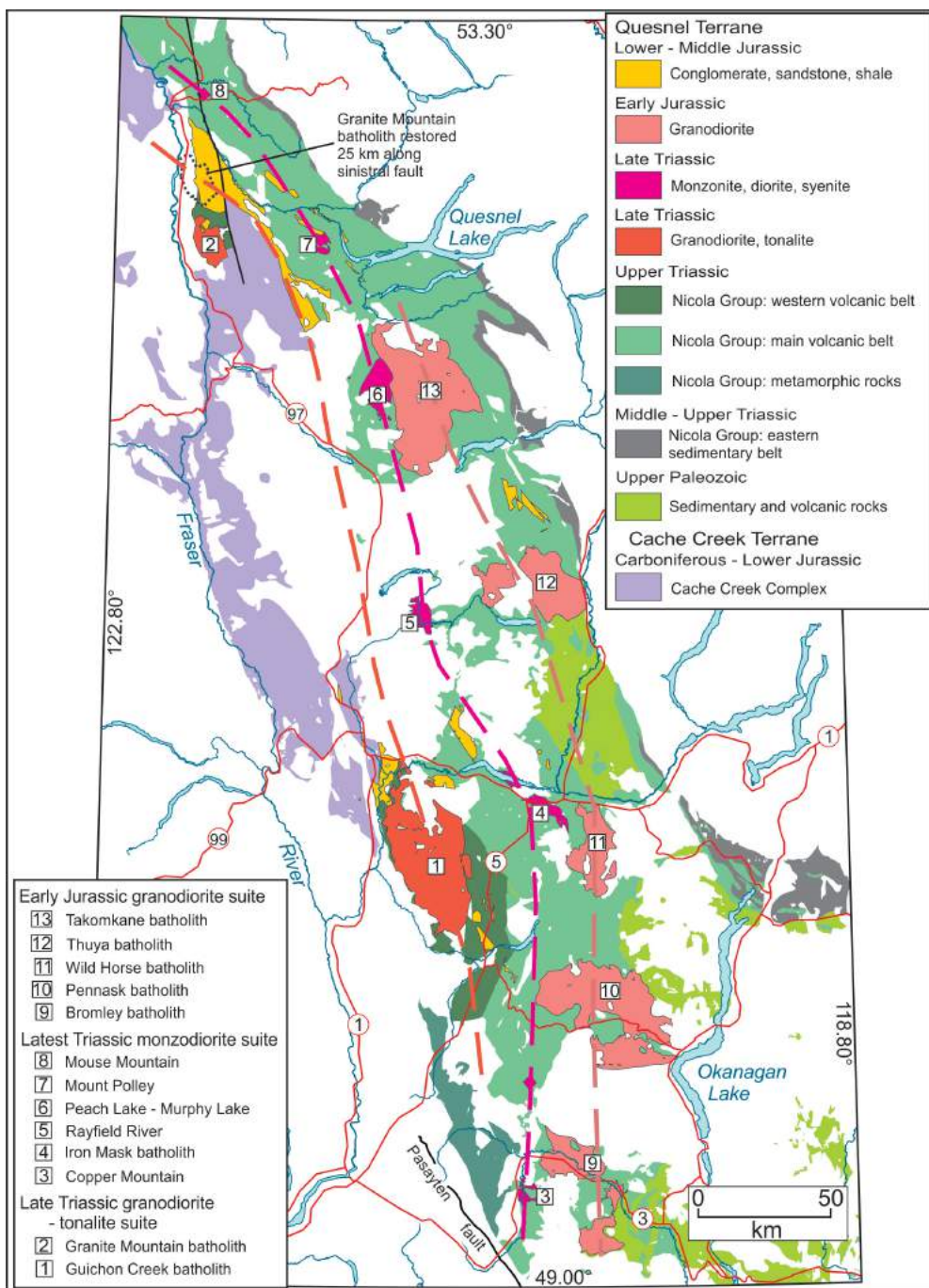


**Figure 2.** Simplified geology map of south-central British Columbia showing location of major plutonic bodies. Dashed lines illustrate parallel belts of calcalkaline or alkaline plutons that show a progressive younging from west to east (from Schiarizza, 2014).

Rocks will be well documented and processed to obtain thin sections and mineral separates that will be evaluated using a range of observable techniques including binocular and petrographic microscopes, SEM and by cathodoluminescence. Selected samples will be evaluated for mineral chemistry using the electron microprobe and LA-MC-ICP-MS to characterize previously observed features. Mineral liberation analysis techniques will be utilized to assess rapid automatic detection of key features of interest. Results, including poster displays and articles for the *Geo-*

*science BC Summary of Activities* series, will be released in the winter of 2015 and 2016.

### Acknowledgments

Geoscience BC is thanked for its generous financial contribution in support of this project. The authors also thank M. Allan of the Mineral Deposit Research Unit for his review of and comments on this report.

## References

- Ballard, J.R., Palin, J.M. and Campbell, I.H. (2002): Relative oxidation states of magmas inferred from Ce(IV)/Ce(III) in zircon: application to porphyry copper deposits of northern Chile; *Contributions to Mineralogy and Petrology*, v. 144, p. 347–364.
- Belousova, E.A., Griffin, W.L., O'Reilly, S.Y. and Fisher, N.I. (2002): Apatite as an indicator mineral for mineral exploration: trace-element compositions and their relationship to host rock type; *Journal of Geochemical Exploration*, v. 76, p. 45–69.
- Bouzari, F., Hart, C.J.R., Barker, S. and Bissig, T. (2011): Porphyry indicator minerals (PIMs): exploration for concealed deposits in central British Columbia; Geoscience BC, Report 2011-17, 31 p., URL <[http://www.geosciencebc.com/i/project\\_data/GBC\\_Report2011-17/GBCReport2011-17\\_report.pdf](http://www.geosciencebc.com/i/project_data/GBC_Report2011-17/GBCReport2011-17_report.pdf)> [November 2014].
- Bysouth, G.D., Campbell, K.V., Barker, G.E. and Gagnier, G.K. (1995): Tonalite-trondhjemite fractionation of peraluminous magma and the formation of syntectonic porphyry copper mineralization, Gibraltar mine, central British Columbia; *in* *Porphyry Deposits of the Northwestern Cordillera of North America*, T.G. Schroeter (ed.), Canadian Institute of Mining, Metallurgy and Petroleum, Special Volume 46, p. 201–213.
- del Real, I., Hart, C.J.R., Bouzari, F., Blackwell, J.L., Rainbow, A. and Sherlock, R. (2014): Relationships between calcalkalic and alkalic mineralization styles at the copper-molybdenum Southeast Zone and copper-gold Deerhorn porphyry deposit, Woodjam property, central British Columbia; *in* *Geoscience BC Summary of Activities 2013*, Geoscience BC, Report 2014-1, p. 63–82, URL [http://www.geosciencebc.com/i/pdf/SummaryofActivities2013/SoA2013\\_delReal.pdf](http://www.geosciencebc.com/i/pdf/SummaryofActivities2013/SoA2013_delReal.pdf) [November 2014].
- Dilles, J.H. and Einaudi, M.T. (1992): Wall-rock alteration and hydrothermal flow paths about the Ann-Mason porphyry copper deposit, Nevada: a 6-km vertical reconstruction; *Economic Geology*, v. 87, p. 1963–2001.
- Lang, J.R., Lueck, B., Mortensen, J.K., Russell, J.K., Stanley, C.R. and Thompson, J.F.H. (1995): Triassic-Jurassic silica-undersaturated and silica-saturated alkalic intrusions in the cordillera of British Columbia: implications for arc magmatism; *Geology*, v. 23, p.451–454.
- Liaghat, S. and Tosdal, R. (2008): Apatite chemical composition and textures as a probe into magmatic conditions at Galore Creek porphyry copper-gold deposit, British Columbia (abstract): 18th Annual V.M. Goldschmidt Conference; *Geochimica et Cosmochimica Acta*, v. 72, no. 12, p. A550.
- Lueck, B.A. and Russell, J.K. (1994): Silica-undersaturated, zoned alkaline intrusions within the British Columbia cordillera; *in* *Geological Fieldwork 1993*, BC Ministry of Energy and Mines, BC Geological Survey, Paper 1994-1, p. 311–315.
- McLeod, G.W., Dempster and T.J., Faithfull, J.W. (2011): Deciphering magma-mixing processes using zoned titanite from the Ross of Mull granite, Scotland; *Journal of Petrology*, v. 52, p. 55–82.
- McMillan, W.J., Thompson, J.F.H., Hart, C.J.R. and Johnston, S.T. (1995): Regional geological and tectonic setting of porphyry deposits in British Columbia and Yukon Territory; *in* T.G. Schroeter (ed.), *Porphyry Deposits of the Northwestern Cordillera of North America*, CIM, Special Volume 46, p. 40–57.
- Schiarizza, P. (2014): Geological setting of the Granite Mountain batholith, host to the Gibraltar porphyry Cu-Mo deposit, south-central British Columbia; *in* *Geological Fieldwork 2013*, BC Ministry of Energy and Mines, BC Geological Survey Paper 2014-1, p. 95–110.
- Schiarizza, P., Bell, K. and Bayliss, S. (2009): Geology and mineral occurrences of the Murphy Lake area, south-central British Columbia (NTS 093A/03); *in* *Geological Fieldwork 2008*, BC Ministry of Energy and Mines, BC Geological Survey, Paper 2009-1, p. 169–188, URL <[http://www.empr.gov.bc.ca/Mining/Geoscience/Publications/Catalogue/Fieldwork/Documents/2008/15\\_Schiarizza.pdf](http://www.empr.gov.bc.ca/Mining/Geoscience/Publications/Catalogue/Fieldwork/Documents/2008/15_Schiarizza.pdf)> [November 2014].
- Streck, M.J. and Dilles, J.H. (1998): Sulfur evolution of oxidized arc magmas as recorded in apatite from a porphyry copper batholith; *Geology*, v. 26, p. 523–526.



# Geological Mapping, Compilation and Mineral Evaluation of the Almond Mountain Map Area, Southern British Columbia (NTS 082E/07)

T. Höy, Consultant, Sooke, BC, thoy@shaw.ca

W. Jackaman, Noble Exploration Services Ltd., Sooke, BC

---

Höy, T. and Jackaman, W. (2015): Geological mapping, compilation and mineral evaluation of the Almond Mountain map area, southern British Columbia (NTS 082E/07); in Geoscience BC Summary of Activities 2014, Geoscience BC, Report 2015-1, p. 69–72.

## Project Summary

The Almond Mountain project includes geological mapping and compilation of a large part of the 1:50 000 scale Almond Mountain map area (NTS 082E/07), located in the Monashee Mountains of southern British Columbia. The project is an extension to the west of mapping, compilation and mineral-potential evaluation of the east half of the 1:250 000 scale Penticton map area (NTS 082E), which included the Grand Forks (NTS 082E/01), Deer Park (NTS 082E/08) and Burrell Creek (NTS 082E/09) map areas (Höy and Jackaman, 2005, 2010, 2013; Figure 1). These projects focused mainly on the potential and controls of Tertiary<sup>1</sup> mineralization along the northern margin of the Grand Forks gneiss complex (Preto, 1970), and recognized and defined a variety of base-metal and precious-metal mineral deposits that appear to be related to prominent north- and northwest-trending regional structures. Geological mapping in the Burrell Creek and Deer Park map areas recognized that metallic mineral deposits, including the Franklin mining camp, are controlled by two prominent structural trends: north-trending Eocene extensional faults and earlier northwest-trending structural zones (Höy, 2013). Furthermore, it was recognized that most deposits occur in the hangingwall of the north-trending faults due, in part, to a genetic relationship to these faults but also to the realization that hangingwall panels expose higher intrusive and structural levels, both of which are more favourable settings for mineralization.

The Almond Mountain project, and the continuation to the north in the Christian Valley map area (NTS 082E/10) in

2016, will extend this work into an area that has attracted some historical and recent exploration, mainly due to successful gold and base-metal exploration in the Greenwood area immediately to the south (Church, 1986; Fyles, 1990; Massey et al., 2010) and farther south in the Republic District of Washington State. However, there has been little university- or government-led exploration research since a regional (1:250 000 scale) mapping and compilation done in the 1980s (Tempelman-Kluit, 1989), with some work focused on Paleozoic successions in the western part of the area by Massey (2006, 2009) and Massey and Duffy (2008).

The Almond Mountain project will include approximately 40 days of geological mapping, which will concentrate on areas of mineral occurrences and higher mineral potential, as well as the evaluation and upgrading of the mineral-occurrence database (BC MINFILE). Geological mapping began late in 2014 and will be completed during the 2015 field season. The project will also include compilation in digital format of all regional geological, geophysical and geochemical data collected under the National Geochemical Reconnaissance (NGR) Program and the BC Regional Geochemical (RGS) Program. This will be combined with mineral occurrence and geology databases to produce several 1:20 000 and 1:50 000 scale maps suitable for directing and focusing mineral exploration. Data, including integrated geological maps, poster displays and *Geoscience BC Summary of Activities* papers, will be released on completion of the Almond Mountain project in the winter of 2015–2016, and for the Christian Valley map area the following year.

The project is intended to integrate all geological data in the east half of the 1:250 000 scale Penticton map area (NTS 082E), including NGR/RGS data and regional geophysical studies. These data, combined with mineral occurrence databases, will provide models that will help both direct and understand the relationship between mineralizing systems and Tertiary extension and magmatism. It is hoped that new mapping and data will spur grassroots prospecting and help focus exploration activity in an area of southern British Columbia that, due partly to limited access in the past, lack of recent government or university input and poorly understood geology, is historically underexplored.

---

<sup>1</sup>*Tertiary* is an historical term. The International Commission on Stratigraphy recommends using 'Paleogene' (comprising the Paleocene to Oligocene epochs) and 'Neogene' (comprising the Miocene and Pliocene epochs). The author used the term 'Tertiary' because it was used in the source material for this report.

**Keywords:** geology, regional compilation, Eocene Coryell alkalic intrusions, Jurassic-Cretaceous intrusions, Eocene extensional tectonics

This publication is also available, free of charge, as colour digital files in Adobe Acrobat® PDF format from the Geoscience BC website: <http://www.geosciencebc.com/s/DataReleases.asp>.

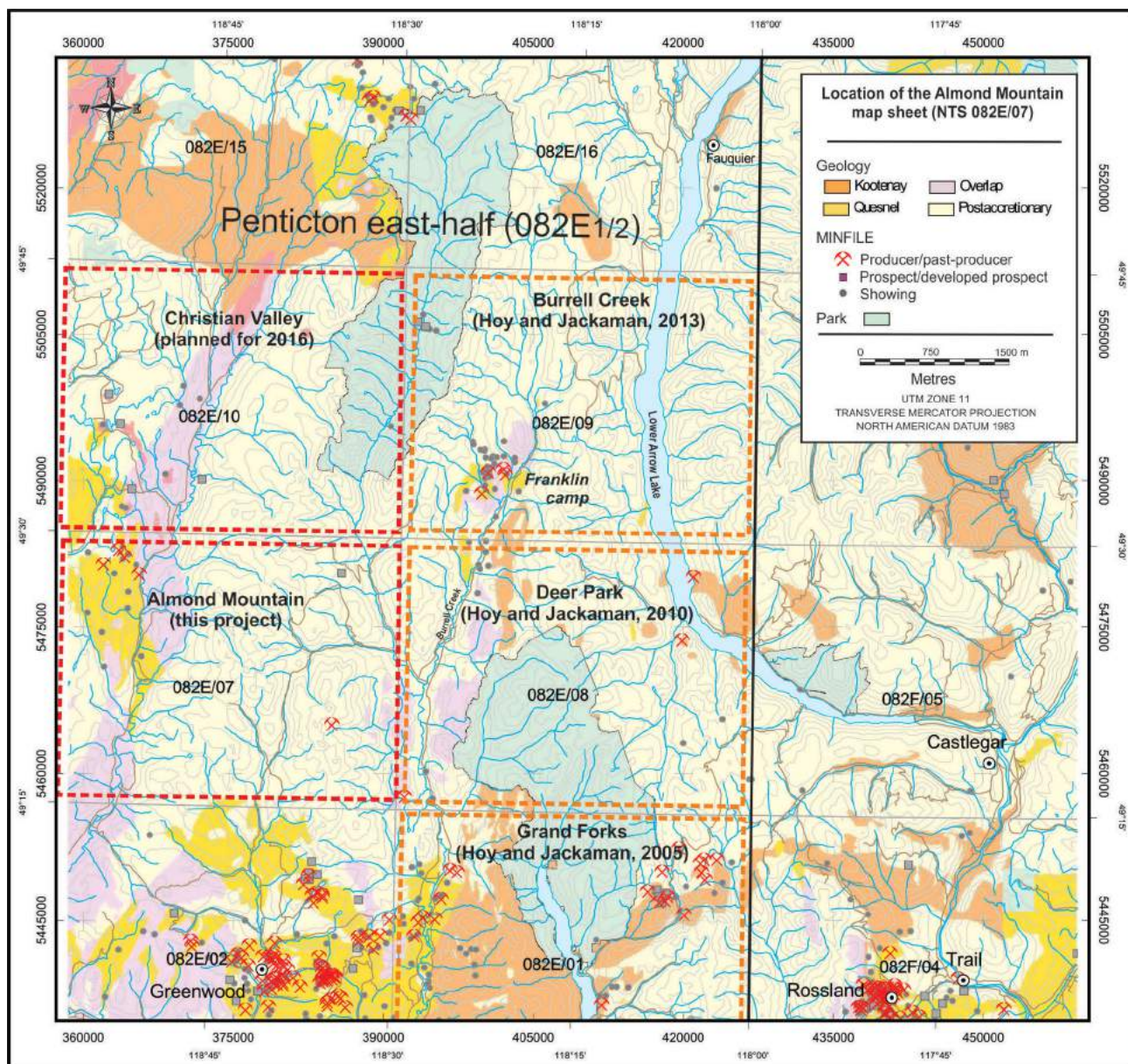


Figure 1. Location of the Almond Mountain map sheet (NTS 082E/07), southern British Columbia.

### Acknowledgments

The authors thank M. Seabrook and G. DeFields for reviewing this paper.

### References

- Church, B.N. (1986): Geological setting and mineralization in the Mount Attwood–Phoenix area of the Greenwood camp; BC Ministry of Energy and Mines, Paper 1986-2, 65 p.
- Fyles, J.T. (1990): Geology of the Greenwood–Grand Forks area, British Columbia; BC Ministry of Energy and Mines, Open File 19.
- Höy, T. (2013): Burrell Creek map area: setting of the Franklin mining camp, southeastern British Columbia; *in* Geoscience BC Summary of Activities 2012, Geoscience BC, Report 2013-1, p. 91–101.
- Hoy, T. and Jackaman, W. (2005): Geology of the Grand Forks map area, British Columbia (NTS 082E/01); BC Ministry of Energy and Mines, Geoscience Map 2005-2, scale 1:50 000.
- Höy, T. and Jackaman, W. (2010): Geology of the Deer Park map sheet (NTS 82E/08); Geoscience BC, Map 2010-7-1, scale 1:50 000.
- Höy, T. and Jackaman, W. (2013): Geology of the Burrell Creek map sheet (NTS 82E/09); Geoscience BC, Map 2013-07-1, scale 1:50 000.
- Massey, N. (2006): Boundary project: reassessment of Paleozoic rock units of the Greenwood area, southern BC; *in* Geological Fieldwork 2005, BC Ministry of Energy and Mines, BC Geological Survey, Paper 2006-1, p. 99–107.
- Massey, N. (2009): Boundary project: geochemistry of volcanic rocks of the Wallace Formation, Beaverdell area, south-central BC; *in* Geological Fieldwork 2008, BC Ministry of En-

- ergy and Mines, BC Geological Survey, Paper 2009-1, p. 143–152.
- Massey, N. and Duffy, A. (2008): Boundary project: McKinney Creek and Beaverdell areas, south-central BC; *in* Geological Fieldwork 2007, BC Ministry of Energy and Mines, BC Geological Survey, Paper 2008-1, p. 87–102.
- Massey, N., Gabites, J.E., Mortensen, J.K. and Ullrich, T.D. (2010): Boundary project: geochronology and geochemistry of Jurassic and Eocene intrusions, southern British Columbia (NTS 082E); *in* Geological Fieldwork 2009, BC Ministry of Energy and Mines, BC Geological Survey, Paper 2010-1, p. 127–142.
- Preto, V.A. (1970): Structure and petrology of the Grand Forks Group, BC; Geological Survey of Canada, Paper 69-22.
- Tempelman-Kluit, D. J. (1989): Geology, Penticton, British Columbia; Geological Survey of Canada, Map 1736A, scale 1:250 000.



# Structural Controls on the Kimberley Gold Trend, Southeastern British Columbia (NTS 082F, G)

M. Seabrook, Consultant, Calgary, AB, [michaelseabrook@calderageology.ca](mailto:michaelseabrook@calderageology.ca)

T. Höy, Consultant, Sooke, BC

---

Seabrook, M. and Höy, T. (2015): Structural controls on the Kimberley gold trend, southeastern British Columbia (NTS 082F, G); in Geoscience BC Summary of Activities 2014, Geoscience BC, Report 2015-1, p. 73–76.

## Project Summary

The Kimberley Gold Trend project involves geological mapping and historical data compilation as part of Geoscience BC's Stimulating Exploration in the East Kootenays (SEEK) program. The project is focused in the Purcell Mountains west-southwest of the town of Cranbrook and covers parts of NTS map areas 082F and G. The purpose of the project is to identify important structural features that are associated with known gold occurrences and to develop a model for the emplacement of gold within the Kimberley gold trend.

The project area is underlain by rocks of the Proterozoic Belt-Purcell Supergroup that have undergone several episodes of regional tectonism (Höy, 1993; Price and Sears, 2000). The Kimberley gold trend is host to four rich placer-gold streams, discovered in the late 19th century, on which mining activities continue to present day. A significant lode-gold source for the rich placer deposits has not been discovered, although many small deposits and occurrences have been located. Most of the large-scale, publicly funded, geological research projects have focused on the synsedimentary Proterozoic base-metal occurrences in the area, due to the attraction of the Sullivan mine near Kimberley. Previous research efforts directed toward gold mineralization in the East Kootenays have suggested that gold is related to intrusive rocks of the Cretaceous Bayonne Plutonic Suite and stocks of similar age (Soloviev, 2010). Observations by the authors, as well as industry geologists, have emphasized the structural controls on gold emplacement, which is the focus of this project.

The Kimberley gold trend lies within a structural corridor bounded to the northwest and southeast by Proterozoic structures that were reactivated in the Mesozoic, namely the St. Mary's and Moyie faults (Figure 1). Between these, formations of the host Belt-Purcell Supergroup are frac-

tured, folded, altered and mineralized in complex patterns that are not well understood. The purpose of this investigation is to determine:

- the age of gold mineralization relative to intrusive events and structures;
- the relationship between gold mineralization and specific fault structures;
- the potential for certain premineralizing structures to produce either structural traps or conduits for gold mineralization; and
- and categorize the alteration style and mineralogy of structural elements, so they can be readily identified in areas of sparse bedrock.

The project includes approximately 40 days of geological mapping, concentrated mainly in three project areas within the Kimberley gold trend. (Included in the planned field-mapping days are several days spent touring known gold occurrences outside the mapping areas to compare their characteristics with those of showings in the mapping areas.) This work will be augmented by compilation of industry work, including several map programs done by the authors for industry clients between 2011 and 2013. The data from the field program will be analyzed to produce digital geology maps that include compilation of geochemistry, geophysics, geology and drill-location data. The digital database will be used to update BC MINFILE occurrences and create additional files, if required. All of the data will be available in widely used digital formats for reliable integration with other datasets.

## Project Progress

Geological mapping of the Kimberley gold trend began in late 2014 and the project is expected to be completed in the spring of 2015. The project results will be published and released to the public as a Geoscience BC report. It is hoped that the release of this data will spur both grassroots exploration and development of known gold targets in an area of southeastern British Columbia that has had relatively little long-term, focused effort in developing its precious-metal potential.

---

**Keywords:** *geology, regional compilations, Belt-Purcell Supergroup, Laramide orogeny, gold deposit evaluation, Cranbrook area*

*This publication is also available, free of charge, as colour digital files in Adobe Acrobat® PDF format from the Geoscience BC website: <http://www.geosciencebc.com/s/DataReleases.asp>.*

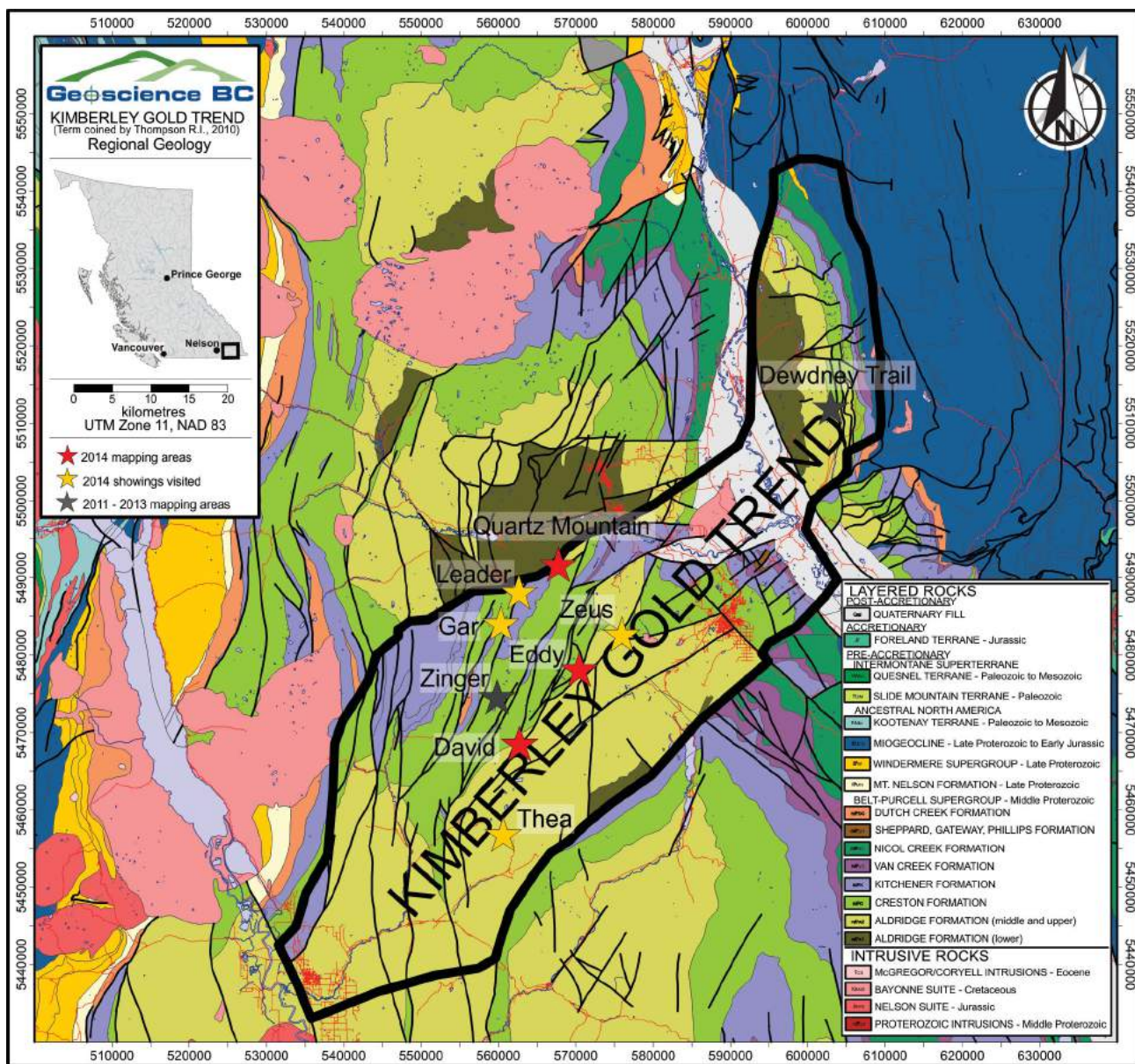


Figure 1. Kimberley gold trend, with locations of mapping projects. Base geology modified from Höy et al. (1995).

### Acknowledgments

This project summary was peer reviewed by Sean Kennedy.

### References

Höy, T. (1993): Geology of the Purcell Supergroup in the Fernie west-half map area, SE British Columbia; BC Ministry of Energy and Mines, BC Geological Survey, Bulletin 84, 157 p., URL <<http://www.empr.gov.bc.ca/Mining/Geoscience/PublicationsCatalogue/BulletinInformation/BulletinsAfter1940/Documents/Bull84.pdf>> [November 2014].

Höy, T., Price, R.A., Legun, A., Grant, B. and Brown, D. (1995): Purcell Supergroup, southeastern British Columbia; BC Ministry of Energy and Mines, BC Geological Survey, Geoscience Map 1995-1, URL <<http://www.empr.gov.bc.ca/Mining/Geoscience/PublicationsCatalogue/Maps/GeoscienceMaps/Documents/GM1995-01.pdf>> [November 2014].

Price, R.A. and Sears, J.W. (2000): A preliminary palinspastic map of the Mesoproterozoic Belt-Purcell Supergroup, Canada and USA: implications for the tectonic setting and structural evolution of the Purcell anticlinorium and the Sullivan deposit; Chapter 5 in *The Geological Environment of the Sullivan Deposit*, British Columbia, J.W. Lydon, T. Höy, J.F. Slack and M.E. Knapp (ed.), Geological Association of Canada, Mineral Deposits Division, Special Publication 1, p. 61–81, URL <[http://geol.queensu.ca/people/price/pdf/SullivanVolCh5\(Price%26Sears\).PDF](http://geol.queensu.ca/people/price/pdf/SullivanVolCh5(Price%26Sears).PDF)> [November 2014].

Soloviev, S.G. (2010): Evaluation of reduced intrusive-related gold mineralization in the area west of Cranbrook, southeastern British Columbia (NTS 082F/08, 16); in *Geological Fieldwork 2009*, BC Ministry of Energy and Mines, BC

Geological Survey, Paper 2010-1, p. 97–111, URL <[http://www.empr.gov.bc.ca/Mining/Geoscience/Publications/Catalogue/Fieldwork/Documents/2009/09\\_Soloviev\\_2009.pdf](http://www.empr.gov.bc.ca/Mining/Geoscience/Publications/Catalogue/Fieldwork/Documents/2009/09_Soloviev_2009.pdf)> [November 2014].

Thompson, R.I. (2011): Geology, exploration program and results from the Dewdney Trail property with recommendations for further exploration, Fort Steele Mining Division, British Co-

lumbia, NTS 82G/12; NI43-101 technical report prepared for PJX Resources Inc. and filed with SEDAR May 27, 2011, 208 p., URL <<http://www.sedar.com/GetFile.do?lang=EN&docClass=24&issuerNo=00031684&fileName=/csfsprod/data118/filings/01750922/00000001/h%3APJX2011May-OfferingTechReport.pdf>> [November 2014].



# Mud Volcanoes in the Purcell Basin and Their Relevance to Mesoproterozoic Massive-Sulphide Ag-Pb-Zn Deposits, Southeastern British Columbia (NTS 082F/01, /08, /09, 082G/04, /05, /12)

S. Kennedy, Consultant, Kimberley, BC, [js\\_kenn@shaw.ca](mailto:js_kenn@shaw.ca)

T. Höy, Consultant, Sooke, BC, [thoy@shaw.ca](mailto:thoy@shaw.ca)

---

Kennedy, S. and Höy, T. (2015): Mud volcanoes in the Purcell Basin and their relevance to Mesoproterozoic massive-sulphide Ag-Pb-Zn deposits, southeastern British Columbia (NTS 082F/01, /08, /09, 082G/04, /05, /12); in Geoscience BC Summary of Activities 2014, Geoscience BC, Report 2015-1, p. 77–78.

## Project Summary

The Purcell Basin fragmental project involves the mapping and rock sampling of various sedimentary fragmental units believed to be related to mud volcanism within the Mesoproterozoic synrift Aldridge Formation in southeastern British Columbia (NTS 082F/01, /08, /09, 082G/04, /05, /12; Figure 1). The project is part of the larger Stimulating Exploration in the East Kootenays (SEEK) program developed by Geoscience BC. The Purcell Basin project is focused on several key areas within the Aldridge Formation, with the intention of creating schematic diagrams of the geometry, local setting and character of the fragmental units. Geochemical analyses of selected alteration assemblages will form a database for later comparison of the study areas. The overarching objective of the project is to highlight the potential for undiscovered massive-sulphide mineralization related to fragmental activity and mud volcanism in the Purcell Basin.

The past-producing Sullivan deposit is a sediment-hosted massive-sulphide Fe-Pb-Zn-Ag deposit that formed within a graben or half graben with a north-south dimension of approximately 13 km and an east-west dimension of 3 to 5 km (Turner et al., 2001; Lydon, 2007). The immediate setting of the deposit has been interpreted as a sedimentary caldera formed from mud-volcano activity (Turner et al., 2001; Lydon, 2007). Venting of hydrothermal fluids during mud-volcano formation controlled sulphide deposition at Sullivan and underpins the importance that these structures have from an economic standpoint.

Mud volcanism in the Aldridge Formation is well documented in numerous locations outside of the Sullivan sub-basin. Recent work by industry has shown that this activity continued episodically from Lower Aldridge to at least

Creston Formation time (Anderson, 2014), a stratigraphic interval in excess of 6000 m (Höy, 1993). Mud-volcano complexes throughout this stratigraphic succession show similar characteristics to those at Sullivan, including alteration types, sulphide mineralization and fragmental facies, thus making them prime exploration candidates for massive-sulphide Ag-Pb-Zn deposits.

## Progress To Date

The 2014 program consisted of approximately 15 days of field mapping and sampling focused on mud-volcano complexes in the Cranbrook area, including those within the Sullivan sub-basin (Figure 1). The project is aimed at providing a geological and geochemical fingerprint for mud-volcano complexes, with a particular focus on comparing the geochemistry from those in the Sullivan area (North Star) to others in the region (Pakk, Rise, Ryder, SBA and Vine West). Geological mapping of fragmental bodies within the complexes focused on their size, alteration and structural controls. The results of this program may define the characteristics of mud-volcano complexes that have higher potential to host massive-sulphide Ag-Pb-Zn deposits.

Data including rock-sample analyses and schematic diagrams will be integrated into a poster display for the Mineral Exploration Roundup 2015 conference and will also be included in a final Geoscience BC report in June of 2015.

## Acknowledgments

This paper was peer reviewed by Michael Seabrook.

## References

- Anderson, D. (2014): Geological mapping of the Silver Fox/St. Eugene claim holdings; BC Ministry of Energy and Mines, Assessment Report 34631, 2 p.
- Anderson, D. and Höy, T. (2001): Fragmental sedimentary rocks, Aldridge Formation, Purcell Supergroup, B.C.; in *The Geological Environment of the Sullivan Deposit*, British Columbia, J.W. Lydon, T. Höy, J.F. Slack and M. Knapp (ed.), Geological Association of Canada, Mineral Deposits Division, Special Publication 1, p. 259-271.

---

**Keywords:** *SEEK, geology, geochemistry, Purcell Basin, mud volcanism, massive sulphide*

*This publication is also available, free of charge, as colour digital files in Adobe Acrobat® PDF format from the Geoscience BC website: <http://www.geosciencebc.com/s/DataReleases.asp>.*

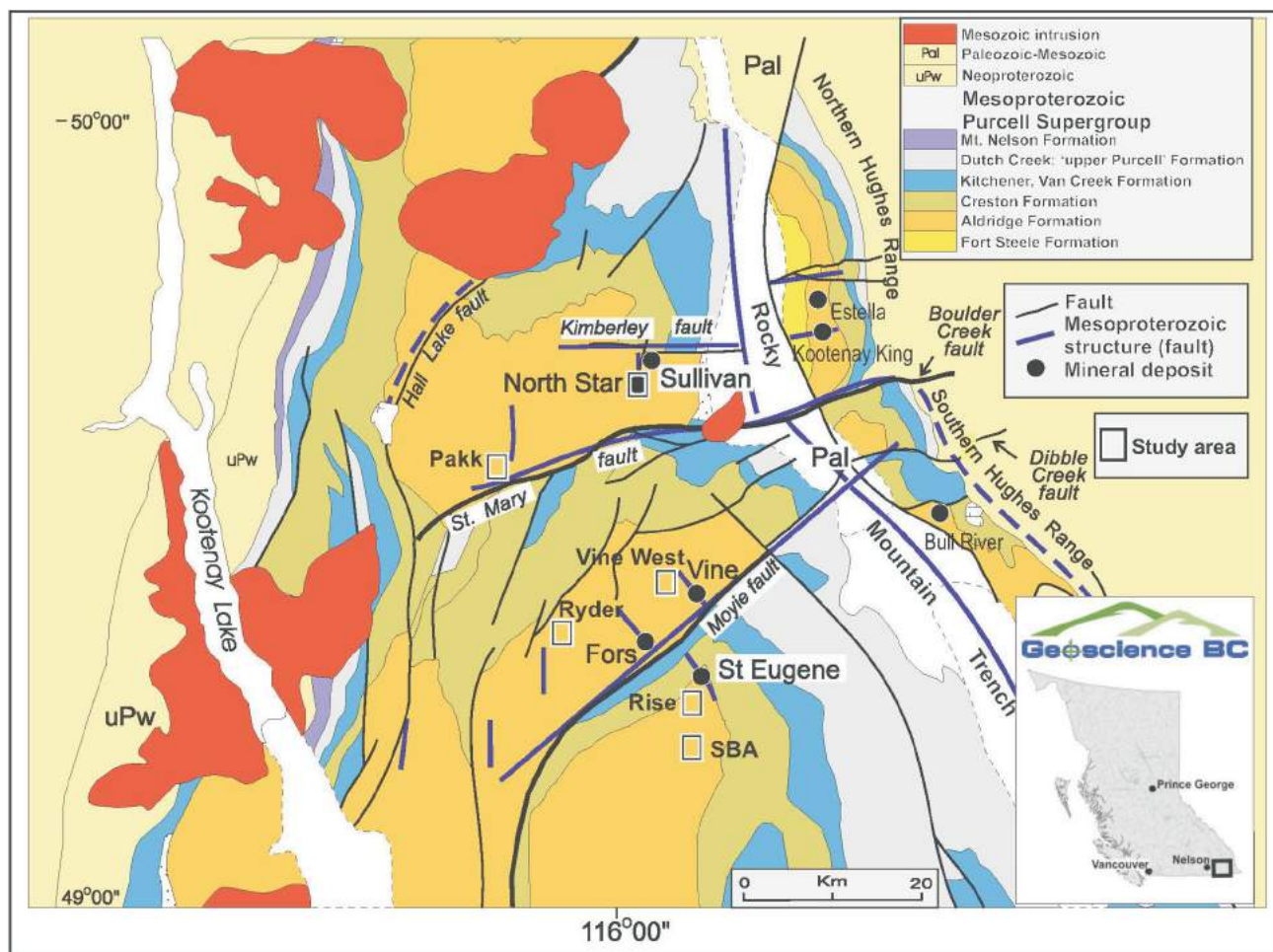


**Figure 1.** Geology of the Cranbrook area (after Anderson and Höy, 2001), showing major Mesoproterozoic structures, massive-sulphide deposits and 2014 study areas, southeastern British Columbia.

Höy, T. (1993): Geology of the Purcell Supergroup in the Fernie west-half map area, southeastern British Columbia; BC Ministry of Energy and Mines, Bulletin 84, 157 p.

Lydon, J.W., 2007. Geology and metallogeny of the Belt-Purcell Basin; in Mineral Deposits of Canada: A Synthesis of Major Deposit-Types, District Metallogeny, the Evolution of Geological Provinces, and Exploration Methods, W.D. Goodfellow (ed.), Geological Association of Canada, Mineral Deposits Division, Special Publication 5, p. 581-607.

Turner, R.J.W., Leitch, C.H.B., Höy, T., Ransom, P.W., Hagen, A. and Delaney, G.D. (2001): Sullivan graben system: district setting of the Sullivan deposit; in The Geological Environment of the Sullivan Deposit, British Columbia, J.W. Lydon, T. Höy, J.F. Slack and M. Knapp (ed.), Geological Association of Canada, Mineral Deposits Division, Special Publication 1, p. 370-407.

## Historical Exploration Data Capture Pilot Project, Northwestern British Columbia (NTS 093L)

C.E. Kilby, Cal Data Ltd., Victoria, BC, ckilby@caldatageol.com

M.A. Fournier, MAF Geographix, Victoria, BC

Kilby, C.E. and Fournier, M.A. (2015): Historical exploration data capture pilot project, northwestern British Columbia (NTS 093L); in Geoscience BC Summary of Activities 2014, Geoscience BC, Report 2015-1, p. 79–84.

### Introduction

There are over 32 000 mineral assessment reports available to the public in the British Columbia Assessment Report Indexing System (ARIS; BC Geological Survey, 2014a). This likely represents the largest privately funded, public geoscience databank in BC. Every exploration project beginning on newly acquired ground should start with a review of the mineral assessment reports that were written at some time in the past about that ground or the surrounding area. The new project must then present the results of some new work, which might be geological mapping, trenching, sampling or drilling. In many cases the reports will contain the geochemistry results from the analysis of samples.

However, the information provided in these reports remains locked in their analogue format. Therefore, in many cases today, preparation for the field season begins with the creation of a geographic information system (GIS) database collecting together all layers of public (and privately obtained) data. How much of the data from the assessment reports actually make it into these databases remains linked to the budget of the project and the time and abilities of the personnel employed. What if the primary data found in these assessment reports were already available as digital layers that could be loaded into a company's GIS? At the very least it could mean work performed in the past would not be duplicated, and beyond that could spur exploration work that may not have been undertaken without the insight of earlier results.

This pilot project aims to extract and convert primary analogue data from the BC assessment reports (and possibly property files and prospector's reports). Types of data being extracted include analytical chemistry information (e.g., geochemical surveys), drillhole samples, trench samples and grab samples, as well as maps displaying unique geological and geophysical information. Data inclusion in

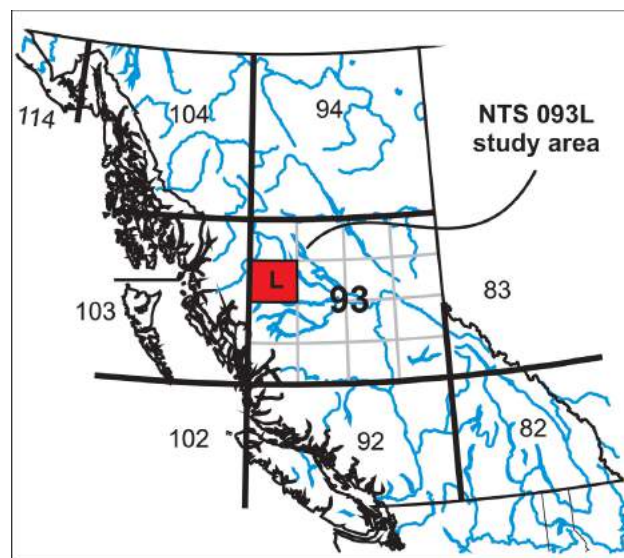


Figure 1. Location of NTS map area 093L, northwestern British Columbia.

the capture process is dependent on a reasonable spatial component for each sample, and collection proceeds in order from most recent to oldest sources. This initial phase is being undertaken on the single NTS 1:250 000 map area 093L (Figures 1, 2), chosen by Geoscience BC's Minerals Technical Advisory Committee, to provide a proof-of-concept product and establish collection procedures. Techniques and protocols for undertaking this work are being developed to facilitate the continuation of the collection should the proof-of-concept products prove valuable. The converted data will be in a format that can be integrated into a GIS and web mapping systems.

### What to Capture?

This pilot project is limited in duration as well as scope. There are over 1100 assessment reports in ARIS for over 360 MINFILE sites (BC Geological Survey, 2014b) within NTS 093L. Due to time limitations, only a portion of these reports can be included in this project. Going forward it makes sense to choose random MINFILE sites and then take advantage of common repetition in reports and maps used in consecutive years by companies on work done on a

**Keywords:** ARIS, MINFILE, GIS, analogue, digital, geopositioning, geochemical data

This publication is also available, free of charge, as colour digital files in Adobe Acrobat® PDF format from the Geoscience BC website: <http://www.geosciencebc.com/s/DataReleases.asp>.

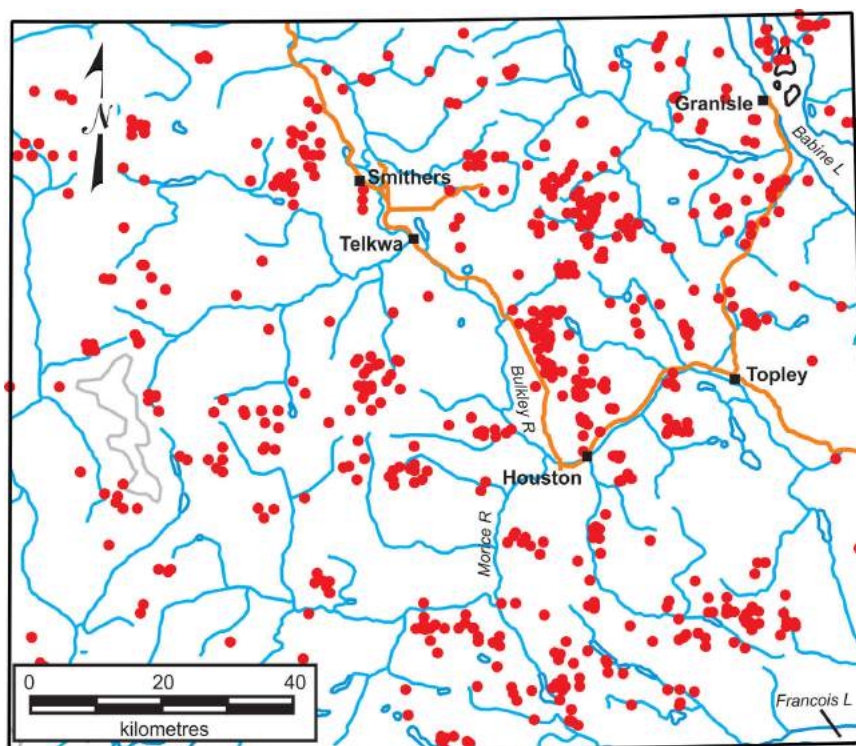


**Figure 2.** Red dots indicate locations of assessment reports filed in British Columbia's Assessment Reporting Index System (BC Geological Survey, 2014a) for NTS map area 093L, northwestern British Columbia.

single mineral site. Any given MINFILE site may have over 30 ARIS reports reaching back to 1947. To limit the amount of time spent on any one mineral site, only reports submitted in the last 30 years will be used. This has nothing to do with the quality of earlier reports; however, it is possible that more time would be spent geopositioning older maps. What it does allow for is the data capture to be distributed more broadly around various MINFILE sites within NTS 093L and should give a more balanced idea of the time spent to do each task required in this process. MINFILE sites with recorded production are also not included in this pilot project. This is due to the reality that after a mine has been in place some or all of the information from soil samples, trenches or drillholes may be of little value as that material may be mined out. However, the same assessment reports could likely contain data of continuing interest around (or beneath) the site; but assessing whether that is the case would be a task beyond the scope of the time available for this project. Assessment reports where map co-ordinates are incompletely provided or not provided at all, which precludes their accurate positioning, are excluded from this work; a number of reports at this point have already been excluded for this reason.

The goal is to collect primary exploration data from each report, such as soil and silt geochemistry, drillhole, trench and rock sample analyses as well as map displays, such as geology and geophysics. Each sample that is spatially

locatable and has associated geochemical information is collected. Each map that can be accurately rectified and provides unique information is collected. In addition, a copy of the original data source (map, assay certificate or report table) is linked to the data as an image or PDF.

A selected report is reviewed and the decision on whether it will be used is based on an assessment of whether the primary information in that report, whatever form it might take, is located on a map that can be geopositioned. The parameters for this decision are described below in the quality control section. Alternatively, locational co-ordinates for all samples may be provided in the report text (such as in an appendix) and would eliminate the need for geopositioning a map and digitizing sample sites. For each report that meets the criteria for locational data, every sample that has associated geochemical information is collected. For a given report, the following material will be collected:

- soil samples with geochemistry,
- silt samples with geochemistry,
- rock samples with geochemistry,
- trench with samples (geochemistry),
- drillholes with samples (geochemistry),
- geology maps with unique work (new, detailed)—this is a geopositioned raster image, and
- geophysical maps (new, property-sized or smaller)—this is a geopositioned raster image.

Geology on maps is not being digitized, but images are being created and geopositioned so that the user can see the geology over a study area. Geology maps tend to be particularly unique in that they usually lean very heavily toward the singular focus of exploration and may contain layers of work by earlier workers. This is a more subjective type of information, more suited to selection (and capture) by the user.

## Capture Techniques

### Maps and Points

Most of the data is captured from analogue maps and tables, which are currently available in PDF format. These maps have been geopositioned against an accurate base, trying multiple projections and datums to achieve a successful fit. Then the appropriate spatial data is rectified and captured in a standard co-ordinate system (geographic projection) using North American Datum 1983 (NAD 83). Geographic co-ordinates are most easily and accurately converted to other projections by most systems. ArcMap, a GIS software application of Environmental Systems Research Institute, Inc. (Esri), is used for the data capture in this project. The ArcView level of ArcGIS provides point feature class shape files and GeoTIFF raster images as the primary products. The captured spatial data is stored in a database along with its metadata documenting the source and spatial accuracy. The rectified maps are saved in the spatial database and ultimately will be provided in a raster format, such as a GeoTIFF. Commonly, the maps contain useful information in addition to the data being captured from them. The availability of the original maps in a format that can be used in a GIS or displayed through a web mapping system is a useful byproduct of the process. Analogue data, such as tables of analyses, laboratory certificates, drillhole and trench logs, are linked to the appropriate captured data point.

Data capture is currently in progress, and it is likely that more than one accurate base may be tried before a map can be successfully geopositioned. The projection and datum used to produce many maps in assessment reports are not always included in the reports, particularly historical maps that predate the use of personal computers in preparing these reports and figures. At this point TRIM data is used to provide added precision to the co-ordinates on maps rectified to date. Once the map is considered geopositioned with a best reasonable outcome it is assigned a level of accuracy (see the discussion on quality control). The sites of interest to this work, such as grid nodes, individual sample sites, drillhole collars and so forth, are then digitized. Where a sample is from an interval, such as in a trench or drillhole, the two bounding co-ordinates will be recorded relative to an anchor co-ordinate, such as drillhole collar or end of trench. Trench and drillhole survey data (when it exists) can be used to calculate the sample positions.

## Geochemical Data

The next step in the process is to capture the geochemical data and link it to each digitized point. The most accurate and cost-effective means to obtain the geochemical data is by contacting the company that completed the assessment report. When a map has been successfully rectified a letter is sent to the company requesting the geochemical data in digital format. Two options are provided for companies; they can provide the lab results from their own digital files, or they can request the lab that did the original work to provide the lab results in digital format. If the geochemical data is provided in this format, it can be added to the database. However, when the data is not provided in a digital format then it must be manually entered into the database. Manual entry is obviously more time consuming and therefore will affect the amount of material project staff are able to complete for this pilot project. Again, for the geochemical components, links to copies of the appropriate pages of the original reports will be provided to allow the user to view the original pages (such as assay certificates).

As this is a pilot project, the results will be evaluated in several ways. As procedures and protocols are created, project staff track their time on the work done. At the end of the project, this will allow the calculation of an average time to geoposition 'x' number of maps, digitize 'x' number of points, and acquire 'x' number of geochemical results. This will help Geoscience BC assess the cost of this work as opposed to the benefit of this work to the exploration community.

## Quality Control

The project work is influenced by error from two sources: error in the original creation of the map or other item being captured, and the error that accumulates during the capture process itself. In the first instance it is only possible to know what errors may exist in the original data if possible sources of error are discussed in the assessment report itself. For example, if a sample site is only generally positioned and plotted on a map, as opposed to actually being given a measured location on site, there is no way to know this unless it is mentioned in the text. If that same sample site was located by chaining from a cut grid on the ground, then its location error would not be significant, depending on how the grid had been placed and how much of this adjacent grid had been accurately located. The sample site could be accurately located by today's GPS equipment and its accuracy would be high, but precision would depend on the device in use. If the same sample site had been located 20 years ago with a handheld GPS the error could be large depending on the dithering, the number of satellites available, the proximity of any features, such as lakes and so forth. In other words, to know the accuracy of the data one uses in an historical assessment report one needs to consider the time and

place when that report was written and consider what is discussed in the report. Make no mistake, the locational accuracy in historical reports can be very high. All of this is beyond the control of this project, but directly affects the work itself and must be kept in mind by all users. This project cannot improve the quality of locational data, but an attempt can be made to minimize the error that is added to data locations as they are captured.

Therefore, there is a significant focus in this project on quality control; essentially minimizing cumulative error in this work. There are two main areas of focus in the cumulative error: the first is in the original georeferencing of a map; and the second is during the process of digitizing the actual points associated with data. Initially, a map is brought into the GIS and an attempt is made to position the map using co-ordinates plotted on the map, as well as other unique positional information, such as lakes, streams, roads, buildings and so forth. Once a best fit is selected, an estimate of the possible error must be made. For this purpose, locational confidence categories (Table 1) are used to provide categories of error to simplify this process. At this point, one category, from A through D, is assigned to the positional accuracy of the map based on the likely error, which is estimated by scanning various sites on the map against the base map. Clearly a map in category A is the desired outcome, where locations on the map will be within 5 m of their true (plotted) location. However, this is often not possible, as many maps have introduced error from things as simple as co-ordinates on the map having been placed in error. There are many other possible sources of error. Whatever the error source may be, scale of the work also affects this assessment. However, if a map has been positioned and the error is estimated to be on the order of 100 m or greater anywhere on the map (poorer than category D), then the map is considered to be too inaccurate to make use of the associated data. There is some grey area in category D (50–100 m), depending on the scale of the map and the data associated with the plotted sites, requiring further consideration as to whether to continue with a map. Final assessment of the error margins remains to be made as the work progresses. Again, the category does not address

the accuracy of the original map. However, as newer maps may contain data points located by GPS, these inherently more accurate maps (better than pre GPS) should only occur within an A or B category. It is important to note that given more time and a desire on the part of a user to ensure the best accuracy possible, a single map could be georeferenced using detailed airphotos or high resolution remote imagery and >200 points to georeference the map, if it was believed that it was worth the time and expenditure. In this project that type of focus would be unrealistic, and the gain in accuracy would be unknown until the work was complete.

The creation of Table 1, and breakdown of the categories into a range of metres of possible error, attempts to set parameters for what accuracy one can expect from the data they are using. It should be noted that the table is still a work in progress. There must be a limit to the level of error a user will deem acceptable in the positioning of sample sites. Drillholes are an example of a site where the location of the collar and the potential value of the analyses from the core suggest that very limited error would be acceptable to a user. In the case of drillholes it is suggested that they should have a locational error within 50 m, or should not be digitized for this program. The final 100 m length for D is initially a random even number; however, it is not surprising at times during exploration work to begin using digital data from a particular source only to discover eventually that the sample sites you have been dealing with are 200 m from where they should be. How would the user then regard the remainder of this data? Digitizing a location can lend an air of precision to sites that are placed inaccurately to begin with. By tightening the total error margin allowed, an evaluation needs to be made regarding how many reports will be eliminated from this capture process. Finally, it is common in the georeferencing process that the sample points nearest the control points are most accurately located, those farther away are not. One way to deal with this problem is to georeference the historical maps by using control points that are closest to the data points being digitized. This might involve several separate steps but ultimately it could help reduce the overall error in locating historical data points.

**Table 1.** Table of locational confidence categories for historical exploration data capture pilot project.

Locational confidence category	Estimate of possible error	Data type
A	0–5 m	borehole collars, georeferencing of maps, grids
B	5–10 m	borehole collars, georeferencing of maps, grids
C	10–50 m	borehole collars (?), georeferencing of maps, grids
D	50–100 m	georeferencing of maps, grids

The second area of cumulative error in the digitizing process is in the accuracy achieved in positioning of sites. This error can be large or small, depending on the quality of the map being used. In this project only points are being digitized, so the potential errors will include things such as the thickness of lines, where they are used to place a measured grid, and the size of the circle or other symbol used to indicate a sample site.

In the typical georeferencing procedure, a scanned map from an existing assessment report was exported to TIFF and subsequently georeferenced in ArcMap using the application software's georeferencing procedure as it relates

to the position of features in TRIM. Attempts to geoposition the raster image using three different projections (UTM, BC Albers and geographic), as well as two datums (NAD 27 and 83), yielded varied results. Neither latitude nor northing capture was reasonable (Figure 3a), and longitude or easting was off by 100 m in each case (Figure 3b). This discrepancy could be attributed to a datum shift, although both NAD 27 and 83 had the same error. Another possible explanation for the discrepancy (most likely) could be that the location of longitude 127°E may not be accurately positioned on the original image. Overall, the rivers, lakes, roads and topology features in the ARIS raster image are reasonably positioned relative to those in TRIM

(Figure 4). Based on an assessment of the overall fit of the geopositioned map, the grid and samples digitized from this map would each be given a locational confidence category of B to C (Table 1) for the estimate of probable locational error, which is stored with each sample in the database.

## Final Product

Presenting this historical data in a manner that makes it easily available for viewing and utilization by the exploration community is the final step in this process. The digitally captured information will be made available in downloadable and interactive formats. The downloadable option will be similar to the current format used in the Geoscience BC geochemistry releases. In the case of drillhole and trench sample data, co-ordinates for both ends of drillhole and trench data, as well as measured survey points, where available, along the length of either, and associated geochemistry will be provided in a simple, flexible format. Each unique set of data will also have the appropriate metadata attached. Map displays will be in a raster format, such as GeoTIFF. The interactive option will see all the information accessible through a web mapping interface, such as those provided by MapPlace and Geoscience BC.

## Summary

Easy access to existing exploration-related information has proven to be a significant incentive in attracting exploration activity to BC. Prospective explorers typically conduct a data search to help them target areas for further investigation. All other things being equal, the jurisdiction with the best, most easily accessible, geological database will attract the most interest. Making existing information readily available for this planning process will attract exploration activity to the province. This pilot project undertakes to convert analogue assessment report primary data to digital format, which will augment and enhance the existing provincial database. This project is a proof-of-concept trial to undertake historical data capture on the single 1:250 000 NTS map area 093L. The project will ultimately develop an un-

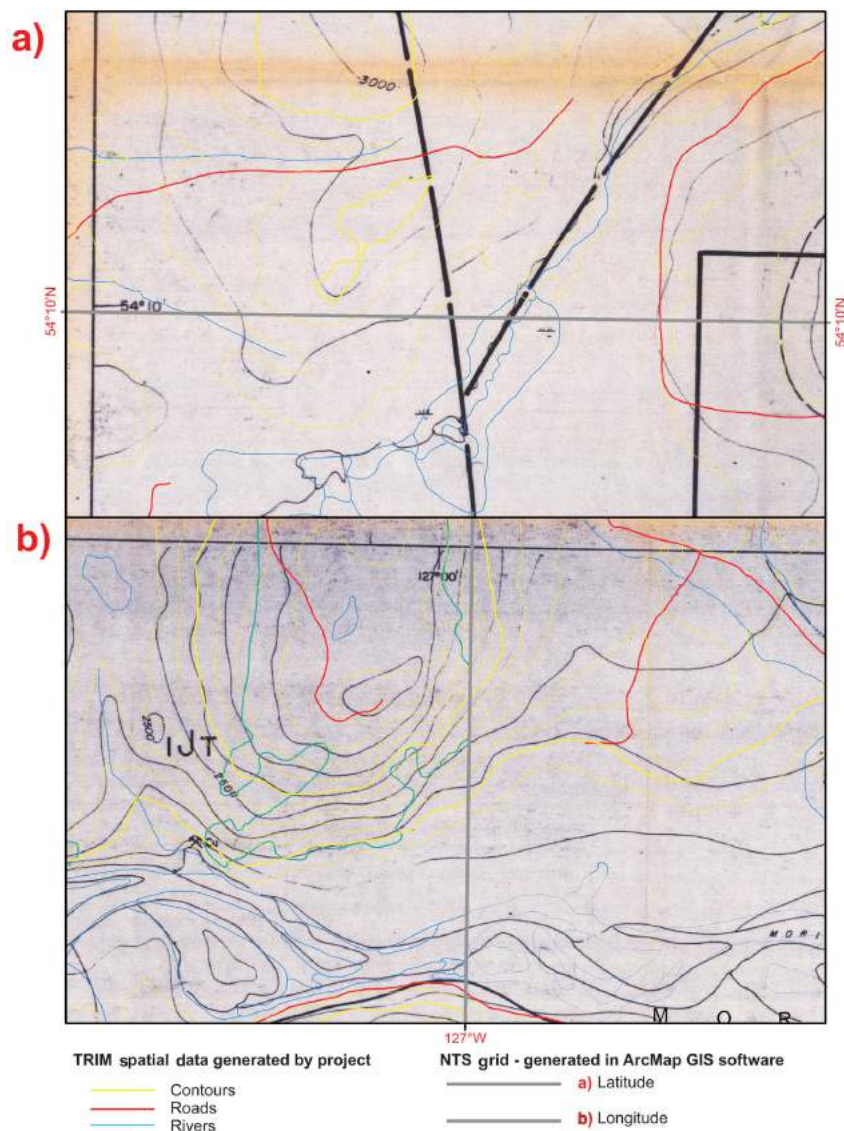


**Figure 3.** Views of the margins of an exploration map from an assessment report, in UTM Zone 9 projection and NAD 83 datum: **a)** the latitude or northing capture, **b)** the longitude or easting capture. A discrepancy of more than 100 m was observed in the easting for projections using both NAD 27 and 83 datums. Note: all coloured lines and red text are new data added and used to geoposition the map image. All black lines, black text and background map are part of page 36 from Assessment Report 21663 (Zastavnikovich and Bzdel, 1992).

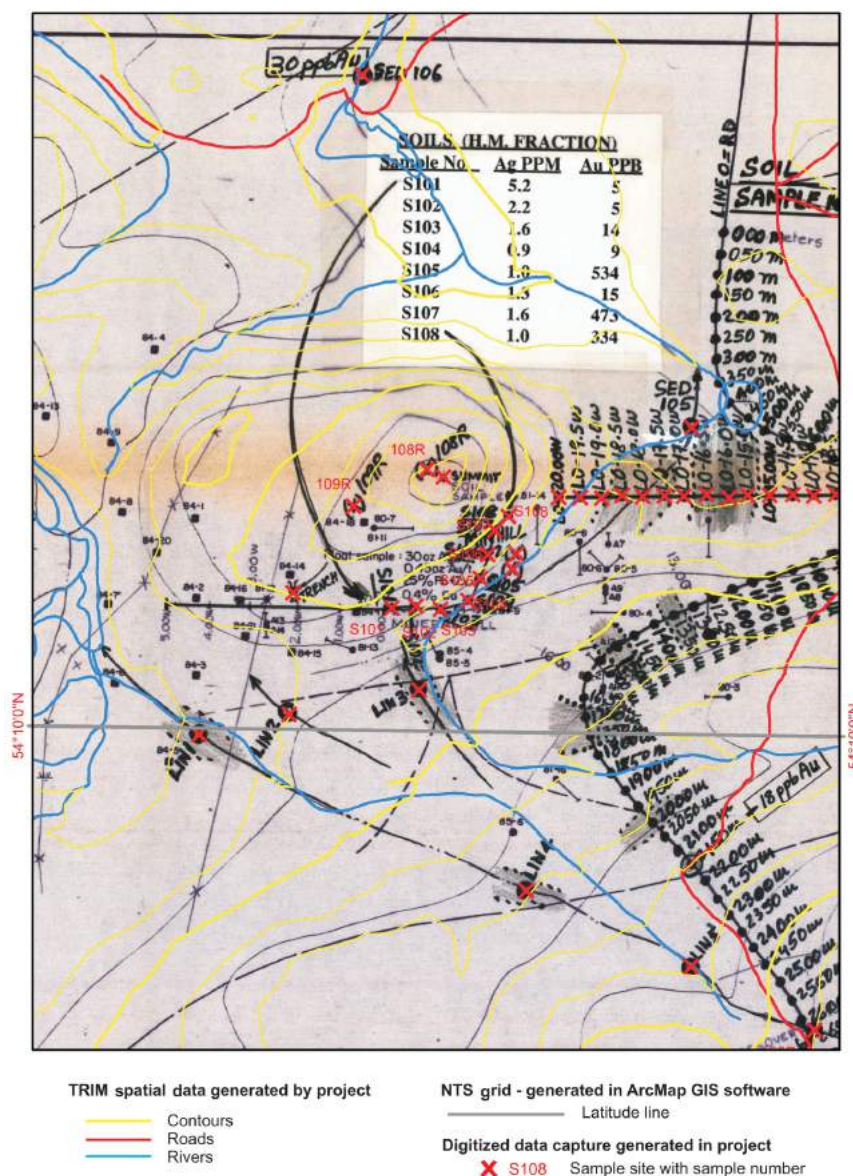


**Figure 4.** Portion of exploration map with the sample points (red crosses) and TRIM data (coloured lines), such as streams, roads and contours, positioned on the historical map. Note: all coloured lines and red text are new data added and used to geoposition the map image. All black lines, black text and background map are part of page 36 from Assessment Report 21663 (Zastavnikovich and Bzdel, 1992).

Understanding of what resources will be required for this work to be performed on additional areas. It will also provide an opportunity to evaluate the benefit of this type of data resurrection.

### Acknowledgments

The authors thank Geoscience BC for funding this pilot project, and the BC Geological Survey, particularly T. Fuller, for help in acquiring data, and Y. Cui and L. Jones for providing insight and knowledge that assisted this project in moving forward. Many thanks to D. MacIntyre who provided a helpful review of the manuscript.

### References

- BC Geological Survey (2014a): Assessment Report Indexing System (ARIS); BC Ministry of Energy and Mines, BC Geological Survey, URL <<http://www.empr.gov.bc.ca/MINING/GEOSCIENCE/ARIS/Pages/default.aspx>> [August 2014].
- BC Geological Survey (2014b): MINFILE BC mineral deposits database; BC Ministry of Energy and Mines, BC Geological Survey, URL <<http://minfile.ca/>> [September 2014].
- Zastavnikovich, S. and Bzdel, L.M. (1992): Geochemical and geophysical assessment report on the Fen 1-4 and Tsalit 4-8 mineral claims, Omineca Mining Division, British Columbia; BC Ministry of Energy and Mines, Assessment Report 21663, 35 p., URL <[http://aris.empr.gov.bc.ca/search.asp?mode=repsum&rep\\_no=21663](http://aris.empr.gov.bc.ca/search.asp?mode=repsum&rep_no=21663)> [December 2014].

# Characterization of Belloy, Kiskatinaw and Debolt Water Disposal Zones in the Montney Play Area, Northeastern British Columbia

**B.J.R. Hayes, Petrel Robertson Consulting Ltd., Calgary, AB, bhayes@petrelrob.com**

**S. Macleod, Petrel Robertson Consulting Ltd., Calgary, AB**

**J. Carey, Petrel Robertson Consulting Ltd., Calgary, AB**

---

Hayes, B.J.R., Macleod, S. and Carey, J. (2015): Characterization of Belloy, Kiskatinaw and Debolt water disposal zones in the Montney play area, northeastern British Columbia; *in* Geoscience BC Summary of Activities 2014, Geoscience BC, Report 2015-1, p. 85–88.

## Introduction

Intensive development of the Montney Formation tight siltstone and shale play in northeastern British Columbia presents new challenges to operators and to the BC Oil and Gas Commission. One of the key challenges is in accessing appropriate water source and disposal zones to support horizontal drilling and multiple hydraulic fracture completions. Source water can be obtained from surface water bodies, shallow nonsaline aquifers or deep saline aquifers. However, spent completion fluids and produced waters must be injected into deep saline aquifers to ensure that no contamination of surface water or nonsaline groundwater takes place.

The Montney Formation unconventional play fairway spans a broad area across the plains and foothills of the Peace River region, as outlined by the BC Oil and Gas Commission (2012; Figure 1). Potential disposal zones in deep saline aquifers exist across the fairway, but their distribution and injectivity characteristics are highly variable. Geoscience BC's Montney Water Project (<http://www.geosciencebc.com/s/Montney.asp>) provides a comprehensive regional inventory of water resources and potential for deep geological disposal sites in the Montney area, and is an excellent starting point for detailed local work on specific water disposal issues.

Recent water injection activity has shown that more work is required to characterize disposal zone capacity in some areas. BC Oil and Gas Commission and Geoscience BC have collaborated to develop a scope of study that addresses many of the water disposal challenges. The Belloy, Kiskatinaw and Debolt formations have been identified as high-priority disposal zone targets, and thus require detailed assessment (Figure 2).

---

**Keywords:** *Montney play area, water disposal, Belloy, Kiskatinaw, Debolt, tight gas*

*This publication is also available, free of charge, as colour digital files in Adobe Acrobat® PDF format from the Geoscience BC website: <http://www.geosciencebc.com/s/DataReleases.asp>.*

## Project Summary

Petrel Robertson Consulting Ltd. (PRCL) has undertaken detailed mapping and characterization of the Belloy, Kiskatinaw and Debolt deep saline aquifers as potential water disposal zones throughout the Montney play fairway. While the Debolt Formation was assessed regionally in the foothills area study of the Montney Water Project (<http://www.geosciencebc.com/s/Montney.asp>), there has been no regional work published on Belloy or Kiskatinaw Formation aquifer potential.

Using all available well control, a map suite is being produced for each potential aquifer, including depth to formation, total thickness and net porous reservoir thickness. Conventional core and drill cuttings data are being used to support reservoir quality assessment; complex mixed carbonate-clastic reservoir lithologies make this assessment more challenging (Figure 3). Available stratigraphic and structural information will support identification of reservoir heterogeneity and compartmentalization that may influence accommodation volumes for injection.

Key tasks supporting this study include:

- Identifying known or potential hydrocarbon pools within the target formations that may be influenced by disposal activity. Disposal too close to existing producers may adversely affect production volumes. Whereas, existing depleted or semidepleted pools may offer potential as present or future disposal sites.
- Identifying hydrocarbon exploitation potential in bounding formations that are expected to provide a seal to injected fluids, as hydraulic fracturing may compromise the integrity of this seal.
- Identifying hydrocarbon exploration and development potential in deeper strata—where wells might be required to penetrate a high-pressure disposal zone.
- Identifying mapped faults, fractures and/or structures that may pose seismic risks when significant water volumes are injected. This work will be compiled from existing maps and literature.

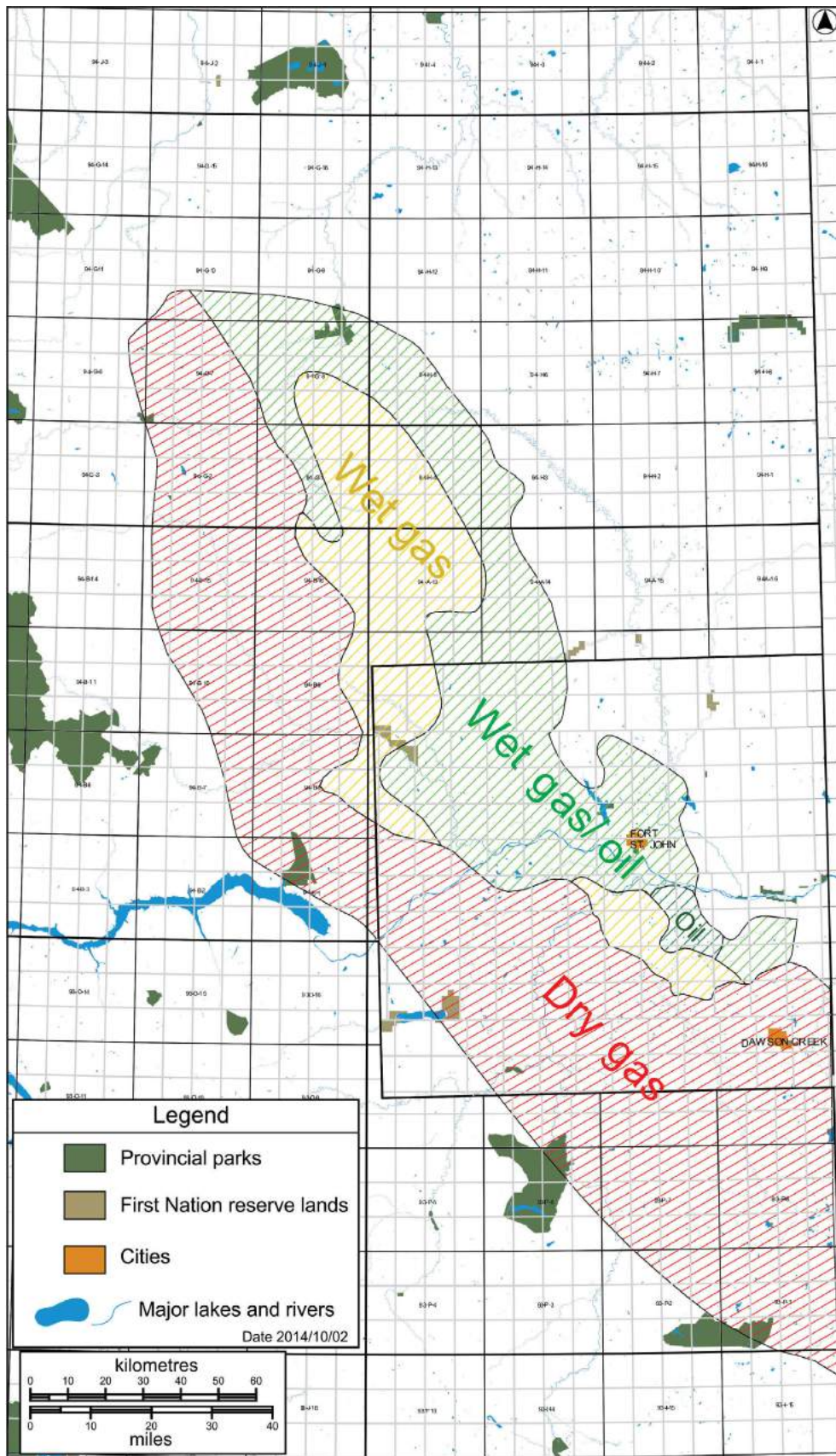
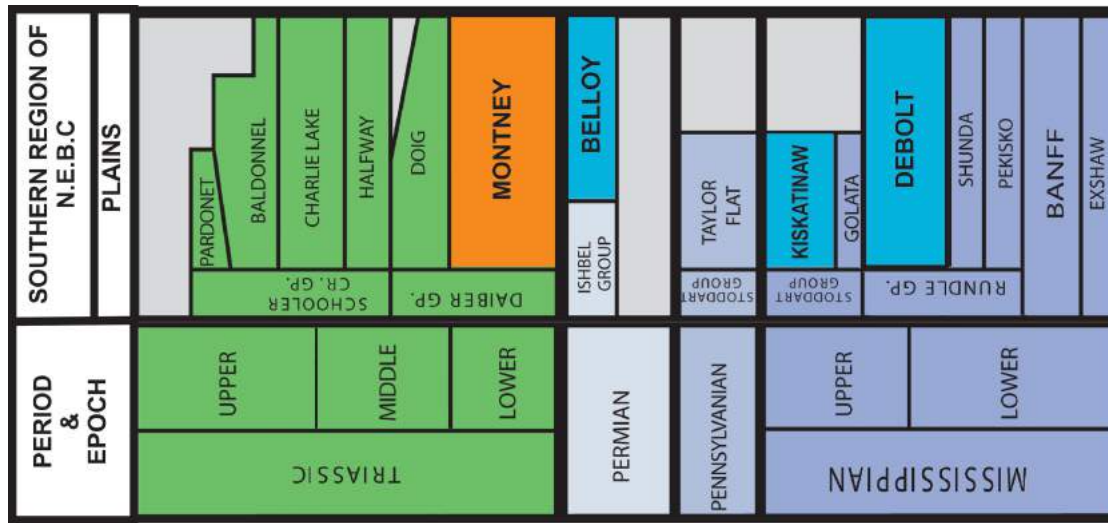
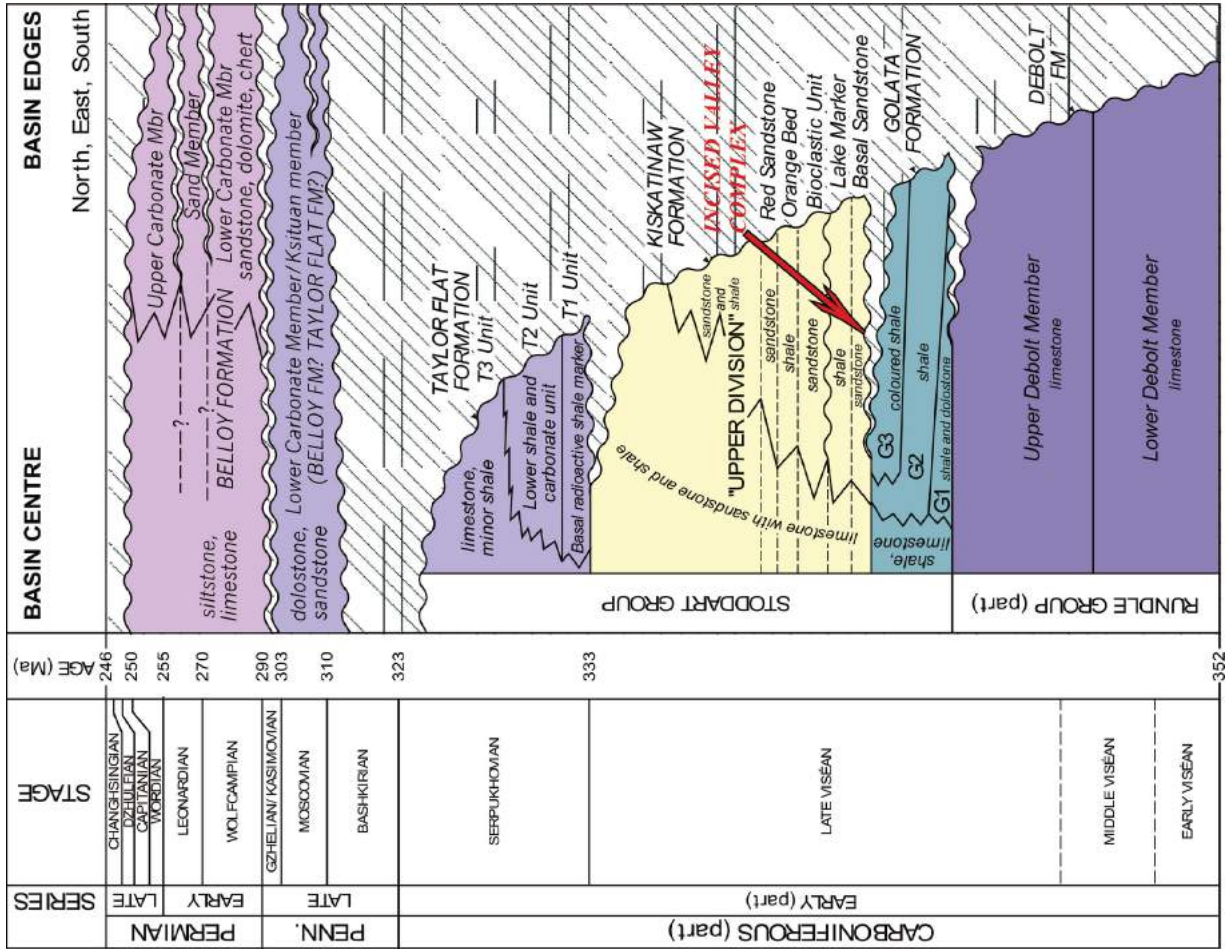


Figure 1. Base map showing Montney Formation play fairway in Peace River area of northeastern British Columbia. Play area boundaries are from BC Oil and Gas Commission (undated).



**Figure 2.** Stratigraphic correlation chart, Peace River plains area of northeastern British Columbia (N.E.B.C.; from BC Ministry of Energy and Mines, 2012). Montney Formation gas reservoir is highlighted in orange, whereas prospective disposal zones in the Belloy, Kiskatinaw and Debolt formations are highlighted in teal.



**Figure 3.** Detailed stratigraphic section of the Debolt Formation through to the Belloy Formation (Carboniferous to Permian) in Peace River plains area of northeastern British Columbia and adjacent Alberta (from Barclay et al., 2002).

To summarize project findings, mapping will be integrated to develop a high/medium/low favourability ranking for each potential aquifer. High favourability will indicate areas with good aquifer characteristics and capacity, with few or no risks arising from hydrocarbon prospectivity or activity, whereas low favourability will indicate poor aquifer characteristics and/or significant risks from existing or prospective hydrocarbon developments within or impacting upon target aquifers.

### **Next Steps**

Upon completion of PRCL's mapping and characterization work, Geoscience BC will engage Canadian Discovery Ltd. to complete a focused assessment of aquifer hydrogeology, including projections of capacity to accept flowback and produced fluids.

### **Acknowledgments**

The authors thank B. McDougall for his review of this paper.

### **References**

- Barclay, J.E., Dunn, L.A. and Krause, F.F. (2002): Estuarine valley fill and interfluvial strata at a significant sequence boundary, Kiskatinaw and Golata formations, Lower Carboniferous (Upper Viséan), north-western Alberta; Canadian Society of Petroleum Geologists Diamond Jubilee Convention, Calgary, Alberta, June 3–7, 2002, Core Convention Abstracts, convention CD, abstract 014S1128.
- BC Ministry of Energy and Mines (2012): Stratigraphic correlation chart; BC Ministry of Energy and Mines, URL <[http://www.empr.gov.bc.ca/titles/ogtitles/otherpublications/documents/stratchart\\_nebc.pdf](http://www.empr.gov.bc.ca/titles/ogtitles/otherpublications/documents/stratchart_nebc.pdf)> [November 2014].
- BC Oil and Gas Commission (undated): Montney Formation play atlas NEBC; BC Oil and Gas Commission, 35 p., URL <<http://www.bcogc.ca/node/8131/download>> [November 2014].

# Quantification of the Gas- and Liquid-in-Place and Flow Characteristics of Shale and Other Fine-Grained Facies in Northeastern British Columbia

R.M. Bustin, Department of Earth and Ocean Sciences, University of British Columbia, Vancouver, BC, bustin@mail.ubc

E. Munson, Department of Earth and Ocean Sciences, University of British Columbia, Vancouver, BC

E. Letham, Department of Earth and Ocean Sciences, University of British Columbia, Vancouver, BC

A.M.M. Bustin, Department of Earth and Ocean Sciences, University of British Columbia, Vancouver, BC

---

Bustin, R.M., Munson, E., Letham, E. and Bustin, A.M.M. (2015): Quantification of the gas- and liquid-in-place and flow characteristics of shale and other fine-grained facies in northeastern British Columbia; *in* Geoscience BC Summary of Activities 2014, Geoscience BC, Report 2015-1, p. 89–94.

## Introduction

The total resource potential of gas shales in British Columbia is estimated to be in the hundreds to thousands of trillions of cubic feet ( $3 \times 10^{10}$  to  $3 \times 10^{11}$  m<sup>3</sup>) of gas and as yet an unquantified amount of liquid hydrocarbons (condensate, natural gas, liquid and oil). Liquid production from shales is particularly important since the liquids currently drive the economics of most unconventional prospects due to depressed gas prices.

Success in developing shales as petroleum reservoirs has not been paralleled with increased understanding of the geological processes that determine gas- and liquid-in-place or their production potential. Simple analyses of the current level of organic maturity has not proved satisfactory in predicting liquids production particularly in areas where maturity, kerogen type, reservoir conditions (pressure and temperature) and rock character changes laterally, such as in northeastern BC.

With the support of Geoscience BC and industry partners, a multifaceted study of strata in northeastern BC has been initiated with the objective to better predict the areal distribution of potential liquid-producing shale and its production potential. The study has two interrelated components: 1) development of better methodologies for quantifying gas- and liquid-in-place in gas shale and shale oil reservoirs and measuring matrix flow characteristics; and 2) quantification of the gas- and liquid-in-place and flow capacity of important shales in northeastern BC using established methodologies and novel ones developed as part of this study. Research is focusing on key horizons, for which considerable data is at hand, including the Muskwa, Exshaw,

Montney, Doig, and Buckinghorse formations, Gordondale Member (formerly the informal Nordegg member) and their equivalents. Additionally, various liquid-producing shales from other basins are being studied for comparative purposes.

In the initial stages of this study, the extensive historical data available on the maturity and source rock properties of the important shale horizons will be compiled and stitched together to create regional surfaces of key properties. The gaps in the regional maps will be augmented by additional sampling and analyses. Access to new cores, supplied by the industry partners, provided the opportunity to do analyses for which achieved samples are ill suited. The maps will be integrated with current production data available in the public domain.

Developing a predictive model for liquid production from shales, which is a goal of the study, requires an in depth understanding of the total petroleum system in northeastern BC. The petroleum system of self-sourced shale reservoirs is complex. Hydrocarbons that are generated depend on kerogen type and thermal history, and hydrocarbons that are retained in shales are a fractionated part of the generated hydrocarbons. Retained hydrocarbons are also subject to alteration with additional burial and possible further selective migration of secondary generated hydrocarbons. During production, the retained hydrocarbons are further fractionated, such that the produced product does not necessarily correspond to that retained in the reservoir. Yet a further complication is the high capillary pressure, which is largely responsible for selective migration, retention and production and varies with pore structure and wettability, which in turn depends on mineralogy, fabric, fluids and thermal history.

In this paper, two questions are addressed: 1) what is the utility of measurements of retained hydrocarbons in shales and how can these data be calibrated or corrected for con-

---

**Keywords:** shale oil, gas shale, unconventional reservoir rocks

*This publication is also available, free of charge, as colour digital files in Adobe Acrobat® PDF format from the Geoscience BC website: <http://www.geosciencebc.com/s/DataReleases.asp>.*

tamination by oil-based drilling fluids; and 2) what is the impact of contamination by drilling or completion fluids on measured wettability of the shales and how does the wettability and hence capillary pressure vary with lithology and thermal maturation.

### Retained Hydrocarbons in Shales

Out of necessity, in this study, there is some dependence on historical data collected on archived core and new analyses of archived core. The most useful measurements for mapping liquid potential of shales, apart from production data, would be a direct measure of the retained hydrocarbons in the rock. The Rock-Eval (Espitalié et al., 1977) type instruments provide a measure of the retained hydrocarbons by heating the samples to 300°C and measuring the amount of hydrocarbons via a calibrated flame ionization detector. The Rock-Eval-type instruments also provide other indices such as  $T_{max}$  (temperature at maximum release of hydrocarbons), which is a measure of thermal maturity, and the hydrogen and oxygen indices (to name a few) that help characterize the kerogen in the rock. Many thousands of these types of measurements exist for strata in northeastern BC and provide a wealth of information and a starting point for this study. Newer instrumentation, referred to as S1 analyzers, can characterize thermally desorbed retained hydrocarbons by chromatography (Agilent Technologies, Inc., 2011), which can be used, for example, to calculate the retained liquid gravity.

Two of the major difficulties in using Rock-Eval or S1 analyzer results are the potential impact of oil-based drilling mud, which is commonly used in wells of interest, and the effect of ‘aging’ on the geochemistry of archived samples. In order to address these issues and to calibrate archived data, two Montney Formation cores, preserved at the well sites, were studied. The cores came from two different areas: one where there is significant liquid production ( $T_{max} \approx 444^\circ\text{C}$ ) and a second area of mainly dry gas production ( $T_{max} \approx 465^\circ\text{C}$ ). The results are presented below. The wells are referred to here as OW (from the oil window) and DG (from dry gas zone).

### Experimental Methodology

Using nitrogen, plugs with a diameter of 0.635 cm (0.25 in.) were cored from preserved whole cores in order to assess the effect of drilling fluid infiltration on organic geochemical properties in tight reservoirs. Sections of the whole core selected for sampling were either 8.89 or 10.16 cm in diameter and greater than 25.00 cm long. Plugs were taken a minimum of one half the diameter of the core from the base ends of the sample, but typically directly in the centre. This ensured that infiltration of drilling fluid from ends of the core sample did not influence results. Plugs were then sectioned into four 1.1 cm pieces and designated zones 1

through 4, where zone 1 is nearest the surface and zone 4 represents the centre of the core (Figure 1). For sample OW-C, an additional subsample (S) from 1 to 2 mm from the core surface was also analyzed.

### Organic Geochemistry

A commercial Rock-Eval-type instrument was used to quantify the hydrocarbons within the preserved plugs as recorded by the first peak (S1) on the pyrograms. Thermal desorption gas chromatography (TDGC) was used in conjunction with source rock analysis (SRA) to quantify the relative contribution of various hydrocarbon molecules to the total hydrocarbons present. Thermal desorption has been used to characterize the hydrocarbon molecules present within oil shales (Crisp et al., 1986), but to the authors’ knowledge no study has been published using TDGC on tight reservoirs to document and fingerprint the infiltration of drilling fluid.

### Results

Results for the S1 analysis are presented in Figure 2 for the OW well and in Figure 3 for the DG well. Each sample is from a different part of the core from the respective wells and hence vary in lithology and fabric.

The S1 values for all samples from both wells are markedly higher toward the margin of the core as a result of contamination by oil-based drilling mud. The S1 decreases from the edge of the core toward the centre. There is little difference between zones 3 and 4 for all but one sample, suggesting zone 4 is not impacted by the drilling mud. The exception is sample DG-A, in which there is a progressive decrease in S1 in all the samples toward the core centre and contamination of even the centre of the core cannot be ruled out. Permeability and other analyses in progress will try to account for the different degrees of core contamination.

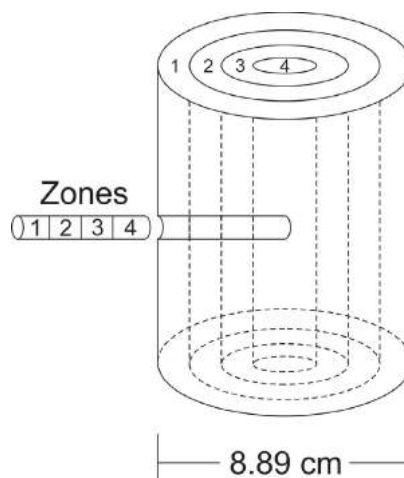


**Figure 1.** Sampling protocol: a plug was drilled into the core using nitrogen and subsequently sectioned into four subsamples, labelled zones 1 through 4 from the surface to the centre.

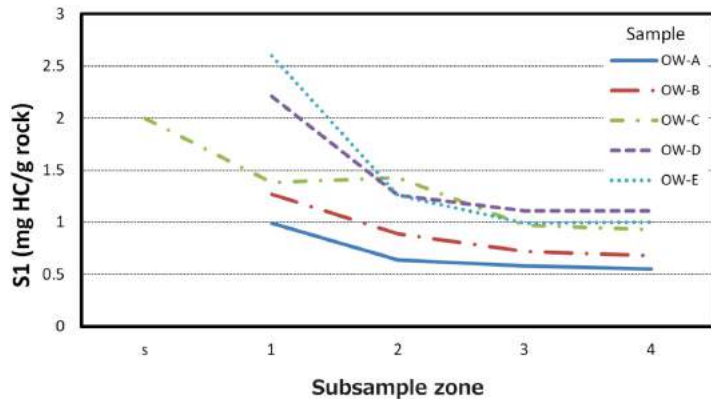


**Figure 2.** Montney Formation oil-window (OW) core. Variation in S1 (mg HC/g rock) from the surface of the core (zone S) to the centre (zone 4) for five subsamples. Refer to Figure 1 for location of subsample zones. Abbreviation: HC, hydrocarbons.

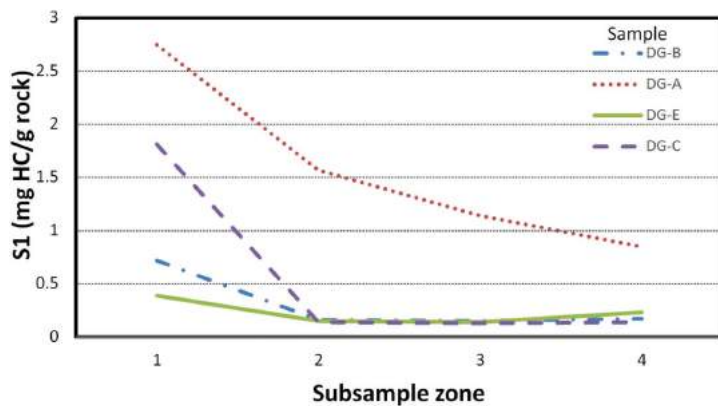


**Figure 3.** Montney Formation dry gas zone (DG) core. Variation in S1 (mg HC/g rock) from the surface of the core (zone 1) to the centre (zone 4) for four subsamples. Refer to Figure 1 for location of subsample zones. Abbreviation: HC, hydrocarbons.

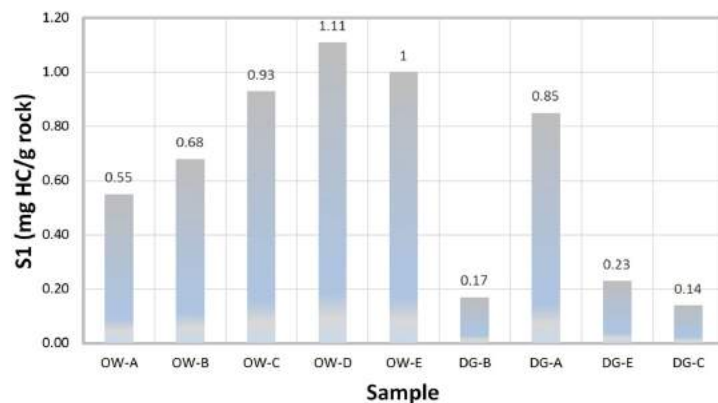


**Figure 4.** Comparison of the S1 values from the centre subsample of each sample and for both wells. The higher S1 values in the samples from the oil-window (OW) well is anticipated due to indigenous oil-in-place (the well produces liquids). The high S1 value of sample DG-A from the dry gas zone (DG) well is due to contamination throughout by oil-based drilling mud.

The difference in S1 values from the centre zone of each sample are compared for both wells in Figure 4. As anticipated, the samples from the oil window (which produce liquids) have higher S1 values due to indigenous oil-in-place. The exception is sample DG-A, which, as noted above, appears to be contaminated throughout by the oil-based drilling mud.

To further investigate the degree of contamination by oil-based drilling mud, subsamples from sample OW-A were subjected to thermal desorption and the products were analyzed. The most notable trends in the results (Figure 5) are an increase in light condensate and an associated decrease in heavy condensate at the margin of the core due to contamination by oil-based mud. The most notable trend is the increase in C8 hydrocarbons toward the core margin.

### Wettability of Shales: Impact of Sampling Techniques, Composition and Maturity

The nanometre- to micrometre-sized pores found in shale and other fine-grained facies result in extremely high capillary pressures. Capillary pressure is one of the principal determinants of hydrocarbon retention, relative permeability and imbibition and thus is important to quantify and is an important metric in this research project. Interfacial tension and pore geometry (size) and wettability (contact angle) determine capillary pressure (Falode and Manuel, 2014). Obtaining reliable measures of contact angles representative of the rocks and fluid systems in the subsurface and understanding compositional and maturity controls on wettability is thus crucial to meeting the broader goals of this research project.

In this paper, the reliability of wettability measurements of drilling-fluid-contaminated core samples was investigated and some preliminary results on the impact of shale composition and thermal maturation are provided.

### Impact of Drilling-Fluid Contamination

To investigate the impact of the interaction between rock and drilling fluids during coring on wettability, profiles of contact angles were collected across samples from edge to edge through the centre of the two cores described earlier (Figure 1). Wettability profiles could then be compared to profiles of retained hydrocarbons, which represent varying levels of contamination with oil-based drilling mud. Interaction with both oil- and water-based drilling muds may alter wettability by coating mineral faces that form pore walls. In this

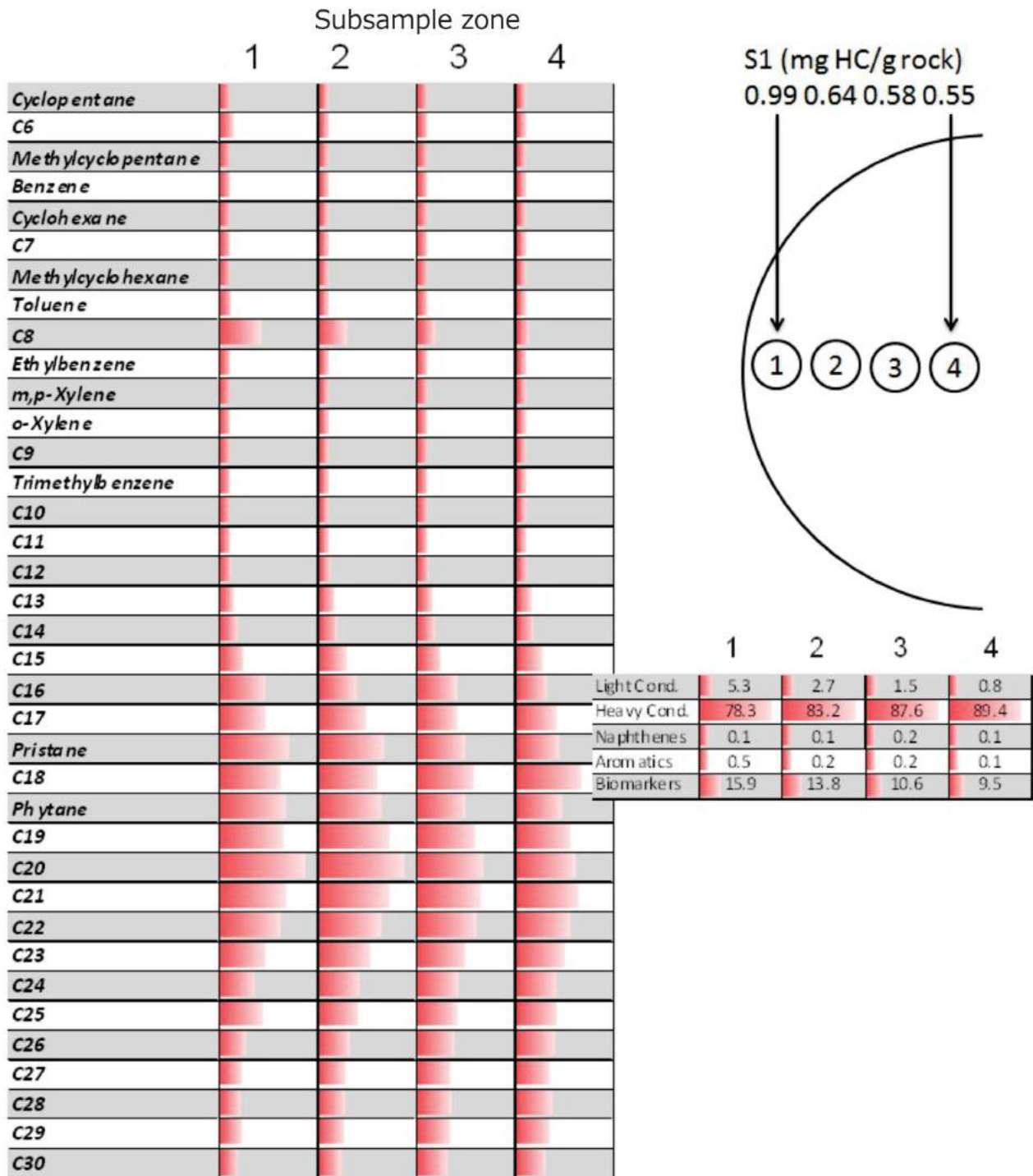


Figure 5. Thermal desorption products of subsamples from sample OW-A. The inset cross-section of the core shows the approximate locations of the subsample zones. The chromatograph data is relative. Abbreviations: Cond, condensate; HC, hydrocarbons.

study, contact angles were measured using the sessile drop method on fresh surfaces prepared under a nitrogen atmosphere.

The contact angle measurements of the two samples across the diameter of the core are shown in Figure 6. The variation in S1 peak across the samples (documented above) is

poorly reflected in the contact angle measurements. With the exception of the sample at about 5 cm there appears to be a trend toward lower contact angles (more water wet) at the more invaded margin of the cores. However, the overall trend is within the variability of repeat measurements (~5–10°) and hence must be interpreted with caution. The lack of a more distinct wettability variation with invasion

across the samples is probably due to the high proportion of new mineral surfaces exposed when cutting the samples, compared to invaded fluid (about 2–5% of the rock volume).

The two tested samples have significantly different contact angles (Figure 6); the contact angle for the OW sample is about 25° higher than the DG sample. Such results are consistent with preliminary data from other formations in the Western Canadian Sedimentary Basin (WCSB) and Eagle Ford trends in Texas, which suggest the wettability of water-based fluids is lowest in the oil window and decreases with both decreasing and increasing thermal maturity.

### Compositional Controls on Wettability

The impact of compositional controls on wettability are being investigated across the WCSB. Preliminary data show a strong correlation between total organic carbon (TOC) and measured contact angles (Bustin, 2014). Contact angles of water in decane and total organic carbon content show positive correlation for Muskwa Formation ( $R^2$  value of 0.72; Figure 7). Contact angles of water in air and total organic carbon content show a positive correlation for Duvernay Formation samples ( $R^2$  value of 0.78; Figure 8). These correlations are expected due to the known hydrophobic nature of organic matter. Other properties display weaker correlations with wettability (e.g., negative correlation of total clays and contact angle). However, with the limited dataset collected thus far, it is not possible to determine if the weaker correlations are spurious correlations (Pearson, 1897) resulting from the fact that the sum of all composition data is a constant (Chayes, 1960), or if in fact mineralogical composition partially controls the observed contact angle variation.

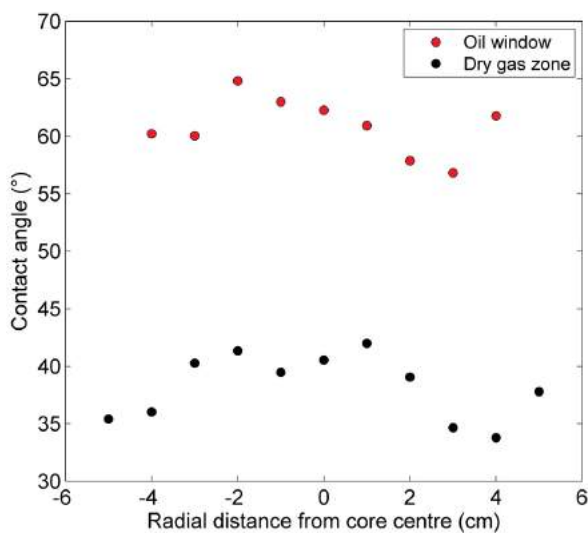


**Figure 6.** Contact angle profiles from edge to edge through the centre of two core samples. Any systematic variation due to drilling fluid invasion is so small that it is within the variability of repeat measurements (~5–10°).

Even with the limited dataset collected so far, wettability shows a large variation within a single formation (e.g., contact angles between ~20 and 100° for water in decane on Muskwa Formation samples, Figure 7). This variation is significant because it translates to very large capillary pressure differences and hence hydrocarbon distribution.

### Summary and Conclusions

In order to establish the utility of Rock-Eval-type data and wettability measurements for mapping and predicting liquid hydrocarbon distribution in shales in northeastern BC, the impact of contamination of core samples by oil-based drilling mud has been investigated. The S1 (mg HC/g rock) analyses that would ideally represent the generated but retained hydrocarbons in fine-grained rocks are strongly contaminated by oil-based drilling mud in Montney Formation strata from the dry gas zone and oil window. Only samples collected from the central 2 cm of 9 cm diameter cores appear to have escaped invasion/imbibition of oil-based drilling mud. Analyses of the hydrocarbons by thermal desorption indicate the invaded portion of core are enriched in light condensate and notably C8 hydrocarbons.

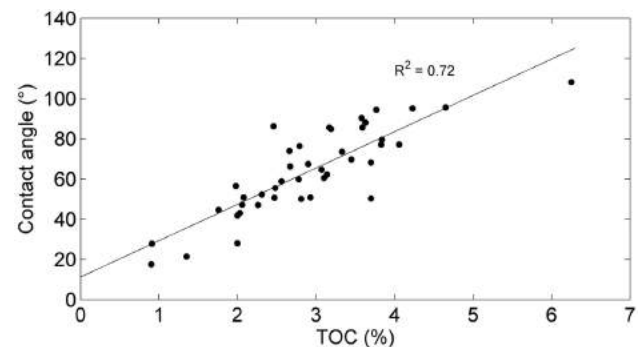


**Figure 7.** Correlation of contact angle for water in decane to total organic carbon (TOC) for all Muskwa Formation samples analyzed to date. Of all properties measured, TOC yields the strongest correlation with wettability.

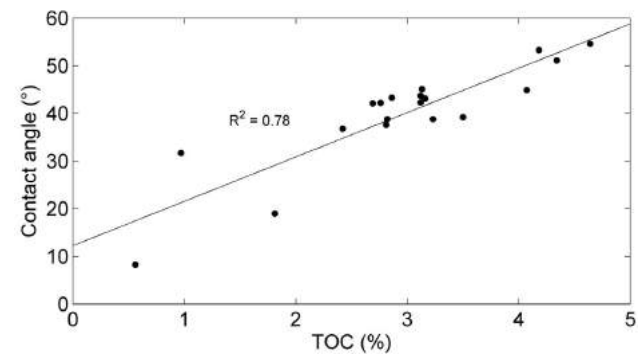


**Figure 8.** Correlation of contact angle for water in air to total organic carbon (TOC) for all Duvernay Formation samples analyzed to date. Of all properties measured, TOC yields the strongest correlation with wettability.

The invasion of drilling fluids into core of conventional reservoir rocks has been investigated using tracers and other techniques (i.e., Menouar et al., 2002; Tracerco, 2014). Intuitively, it has been assumed, although not demonstrated, that ultra-low permeability rocks are less susceptible to infiltration by completion or drilling fluids. However, because of the high capillary pressures of tight rocks, imbibition may be pronounced, as found in this study. These results clearly illustrate that care must be taken when selecting samples for mapping retained hydrocarbons and that the saturation calculations routinely performed by commercial laboratories, even on preserved cores, must be viewed with extreme caution.

The variation in wettability (contact angles) measured on new core surfaces perpendicular to the core axes do not show a significant trend with degree of invasion/imbibition of drilling oil. Such results probably reflect the dominance of new mineral surfaces created during sample preparation and the relatively small pore volume of the samples. The core from the oil window had higher contact angles (~25°) than the core from the dry gas zone. Such results are consistent with the preliminary mapping data, which shows wettability appears to pass through a minimum in the oil window for the Duvernay, Muskwa and Montney formations. Trends in wettability with maturity can be overprinted by variation in wettability with lithology. Preliminary wettability measurements on the Muskwa and Duvernay formations show a strong dependence on the amount of total organic carbon present, which undoubtedly reflects the strong hydrophobicity of the organic fraction.

### Acknowledgments

The authors thank Trican Geological Services for carrying out the thermal desorption and Rock-Eval-type analyses. This paper has benefitted from the careful review of R. Wust of Trican Geological Services.

### References

- Agilent Technologies, Inc. (2011): Hydrocarbons C3–C32 thermal desorption of rock sample; Agilent Technologies, Inc., Application Note, Energy and Fuels, 3 p., URL <<http://www.chem.agilent.com/Library/applications/A00059.pdf>> [November 2014].
- Bustin, R.M. (2014): Petrophysics and hydrocarbon generation, retention and production from ultra-low permeability rocks: musings and learnings with implications for liquid potential from NEBC shales; 8th BC Unconventional Gas Technical Forum, June 5–6, 2014, Victoria, BC, presentation.
- Chayes, F. (1960): On correlation between variables of constant sum; *Journal of Geophysical Research*, v. 65, issue 12, p. 4185–4193.
- Crisp, P.T., Ellis, J., De Leeuw, H.W. and Schenck, P.A. (1986): Flash thermal desorption as an alternative to solvent extraction for the determination of C8-C35 hydrocarbons in oil shales; *Analytical Chemistry*, v. 58, p. 258–261.
- Espitalié, J., Laporte, J.L., Madec, M., Marquis, F., Leplat, P., Paulet, J. and Boutefeu, A. (1977): Méthode rapide de caractérisation des roches mères, de leur potentiel pétrolier et de leur degré d'évolution; *Revue Institut Français du Pétrole*, v. 32, no. 1, p. 23–42.
- Falode, O. and Manuel, E. (2014): Wettability effects on capillary pressure, relative permeability, and irreducible saturation using porous plate; *Journal of Petroleum Engineering*, v. 2014, article 465418, 12 p.
- Menouar, H., Aman, H.M., Al-Majed, A., Khan, M.A. and Jilani, S.J. (2002): Use of a non-destructive method to estimate drilling fluid invasion depths in core, application to formation damage; *Society of Core Analysts*, SCA2002-19, 12 p.
- Pearson, K. (1897): Contributions to the mathematical theory of evolution. On a form of spurious correlation which may arise when indices are used in the measurement of organs; *Proceedings of the Royal Society of London*, v. 60, p. 489–498.
- Tracerco (2014): Drilling mud core invasion measurement-oil based drilling mud; Tracerco case study, 2 p., URL <<http://www.tracerco.com/case-studies/drilling-mud-core-invasion-measurement>> [November 2014].

# Carbonate Alteration Footprints of Carbonate-Hosted Zinc-Lead Deposits in Southeastern British Columbia (NTS 082F/03): Applying Carbon and Oxygen Isotopes

N.L. Cook, Mineral Deposit Research Unit, University of British Columbia, Vancouver, BC, [ncook@eos.ubc.ca](mailto:ncook@eos.ubc.ca)

C.J.R. Hart, Mineral Deposit Research Unit, University of British Columbia, Vancouver, BC

---

Cook, N.L. and Hart, C.J.R. (2015): Carbonate alteration footprints of carbonate-hosted zinc-lead deposits in southeastern British Columbia (NTS 082F/03): applying carbon and oxygen isotopes; *in* Geoscience BC Summary of Activities 2014, Geoscience BC, Report 2015-1, p. 95–102.

## Introduction

The hydrothermally altered hostrocks that result from the formation of many mineral deposit systems, such as porphyry, volcanogenic massive sulphide (VMS), epithermal and orogenic gold, can form large concentric haloes of visibly altered rocks that define the alteration footprints of that specific ore deposit type. By contrast, deposits that form in carbonate hostrocks typically have narrower and less-intensely developed alteration footprints, and so these hydrothermal systems generate significantly smaller visible and geochemical haloes. However, carbonate-hosted deposits can have cryptic or invisible alteration footprints that are much broader when detected with analyses of light stable isotopes. It has been shown that stable isotope alteration can be detected at distances of up to 3 km laterally around the mineralization core. As such, stable isotope alteration haloes are typically larger than the limits of the orebody, visible alteration or even geochemical anomalies (Barker et al., 2013).

Light stable isotopes of common elements in ore systems, such as carbon, oxygen, hydrogen and sulphur, have been utilized to understand fluid-rock interactions in and around ore deposits for more than 40 years (Nesbitt, 1996). The intensity of this isotopic alteration increases from peripheral regions into the centre of mineralization with greater shifts toward lighter isotopic ratios occurring with more fluid-rock interaction. These lighter stable isotope ratios can therefore provide information about fluid flow during mineralization. This in turn can enable the mapping of the extent of fluid interactions, discern fracture-controlled versus pervasive permeability, determine alteration temperatures, assess alteration intensity, and contribute to the development of ore deposit and exploration models (Barker et al., 2013).

---

**Keywords:** carbonate, British Columbia, Zn-Pb deposits, C and O isotopes, isotopic footprint

*This publication is also available, free of charge, as colour digital files in Adobe Acrobat® PDF format from the Geoscience BC website: <http://www.geosciencebc.com/s/DataReleases.asp>.*

This particular project is focused on characterizing the carbonate alteration footprints of the relatively poorly understood Zn-Pb deposits in southeastern British Columbia. These deposits are poorly classified and have been variably attributed to a range of mineral deposit models, such as sedimentary exhalative, Irish-type, carbonate replacement-type and skarns (Fyles, 1970; Simandl and Paradis, 2009), and further complications arise because many deposits also include oxidized Zn ores (Simandl and Paradis, 2009).

This paper aims to outline the Masters project initiated at the Mineral Deposit Research Unit (MDRU) at the University of British Columbia. This project is included in the MDRU's Carbonate Alteration Footprints Project. The main project objectives are as follows:

- determine the size and intensity of alteration surrounding different types of carbonate-hosted Zn-Pb deposits within southeastern BC,
- characterize and map fluid flow pathways and assess the intensity of fluid-rock interactions as vectoring tools,
- assess stable isotope alteration from proximal intrusion-related through to distal carbonate-hosted ore systems, and
- determine the optimal sampling protocols and strategies to utilize stable isotopes as an exploration tool.

## Regional Geology

### Geology

Southeastern BC is underlain by the central part of the Kootenay Arc, a curving belt of complexly deformed sedimentary, volcanic and metamorphic rocks extending from Revelstoke southeast, south and southwest across into northeastern Washington (Fyles, 1967). These rocks represent the ancient western margin of the ancestral North American miogeocline. The rock units of the central Kootenay Arc comprise Lower Cambrian micaceous quartzite of the Reno Formation overlain by the Cambrian Laib Formation, containing the Truman, Reeves and Emerald members (Figure 1). The Truman member of the lower Laib Formation consists of a thin sequence of interbedded

Period	Southeastern British Columbia	
Ordovician	Active Formation	
Middle Cambrian	Nelway Formation	
Lower Cambrian	Laib Formation	upper Laib Formation
		Emerald member
		Reeves member
		Truman member
		Reno Formation
	Quartzite Range Formation	

**Figure 1.** Schematic stratigraphic log of the regional geology in southeastern British Columbia (modified from Fyles, 1970).

phyllite and limestone. The Reeves member mainly consists of fine- to medium-grained limestone, which has been locally altered to dolostone. This limestone characteristically displays grey, black and white banding typically a few centimetres in width. The dolostone often weathers buff, is poorly banded or massive, and is normally finer grained than the limestone. The Emerald member overlies the Reeves member limestone and is characterized by a black to grey, foliated, carbonaceous, often crenulated, phyllite unit. At the top of the Laib Formation (the upper Laib Formation) is an undivided series of phyllite units with lesser intercalated beds of micaceous quartzite and limestone (Fyles and Hewitt, 1959).

The Laib Formation is overlain by the Middle Cambrian Nelway Formation (Figure 1), a second unit of limestone and dolomite. Above the Nelway Formation is the Ordovician Active Formation (Figure 1); a unit of black argillite slate with minor calcareous lenses (Fyles and Hewitt, 1959). Throughout southeastern BC there are numerous intrusions of Mesozoic granite, leucocratic granite and syenite. These have traditionally been considered part of the Nelson batholith suite, which has been dated as Middle Jurassic (Little, 1960).

## Structure and Metamorphic History

The rocks of the Kootenay Arc have a complex structural history involving at least three phases of folding, major regional low-angle faults and multiple smaller faults (Fyles and Hewitt, 1959). Notably, the regional trend is to the northeast, which is contrary to the typical northwesterly trend of the Cordillera.

Regional metamorphism reaches to lower greenschist facies and is thought to have been synchronous with the earliest phase of deformation. Contact metamorphism is locally associated with the intrusion of the Middle Jurassic igneous rocks and postdates all phases of folding (Fyles and Hewitt, 1959).

## Mineralization

Carbonate-hosted Zn-Pb deposits occur along the entire length of the Kootenay Arc with the largest deposits occurring in the vicinity of Salmo, BC and Metaline Falls, Washington, on either side of the Canada–United States border. From north to south, the major carbonate-hosted Zn-Pb deposits of the Kootenay Arc include the Duncan, H.B., Jersey, Remac and Pend Oreille deposits (Figure 2). These deposits can be split into two end-members (Fyles, 1970):

- Salmo-type deposits consist of stratiform lenses of pyrite, sphalerite and galena in zones of dolomite in the highly deformed Lower Cambrian Reeves member limestone. These types of deposits include the Duncan (near the north end of Kootenay Lake), the H.B., Jersey and Remac orebodies.
- Metaline-type deposits consist of stratiform lenses in the relatively undeformed, stratigraphically younger, Middle Cambrian Nelway Formation carbonate rocks. These types of deposits include those situated near Metaline Falls, Washington, in particular, the Pend Oreille deposit.

## Deposit Geology

The three deposits that this project is focused on are Remac, Jersey and H.B. (Figure 2). The property geology for each of these deposits is discussed further below.

### Remac

The Remac property is located east of the junction of the Salmo and Pend-d'Oreille rivers, approximately 56 km south-southwest of Nelson and 25 km southeast of Trail (Figure 2). Between 1949 and 1971, whilst the mine was active, 5.8 million tonnes of ore was recovered at 3.5% Zn, 1.39% Pb, 0.02% Cd and 3.12 g/t Ag (MINFILE 082FSW026, BC Geological Survey, 2014). Three regional-scale packages of rocks are present at the property: the Reeves member, the Active Formation and the Nelway Formation. These rock units typically strike west-southwest and dip steeply to moderately to the south (Fyles and

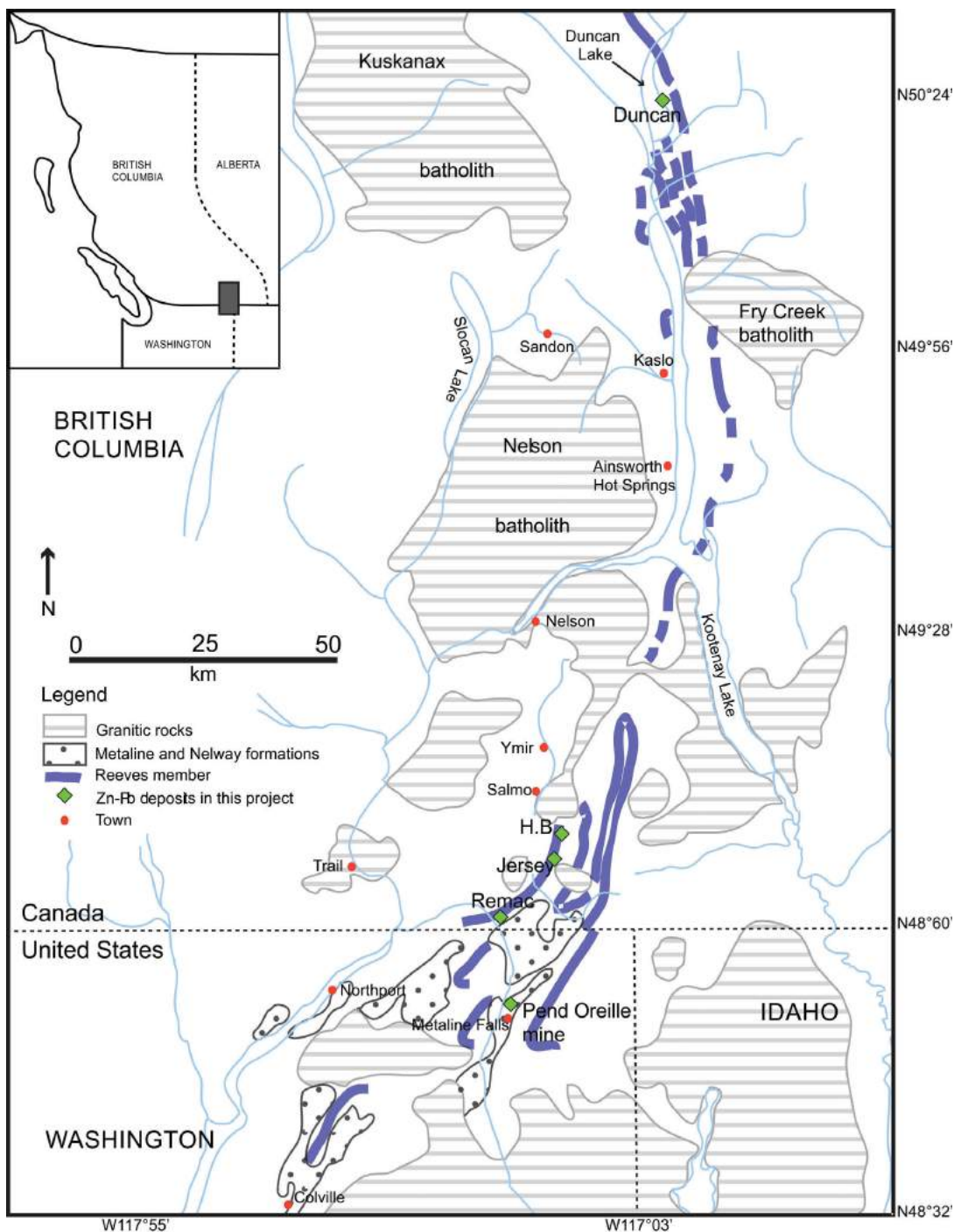


**Figure 2.** Location map of the three properties studied in this project and their corresponding bedrock geology, southeastern British Columbia (modified from Fyles, 1970).

Hewitt, 1959). All significant Zn-Pb mineralization within the Remac property occurs in the Reeves member carbonate rocks, which can be split into three property-scale subunits (Kushner, 2009).

The northern Reeves horizon is an extensive unit of massive to bedded limestone that appears to be devoid of base metal mineralization. The central Reeves horizon is host to

all the past Zn-Pb production from the mine and the majority of other known Zn-Pb mineralization on the property. The southern Reeves horizon is host to scattered zones of Zn-Pb mineralization (Kushner, 2009).

The Reeves member limestone is medium grained, weathers blue-grey and is thinly banded between white, grey and sometimes black intervals. These laminations are generally

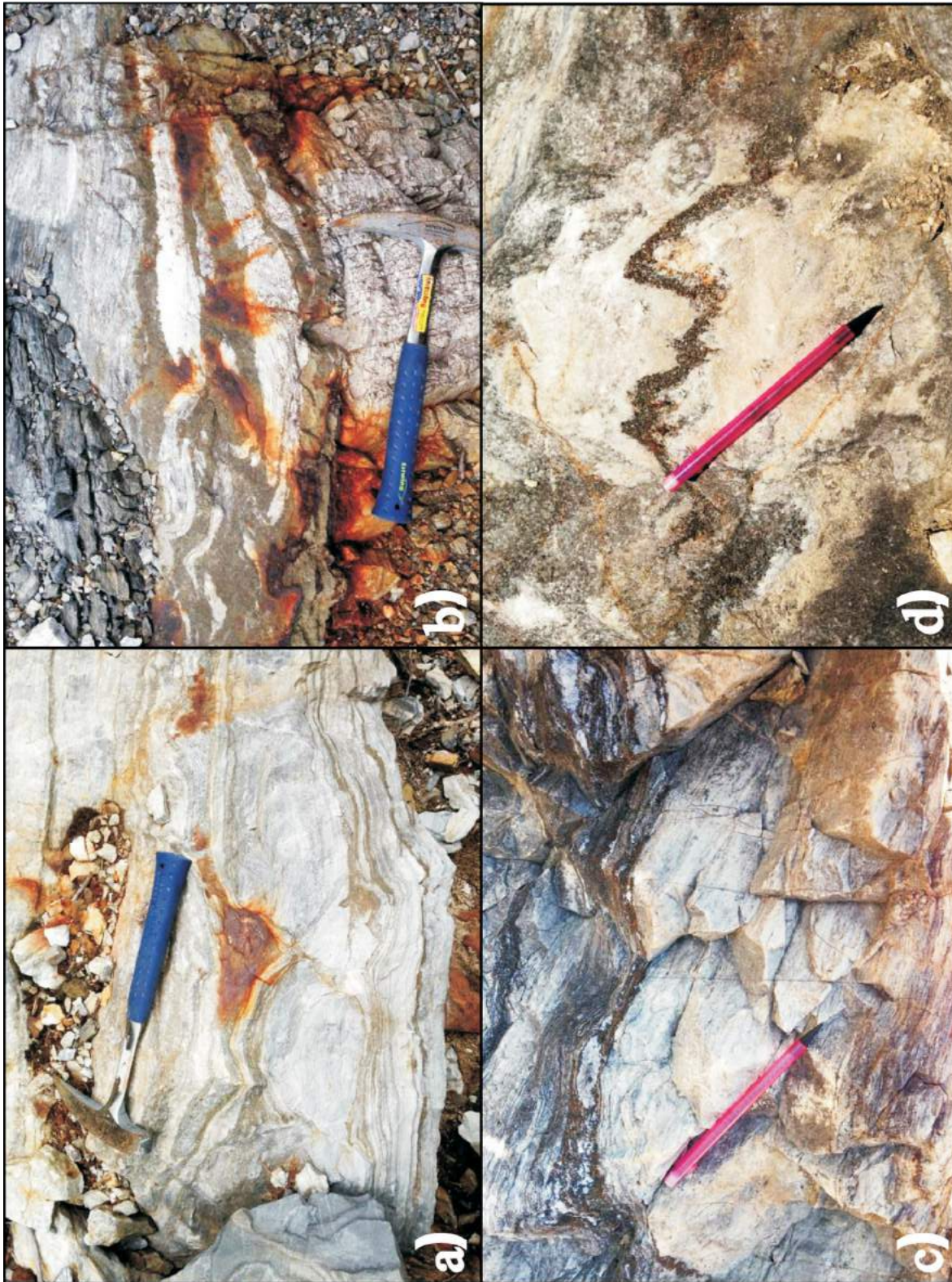


**Figure 3.** Collage of photographs to show the mineralization styles seen at the Remac (a, b) and Jersey (c, d) deposits, southeastern British Columbia. **a)** Deformed lenses of sulphides within the Reeves member at the Remac deposit; mineralization wraps around a dolomite boudin. **b)** Deformed lenses of pyrite within the Reeves member at the Remac deposit. **c)** Stratiform lenses of pyrite, sphalerite and galena within the Reeves member dolomite at the Jersey deposit. **d)** Deformed band of pyrite within the Reeves member limestone at the Jersey deposit.

on the scale of one to several centimetres. Primary sulphide mineralization at the Remac property consists of laminations and lenses of massive and disseminated pyrite, honey-coloured sphalerite, galena and trace chalcopyrite within the Reeves member. The sulphide bodies are structurally conformable and stratabound, and often contain a high-grade central core that typically feathers out along strike. The sulphide bodies are typically contained within dolomite envelopes, some of which extend for considerable distances along strike (Figure 3a, b). The dolomites tend to be finer grained and more massive than the nearby limestone (Kushner, 2009).

Conformably overlying the ore-bearing limestone of the Reeves member are black, carbonaceous phyllite and schist of the Emerald member of the Laib Formation. The characteristic rock type that comprises the Emerald member is a black to grey, foliated, often crenulated, phyllite unit. Disconformably overlying the Laib Formation is the Ordovician Active Formation. The Active Formation consists of black argillite slate and minor calcareous members (Fyles and Hewitt, 1959).

Rocks present on the Remac property are deformed by two major west-southwest-trending, isoclinal folds: the Salmo River anticline and the Reeves syncline. These folds have moderate to steep southerly dipping axial planes. The rocks are also cut by a series of north-northeasterly trending normal faults. These faults dip 45 to 60° to the east, and have resulted in a downfaulted repetition of the stratigraphic and mineralized sequence eastward in a number of separate fault blocks (Fyles and Hewitt, 1959).

### Jersey

The Jersey property sits at the summit between Sheep and Lost creeks, roughly 11 km southeast of Salmo (Figure 2). Between 1949 and 1970, whilst the mine was active, 6.4 million tonnes of ore was recovered at 4.1% Zn and 1.2% Pb. Measured and indicated ore reserves as of April 1, 1965, are reported at 671 075 tonnes grading 4.1% Zn and 1.2% Pb (MINFILE 082FSW009). The property is underlain by rocks of the Truman member, composed of interbedded thin grey and white, locally dolomitic limestone. The Emerald member is a black argillite unit. The Reeves member consists of limestone and dolomite and the upper Laib Formation is composed of green phyllite and micaceous quartzite. These sedimentary rocks are intruded by small plugs, dikes and sills of Cretaceous granite and those that are in contact with the granitic bodies are typically skarnified, resulting in a variety of skarn rocks ranging from recrystallized coarse-grained marble to garnet-pyroxene-bearing skarn (Giroux and Grunenberg, 2010).

The Zn-Pb deposits on the Jersey property are hosted by fine-grained, poorly layered to massive dolomite of the Reeves member (Simandl and Paradis, 2009). This miner-

alization (Figure 3c, d) occurs near to the base of the Reeves member and forms stratiform lenses of pyrite, sphalerite and galena in dolomitized zones (Simandl and Paradis, 2009). The dolomites are texturally distinct from the medium-grained, well banded, grey and white limestone unit of the Reeves member. The deposits, their dolomitic envelopes and the limestone hostrock generally lie within secondary isoclinal folds along the limbs of regional anticlinal structures (Giroux and Grunenberg, 2010). Five ore bands, ranging in thickness from 0.3 to 9.0 m have been identified. These bands in order of stratigraphic sequence are

- 1) upper lead band,
- 2) upper zinc band,
- 3) middle zinc band,
- 4) lower zinc band, and
- 5) lower lead band.

The Truman member of the Laib Formation forms the mine footwall rocks. It consists of dense, reddish green skarns and a brown argillite that hosts W and Mo mineralization (Giroux and Grunenberg, 2010).

Several zones of significant and locally very different mineralization have been identified. Historically, mined areas produced Zn, Pb and W, with known areas of high Mo, Au, Bi, As, Cu, Ag, Cd and Ba concentrations (Giroux and Grunenberg, 2010).

The rocks present on the Jersey property have been deformed by three phases of folding. Within the mine area, structure is dominated by a major north-northeast-trending anticline, which is also present at the Remac property, known as the Salmo River anticline. The property mineralization is associated with the east limb of this anticline (Giroux and Grunenberg, 2010). Three small stocklike bodies of Cretaceous granite intrude the Salmo River anticline and locally cut the ore zones near the Jersey mine. From south to north these are the Jersey, Emerald and Dodger stocks (Giroux and Grunenberg, 2010).

### H.B.

The H.B. property is located on Aspen Creek, a tributary of Sheep Creek, 8 km southeast of Salmo (Figure 2). Between 1912 and 1978, whilst the mine was active, 6.7 million tonnes of ore was recovered at 4.1% Zn and 0.1% Pb. Measured and indicated reserves as of December 31, 1978, are reported at 36 287 tonnes grading 4.1% Zn and 0.1% Pb (MINFILE 082FSW004). The property is underlain by the Reeves member limestone and the Lower to Middle Ordovician Active Formation. These units contact each other along a fault, with the Active Formation rocks overthrust from the east over the Reeves member rocks (Giroux and Grunenberg, 2010). Two distinct calcareous layers of the Reeves member can be recognized in the area, an upper unit about 110 m thick separated from a lower 12 m member by 15 to 30 m of micaceous, brown, limey argillite. The H.B.

orebodies occur roughly 100 m to the west of the thrust fault. It is thought that the mineralization is related to the intrusion of granitic stocks of the Middle to Late Jurassic Nelson intrusion. However, the only intrusions present in the mine are post-ore diabase dikes up to 3 m thick (Giroux and Grunenberg, 2010).

The mineralized zones are located within dolomitized limestone of the Reeves member and contain banded galena, sphalerite, pyrite and pyrrhotite similar to that seen at the Jersey property except that Pb dominates (Giroux and Grunenberg, 2010).

In the vicinity of the H.B. mine, the beds are folded into a broad synclorium, and the limestone layers in the mine are on the west limb of this structure. The principal ore zones consist of three, steeply dipping, parallel zones lying approximately side by side and extending as pencil-like shoots for about 900 m along the south plunge of the controlling structures (Giroux and Grunenberg, 2010).

### Light Stable Isotopes

Studies of light stable isotopes (S, C, O and H) have attempted to characterize isotopic footprints of a variety of carbonate-hosted ore systems, but have yet to be extensively used in BC's Zn-Pb deposits. It has been shown that light stable isotope studies, when used in conjunction with geological data, fluid inclusion studies and geochemical data, can not only identify fluid components, but also place important constraints on their evolution in the system, for example, origin of the ore fluid (Rye, 1993). The use of stable isotopes in these systems is enabled by the fact that their host ore fluids undergo considerable fluid-rock interaction.

Stable isotope analyses are traditionally measured using gas-source isotope ratio mass spectrometry (IRMS). However, C and O isotope ratios can now be analyzed using infrared absorption to measure isotopic signatures in different gas species. One such infrared absorption technique, which has been developed and applied at MDRU, is off-axis-integrated cavity output spectroscopy (OA-ICOS). The OA-ICOS uses a laser source, which produces light at an infrared wavelength suitable for interacting with the gas species of interest (Barker et al., 2013).

The stable isotope composition of hostrocks that have interacted with hydrothermal fluid will depend on a variety of factors:

- the isotopic composition of unaltered hostrock,
- the isotopic composition of the hydrothermal fluid, and
- the temperature of dissolution and precipitation.

In general, rocks that have seen higher degrees of fluid-rock interaction, or where fluid-rock interaction occurred at higher temperatures, will have a greater shift toward lighter isotopic ratios. Therefore, hostrocks in the vicinity

of mineralization should be expected to have the lightest isotopic values compared to rocks farther from mineralization. Furthermore, the size and distribution of isotopic alteration is likely controlled by the total flux of hydrothermal fluid and, as such, is controlled by permeability, mineralogy, grain size, temperature and fluid-rock ratios in the surrounding hostrocks (Barker et al., 2013).

### Conclusion

This project aims to improve the current understanding of southeastern BC's poorly understood Zn-Pb deposits by applying stable isotope studies to map out their alteration footprints. Stable isotopes have been used to successfully understand fluid-rock interactions in and around a variety of ore deposits for more than 40 years (Nesbitt, 1996). It stands to reason that the same techniques can be applied to less well understood deposit types in order to aid in the mapping of the extent of fluid interactions, discern fracture-controlled versus pervasive flow, determine fluid temperatures, assess alteration intensity, and contribute to the development of ore deposit and exploration models. It is hoped that this technique will improve the current deposit model for Zn-Pb systems in southeastern BC and could potentially be used as an exploration tool to find similar, undiscovered deposits in the area. This, in turn, may revive southeastern BC as a region of potential economic development and so generate more interest in the nearby communities of Salmo, Nelson and Trail.

To date, fieldwork has been conducted on the Remac, Jersey and H.B. deposits to collect a variety of carbonate samples for C and O isotope analysis. Roughly 500 samples were collected in September 2014 with particular focus being put on sampling: unaltered, unmineralized, carbonate hostrocks distal to the main ore zones; all observable dolomite phases; mineralized samples proximal to the main ore zones; and any late-stage carbonate veins. Furthermore, representative samples of all main rock types have been collected for thin-section petrography. Preliminary C and O isotope analysis will be conducted on these samples in the coming months in addition to petrography, carbonate staining, ultraviolet-light analysis and scanning electron microscope-cathodoluminescence (SEM-CL) analysis. It is anticipated that all of these techniques will characterize the carbonate alteration footprint of these poorly understood Zn-Pb deposits and provide a paragenetic sequence of events for each deposit, which in turn may be used to improve the current deposit models in this area. This Masters project is anticipated to be completed in January 2016.

### Acknowledgments

This research is part of the Carbonate Alteration Footprints Project, which is being undertaken at the Mineral Deposit Research Unit at the University of British Columbia. The

project is supported by a consortium of industry sponsors. Geoscience BC is acknowledged and thanked for the scholarship provided to aid the first author's efforts in working on this project. The help and support at the Jersey and H.B. mines from E. Lawrence, the consultant for Sultan Minerals Inc., and J. Denny at the Chamber of Mines of Eastern BC is greatly appreciated. G. Dipple at the University of British Columbia is also thanked for a helpful peer review of this paper.

## References

- Barker, S., Dipple, G., Hickey, K., Lepore, W. and Vaughan, J. (2013): Applying stable isotopes to mineral exploration: teaching an old dog new tricks; *Economic Geology*, v. 108, p. 1–9.
- BC Geological Survey (2014): MINFILE BC mineral deposits database; BC Ministry of Energy and Mines, BC Geological Survey, URL <<http://minfile.ca/>> [November 2014].
- Fyles, J.T. (1967): Geology of the Ainsworth-Kaslo area, British Columbia; BC Ministry of Energy and Mines, Bulletin no. 53, 133 p., URL <<http://www.empr.gov.bc.ca/Mining/Geoscience/PublicationsCatalogue/BulletinInformation/BulletinsAfter1940/Documents/Bull53.pdf>> [November 2014].
- Fyles, J.T. (1970): Geological setting of the lead-zinc deposits in the Kootenay Lake and Salmo areas of British Columbia; *in* Lead-Zinc Deposits in the Kootenay Arc, Northeastern Washington and Adjacent British Columbia, A.E. Weissenborn (ed.), State of Washington, Department of Natural Resources, Bulletin no. 61, p. 45–53, URL <[http://www.dnr.wa.gov/publications/ger\\_b61\\_lead\\_zinc\\_dep\\_kootenay.pdf](http://www.dnr.wa.gov/publications/ger_b61_lead_zinc_dep_kootenay.pdf)> [November 2014].
- Fyles, J.T. and Hewlett, C.G. (1959): Stratigraphy and structure of the Salmo lead-zinc area; BC Ministry of Energy and Mines, Bulletin no. 41, 162 p., URL <<http://www.empr.gov.bc.ca/Mining/Geoscience/PublicationsCatalogue/BulletinInformation/BulletinsAfter1940/Documents/Bull41.pdf>> [November 2014].
- Giroux, G. and Grunenberg, P. (2010): Resource estimation for the Jersey lead zinc deposit, Jersey-Emerald property, BC (Nelson Mining Division BC, NTS 82F.004/005/014/015); report for Sultan Minerals Inc., 67 p., URL <[http://www.sultanminerals.com/i/pdf/ni43-101\\_jerseyleadzinc.pdf](http://www.sultanminerals.com/i/pdf/ni43-101_jerseyleadzinc.pdf)> [November 2014].
- Kushner, W. (2009): Technical drilling program on the ReMac zinc project, Nelson Mining Division, British Columbia; BC Ministry of Energy and Mines, Assessment Report 30 001, 210 p., URL <[http://aris.empr.gov.bc.ca/search.asp?mode=repsum&rep\\_no=30001](http://aris.empr.gov.bc.ca/search.asp?mode=repsum&rep_no=30001)> [November 2014].
- Little, H.W. (1960): Nelson map area, west half, British Columbia; *in* Geological Survey of Canada, Memoir 308, 205 p., URL <<http://geoscan.nrcan.gc.ca/starweb/geoscan/servlet.starweb?path=geoscan/download.web&search1=R=100535>> [November 2014].
- Nesbitt, B.E. (1996): Applications of oxygen and hydrogen isotopes to exploration for hydrothermal mineralization; featured article *in* SEG Newsletter no. 27, Society of Economic Geologists, p. 1–13.
- Rye, R.O. (1993): The evolution of magmatic fluids in the epithermal environment: the stable isotope perspective; *Economic Geology*, v. 88, p. 733–752.
- Simandl, G.J. and Paradis, S. (2009): Carbonate-hosted, nonsulphide, zinc-lead deposits in the southern Kootenay Arc, British Columbia (NTS 082F/03); *in* Geological Fieldwork 2008, BC Ministry of Energy and Mines, Paper 2009-1, p. 205–218, URL <[http://www.empr.gov.bc.ca/Mining/Geoscience/PublicationsCatalogue/Fieldwork/Documents/2008/17\\_Simandl.pdf](http://www.empr.gov.bc.ca/Mining/Geoscience/PublicationsCatalogue/Fieldwork/Documents/2008/17_Simandl.pdf)> [November 2014].



## Preliminary Results from a Trace-Element Study of Amphibole-Cumulate Rocks from the Bonanza Arc, Vancouver Island, British Columbia (NTS 092A/09)

R.J. D'Souza, School of Earth and Ocean Science, University of Victoria, Victoria, BC, rdsouza@uvic.ca

D. Canil, School of Earth and Ocean Science, University of Victoria, Victoria, BC

---

D'Souza, R.J. and Canil, D. (2015): Preliminary results from a trace-element study of amphibole-cumulate rocks from the Bonanza Arc, Vancouver Island, British Columbia (NTS 092A/09); *in* Geoscience BC Summary of Activities 2014, Geoscience BC, Report 2015-1, p. 103–110.

### Introduction

Porphyry-Cu deposits, which are closely associated with convergent-margin (i.e., arc) settings, are sources for much of the world's Cu and almost the entire supply of the world's Mo (Sinclair, 2007). Rare metals, including Pt, Pd and W, are also found in porphyry-Cu systems. However, despite the genetic association of such deposits with convergent margins, not all arcs are prospective for the formation of porphyry-Cu deposits. For example, the Jurassic Bonanza Arc on northern Vancouver Island hosted the Island Copper mine (Canada's third largest, active from 1970 to 1995), but no similar deposit has been discovered elsewhere on Vancouver Island, despite the extensive exposure of the Bonanza Arc rocks.

The key to whether or not magmas are enriched in Cu depends critically on the oxidation state of the magma and the speciation of S. Under reducing conditions, S is present as sulphide and the chalcophile elements (Cu, Au, Mo, etc.) are sequestered in the immiscible sulphide melt and lost from the magma. Under more oxidizing conditions, however, S is present as sulphate and thus Cu remains in the silicate magma. A recent study by Chiaradia (2014) reported that arcs with crust >30 km in thickness tend to produce Cu-poor volcanic rocks, whereas arcs <20 km in thickness produce Cu-rich volcanic rocks, contrary to prior observations of porphyry deposits with thick arcs (e.g., Sinclair, 2007; Sillitoe, 2010). Chiaradia (2014) attributed his observations to magnetite fractionation at depth from water-rich magmas, which would produce a reduced magma in which sulphide is stable and able to remove the chalcophile elements. This produces a sulphide-rich lower crust that could be melted by later magmas to produce porphyry-Cu deposits (Lee et al., 2012; Chiaradia, 2014).

In addition to their association with economic ore deposits, arcs are also thought to be the locus of continental growth, based on the similarity between the andesitic bulk composition of arcs and that of the bulk continental crust (e.g., Taylor, 1977; Rudnick and Fountain, 1995; Rudnick and Gao, 2014). However, Lee et al. (2012) noted some discrepancies between these compositions. Specifically, the bulk continental crust is depleted in Cu, Sc, Ni and Cr relative to parental arc magmas. Whereas Cu depletion is likely due to sulphide fractionation, Lee et al. (2012) postulated that the coupled depletion in Sc, Cr and Ni indicates the effect of pyroxene or amphibole fractionation in the lower crust of arcs. Amphibole fractionation in the lower crust of arcs would effectively filter ascending magmas of up to 20% of their water and form a fertile, incompatible-element-rich lower crust (Davidson et al., 2007). Release of this water from this 'sponge' could enhance melt production in the lower crust (Davidson et al., 2007) and promote the melting of sulphides to produce the Cu-rich melts that could form porphyry-Cu deposits (Chiaradia, 2014).

This paper describes the results of preliminary work to test the hypotheses of Davidson et al. (2007) and Lee et al. (2012) using intrusive rocks of the Jurassic Bonanza Arc exposed on Vancouver Island. Trace-element chemistry of amphiboles and pyroxenes from sulphide-bearing, amphibole-rich cumulate ultramafic rocks that have been described in the Bonanza Arc by Larocque and Canil (2010) is examined to determine whether amphibole crystallization could control magma evolution. The origin of amphibole in these rocks is contentious, with arguments having been made for both primary (e.g., Larocque and Canil, 2010) and secondary (e.g., Fecova, 2009) origin.

A recent study by Smith (2014) on lower crustal xenoliths in volcanic rocks from the Solomon Islands concluded that the amphibole in those samples was formed by melt reaction of primary clinopyroxene. Trace-element distributions in the cumulate rocks from the Bonanza Arc may indicate whether amphibole is a primary fractionating phase or a secondary melt-reaction product. Answers to this question provide an important test of the hypothesis that amphibole crystallization can drive the chemical evolution of an arc

---

**Keywords:** geochemistry, Bonanza Arc, amphibole, pyroxene, sulphides

This publication is also available, free of charge, as colour digital files in Adobe Acrobat® PDF format from the Geoscience BC website: <http://www.geosciencebc.com/s/DataReleases.asp>.

(Davidson et al., 2007). If the amphibole in the Bonanza Arc cumulate rocks is a primary magmatic phase, this would imply the existence of water-rich, incompatible-element-rich, lower crustal rocks that could have been the source of later magmas that formed porphyry-Cu deposits (Chiaradia, 2014).

### Industry Application

In addition to testing whether amphibole is indeed controlling the magma evolution and behaviour of incompatible elements in the lower crust, as predicted by Davidson et al. (2007) and Lee et al. (2012), this study will contribute to the understanding of the processes by which some arcs and not others are prospective for the formation of porphyry-Cu deposits. The observation by Chiaradia (2014) of the inverse relationship between volcanic Cu content and arc thickness is not consistent with the observation of porphyry-Cu deposits in association with thick arcs. Testing the hypothesis postulated by Chiaradia (2014) for this inverse relationship has the potential to refine current exploration strategies and expand understanding of the formation of these deposits.

### Regional Geology

The Jurassic Bonanza Arc on Vancouver Island (Figure 1) was emplaced within a pre-Jurassic crust comprising a Triassic oceanic plateau (the Karmutsen basalts) and a Devonian arc (the Sicker Group; Muller and Yorath, 1977). A compilation of U-Pb (zircon) and Ar-Ar (hornblende) ages from the Bonanza Arc (D'Souza et al., work in progress) shows that the arc was emplaced between 203 and 160 Ma, with a large peak at 170 Ma. Although the Bonanza Arc is considered to be correlative with the Jurassic Talkeetna Arc in Alaska (DeBari et al., 1999), the Talkeetna Arc differs in that it was emplaced directly on oceanic crust (DeBari and Coleman, 1989). Rare garnet-bearing cumulate rocks have

also been discovered within the Talkeetna Arc section but have not been reported from the Bonanza Arc (DeBari et al., 1999).

The Bonanza Arc consists of volcanic rocks and their plutonic counterpart, which has traditionally been divided into two groups: the Westcoast Crystalline Complex and the Island Plutonic Suite (Muller and Yorath, 1977). The volcanic rocks consist of basalt, andesite, dacite and rhyolite that have been emplaced as flows, breccias and tuffs. The Westcoast Crystalline Complex is a variably foliated unit comprising hornblendite, gabbro and granodiorite. Application of Al-in-hornblende barometry indicates that this unit equilibrated at depths of 10–17 km (with high uncertainty; Canil et al., 2010). The Island Plutonic Suite is typically unfoliated and, on average, more felsic than the Westcoast Crystalline Complex; the former comprises quartz diorite, granodiorite, quartz monzonite and tonalite. The Island Plutonic Suite was emplaced at depths of 2–10 km, as indicated by Al-in-hornblende barometry (Canil et al., 2010). Aside from the presence of foliation, the distinction between the Island Plutonic Suite and the Westcoast Crystalline Complex is, in practice, difficult to observe in the field. Amphibole-rich cumulate rocks have been reported as schlieren and layers within intermediate plutonic rocks.

### Amphibole in the Bonanza Arc: Primary or Melt-Reaction Product?

On the basis of geochemical modelling, Fecova (2009) concluded that the amphibole in the Bonanza Arc was a product of reaction between primary clinopyroxene and a later melt. Similarly, DeBari and Coleman (1989) and Greene et al. (2006) interpreted the amphibole in plutonic rocks from the Talkeetna Arc as not being primary but instead to have formed as a result of fluid enrichment, melt reaction or subsolidus re-equilibration of cumulus clinopyroxene. Conversely, Larocque and Canil (2010) argued that the major-element geochemistry indicates that amphibole is a primary fractionating phase in the Bonanza Arc. D'Souza et al. (work in progress) determined a Rb-Sr isochron age for samples of the Bonanza Arc (including amphibole-bearing ones) of ca. 160 Ma, coinciding with the age of magmatism. They argued that the closeness of the Rb-Sr isochron age and the emplacement age supports the argument that amphibole is a primary fractionating phase in these magmas, as the Rb-Sr isochron would have been reset by amphibole formation by reaction of clinopyroxene with a later melt. Petrographic evidence appears equivocal (Fecova, 2009; Larocque and Canil, 2010) because clinopyroxene is observed to grade into amphibole in some samples, indicating a fluid-reaction origin, whereas chadacrysts of amphibole are seen within oikocrysts of relatively pristine olivine in other samples, implying a primary origin (Figure 2).

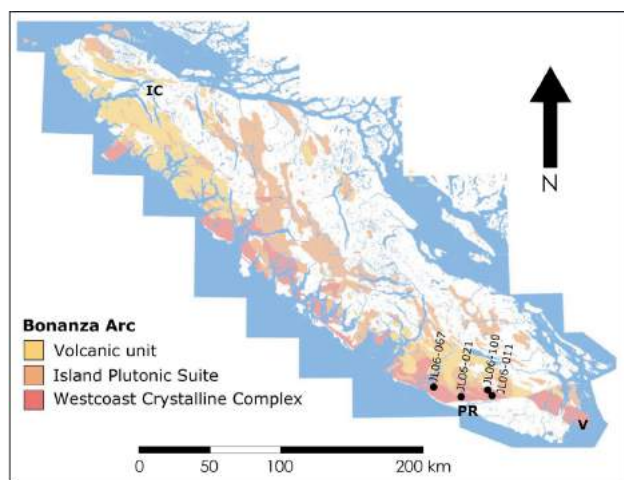


**Figure 1.** Simplified geology of Vancouver Island, showing the Jurassic Bonanza Arc and pre-existing igneous rocks. Locations of samples analyzed in this study are shown and labelled. Abbreviations: IC, Island Copper minesite; PR, Port Renfrew; V, Victoria.

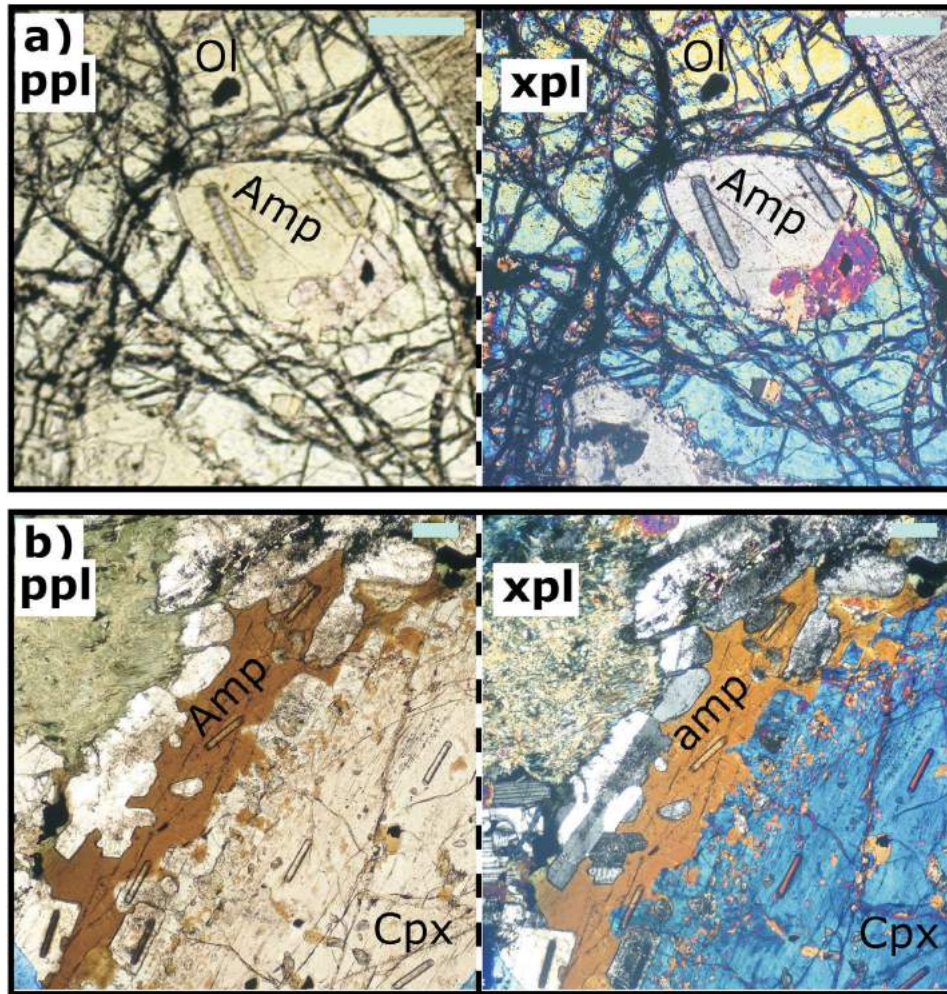


**Figure 2.** Photomicrographs of **a)** an amphibole chadacryst within an olivine oikocryst, JL06-021; **b)** a gradational contact between amphibole and clinopyroxene, JL06-100. Scale bar in all images is 200  $\mu\text{m}$ , the length of the ablation pits in the images. Images shown were taken in plane polarized light (ppl) and cross-polarized light (xpl).

## Methods

Trace-element compositions were analyzed for amphibole, clinopyroxene, orthopyroxene and plagioclase in four amphibole-bearing cumulate samples (Table 1) from exposures near Port Renfrew for which mineral chemistry and bulk-rock compositions are available (Larocque, 2008; locations in Figure 1). These samples were selected because they contained all the phases of interest and also appeared under the microscope to show little alteration.

Rare-earth-element (REE) and other trace-element concentrations were determined at the School of Earth and Ocean Sciences, University of Victoria using a New Wave Research UP213 laser-ablation system and a Thermo X-Series II inductively coupled plasma-mass spectrometer with an argon-gas carrier system. Four ablation passes were conducted along a raster line that was 200  $\mu\text{m}$  long and 40  $\mu\text{m}$  wide, using an average laser power of  $\sim 14 \text{ J/cm}^2$ . Gas-blank compositions were also determined for every analysis and

United States Geological Survey standard glass BCR2g was analyzed after every six to eight analyses. The BCR2g standard glass and National Institute of Standards and Technology (NIST) standard glasses 615, 613 and 611 were analyzed at the start and end of every sample. These standards were analyzed under the same conditions used for phases in the samples.

After data collection, the individual spectra of counts per second versus time were examined for each analysis and sections that showed flat plateaus were manually selected. Ramps and saw-tooth patterns in such spectrum were edited, as they are likely due to laser or plasma instability and the presence of unseen inclusions, respectively. The data were reduced to concentrations in parts per million in a spreadsheet using Ca and Si concentrations (determined by microprobe; Larocque, 2008) as internal standards. All analyses were also corrected for instrument drift using the analyses of BCR2g collected during the session. GeoReM (Jochum

**Table 1.** Petrographic summary of the samples analyzed in this study, from exposures near Port Renfrew.

Sample	Rock type	Mineralogy (mode - species)				
		Amphibole	Pyroxene	Feldspar	Olivine	Other
JL06-021	Olivine cumulate	62% - tschermakite	6% - enstatite, diopside	20% - plagioclase	12% - chrysolite	-
JL06-011	Plagioclase cumulate	60% - magnesiohornblende, tschermakite	23% - enstatite, diopside	12% - An <sub>53-90</sub> Ab <sub>10-53</sub> Or <sub>0-8</sub>	-	5% - Fe-Ti oxide
JL06-067	Plagioclase cumulate	64% - magnesiohornblende, tschermakite	3% - diopside	30% - An <sub>52-92</sub> Ab <sub>9-48</sub> Or <sub>0.5-1</sub>	-	1% - Fe-Ti oxide; 2% - biotite
JL06-100	Plagioclase cumulate	29% - tschermakite	6% - augite, diopside	65% - An <sub>46-54</sub> Ab <sub>46-51</sub> Or <sub>0.6-4</sub>	-	-

et al., 2005) preferred values were used for the NIST and BCR2g standard element concentrations.

## Results

Chondrite-normalized REE profiles (Figure 3) for the amphibole and pyroxene in all four samples are convex upward, with the apex at Sm. This convex-upward shape is similar to the shape of the REE profile for the JL06-011 and JL06-021 whole-rock analyses, reflecting the high proportion of amphibole and pyroxene in these samples. There are two amphibole populations in sample JL06-067: one that is similar in profile curvature to the amphibole in the other samples (dark green on Figure 3) and another that shows higher La and Ce abundances, and therefore has less curved profiles (light green on Figure 3).

The two populations of amphibole are also evident on a plot of the Eu anomaly (calculated using Equation 1, where Eu\* is the expected Eu abundance, given the observed chondrite-normalized Sm and Gd abundances) versus the chondrite-normalized La/Sm ratio (Figure 4). The amphibole analyses show varying Eu anomalies, from positive (JL06-021) to none or slightly negative (JL06-011, JL06-021) to strongly negative (JL06-100). A strong negative correlation was observed between the Eu anomaly and La/Sm ratio in the main amphibole population, except for the subvertical array described by amphiboles from JL06-021 (i.e., amphiboles that are both chadacrysts within olivine oikocrysts and oikocrysts to olivine chadacrysts). The high La/Sm population of amphibole from JL06-067 shows a small range in Eu anomaly (1.1–1.3) and little variation with La/Sm ratio.

$$Eu/Eu^* = Eu_N / ((Sm_N + Gd_N) / 2) \quad (1)$$

The pyroxenes have REE profiles that are similar in shape (i.e., convex upward, Figure 3) to the amphiboles. The pyroxenes have lower REE abundances than the amphiboles, except in JL06-011, where the middle and heavy REE (Sm to Lu) abundances of amphibole and pyroxene overlap. Pyroxene in JL06-011 and JL06-067 shows larger, negative Eu anomalies than amphibole, whereas the opposite is observed in JL06-100. In Figure 4, the pyroxene shows a range in La/Sm ratio similar to that of the amphibole (ex-

cept the high La/Sm amphibole from JL06-067). In Figure 4, the Eu anomalies in the pyroxene data fall within the range of those in the amphibole data but are more restricted (0.6–1.1) and do not display any strong trends.

On a plot of the extended trace-element profiles (normalized to primitive-mantle values; Figure 5), the most striking features are the sharp negative Cu and Zn anomalies that are seen in the analyzed phases of all samples. The values for MnO, MgO and FeO\* on Figure 5 are averaged from the microprobe data for each phase in a given sample. Within each sample, the trace-element profiles for amphibole and pyroxene are remarkably similar, with the only noticeable difference being that amphibole generally shows higher Co and V abundances than pyroxene.

Whereas two amphibole populations in JL06-067 are visible in Figures 3 and 4, these same populations are not easily distinguished in the extended trace-element profiles (Figure 5). The amphibole analyses that constitute the high-La/Sm population have been highlighted in light green on Figure 5 and show generally lower Yb, Lu, Y, V and Cu than the low-La/Sm amphibole population. There are, however, no consistent and distinct differences between these two amphibole populations in Figure 5.

## Discussion

The convex-upward shape of the REE profiles of the amphibole (Figure 3) is similar to those of the pyroxene, except that the latter are flatter in the middle to heavy REE (Sm to Lu). These profiles reflect the high partition coefficients for amphibole and pyroxene (relative to basaltic melt) for the middle and heavy REE, respectively (Green et al., 2000; Tiepolo et al., 2007). The relative enrichments and shape of the REE profiles of the amphibole and pyroxene in the present study are similar to those reported by Smith (2014) for amphibole and pyroxene from cumulate nodules in volcanic rocks on the Solomon Islands.

As both phases have generally similar partition coefficients for the REE (Green et al., 2000; Tiepolo et al., 2007), some differences between the profiles of these two phases, notably the Eu anomaly (Figure 4), are important. Except for amphibole from JL06-021 and the high La/Sm population

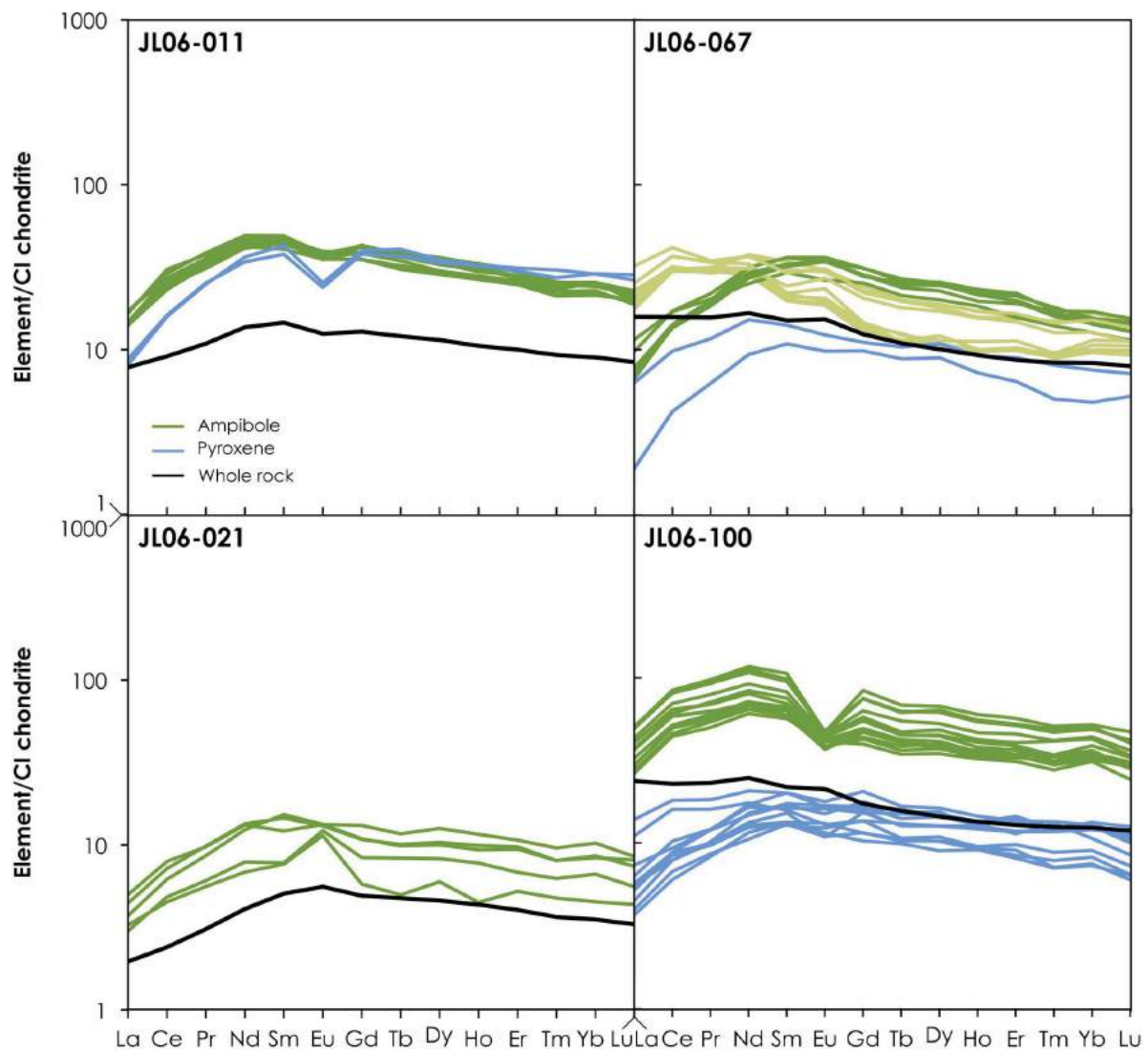


**Figure 3.** Chondrite-normalized (McDonough and Sun, 1995) rare-earth-element (REE) profiles for amphibole, pyroxene and the whole rock in each sample analyzed in this study. Amphiboles in JL06-067 are separated into two groups on the basis of REE-profile shape, as discussed in the text.

from JL06-067, the Eu anomaly in amphibole becomes more negative as the REE profile between La and Sm becomes flatter (i.e.,  $Eu/Eu^*$  decreases as  $La/Sm$  increases). A negative Eu anomaly is commonly attributed to the crystallization of plagioclase from a melt, as Eu is very compatible in that phase. In individual samples and in the entire dataset (except for JL06-021 and the high- $La/Sm$  population in JL06-067), the  $La/Sm$  ratio of the amphibole increases continuously (Figure 4) due to the simultaneous increase in La and Sm concentration, albeit at different rates (Figure 6). The increasingly negative Eu anomaly might be consistent with continuous amphibole production prior to and during plagioclase crystallization. The increasing La and Sm concentration of amphibole (Figure 6) is in accord with this idea, as these elements are incompatible in plagioclase. Furthermore, amphibole displays Eu anom-

lies that are less negative compared to pyroxene in JL06-011 (Figures 3, 6), implying that amphibole may have crystallized prior to or during plagioclase crystallization, which itself occurred prior to clinopyroxene crystallization.

The high- $La/Sm$  amphibole population from JL06-067 describes a subhorizontal trend on Figure 4. The same population also shows only a small range in Sm content but a much larger range in La (Figure 6), which is correlated positively with the Eu anomaly. The similarity of the REE abundance and profile shape of these amphiboles (Figure 3) to those from analyses of ‘amphibole rim on nodule’ (Daniel, 2014) likely points to a similar origin, presumably by reaction with melt. Such an origin might also be responsible for the higher Co concentration observed in the high- $La/Sm$  amphibole population in JL06-067 (Figure 5).

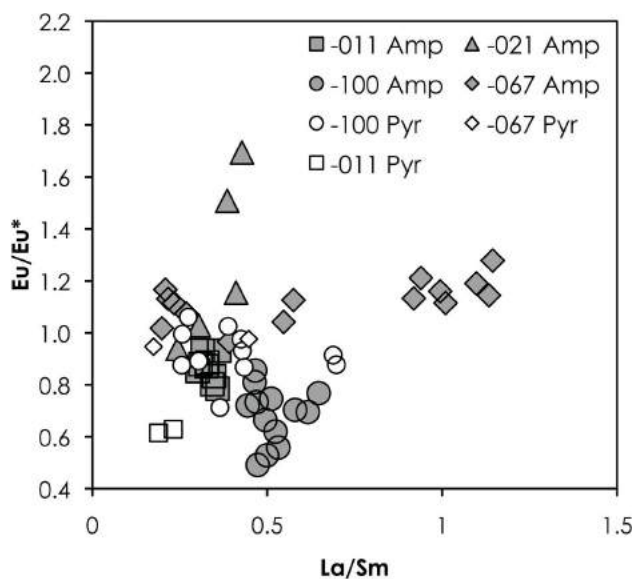


**Figure 4.** Eu anomaly versus La/Sm ratio of the amphibole and pyroxene in each sample analyzed in this study. Both ratios are chondrite normalized (McDonough and Sun, 1995). See text for calculation of the Eu anomaly.

Pyroxene analyses have Eu anomalies ranging from slightly positive to slightly negative and show no variation with increasing La/Sm (Figure 4). The increase in La/Sm for the pyroxenes is due mainly to an increase in their La concentration, as Sm content stays generally constant within a sample (Figure 6). The lack of variation in the pyroxene Eu anomaly (Figure 4) may imply that pyroxene crystallization occurred over a small window straddling the onset of plagioclase crystallization. Additionally, pyroxene analyses from samples JL06-067 and JL06-100 plot as a subvertical array that is continuous with analyses of amphibole from JL06-021 (Figure 6b), which could indicate that the amphibole in JL06-021 crystallized before plagioclase, whereas the pyroxene crystallized after. Another possibility is that the amphibole in JL06-021 was originally pyroxene that reacted with a later-transiting melt to form amphibole, although this explanation is at odds with the observation that some amphibole in this sample forms as chadacrysts within olivine oikocrysts.

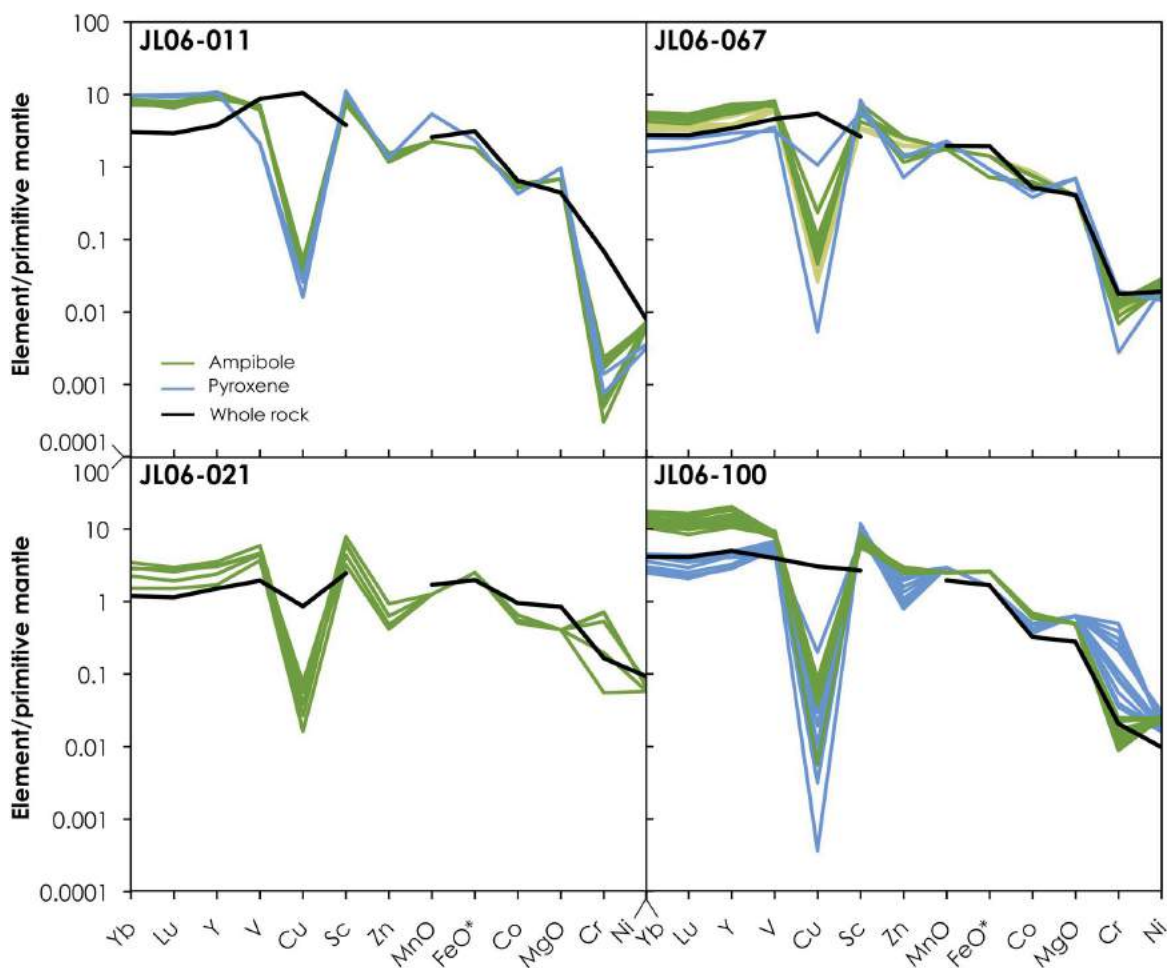


**Figure 5.** Primitive-mantle-normalized (Palme and O'Neill, 2014), extended trace-element profiles for amphibole, pyroxene and the whole rock in each sample analyzed in this study.

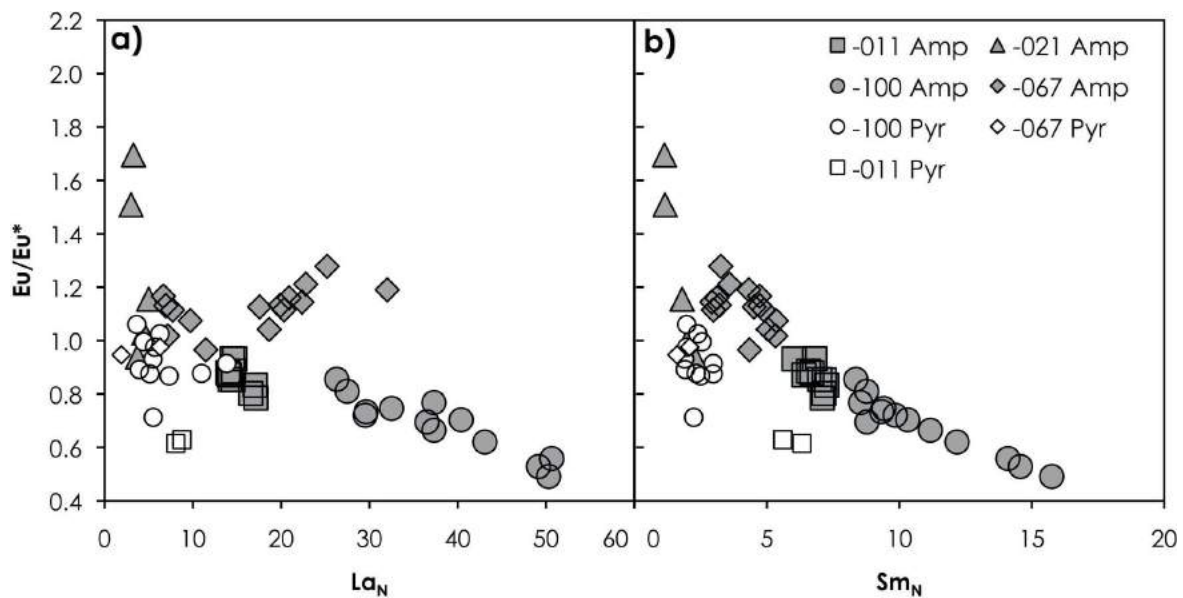


**Figure 6.** Europium anomaly versus La (a) and Sm (b) concentration of the amphibole and pyroxene analyzed in this study.

## Conclusions

The authors' interpretations indicate that amphibole in some plagioclase cumulates crystallized prior to plagioclase and pyroxene (i.e., the low-La/Sm amphiboles from sample JL06-067), during plagioclase crystallization but before pyroxene (JL06-011), or after plagioclase and pyroxene crystallization (JL06-100). Some amphiboles (e.g., high-La/Sm amphibole from JL06-067) show REE and trace-element concentrations that could imply that the amphibole was produced by reaction of pyroxene with a later melt. The origin of amphibole in JL06-021 is enigmatic, as it is present as chadacrysts within olivine and as oikocrysts to olivine; however, both populations show pyroxene-like variation in Eu anomaly, La/Sm ratio and abundance of La and Sm.

## Future Work

Analyses of the trace-element abundances in amphibole from other samples, as well as analyses of the coexisting olivine, plagioclase, sulphides and magnetite, are planned in the near future. This work will help in elucidating the role of H<sub>2</sub>O and amphibole crystallization along the liquid lines of descent in the Bonanza Arc magmas and their role in causing magnetite or sulphide saturation in the arc crust. The latter phases may have played a role in chalcophile abundance in Bonanza Arc magmas (Chiaradia, 2014).

## Acknowledgments

The authors thank J. Spence for assistance and training in data collection and reduction using the laser-ablation inductively coupled plasma-mass spectrometer at the University of Victoria. Thanks also go to A. Locock and A. Blinova for thoughtful reviews of this study.

## References

- Canil, D., Styan, J., Larocque, J., Bonnet, E. and Kyba, J. (2010): Thickness and composition of the Bonanza arc crustal section, Vancouver Island, Canada; *Geological Society of America Bulletin*, v. 122, p. 1094–1105.
- Chiaradia, M. (2014): Copper enrichment in arc magmas controlled by overriding plate thickness; *Nature Geoscience*, v. 7, p. 43–46, doi:10.1038/ngeo2028
- Davidson, J., Turner, S., Handley, H., MacPherson, C. and Dosseto, A. (2007): Amphibole “sponge” in arc crust?; *Geology*, v. 35, p. 787–790.
- DeBari, S.M. and Coleman, R.G. (1989): Examination of the deep levels of an island arc: evidence from the Tonsina ultramafic assemblage, Tonsina, Alaska; *Journal of Geophysical Research*, v. 94, p. 4373–4391.
- DeBari, S.M., Anderson, R.G. and Mortensen, J.K. (1999): Correlation among lower to upper crustal components in an island arc: the Jurassic Bonanza arc, Vancouver Island, Canada; *Canadian Journal of Earth Sciences*, v. 36, p. 1371–1413.
- Fecova, K. (2009): Conuma River and Leigh Creek intrusive complexes: windows into mid-crustal levels of the Jurassic Bonanza arc, Vancouver Island, British Columbia; M.Sc. thesis, Simon Fraser University, 245 p.
- Green, T.H., Blundy, J.D., Adam, J. and Yaxley, G.M. (2000): SIMS determination of trace element partition coefficients between garnet, clinopyroxene and hydrous basaltic liquids at 2–7.5 GPa and 1080–1200°C; *Lithos*, v. 53, p. 165–187.
- Greene, A.R., DeBari, S.M., Kelemen, P.B., Blusztajn, J. and Clift, P.D. (2006): A detailed geochemical study of island arc crust: the Talkeetna arc section, south-central Alaska; *Journal of Petrology*, v. 47, p. 1051–1093.
- Jochum, K.P., Nohl, U., Herwig, K., Lammel, E., Stoll, B. and Hofmann, A.W. (2005): GeoReM: a new geochemical database for reference materials and isotopic standards; *Geostandards and Geoanalytical Research*, v. 29, p. 333–338.

- Larocque, J. (2008): The role of amphibole in the evolution of arc magmas and crust: the case from the Jurassic Bonanza arc section, Vancouver Island, Canada; M.Sc. Thesis, University of Victoria, 115 p.
- Larocque, J. and Canil, D. (2010): The role of amphibole in the evolution of arc magmas and crust: the case from the Jurassic Bonanza arc section, Vancouver Island, Canada; *Contributions to Mineralogy and Petrology*, v. 159, p. 475–492.
- Lee, C.-T.A., Luffi, P., Chin, E.J., Bouchet, R., Dasgupta, R., Morton, D.M., Le Roux, V., Yin, Q.-z. and Jin, D. (2012): Copper systematics in arc magmas and implications for crust-mantle differentiation; *Science*, v. 336, p. 64–68.
- McDonough, W.F. and Sun, S.-s. (1995): The composition of the Earth; *Chemical Geology*, v. 95, p. 223–253.
- Muller, J.E. and Yorath, C.J. (1977): Geology of Vancouver Island; Geological Association of Canada–Mineralogical Association of Canada, Joint Annual Meeting, April 21–24, 1977, Vancouver, British Columbia, Field Trip 7 Guidebook, 53 p.
- Palme, H., and O’Neill, H.S.C. (2014): Cosmochemical estimates of mantle composition; *in* *The Mantle and Core*, R.W. Carlson (ed.), *Treatise on Geochemistry*, Volume 2, Elsevier, p. 1–38, doi:10.1016/B978-0-08-095975-7.00201-1
- Rudnick, R.L. and Gao, S. (2014): Composition of the continental crust; *in* *The Crust*, R.L. Rudnick (ed.), *Treatise on Geochemistry*, Volume 3, Elsevier, p. 1–51, doi:10.1016/B978-0-08-095975-7.00301-6
- Rudnick, R.L. and Fountain, D.M. (1995): Nature and composition of the continental crust: a lower crustal perspective; *Reviews of Geophysics*, v. 33.3, p. 267–309.
- Sillitoe, R.H. (2010): Porphyry copper systems; *Economic Geology*, v. 105, p. 3–41.
- Sinclair, W.D. (2007): Porphyry deposits; *in* *Mineral Deposits of Canada: A Synthesis of Major Deposit-Types, District Metallogeny, the Evolution of Geological Provinces, and Exploration Methods*, W.D. Goodfellow (ed.), Geological Association of Canada, Mineral Deposits Division, Special Publication 5, p. 223–243.
- Smith, D.J. (2014): Clinopyroxene precursors to amphibole sponge in arc crust; *Nature Communications*, v. 5, art. 4329, doi:10.1038/ncomms5329
- Taylor, S.R. (1977): Island arc models and the composition of the continental crust; *in* *Island Arcs, Deep Sea Trenches and Back-Arc Basins*, M. Talwani and W.C. Pitman III (ed.), American Geophysical Union, Maurice Ewing Series, v. 1, p. 325–335.
- Tiepolo, M., Oberti, R., Zanetti, A., Vannucci, R. and Foley, S.F. (2007): Trace-element partitioning between amphibole and silicate melt; *Reviews in Mineralogy and Geochemistry*, v. 67, p. 417–452.

# Evaluation of Mozley C800 Laboratory Mineral Separator for Heavy Mineral Concentration of Stream Sediments in Exploration for Carbonatite-Hosted Specialty Metal Deposits: Case Study at the Aley Carbonatite, Northeastern British Columbia (NTS 094B)

**D.A.R. Mackay**, School of Earth and Ocean Sciences, University of Victoria, Victoria, BC, mackay87@uvic.ca

**G.J. Simandl**, British Columbia Ministry of Energy and Mines, British Columbia Geological Survey, Victoria, BC and School of Earth and Ocean Sciences, University of Victoria, Victoria, BC

**B. Grcic**, Inspectorate Exploration & Mining Services Ltd., Richmond, BC

**C. Li**, Inspectorate Exploration & Mining Services Ltd., Richmond, BC

**P. Luck**, British Columbia Ministry of Energy and Mines, British Columbia Geological Survey, Victoria, BC

**M. Redfearn**, Inspectorate Exploration & Mining Services Ltd., Richmond, BC

**J. Gravel**, Acme Analytical Laboratories, Vancouver, BC

---

Mackay, D.A.R., Simandl, G.J., Grcic, B., Li, C., Luck, P., Redfearn, M. and Gravel, J. (2015): Evaluation of Mozley C800 laboratory mineral separator for heavy mineral concentration of stream sediments in exploration for carbonatite-hosted specialty metal deposits: case study at the Aley carbonatite, northeastern British Columbia (NTS 094B); *in* Geoscience BC Summary of Activities 2014, Geoscience BC, Report 2015-1, p. 111–122.

## Introduction

Finding tools to explore for overburden-covered or poorly exposed ore deposits is one objective of Natural Resources Canada's Targeted Geoscience Initiative 4 (TGI-4). Indicator minerals and geochemical studies are particularly effective tools. General principles about stream sediment surveys are given by Levinson (1974), Hawkes (1976), Rose et al. (1979) and Fletcher (1997). Lett (2007), Friske (2005) and McCurdy et al. (2006, 2009) provided guidelines for regional geochemical surveys. Methods for regional indicator mineral studies at the regional scale are also well established (McCurdy et al., 2006, 2009; McClenaghan, 2011). Indicator mineral studies generally require large samples that need to be treated by heavy liquid separation, isodynamic magnetic separation, optical identification and hand picking. The limited budgets of exploration companies targeting specific deposit types or commodities, or following up on regional geochemical or indicator mineral surveys, necessitate a more focused, customized approach. One of the objectives of the specialty metal component of the TGI-4 is to develop simpler, more inexpensive methods to explore for rare earth element (REE), niobium (Nb) and, potentially, tantalum (Ta) deposits. This research comprises three stages.

Stage one involved stream sediment sample collection, characterization of the carbonatite-related deposits and chemical analyses of the sediments from the Aley carbonatite (large, high-grade Nb deposit; Mackay and Simandl, 2014a), Wicheeda Lake carbonatite (high-grade REE deposit; Mackay and Simandl, 2014b) and Lonnie carbonatite (modest-grade Nb and REE deposit; Luck and Simandl, 2014). Geochemical stream sediment surveys commonly rely on the <177 µm (–80 mesh) size fraction (Fletcher, 1997). In contrast, the size fractions commonly used for hand picking and indicator mineral studies vary from 0.25 to 2.0 mm (McClenaghan, 2011). The stage one orientation surveys examined the optimal grain-size fraction for indicator mineral studies. Stage two comprises evaluation of rapid, low-cost methods to produce heavy-mineral concentrates for specialty metal exploration, using indicator minerals containing Nb, Ta and light rare earth elements (LREE [La, Ce, Pr, Nd]). Processing results for synthetic standards (prepared for this purpose) and Aley carbonatite stream sediments using the Mozley C800 laboratory mineral separator (MMS) are presented here. Stage three considers the use of custom microscope, scanning electron microscope (SEM), QEMSCAN<sup>®</sup>, mineral liberation analyzer (MLA) and electron microprobe analyses to reduce the need for hand picking of minerals and will be presented elsewhere.

---

**Keywords:** *indicator minerals, carbonatite, niobium, tantalum, rare earth elements, specialty metals*

*This publication is also available, free of charge, as colour digital files in Adobe Acrobat<sup>®</sup> PDF format from the Geoscience BC website: <http://www.geosciencebc.com/s/DataReleases.asp>.*

## Deposit Characterization, Geological Setting

The Aley carbonatite is 290 km north of Prince George, British Columbia (Figure 1 inset), and outcrops over a 3 to 3.5 km diameter area (Figure 1; Mäder, 1986; McLeish,

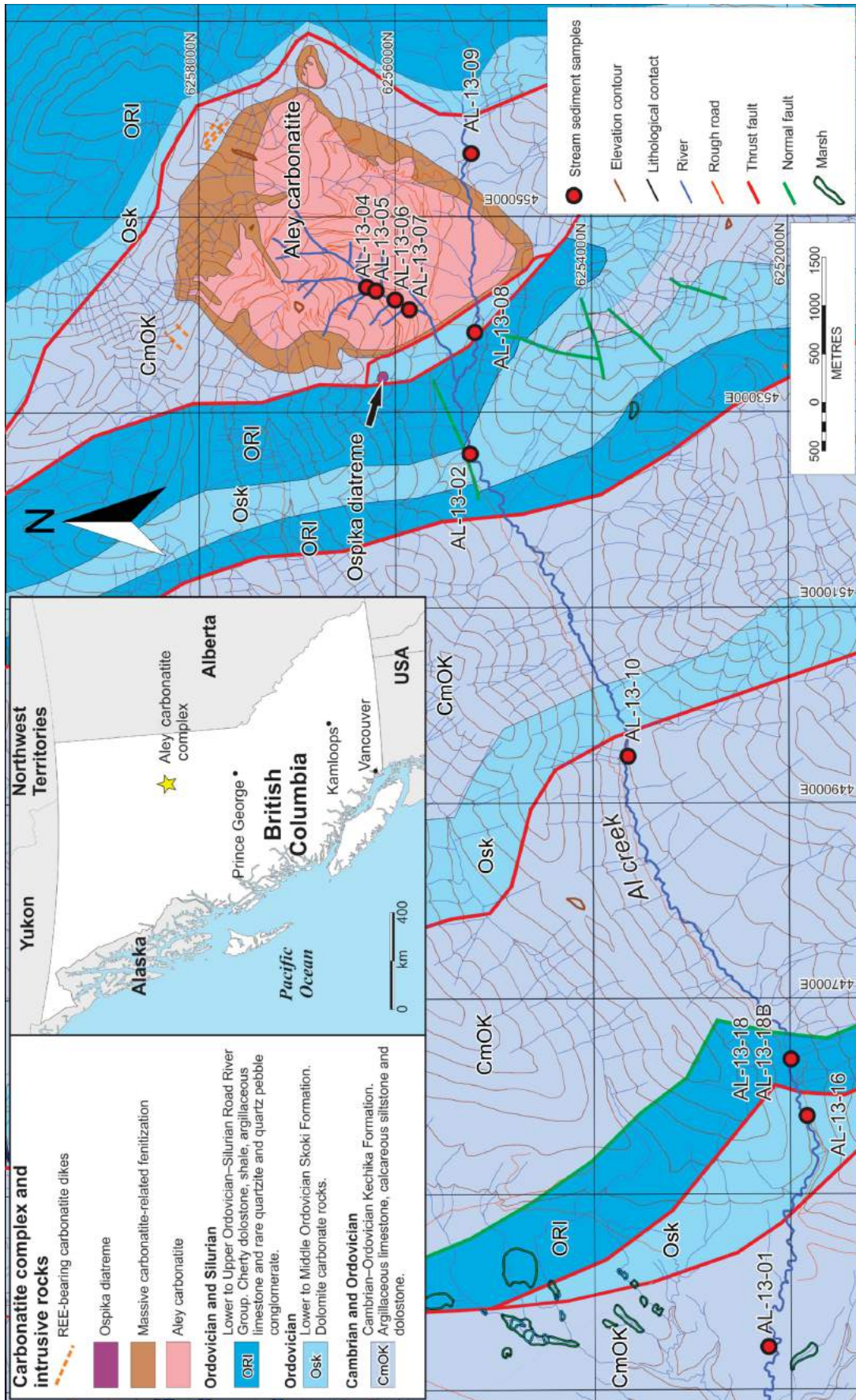


Figure 1. Location and geology of the Aley carbonatite, northeastern British Columbia. Stream sediment sample locations are denoted by red circles. Modified after Pride (1983), Mäder (1986), Massey et al. (2005), McLeish (2013) and Mackay and Simandl (2014a). Abbreviation: REE, rare earth element.

2013). Measured and indicated resources are 113 million tonnes at 0.41% Nb<sub>2</sub>O<sub>5</sub> and 173 million tonnes at 0.35% Nb<sub>2</sub>O<sub>5</sub>, respectively, with a cutoff grade of 0.20% Nb<sub>2</sub>O<sub>5</sub> (Simpson, 2012). The main phase of the carbonatite is predominantly dolomite surrounded by a minor calcite carbonatite phase. The dolomite carbonatite contains apatite, pyrite, calcite, fersmite, columbite-(Fe) and pyrochlore (Kressell et al., 2010). Magnetite pods tens of centimetres to metres in size are found throughout. These pods also contain apatite, phlogopite, pyrochlore, columbite-(Fe), fersmite, zircon and carbonate minerals (Mäder, 1986; Kressall et al., 2010). The carbonatite is surrounded by a zone of fenitized (Na and K hydrothermally altered) country rock containing richterite, arfvedsonite, aegirine and albite. Fenitization intensity varies from pervasive massive alteration (near the carbonatite contact) to millimetre- to centimetre-scale veins containing Na-amphiboles and feldspars (distal to the carbonatite contact).

The Aley carbonatite intruded into platformal carbonate and siliciclastic rocks of the Cambrian–Ordovician Kechika Formation, Lower to Middle Ordovician Skoki Formation and Lower to Upper Ordovician–Silurian Road River Group (Figure 1; Irish, 1970; Mäder, 1986; Pyle and Barnes, 2001). The carbonatite is older than 365.9 ± 2.1 m.y.

(McLeish, 2013) and younger than the Lower to Upper Ordovician–Silurian Road River Group (Mäder, 1986; Pyle and Barnes, 2001). Regional lower-greenschist-facies metamorphism coincided with compressional deformation at ca. 155 and 50 m.y. (Read et al., 1991; Pell, 1994) and overprints the rocks in the area, including the carbonatite (Mäder, 1986; McLeish, 2013).

### Summary of Previous Work

Twelve stream sediment samples were collected from the stream draining the Aley carbonatite (Mackay and Simandl, 2014a). Eleven samples were collected directly over and downstream (up to 11.5 km) of the carbonatite; one was collected upstream (Figure 1). Samples were prescreened in the field; material that passed through an 8 mm sieve was kept in permeable canvas bags. Samples were dry sieved into eight size fractions (>4 mm, 2–4 mm, 1–2 mm, 500 µm–1 mm, 250–500 µm, 125–250 µm, 63–125 µm and <63 µm). The follow-up laboratory sample preparation, dry sieving procedure and analytical methods leading to the selection of the ideal size fraction for the follow-up study are described by Luck and Simandl (2014) and Mackay and Simandl (2014a). Dry sieved but otherwise unprocessed stream sediment samples will be referred to here on as raw samples.

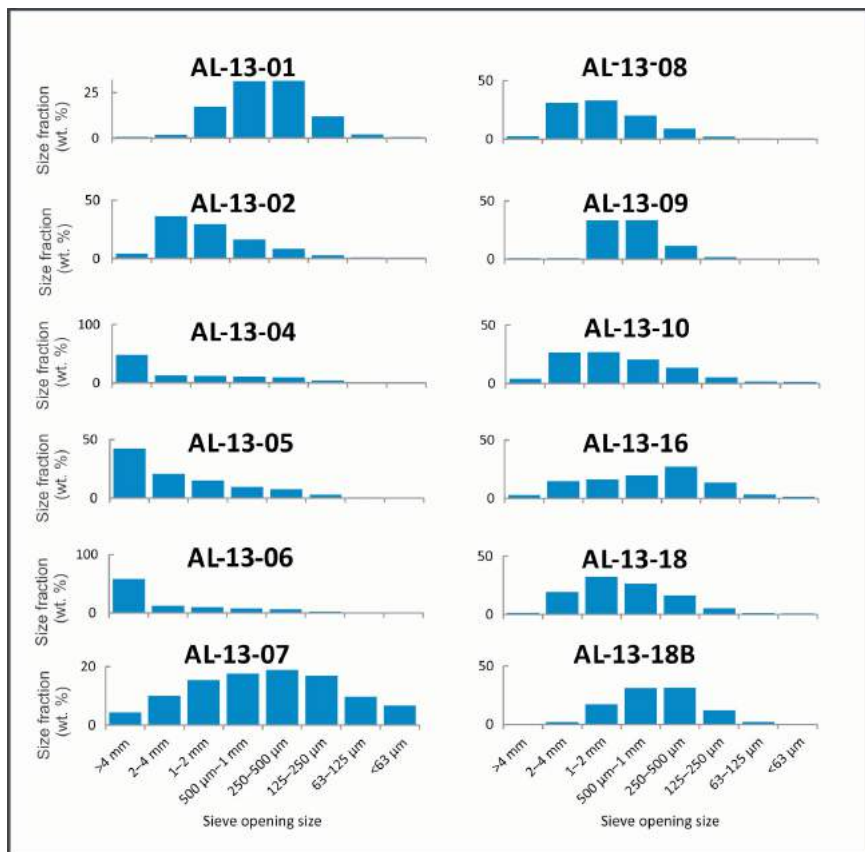


**Figure 2.** Weight percent distribution of material for different size fractions in dry sieved stream sediment samples from the Aley carbonatite drainage area, northeastern British Columbia (Mackay and Simandl, 2014a)

The distribution of size fractions in stream sediments from the Aley carbonatite vary in different reaches of the creek (Figure 2). Samples downstream of the deposit (AL-13-01, AL-13-02, AL-13-08, AL-13-10, AL-13-16, AL-13-18, AL-13-18B) show a more balanced size-fraction distribution (either slightly skewed toward a coarser fraction or approaching a normal bell-shape distribution) than those from over the deposit (AL-13-04, AL-13-05, AL-13-06). The latter samples show distribution patterns skewed toward the coarsest fractions. Sample AL-13-07 was also collected over the deposit but where the stream gully cuts through >5 m of overburden (down-slope of a major scree slope) and shows a normal distribution of material between size fractions. Sample AL-13-09 collected upstream of the deposit (in a meandering reach of the creek) is somewhat unique, with very little material coarser than 2 mm.

Approximately 10 g of each raw sample was split using a riffle-style split-

ter, milled, prepared in standard X-ray diffraction sample cups and analyzed using a Thermo Scientific Niton® FXL-950 as described by Luck and Simandl (2014). The 125–250 µm fraction (Figure 3) shows elevated levels of elements associated with carbonatite-hosted Nb deposits (Nb, Ta and LREE [La, Ce, Pr, Nd]) relative to other size fractions. This, and equivalent studies at the Wicheeda Lake

(Mackay and Simandl, 2014b) and Lonnie carbonatites (Luck and Simandl, 2014), indicates that the 125–250 µm fraction is the most appropriate to explore for specialty metal deposits in the Canadian Cordillera. Based on the distribution of material in the different size fractions of each sample and the concentration of potential pathfinder elements associated with carbonatite-hosted Nb deposits, the

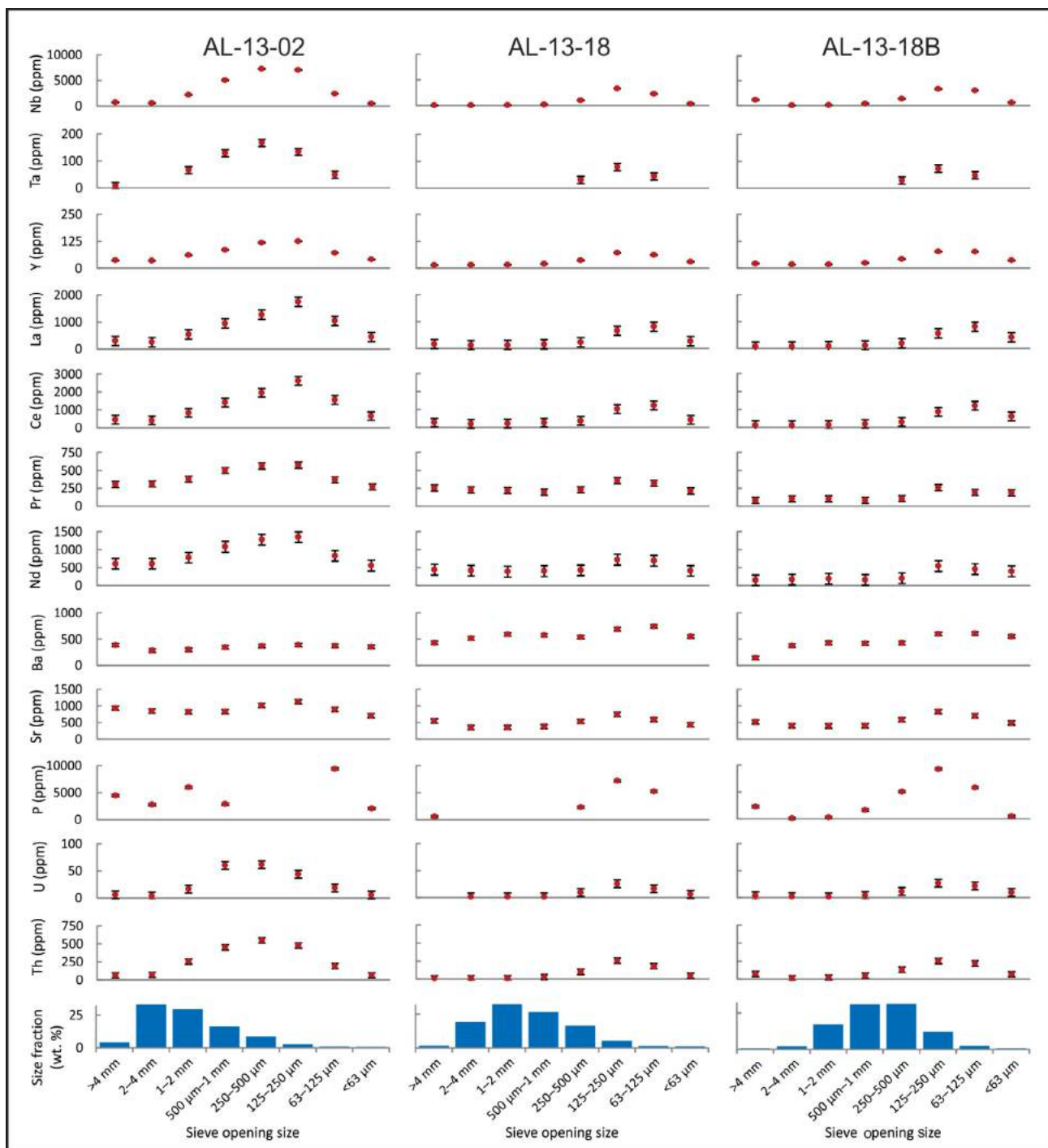


**Figure 3.** Concentration of selected elements associated with carbonatites for each size fraction of stream sediment samples from the Aley carbonatite drainage area, northeastern British Columbia. Modified after Mackay and Simandl (2014a).

125–250  $\mu\text{m}$  size fraction was selected for geochemical and indicator mineral studies. The 63–125  $\mu\text{m}$  and 250–500  $\mu\text{m}$  size fractions could have also been used.

### Assessment of the Mozley C800 Laboratory Mineral Separator Procedure

The Mozley C800 laboratory mineral separator (MMS) is a light and compact alternative to the shaker tables and gravity concentrators that are commonly used by metallurgists. The v-profile tray, best suited for coarse grain sizes (100  $\mu\text{m}$ –2 mm), was used for this study instead of a flat tray, traditionally used for finer grain sizes ( $\sim$ 100  $\mu\text{m}$  or less). The MMS set up parameters were: 1.75° longitudinal slope; 70 rpm table speed; 6.35 cm amplitude (throw or stroke); and 1.6 L/min water flow rate. Specifications and detailed operating procedures for the MMS are described in the instrument manual (Mozley Inc., undated). Optimal operating conditions are determined by running synthetic standards.

#### Processing Procedure

The operating procedure is relatively simple once optimal conditions for sample processing are identified. Dry sieved (125–250  $\mu\text{m}$  size fraction) samples weighing  $\sim$ 75 g are



**Figure 4.** A sample being poured onto a Mozley C800 laboratory mineral separator. Water is supplied to the v-profile tray by the wash water pipe (copper tube) and the irrigation pipes (two white plastic tubes with water outlets at regular intervals). The direction of water flow is denoted by black arrows.

gradually poured from a beaker onto the table and thoroughly wetted at the wash water pipe (Figure 4). A spray bottle is used to remove all material from the beaker. Tailings (low density material) separate first, moving longitudinally down the trough in the direction of water flow. The tailings are collected at the end of the table. Once the selected time interval is reached, the table and water are turned off. Tailings, middlings and concentrate are separated and carefully washed into separate containers. The concentrate consists of the highest density material in the sample. The middlings are a transition zone between the tailings and concentrate. They contain medium-density material and a mixture of low- and high-density minerals. The division of sediment into concentrate, middlings and tailings is visually discernable by shape and, to a lesser extent, colour (which in this study reflects the proportion of heavy minerals; Figure 5).

Following a sample run, suspended particles are allowed to settle, excess water is decanted from the concentrate, middlings and tailings containers and the fractions are dried overnight at 90°C then weighed for quality control and bagged separately. This procedure allows for samples to be reconstituted and reprocessed if needed. The same procedure was used to process all synthetic samples (standards) and multiple splits of a natural stream sediment sample collected in the field to determine optimal operating conditions and run time. Once the optimal operating conditions were determined, table speed, slope, water flow rate, throw amplitude and size of the samples were kept constant. A portion ( $\sim$ 75 g) of the 125–250  $\mu\text{m}$  fraction of each stream sediment sample was split and processed on the MMS. After processing, concentrate, middlings and tailings were analyzed by portable X-ray fluorescence (pXRF) spectrometer.

#### Optimizing Operating Conditions Based on Synthetic Samples

Testing and optimizing operating conditions for the MMS were performed using synthetic standards and a quintet of subsamples split from the natural sample AL-13-16. Synthetic standards contained 75 g of material made up of magnetite (0.33–10 wt. %), garnet (0.33–10 wt. %), fluorite (0.33–10 wt. %) and quartz (remaining portion of the stan-

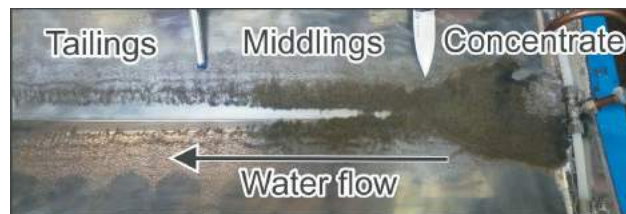


**Figure 5.** View of the surface of the Mozley C800 laboratory mineral separator table and sample material after a completed run. Concentrate, middlings and tailings are separated based on pattern and colour of the material stream.

standard sample). All constituents of the synthetic standards were milled and sieved to the 125–250 µm size fraction (compatible with the size fraction identified previously for testing). Magnetite in MMS concentrates increased by 5.5 to 228.2 times relative to unprocessed synthetic standards. The strong correlation ( $R^2=0.98$ ) between magnetite contained in unprocessed standard samples and MMS concentrates indicates consistent and predictable concentration of standards (Figure 6).

### Optimizing Operating Conditions Using Natural Samples

One of the larger natural samples (AL-13-16) was split using a riffle splitter into five identical subsamples (~75 g)

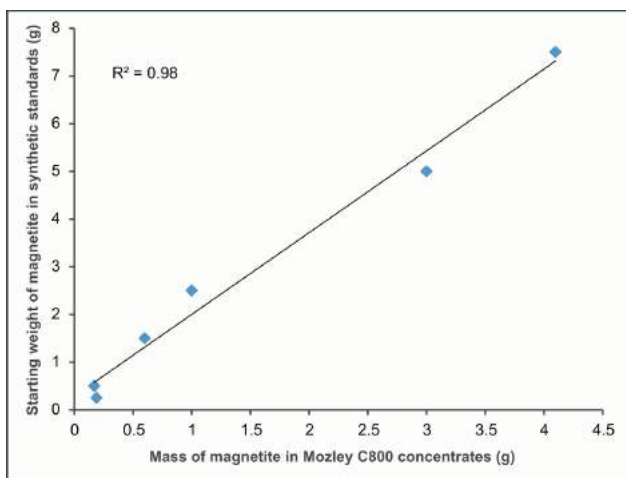


**Figure 6.** Comparison of the weight of magnetite contained in unprocessed synthetic standards with corresponding weight of magnetite in Mozley C800 laboratory mineral separator concentrates (from Aley carbonatite drainage area, northeastern British Columbia).

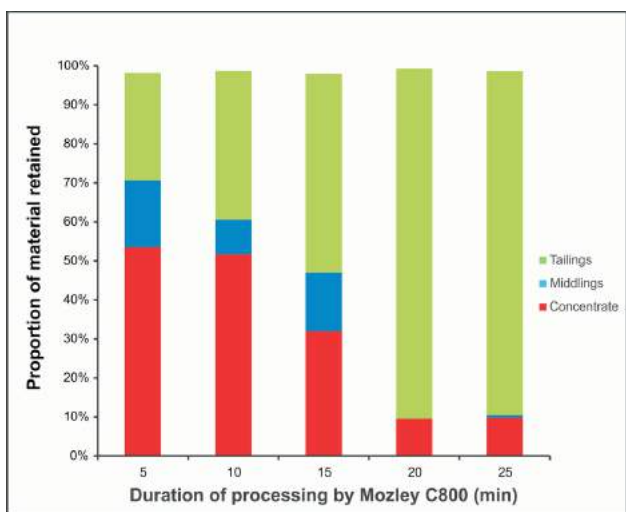


**Figure 7.** Proportions of concentrate, middlings and tailings in five subsamples of AL-13-16 (Aley carbonatite drainage area, northeastern British Columbia) after processing on the Mozley C800 laboratory mineral separator for 5, 10, 15, 20 and 25 minutes.

and these subsamples were processed for 5, 10, 15, 20 and 25 minutes (Figure 7). The proportion of retained concentrate decreases with increasing processing time when all other parameters are kept constant (Figure 7). Reproducibility of the MMS was tested on three subsamples (~77 g each) of AL-13-16 processed for 25 minutes. The retained concentrate fraction varied only slightly with observed weights representing 12, 9.4 and 9.9% of the initial sample weights. Based on these tests, a processing time of 15 minutes was selected for processing stream samples from the Aley carbonatite. The 15-minute run time is a compromise that ensures adequate concentration of heavy minerals (magnetite) and minimal loss to tailings.

## Results

### Mozley C800 Laboratory Mineral Separator and Geochemical Analyses

Separation by MMS of the 125–250 µm fraction of stream sediment samples from the Aley carbonatite drainage area produced a range in proportions of concentrate (3.8–32.0%), middlings (0–17.1%) and tailings (51.0–94.1%). Ten out of twelve samples show 24.7 to 32.0% of material retained in concentrate, consistent with the desired proportion of material retained in concentrate for the sample (AL-13-16) used to test the separation procedure (Figure 8). Only sample AL-13-09 shows noticeably lower proportions of retained concentrate (3.8%).

Raw samples (Table 1) and MMS concentrates (Table 2) from the Aley carbonatite drainage area were analyzed by pXRF following the procedure described by Luck and Simandl (2014) and Mackay and Simandl (2014a). Abundances of Nb in MMS concentrates increased by a factor of 2.7 to 17.2 (average of 4.3) relative to the raw samples (Figure 9a). For samples with available analyses, concentration

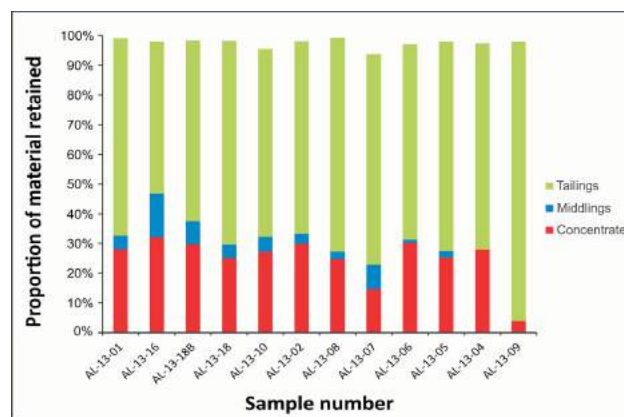


**Figure 8.** Proportions of Mozley C800 laboratory mineral separator concentrates, middlings and tailings for stream sediment samples from the Aley carbonatite drainage area, northeastern British Columbia. Samples were processed for 15 minutes. Samples appear in order of their geographic location from west to east (see Figure 1 for sample locations).

of Nb is 2.4 to 9.9 times higher in concentrates relative to middlings (Table 2). The MMS concentrates also show large increases in the concentration of Ta (factor of 1.5 to 11.7; average of 3.1) and LREE (factor of 2.6 to 12.6; average of 3.9) relative to raw samples (Figure 9b, c).

## Discussion

Processing samples using a MMS permits separation of dense indicator minerals. Pyrochlore (4.2–6.4 g/cm<sup>3</sup>), columbite-(Fe) (5.3–7.3 g/cm<sup>3</sup>), fersmite (4.69–4.79 g/cm<sup>3</sup>), monazite (4.8–5.5 g/cm<sup>3</sup>) and REE-fluorocarbonates, such as bastnaesite (4.95–5.00 g/cm<sup>3</sup>) and synchysite (3.90–4.15 g/cm<sup>3</sup>), have been identified in mineralogical studies of the Aley carbonatite (Mäder, 1986; Kressall et al., 2010; Chakhmouradian et al., 2014) and targeted as indicator minerals for carbonatite-hosted specialty metal deposits in this study. These minerals have similar or greater densities than magnetite (5.1–5.2 g/cm<sup>3</sup>) in the synthetic standards used herein. Based on the consistent and effective concentration of magnetite from the synthetic standards, the targeted heavy mineral fraction should be retained effectively in MMS concentrates.

Comparison of the results of the pXRF analyses of raw samples and MMS concentrates, middlings and tailings shows that the concentration of Nb-, Ta- and LREE-bearing heavy minerals was successful. High concentrations of Nb (average increase by a factor of 4.3) in MMS concentrates relative to tailings and corresponding raw samples (Figure 9a) indicate that most of the Nb-bearing minerals (pyrochlore, columbite-(Fe) and fersmite) were successfully concentrated by the MMS. The correlation ( $R^2=0.94$ ) between Nb in raw samples and MMS concentrates (Figure 10a) indicates that the procedure consistently and efficiently concentrates pyrochlore, columbite-(Fe) and fersmite in all samples in the range of 2000 to 30 000 ppm Nb. The correlation ( $R^2=0.86$ ) between Fe in raw samples and

concentrates indicates magnetite was successfully concentrated.

High Ta contents (average increase by a factor of 3.1) in MMS concentrates relative to tailings and raw samples (Figure 9b) are likely due to pyrochlore and columbite-(Fe); however the Ta/Nb ratio for these minerals in carbonatites is typically very low. The lack of correlation between Ta concentrations in raw samples and concentrate ( $R^2=0.23$ ; Figure 10b) is likely due to low (near detection limit) contents. Also, the elemental concentration for two concentrates (AL-13-09 and AL-13-05) had to be calculated because the amount of material retained following Mozley separation was insufficient for chemical analyses (Table 2). In these cases, elemental concentration can be calculated based on initial concentrations measured in raw samples and analyses of tailings and middlings (normalized to wt. % of retained material). Error propagation from analyses near detection limits combined with error in weights of raw samples, concentrates, middlings and tailings makes calculated concentrations unreliable. Despite this, the calculated elemental concentrations for AL-13-05 do not appear to dramatically affect the results. Sample AL-13-09 was collected upstream of the Aley carbonatite and is unique in the sample set (Figure 1). It shows a different grain size distribution relative to the other samples (Figure 2), and lower proportions of retained concentrate (3.8%; Figure 8). Elemental concentrations of Nb, Ta and LREE in raw samples are also much lower than in other samples (Figure 9). This may reflect background levels of heavy minerals in the Aley carbonatite area, and the different flow characteristics of the creek (meandering reach) upstream of the deposit.

Concentrations of LREE are also high (average increase by a factor of 3.9) in MMS concentrates relative to tailings and raw samples (Figure 9c). Combined with correlations for

**Table 1.** Relative concentrations (in ppm) of major and minor elements associated with carbonatite from raw stream sediment samples, analyzed by portable X-ray fluorescence spectrometer. Samples are listed from upstream of, to directly over, and with increasing distance downstream of the Aley carbonatite, northeastern British Columbia. See Figure 1 for sample locations. From Mackay and Simandl (2014a).

Sample no.	Nb	Ta	La	Ce	Pr	Nd	Y	Ba	Sr	P	U	Th	Fe	Ca
AL-13-09	444	28	184	288	188	351	29	324	177	1885	9	53	15968	78201
AL-13-04	9971	131	1592	2647	660	1585	170	355	2013	n.d.	31	589	90204	209044
AL-13-05	8647	120	1521	2466	614	1453	156	379	1655	n.d.	32	534	87093	198956
AL-13-06	7977	123	1536	2447	623	1443	155	380	1591	n.d.	36	497	90654	193408
AL-13-07	615	23	316	505	289	580	34	244	688	4215	6	68	22375	186264
AL-13-08	6695	135	2010	2977	599	1421	124	421	1054	n.d.	40	461	79669	160338
AL-13-02	7036	134	1746	2599	565	1326	125	379	1126	n.d.	43	474	77903	169329
AL-13-10	5543	110	1280	1918	520	1161	104	505	944	n.d.	40	376	65852	165451
AL-13-18	3311	78	662	1025	355	721	71	688	747	7221	26	255	42845	154081
AL-13-18B	3361	73	561	866	259	542	77	598	827	9203	27	251	39801	166097
AL-13-16	5246	101	1083	1648	470	1028	93	910	745	n.d.	36	355	59782	149924
AL-13-01	3495	79	596	936	346	724	72	670	711	7117	26	266	40852	156997

Abbreviation: n.d., not detected

**Table 2.** Relative concentrations (in ppm) of major and minor elements associated with carbonatite from Mozley C800 laboratory mineral separator concentrates, middlings and tailings and tailings from stream sediment samples, analyzed by portable X-ray fluorescence spectrometer. Samples are listed from upstream of, to directly over, and with increasing distance downstream of the Aley carbonatite, northeastern British Columbia. See Figure 1 for sample locations. Error propagation and elemental concentrations near the limit of detection greatly reduce the reliability of calculated values.

Sample no.	Nb	Ta	La	Ce	Pr	Nd	Y	Ba	Sr	P	U	Th	Fe	Ca
<b>Concentrate</b>														
AL-13-09 <sup>1</sup>	7635	327	1725	2688	1222	2210	223	976	842	34659	109	791	80156	162926
AL-13-04	26514	193	3857	6347	1061	2853	343	364	2076	n.d.	73	788	194756	193214
AL-13-05 <sup>1</sup>	26389	325	4130	6593	1295	3235	365	664	2030	n.d.	87	1516	213404	222021
AL-13-06	21571	217	3785	6031	1029	2730	319	407	1779	n.d.	76	785	185251	190196
AL-13-07	2262	48	694	1076	354	762	72	218	987	10791	14	164	37475	223300
AL-13-08	23076	292	7325	11001	1373	3832	339	501	1275	n.d.	120	987	233457	150235
AL-13-02	21400	335	5541	8420	1153	3198	327	459	1464	n.d.	133	961	210258	175782
AL-13-10	17271	279	4047	6154	963	2611	277	773	1383	n.d.	111	942	169748	185713
AL-13-18	11923	176	2341	3600	734	1804	203	1225	1184	n.d.	84	573	114173	191843
AL-13-18B	10227	182	1868	2906	640	1534	184	1084	1204	n.d.	80	591	88135	194940
AL-13-16	14603	290	3023	4605	798	2006	229	1595	1059	n.d.	95	874	139688	172378
AL-13-01	11481	183	1795	2808	616	1486	189	1018	1112	n.d.	78	700	95421	169733
<b>Middlings</b>														
AL-13-07	939	27	325	502	184	359	46	158	874	6941	7	87	23952	213935
AL-13-18B	1547	23	327	529	163	362	60	335	996	11701	13	126	25994	190527
AL-13-16	1483	27	413	672	280	553	57	410	957	10436	13	124	26276	188037
<b>Tailings</b>														
AL-13-09	163	17	126	197	150	283	22	305	154	597	5	24	13718	76492
AL-13-04	3704	55	792	1356	476	1026	110	298	2027	21556	15	273	52382	215621
AL-13-05	2804	54	676	1134	406	901	91	299	1619	15708	14	214	47007	202470
AL-13-06	2487	47	689	1133	425	904	86	310	1524	13871	15	196	46808	194605
AL-13-07	279	n.d.	231	370	257	500	25	244	640	1686	6	39	18900	178263
AL-13-08	612	33	275	450	243	489	34	296	948	3624	10	62	21832	156680
AL-13-02	741	38	307	478	257	516	37	296	947	3959	11	74	22482	157974
AL-13-10	298	n.d.	190	330	220	426	27	318	744	2388	7	41	19832	151534
AL-13-18	320	17	164	282	192	354	26	501	590	1865	6	36	18935	140844
AL-13-18B	239	n.d.	180	294	211	412	25	473	625	2255	5	37	17959	149069
AL-13-16	242	22	171	265	199	352	23	552	529	<90	6	35	19601	124735
AL-13-01	284	28	157	271	190	347	24	496	528	1845	7	34	17322	137060

<sup>1</sup> Calculated values

Abbreviation: n.d., not detected

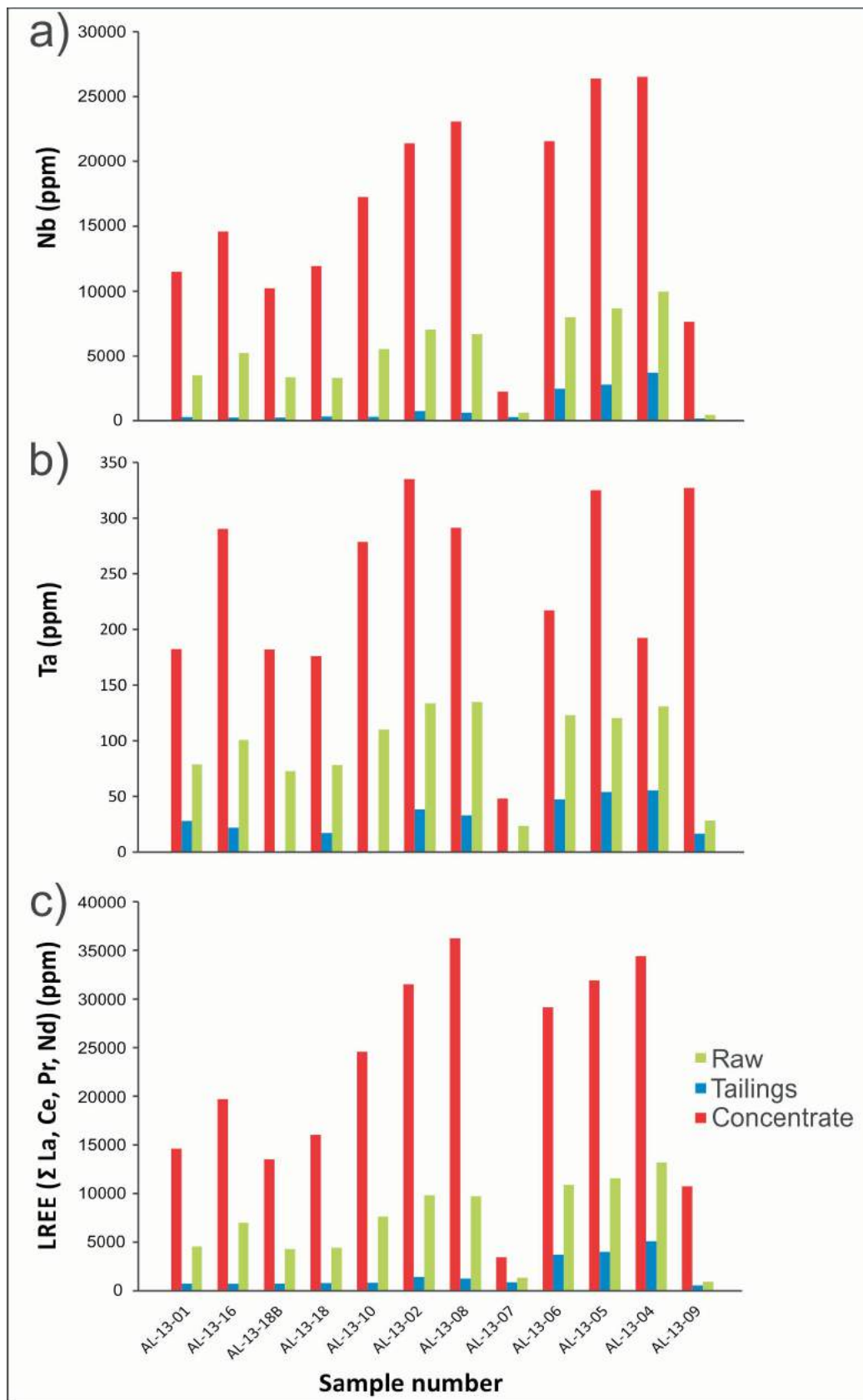
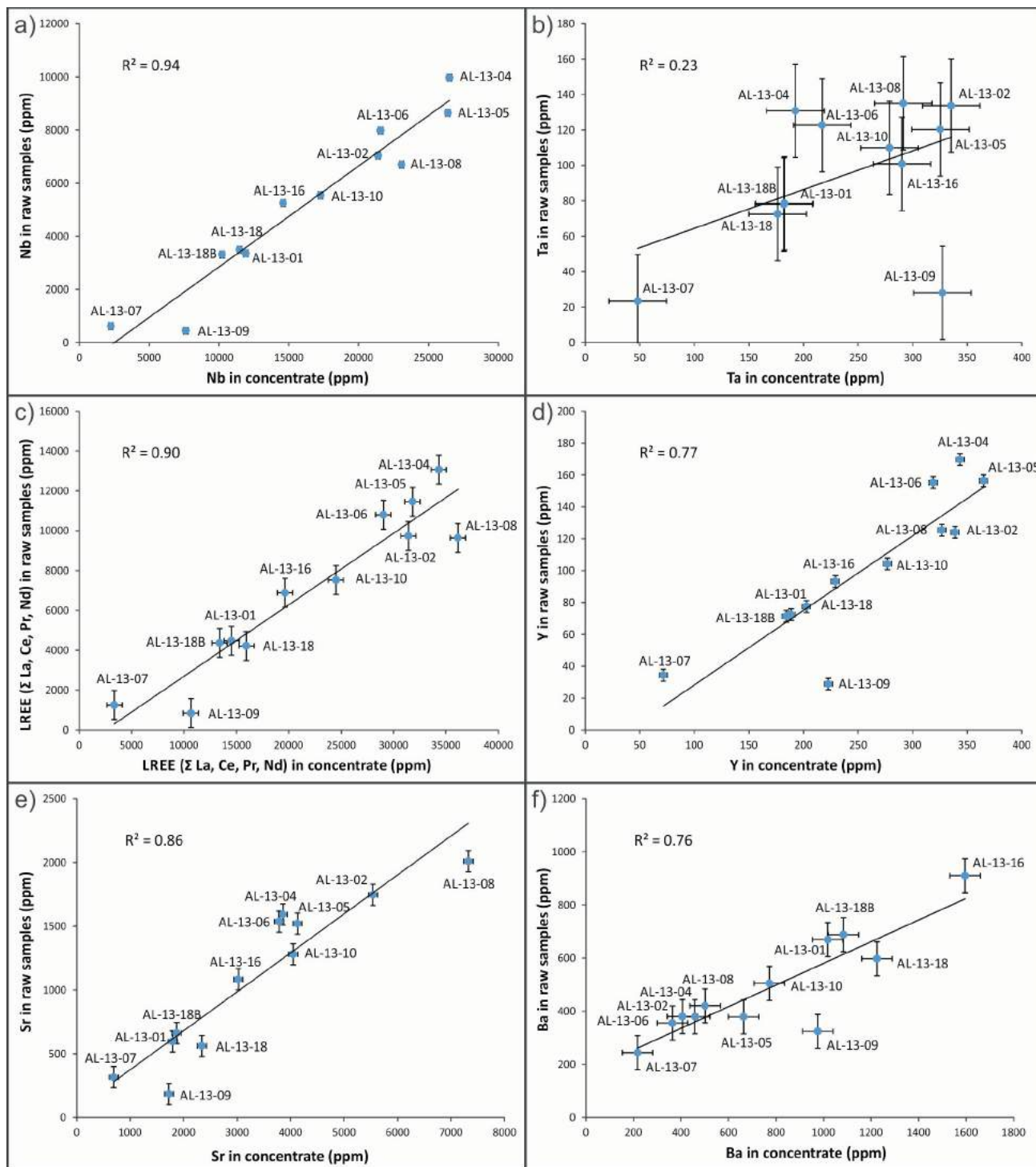


Figure 9. Comparison of a) Nb, b) Ta and c) LREE (ΣLa, Ce, Pr, Nd) concentrations in Mozley C800 laboratory mineral separator concentrates, tailings and corresponding raw samples. Samples appear in order of their geographic location from west to east (see Figure 1 for sample locations).



**Figure 10.** Comparison of the concentrations of **a)** Nb, **b)** Ta, **c)** light rare earth elements (LREE), **d)** Y, **e)** Sr and **f)** Ba in Mozley C800 laboratory mineral separator concentrates versus raw samples (from Aley carbonatite drainage area, northeastern British Columbia). Error bars ( $2\sigma$ ) are based on repeated portable X-ray fluorescence analyses of standards.

LREE ( $R^2=0.90$ ; Figure 10c) and Y ( $R^2=0.77$ ; Figure 10d), this indicates that heavy minerals, such as monazite and REE-bearing fluorocarbonates (e.g., bastnaesite and synchysite), were concentrated during Mozley separation in the range of 3000–40 000 ppm LREE. Correlation for Sr ( $R^2=0.86$ ; Figure 10e) and Ba ( $R^2=0.76$ ; Figure 10f) in raw samples and MMS concentrate indicate that the carbonatite signature in stream sediments is preserved following MMS concentration. The low coefficients of determination for Th ( $R^2=0.44$ ) and U ( $R^2=0.43$ ) are due to low concentrations (near detection limits) in samples AL-13-09 and AL-13-07 and the error propagation issue described for Ta.

The MMS is lighter and easier to transport than other density separator equipment, such as shaker tables. The method presented by this study is able to effectively detect and amplify a weak carbonatite signature up to 11.5 km from its source. The small sample size required for Mozley separation also allows for increased sampling efficiency during exploration programs.

## Conclusions

The Mozley C800 laboratory mineral separator is a compact, simple to operate instrument that can be transported and optimized for specific drainages, deposits or commodities. After selecting the most favourable size fraction (125–250  $\mu\text{m}$ , dry sieved, in this study), the MSS was used to increase the heavy mineral content of the stream sediment samples from the drainage area surrounding the Aley carbonatite-hosted specialty metal deposit. This is substantiated by increased concentrations of Nb (average factor of 4.3), Ta (average factor of 3.1) and LREE (average factor of 3.9) in MMS concentrates relative to corresponding raw samples. Correlations between Nb, LREE and Y concentrations in the raw stream sediment samples and corresponding concentrates indicate that Nb- and LREE-bearing minerals (such as pyrochlore, columbite-(Fe) and REE-bearing fluorocarbonates) were consistently concentrated, and that a predictable relationship between indicator mineral counts in raw stream sediments samples and concentrates should be expected. Extending this study, the plan is to examine microscope, SEM, QEMSCAN, MLA and electron microprobe methods to eliminate the need to hand pick indicator minerals.

## Acknowledgments

This project was funded by the Targeted Geoscience Initiative 4 (2010–2015), a Natural Resources Canada program. The specialty metal component of this program was carried out collaboratively with the Geological Survey of Canada and British Columbia Geological Survey. Inspectorate Exploration & Mining Services Ltd. and Acme Analytical Laboratories are thanked for their generous support. Logistical and helicopter support by Taseko Mines Limited and a

scholarship from Geoscience BC to the first author are also greatly appreciated. The manuscript has benefitted from constructive comments by an anonymous reviewer.

## References

- Chakhmouradian, A.R., Reguir, E.P., Kressall, R.D., Crozier, J., Pisiak, L.K., Sidhu, R. and Yang, P. (2014): Carbonatite-hosted niobium deposit at Aley, northern British Columbia (Canada): mineralogy, geochemistry and petrogenesis; *Ore Geology Reviews*, v. 64, p. 642–666, URL <<http://dx.doi.org/10.1016/j.oregeorev.2014.04.020>> [September 2014].
- Fletcher, W.K. (1997): Stream sediment geochemistry in today's exploration world: *in* Proceedings of Exploration 97: Fourth Decennial International Conference on Mineral Exploration, A.G. Gubins (ed.), Prospectors and Developers Association of Canada, Toronto, Canada, Paper 32, p. 249–260.
- Hawkes, H.E. (1976): The downstream dilution of stream sediment anomalies; *Journal of Geochemical Exploration*, v. 6, p. 345–358.
- Irish, E.J.W. (1970): Geology of the Halfway River map area, British Columbia; Geological Survey of Canada, Paper 69-11, 154 p.
- Kressall, R., McLeish, D.F. and Crozier, J. (2010): The Aley carbonatite complex – part II petrogenesis of a Cordilleran niobium deposit; *in* International Workshop on the Geology of Rare Metals, G.J. Simandl and D.V. Lefebure (ed.), Extended Abstracts Volume, November 9–10, 2010, Victoria, Canada, BC Ministry of Energy and Mines, BC Geological Survey, Open File 2010-10, p. 25–26.
- Lett, R. (2007): Workshop notes: drainage geochemical surveys–stream sediments, lake sediments, moss mats, heavy minerals: BC Ministry of Energy and Mines, BC Geological Survey, Geofile 2007-6, 63 p., URL <<http://www.empr.gov.bc.ca/Mining/Geoscience/PublicationsCatalogue/GeoFiles/Documents/GF2007-06.pdf>> [October 2014].
- Levinson, A.A. (1974): Introduction to Exploration Geochemistry (Second Edition); Applied Publishing Ltd., Wilmette, Illinois, 924 p.
- Luck, P. and Simandl, G.J. (2014): Portable X-ray fluorescence in stream sediment chemistry and indicator mineral surveys, Lonnie carbonatite complex, British Columbia; *in* Geological Fieldwork 2013, BC Ministry of Energy and Mines, BC Geological Survey, Paper 2014-1, p. 169–182, URL <[http://www.empr.gov.bc.ca/Mining/Geoscience/PublicationsCatalogue/Fieldwork/Documents/2013/10\\_Luck\\_Simandl.pdf](http://www.empr.gov.bc.ca/Mining/Geoscience/PublicationsCatalogue/Fieldwork/Documents/2013/10_Luck_Simandl.pdf)> [September 2014].
- Mackay, D.A.R. and Simandl, G.J. (2014a): Portable X-ray fluorescence to optimize stream sediment chemistry and indicator mineral surveys, case 1: carbonatite-hosted Nb deposits, Aley carbonatite, British Columbia, Canada; *in* Geological Fieldwork 2013, BC Ministry of Energy and Mines, BC Geological Survey, Paper 2014-1, p. 183–194, URL <[http://www.empr.gov.bc.ca/Mining/Geoscience/PublicationsCatalogue/Fieldwork/Documents/2013/11\\_Mackay\\_Simandl\\_\(Aley\).pdf](http://www.empr.gov.bc.ca/Mining/Geoscience/PublicationsCatalogue/Fieldwork/Documents/2013/11_Mackay_Simandl_(Aley).pdf)> [September 2014].
- Mackay, D.A.R. and Simandl, G.J. (2014b): Portable X-ray fluorescence to optimize stream sediment chemistry and indicator mineral surveys, case 2: carbonatite-hosted REE deposits, Wicheeda Lake, British Columbia, Canada; *in* Geological Fieldwork 2013, BC Ministry of Energy and

- Mines, BC Geological Survey, Paper 2014-1, p. 195–206, URL <[http://www.empr.gov.bc.ca/Mining/Geoscience/PublicationsCatalogue/Fieldwork/Documents/2013/12\\_Mackay\\_Simandl\\_\(Wicheeda\).pdf](http://www.empr.gov.bc.ca/Mining/Geoscience/PublicationsCatalogue/Fieldwork/Documents/2013/12_Mackay_Simandl_(Wicheeda).pdf)> [September 2014].
- Mäder, U.K. (1986): The Aley carbonatite complex; M.Sc. thesis, University of British Columbia, 176 p.
- Massey, J.W.H., McIntyre, D.G., DeJardins, P.J. and Cooney, R.T. (2005): Digital geology map of British Columbia; BC Ministry of Energy and Mines, BC Geological Survey, Open File 2005-2, DVD.
- McClenaghan, M.B. (2011): Overview of common processing methods for recovery of indicator minerals from sediments and bedrock in mineral exploration; Geochemistry: Exploration, Environment, Analysis, v. 11, p. 265–278.
- McCurdy, M.W., Kjarsgaard, I.M., Day, S.J.A., McNeil, R.J., Friske, P.W.B. and Plouffe, A. (2009): Indicator mineral content and geochemistry of stream sediments and waters from northeast British Columbia (NTS 94A, 94B, 94G, 94H, 94I, 94K, 94N, 94O, 94P); BC Ministry of Energy and Mines, BC Geological Survey, Report 2009-2 and Geological Survey of Canada, Open File 6311, 19 p.
- McCurdy, M.W., Prior, G.J., Friske, P.W.B., McNeil, R.J., Day, S.J.A. and Nicholl, T.J. (2006): Geochemical, mineralogical and kimberlites indicator mineral electron microprobe data from silts, heavy mineral concentrates and water from a National Geochemical Reconnaissance stream sediment and water survey in northern and southwestern Buffalo Head Hills, northern Alberta (parts of 84B, 84C, 84F, and 84G); Alberta Energy and Utilities Board, Alberta Geological Survey, Special Report 76 and Geological Survey of Canada, Open File 5057, 16 p.
- McLeish, D.F. (2013): Structure, stratigraphy, and U-Pb zircon-titanite geochronology of the Aley carbonatite complex, northeast British Columbia: evidence for Antler-aged orogenesis in the foreland belt of the Canadian Cordillera; M.Sc. thesis, University of Victoria, 131 p.
- Millonig, L.J., Gerdes, A. and Groat, L.A. (2012): U-Th-Pb geochronology of meta-carbonatites and meta-alkaline rocks in the southern Canadian Cordillera: a geodynamic perspective; *Lithos*, v. 152, p. 202–217.
- Mozley Inc. (undated): Installation, operation and maintenance manual: C800 laboratory mineral separator; Mozley Inc., Gloucester, United Kingdom, 26 p.
- Pell, J. (1994): Carbonatites, nepheline syenites, kimberlites and related rocks in British Columbia; BC Ministry of Energy and Mines, BC Geological Survey, Bulletin 88, 136 p.
- Pride, K.R. (1983): Geological survey on the Aley claims; BC Ministry of Energy and Mines, Assessment Report 12018, 16 p.
- Pyle, L.J. and Barnes, C.R. (2001): Conodonts from the Kechika Formation and Road River Group (Lower to Upper Ordovician) of the Cassiar terrane, northern British Columbia; *Canadian Journal of Earth Sciences*, v. 8, p. 1387–1401.
- Read, P.B., Woodsworth, G.J., Greenwood, H.J., Ghent, E.D. and Evenchick, C.A. (1991): Metamorphic map of the Canadian Cordillera; Geological Survey of Canada, Map 1714A, scale 1:2 000 000.
- Rose, A.W., Herbert, H.E. and Webb, J.S. (1979): *Geochemistry in Mineral Exploration* (second edition); Academic Press, London, United Kingdom, 657 p.
- Simpson, R.G. (2012): Technical report – Aley carbonatite niobium project; Taseko Mines Limited, unpublished company report, 66 p.

# Assessing Fracture Network Connectivity of Prefeasibility-Level High-Temperature Geothermal Projects Using Discrete Fracture Network Modelling at the Meager Creek Site, Southwestern British Columbia (NTS 092J)

S.W. Mak, Geological Engineering/EOAS, University of British Columbia, Vancouver, BC, smak@eos.ubc.ca

E. Eberhardt, Geological Engineering/EOAS, University of British Columbia, Vancouver, BC

J.A. Meech, NBK Institute of Mining Engineering, University of British Columbia, Vancouver, BC

---

Mak, S.W., Eberhardt, E. and Meech, J.A. (2015): Assessing fracture network connectivity of prefeasibility-level high-temperature geothermal projects using discrete fracture network modelling at the Meager Creek site, southwestern British Columbia (NTS 092J); in Geoscience BC Summary of Activities 2014, Geoscience BC, Report 2015-1, p. 123–128.

## Introduction

Geothermal energy represents a clean, renewable, base-load source of energy that is underutilized in Canada. The current status of geothermal energy usage in Canada is limited to heating/cooling systems for residential and commercial infrastructure through the use of low-temperature heat exchangers. Despite having a wide distribution of potential high-temperature geothermal sites, there is currently no commercial electricity production derived from geothermal energy in Canada. The amount of energy stored within Canada's in-place geothermal resources is estimated to be greater than one million times current electrical consumption, although only a fraction of this energy can be accessed. The location of high-temperature geothermal sites that have the greatest potential of being developed are concentrated in the western provinces of British Columbia and Alberta, the Yukon and the Northwest Territories (Grasby et al., 2011).

The Meager Creek geothermal site, located approximately 150 km north of Vancouver, BC, has been characterized as the most promising high-temperature geothermal site in Canada (Jessop et al., 1991), with an estimated net electrical capacity of 250 MW (Ghomshei et al., 2004). Exploration of the site began in the early 1970s and production testing began in the early 1980s. Despite several attempts to develop the resource, the most recent occurring around 2005, sustainable yields of geothermal fluids have never been maintained at the site. The principle reason behind the lack of success of these past attempts is that none of the production wells drilled intersected a sufficiently large, connected, permeable fracture network. To date, no extensive fracture network analysis has been completed of the base-

ment rocks underlying the Meager Creek site and the natural connectivity of the existing fracture network remains unknown.

The viability of high-temperature geothermal projects is largely controlled by the connectivity of the fracture network within the reservoir rocks. The reason for this is that the amount of heat that can be extracted from a geothermal resource is dependent on the rate at which high-temperature fluids can be produced from geothermal wells. The geothermal resource at the Meager Creek site is hosted in low-permeability crystalline rocks and the circulation of geothermal fluids is largely confined to networks of interconnected fractures. It follows that if the connectivity of the existing fracture network can be characterized, the likelihood that the site can be successfully developed can be better assessed.

Fracture network connectivity cannot be measured directly, but must be inferred through the development and analysis of representative fracture models. Discrete fracture network (DFN) modelling is a stochastic method that is capable of simulating the geometric properties of individual fractures and the spatial relationships between fractures that develop within a rock mass. Unlike equivalent continuum methods, which treat the rock mass as a porous medium, DFN models explicitly represent the geometric characteristics of connected fracture networks through the stochastic simulation of discrete fractures across a model volume (Jing and Hudson 2002).

## Research Objective

The goal of this research is to use historical geomechanical and hydrogeological data collected from the Mount Meager area to assess the natural fracture connectivity of the reservoir rocks that host the geothermal resource at the Meager Creek site using DFN modelling. This assessment will contribute to a greater understanding of why past attempts to develop the site were unsuccessful and help determine whether specific measures can be taken to increase the like-

---

**Keywords:** geothermal, discrete fracture network, DFN, connectivity

This publication is also available, free of charge, as colour digital files in Adobe Acrobat® PDF format from the Geoscience BC website: <http://www.geosciencebc.com/s/DataReleases.asp>.

likelihood of successfully developing high-temperature geothermal resources in the future.

### Sources of Fracture Data

The development of DFN models begins with the collection of individual fracture properties. The fracture data required for the development of DFN models is typically collected from core logging, geophysical surveys of borehole walls and/or structural mapping of exposed bedrock outcrops. The primary source of fracture data used in this study consists of data collected during drilling and outcrop-mapping campaigns that were part of exploratory field investigations conducted in the area surrounding Mount Meager from 1974 to 1982. The initial field investigations of the site were carried out by the British Columbia Hydro and Power Authority (BC Hydro) and the federal Department of Energy, Mines and Resources. Although field investigations at the Meager Creek site occurred intermittently until approximately 2005, geomechanical and hydrogeological data collected after 1982 were not publicly available at the time of this study. The location of drillholes and mapping stations within the Meager Creek project area are shown in Figure 1.

### Fracture Data from Exploratory Diamond Drilling

The collection of fracture data from exploratory boreholes, either through oriented-core or televiwer logs, is essential for estimating fracture network connectivity of geothermal reservoirs. This is because fracture properties measured in surface outcrops may not be representative of the characteristics of the fracture network at depth. Geological data collected during exploratory drilling that was used in this study to develop DFN models of the Meager Creek site included

- lithology and alteration logs,
- rock-quality designation (RQD),
- depths at which fluid circulation was lost during drilling, and
- depths of dikes, shears and fault zones.

Fracture frequency (number of fractures intersected per metre) and fracture orientation (dip and dip direction of individual fractures) are two fracture parameters that are necessary for the development of site-specific DFN models. These two fracture parameters have a strong influence on fracture network simulations and, in turn, fracture-network

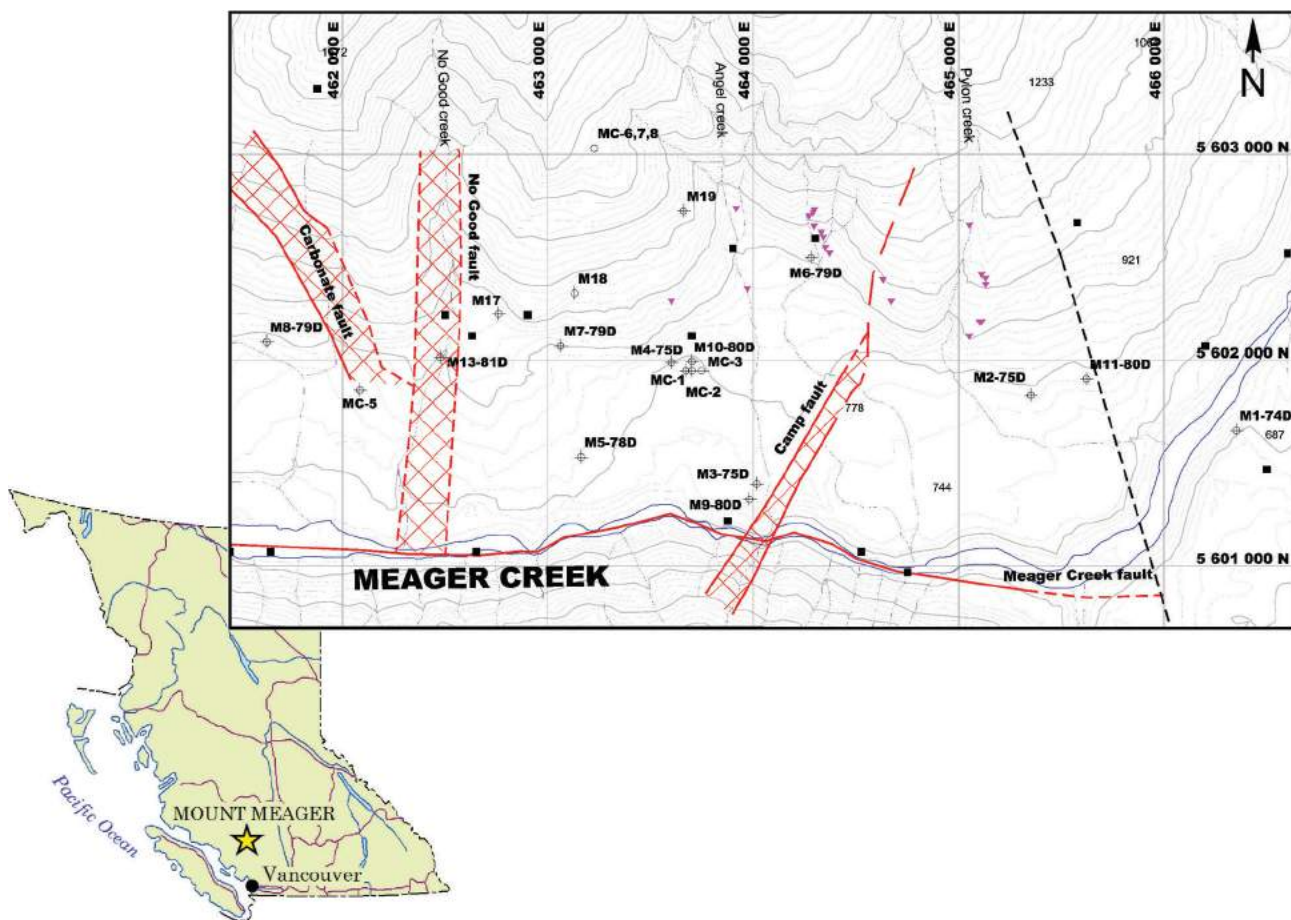


Figure 1. The Meager Creek geothermal project site, southwestern British Columbia, showing drillholes and mapping stations.

connectivity estimates. It follows that the collection of fracture frequency and fracture orientation measurements should be prioritized during exploration drilling.

### Fracture Data from Structural Mapping

Fracture data collected from structural mapping of rock outcrops can be used to identify major fracture sets and estimate the distribution of fracture sizes and fracture intensity within the rock mass. Historical structural mapping of exposed outcrops within the Mount Meager area was completed in 1980 and 1981. The structural-mapping database was augmented by geotechnical mapping of rock outcrops located north of the Lillooet River by the author during the summer of 2013. The type of fracture data collected included

- fracture orientation (dip and dip direction),
- fracture type,
- fracture trace length,
- fracture spacing, and
- mapping station co-ordinates.

### Interpretation of Fracture Network Characteristics for DFN Model Development

The following fracture network characteristics were interpreted from the geological and hydrogeological data collected from previous field investigations to generate representative DFN models of the Meager Creek site:

- peak orientation and distribution parameters of major fracture sets
- distribution of observed fracture spacing
- distribution of fracture trace lengths
- estimates of fracture intensity

### Characterization of Major Fracture Sets

The range of dip and dip direction of major fracture sets that occur within the Meager Creek site was determined by plotting poles of individual fractures on contoured, lower hemisphere, equal-area stereonet for individual mapping stations and comparing peak orientations of observed fracture sets over the Meager Creek site. Peak orientations that were observed over several mapping stations were interpreted as major fracture set orientations. Seven fracture sets were identified and were labelled fracture sets A to G. Figure 2 is a plot of all fractures mapped within the Meager Creek area, along with the range of dip and dip direction for each fracture set. Peak orientations and distribution parameters for each fracture set are summarized in Table 1. The Fisher constant for each fracture set was assessed using a Fisher-distribution analysis, which assumes that all observed fracture orientations within a fracture set are scattered around a single true orientation.

### Fracture Spacing Distribution

Fracture spacing is the measured distance between adjacent fractures intersected along a scanline. By fitting a statistical distribution to a population of fracture spacing measurements, inferences can be made regarding the spatial relationship between neighbouring fractures. Fracture spacing was not recorded during the 1980 and 1981 structural-mapping campaigns; however, it was recorded during structural mapping completed during the summer of 2013. It was found that the distribution of fracture spacing measurements could be fit using a negative exponential distribution. The fitted spacing distribution was then used to define the spatial relationship between neighbouring fractures in the DFN model simulations.

### Fracture Size Distribution

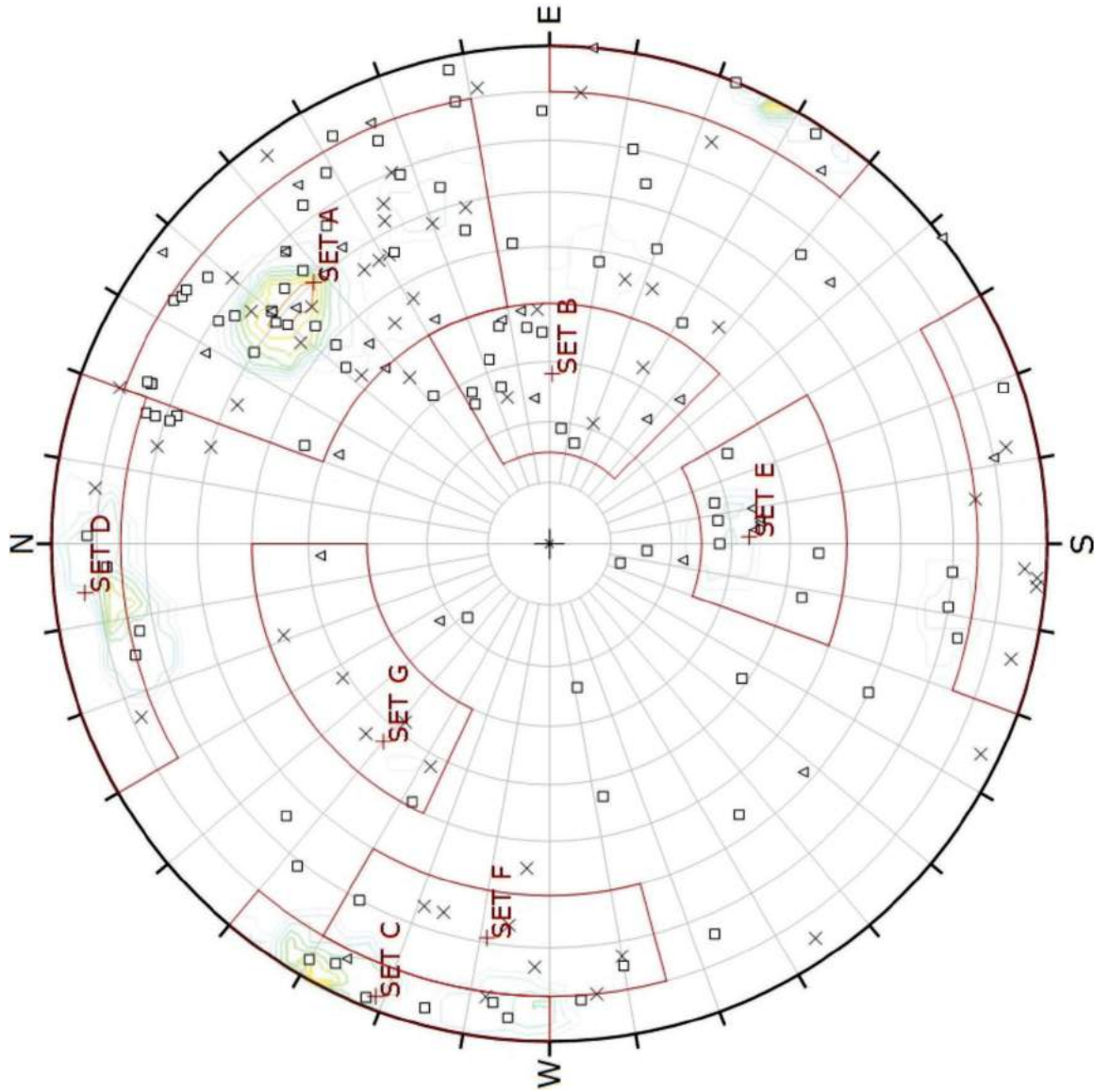
The true size of a fracture is rarely known with a high degree of certainty because direct observation and measurement of entire fracture planes is often impossible or impractical. Fracture size is typically inferred from the length of the line of intersection between the fracture and a two-dimensional plane, referred to as the fracture trace length. The distribution of fracture sizes was determined by estimating an equivalent radius distribution from trace length measurements that were collected during the summer of 2013. The DFN models were populated with fractures using the derived equivalent radius distribution so that the fracture size distributions in the models are statistically equivalent to the distribution of trace lengths observed in the field.

### Estimation of Fracture Intensity

Fracture intensity is a measure of fracture density within a rock mass. Typically, fracture intensity is inferred from fracture frequency measurements that are measured from core sample downhole surveys of open boreholes. Fracture frequency was not recorded during the exploratory drilling program. Attempts to derive fracture frequency values from logged RQD were unsuccessful. Consequently, a range of fracture intensity values was used as input in the DFN simulations. This led to a wide range of fracture-network connectivity estimates of the Meager Creek site. In future, fracture-network connectivity estimates can be significantly constrained if fracture frequency data is made available.

### Results from Fracture-Network Connectivity Assessments

The DFN models were constructed based on two different geological models to analyze the effects of large-scale faults on fracture-network connectivity estimates. The first geological model assumes that regional-scale faults have no effect on fracture network connectivity. The second geo-



Symbol	Area	Quantity
△	East of Camp fault	32
×	North reservoir	81
□	South reservoir	307

Colour	Density concentrations
	0.00 - 1.20
	1.20 - 2.40
	2.40 - 3.60
	3.60 - 4.80
	4.80 - 6.00
	6.00 - 7.20
	7.20 - 8.40
	8.40 - 9.60
	9.60 - 10.80
	10.80 - 12.00

Maximum density	11.54%
Contour data	Pole vectors
Contour distribution	Schmidt
Counting circle size	1.0%

Plot mode	Pole vectors
Vector count	420 (176 entries)
Hemisphere	Lower
Projection	Equal area

Figure 2. Combined, lower hemisphere, equal-area stereonet plot of all fracture data collected from all structural-mapping stations within the Meager Creek area, southwestern British Columbia.

**Table 1.** Summary of peak orientations and distribution parameters for major fracture sets based on surface-mapping data collected at the Meager Creek site, southwestern British Columbia. Abbreviation: DDR, dip direction.

Major sets	Average orientation		Dip range		DDR range	
	Dip (°)	DDR (°)	Min (°)	Max (°)	Min (°)	Max (°)
Set A	60	223	40	80	200	260
Set B	30	257	15	40	240	315
Set C	89	118	80	90	090	130
Set D	77	172	80	90	270	310
			75	90	150	200
Set E	31	350	25	50	330	020
Set F	66	109	60	80	075	120
Set G	44	124	30	50	115	180

logical model incorporates an extensive east-striking fault that dips toward the north at approximately 50°, with an associated fault-damage zone 100 m in width. The fault-damage zone is assigned a greater fracture intensity value relative to the rocks that constitute the hangingwall and footwall of the fault. The fault geometry used in the model is reflective of the Meager Creek fault geometry, which was mapped in exposed outcrops along the banks of Meager Creek.

Numerous studies have reported that fluid flow in fractured media is typically limited to a small percentage of the total number of observed fractures (Long et al., 1991; Cohen, 1995). This was accounted for in the DFN simulations by assigning transmissivity values to individual fractures and utilizing transmissivity thresholds to exclude a certain percentage of fractures from contributing to the development of connected fracture networks. Table 2 summarizes the range of total connected surface area that may exist at the Meager Creek site for various fracture intensity values and transmissivity thresholds.

## Discussion of Results

Fracture-network connectivity analysis results indicate that although the geothermal resource at the Meager Creek site is hosted in low-permeability reservoir rocks, the presence of the Meager Creek fault may provide sufficient connectivity for the upwelling and circulation of heated geothermal fluids to possibly permit the future development of a commercial geothermal project at the site. The higher fracture intensity value assigned to the fault-damage zone allows clusters of connected fractures to develop along the fault plane, even in a scenario where only a low percentage of transmissive fractures are present in the model. The effect of the Meager Creek fault on fracture network connectivity is shown in Figure 3.

Significant uncertainty is associated with the fracture connectivity assessments of the Meager Creek site due to the absence of certain geological information that was not

collected during the initial field investigations. This data included measurements of fracture orientation and the depth of all fractures encountered during drilling. The data collected from structural mapping could not be corrected for sampling biases, which increases the potential margin of error in the delineation of fracture set orientations and trace length distribution. Sampling biases can be easily corrected if a more rigorous mapping methodology is adopted, which would require that the following data be recorded at each mapping station:

- orientation of the mapping station (dip/dip direction of the mapped surface)
- type of sampling method used, more specifically line mapping (where the orientation and length of the sampling line should be recorded) vs. window mapping (where the total area and shape of the window, whether rectangular, square or circular, should be recorded)
- minimum trace length that was measured
- number of fractures that extend beyond the boundaries of the mapping station
- number of observable fracture termination points, if any, for each fracture

## Summary

The collection of geological data for the purpose of characterizing fracture networks can be costly, and at times impossible, due to the extreme depths of geothermal reservoirs and the effects of high temperature on borehole-instrumentation performance (Armstead and Tester, 1987). Moreover, these costs are incurred early in the project lifetime, when there is minimal geological data available for fracture network characterization. It follows that geothermal projects at the prefeasibility-level suffer from high developmental risks due to high exploration costs, coupled with high geological uncertainty associated with the nature of fracture-network connectivity assessments. The use of DFN modelling provides a means to manage part of this risk by allowing the connectivity of natural fracture net-

**Table 2.** Estimated ranges of connected surface area derived from fracture connectivity analyses of simulated DFN models.

	Fracture intensity: total surface area of fractures per cubic metre of rock (m <sup>2</sup> /m <sup>3</sup> )	Percentage of transmissive fractures (%)	Total connected surface area (m <sup>2</sup> )
Uniform rock mass model	0.5	100%	5.41E+08
	0.5	30%	1.22E+08
	0.5	25%	7.39E+07
	0.5	20%	1.91E+06
	0.5	15%	0.00E+00
Meager Creek fault model	0.5	100%	2.791E+08
	0.5	30%	6.200E+07
	0.5	25%	3.405E+07
	0.5	20%	1.385E+07
	0.5	15%	1.359E+06
	0.5	10%	0.000E+00

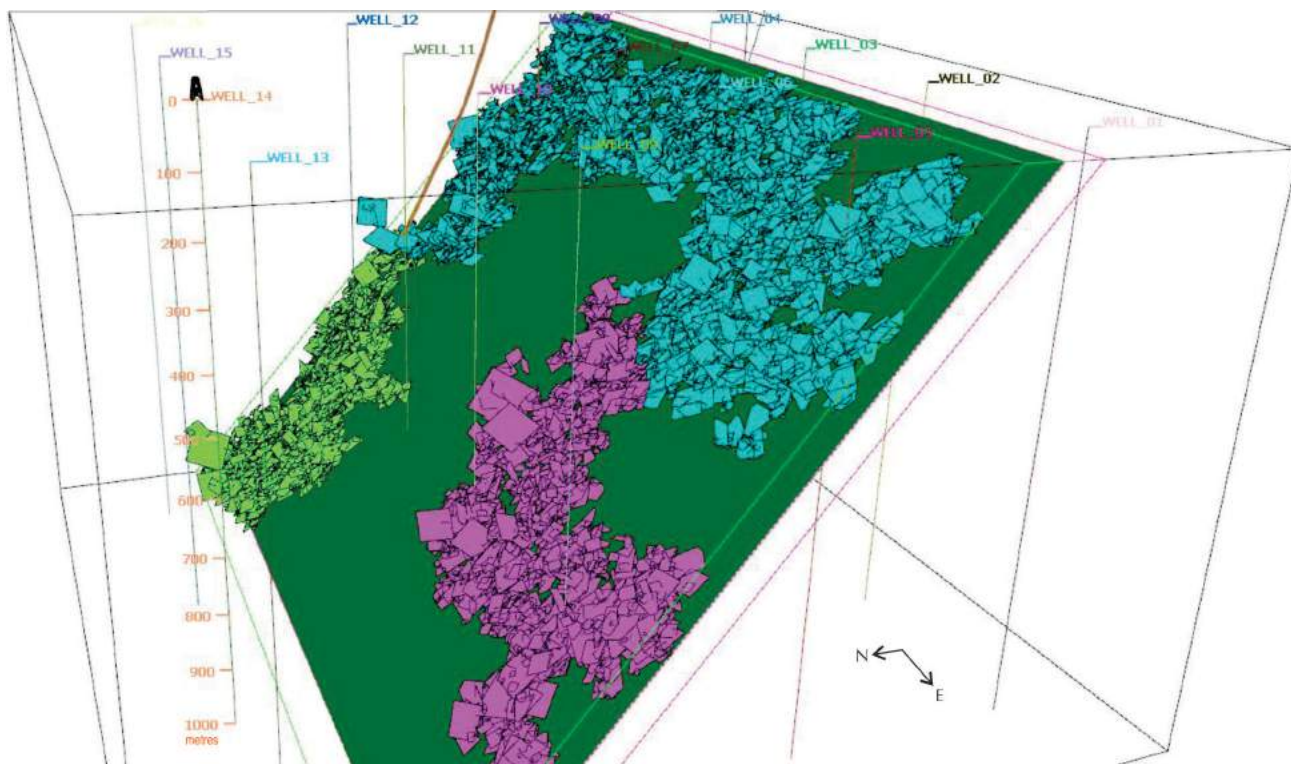


**Figure 3.** A DFN (discrete fracture network) model simulation, showing the development of three connected fracture networks (in green, blue and magenta) along the damage zone of the Meager Creek fault, southwestern British Columbia. Each polygon represents a single discrete fracture.

works to be assessed using fracture information that can be easily collected during exploration or prefeasibility-level field investigations.

### Acknowledgments

This research was funded in part by the Natural Sciences and Engineering Research Council (NSERC) and the Pacific Institute for Climate Solutions (PICS). A special thanks is extended to M. Ghomshei, whose years of experience in the geothermal industry and familiarity with the Meager Creek site were invaluable to this research.

### References

Armstead, H. and Tester, J. (1987): *Heat Mining: a New Source of Energy*; E. & F.N. Spon Ltd., New York, p. 478.

Cohen, A. (1995): *Hydrogeologic characterization of fractured rock formations: a guide for groundwater remediators*; Report LBL-38142, p. 144, doi:10.2172/219408

Ghomshei, M., Sanyal, S., Macleod, K., Henneberger, R., Ryder, A., Meech, J. and Fairbank, B. (2004): *Status of the South*

*Meager Geothermal Project British Columbia, Canada: resource evaluation and plans for development*; Geothermal Resources Council Transactions, v. 28, p. 339–344.

Grasby, S.E., Allen, D.M., Bell, S., Chen, Z., Ferguson, G., Jessop, A., Kelman, M., Ko, M., Majorowicz, J., Moore, M., Raymond, J. and Therrien, R. (2011): *Geothermal energy resource potential of Canada*; Geological Survey of Canada, Open File 6914, 301 p.

Jessop, A., Ghomshei, M. and Drury, M. (1991): *Geothermal energy in Canada*; Geothermics, v. 20, issue 5/6, p. 369–385.

Jing, L. and Hudson, J. (2002): *Numerical methods in rock mechanics*; International Journal of Rock Mechanics and Mining Sciences, v. 39, issue 4, p. 409–427.

Long, J., Karasaki, K., Davey, A., Peterson, J., Landsfeld, M., Kemen, J. and Martel, S. (1991): *An inverse approach to the construction of fracture hydrology models conditioned by geophysical data: an example from the validation exercises at the Stripa mine*; International Journal of Rock Mechanics and Mining Sciences & Geomechanics Abstracts, v. 28, issue 2/3, p. 121–142, doi:10.1016/0148-9062(91)92162-R

# Structural Geology of the Granite Lake Pit, Gibraltar Copper-Molybdenum Mine, South-Central British Columbia (NTS 093B/08, /09): Preliminary Observations

N. Mostaghimi, University of British Columbia, Vancouver, BC, nmostagh@eos.ubc.ca

L. Kennedy, University of British Columbia, Vancouver, BC

---

Mostaghimi, N. and Kennedy, L. (2015): Structural geology of the Granite Lake pit, Gibraltar copper-molybdenum mine, south-central British Columbia (NTS 093B/08, /09): preliminary observations; *in* Geoscience BC Summary of Activities 2014, Report 2015-1, p. 129–140.

## Introduction

The Gibraltar mine is a large calcalkaline copper-molybdenum porphyry deposit located about 10 km north of McLeese Lake, British Columbia, and hosted by tonalite of the Late Triassic Granite Mountain batholith (Figure 1). The Gibraltar deposit (MINFILE 093B 005, 006, 007, 008, 011, 012, 013; BC Geological Survey, 2014) is deformed, possessing a poorly to well-developed penetrative foliation, ductile shear zones and crosscutting brittle shear zones and faults (Ash and Riveros, 2001; Oliver, 2007a; Oliver et al., 2009; van Straaten et al., 2013). There is a known spatial association between the ore bodies and zones of ductile deformation; however, the relative timing of intrusion, mineralization and deformation has not been resolved.

This project is part of the Geological Survey of Canada's Intrusion Related Ore Systems TGI-4 program, where the Gibraltar copper-molybdenum open-pit mine is one of several mineralized systems currently being investigated. The objectives of this study are to 1) unravel the geometry and kinematics of deformation that have affected ore distribution, 2) place constraints on the timing of deformation structures and 3) determine if batholith emplacement and mineralization were synkinematic with the earliest deformation structures or if structural modification of the deposit occurred after emplacement and mineralization.

In this paper, the authors present preliminary field observations from detailed structural mapping of select benches in the Granite Lake operational pit (Figure 2).

## Regional Geological Setting

The geological setting of the Granite Mountain batholith is shown in Figure 1. The oldest rocks in the region include

---

**Keywords:** Gibraltar mine, copper-molybdenum deposit, porphyry, deformation, structural geology, Granite Mountain batholith

*This publication is also available, free of charge, as colour digital files in Adobe Acrobat® PDF format from the Geoscience BC website: <http://www.geosciencebc.com/s/DataReleases.asp>.*

late Paleozoic through early Mesozoic oceanic rocks (mainly chert, limestone and basalt) of the Cache Creek Complex (Cache Creek terrane), and Late Triassic through Middle Jurassic arc volcanic, volcanoclastic and plutonic rocks of the Quesnel terrane. Younger rocks include granitic plutons of the Middle Jurassic and Early Cretaceous, Eocene volcanic and sedimentary rocks, Oligocene–Pliocene clastic sedimentary sequences that occur along parts of the Fraser River, and widespread Miocene–Pleistocene basalt of the Chilcotin Group. Drummond et al. (1976), Tipper (1978) and Bysouth et al. (1995) thought that the Granite Mountain batholith was intrusive into the Cache Creek Complex, in part because of widespread Cache Creek exposures to the east and south of the batholith. Conversely, Ash et al. (1999a, b) and Schiarizza (2014) suggest that contacts between the batholith and the Cache Creek Complex are faults, but that intrusive contacts are preserved along the northeastern margin of the batholith where it and related plutonic rocks of the Burgess Creek stock cut an Upper Triassic volcanoclastic and volcanic sequence correlated with the Nicola Group of the Quesnel terrane. These relationships suggest that the Granite Mountain batholith is within the Quesnel terrane, and part of a panel of Quesnel terrane rocks that is faulted against the Cache Creek terrane to the west of the main Quesnel belt (Figure 1). Its age and location within the western part of Quesnel terrane suggest that the Granite Mountain batholith is broadly correlative with the Late Triassic Guichon Creek batholith, which hosts the Highland Valley copper-molybdenum porphyry deposits 250 km to the south-southeast.

## Previous Work

Early workers proposed that emplacement of the Granite Mountain batholith was syntectonic such that batholith emplacement, deformation, metamorphism and mineralization were a continuous process (Sutherland Brown, 1974; Drummond et al., 1976; Bysouth et al., 1995). Bysouth et al. (1995) presented a model where deformation of the batholith, including the formation of penetrative foliation and ductile shear zones (generally thrust faults), was related to the accretion of the Cache Creek terrane to the

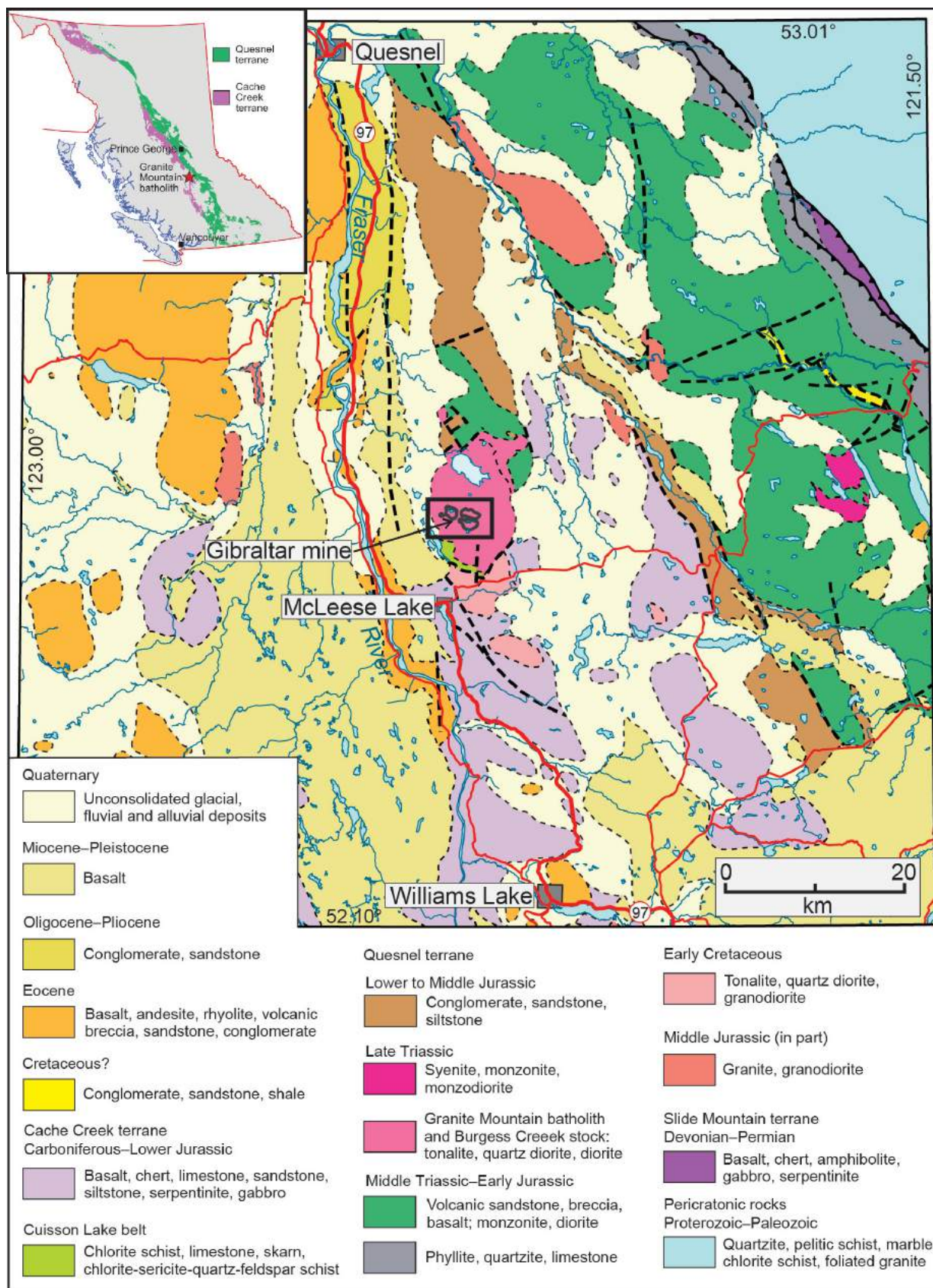


**Figure 1.** Geology of the area surrounding the Granite Mountain batholith, showing the location and setting of the Gibraltar copper-molybdenum mine (modified from Scharizza, 2014). Inset of British Columbia (top left) showing the location of the Granite Mountain batholith and the distribution of the Quesnel, Cache Creek and Slide Mountain terranes (from Scharizza, 2014).

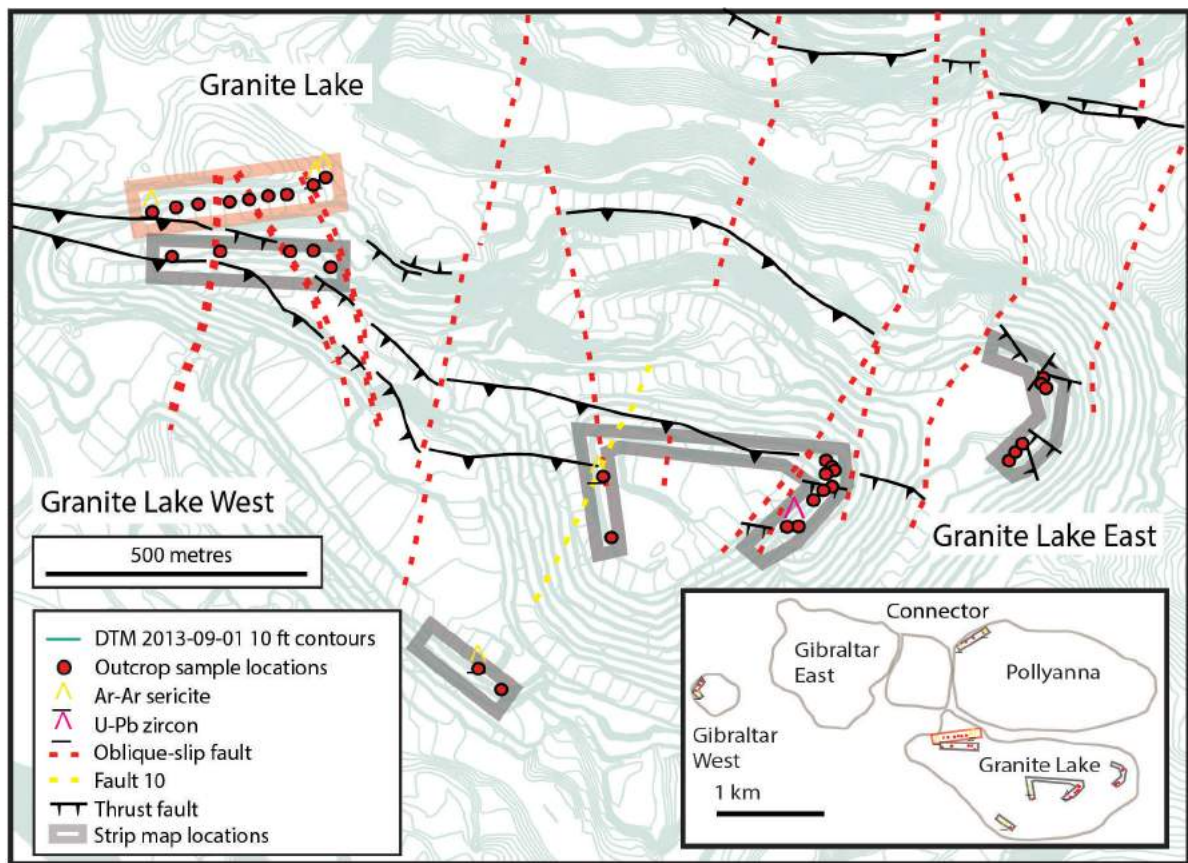


**Figure 2.** Granite Lake pit topography. Granite Lake faults offset by late north-south high-angle oblique-slip faults (dashed red lines) modified from Oliver (2008). The pit contours are from 2013, whereas the Granite Lake fault traces are from 2008 and have not been updated to the current locations where they crop out within the pit. Inset: four main pits of Gibraltar mine outlined from 2013 with the proposed Connector pit and strip map locations (modified from Jones, 2011). The strip map in Figure 3 is highlighted in red.

Quesnel terrane and was initiated before ore deposition but continued after the metals were deposited, creating the present foliated nature of the ore, alteration and hostrock (Bysouth et al., 1995). In contrast, Ash et al. (1999a, b) suggested that the ductile shear zones within the Gibraltar deposit formed during faulting of the batholith against the Cache Creek terrane, implying that either mineralization postdates intrusion or ore was remobilized into the shear zones. Late Triassic Re-Os ages on molybdenum that overlap the age of the host tonalite indicate that intrusion and mineralization are genetically linked (Harding, 2012). Van Straaten et al. (2013) argued that because ductile deformation zones contain abundant, folded, sheared and transposed hydrothermal mineralized veins, mineralization occurred either before or during deformation. The relative timing of mineralization and ductile deformation in the Gibraltar copper-molybdenum mine has not been resolved.

Deformation in the Gibraltar pits is complex because there are no true marker horizons; therefore, determining offsets and kinematics can be difficult. In general, the geometry, relative timing and kinematics of most deformation structures were documented by early workers (Sutherland

Brown, 1974; Drummond et al., 1976; Bysouth et al., 1995) and more recently by Ash et al. (1999b), Ash and Riveros (2001), Oliver et al. (2009) and van Straaten et al. (2013). The earliest tectonic fabric is a poorly to well-developed, gently to moderately southwest-dipping  $S_1$  foliation defined by chlorite and/or sericite and elongate to recrystallized quartz porphyroclasts. This foliation is best developed in proximity to high-strain zones and ranges from phyllonitic to schistose to gneissic in texture (Drummond et al., 1973; Ash and Riveros, 2001; van Straaten et al., 2013). Ash and Riveros (2001) recognized early ‘sub-horizontal shear zones’ that are laterally discontinuous and deform  $S_1$ . Large (tens to hundreds of metres wide), southeast- to east-trending, shallowly dipping, ductile, high-strain zones with top to the northeast sense of movement commonly host, or are spatially associated with, mineralization (e.g., Oliver, 2007a, b; Oliver et al., 2009). Oliver et al. (2009) suggest that the  $S_1$  foliation and the ductile high-strain zones formed during emplacement of the batholith and therefore exert a fundamental control on mineralization and alteration. It is likely that the formation of  $S_1$ , the subhorizontal shear zones and the ductile, compressive shear zones represent a progressive deformation. Brittle-ductile, more dis-

crete (thinner) southwest-dipping thrust faults, also with a top to the northeast shear sense are interpreted as having formed during cooling of the pluton and/or exhumation of the pluton after ductile shearing (van Straaten et al., 2013). Steeply dipping, north-striking, dextral normal fault zones offset the orebody and have similar kinematics as regional Late Cretaceous–Paleogene structures such as the Fraser, Quesnel and Pinchi fault systems.

## Ore Deposit Geology

### Lithology

The Granite Mountain batholith is subdivided into three mappable phases: Border phase quartz diorite, Mine phase tonalite and Granite Mountain phase trondhjemite (Bysouth et al., 1995). The Mine phase tonalite hosts the copper-molybdenum mineralization in the Granite Lake, Gibraltar East, Gibraltar West and Pollyanna pits (Figure 2). The Border phase quartz diorite is composed of 15% quartz, 45–50% plagioclase and 35% chloritized hornblende and is found in the southwestern segment of the batholith (van Straaten et al., 2013). The Mine phase tonalite comprises 15–25% quartz, 40–50% plagioclase and 25–35% chlorite (van Straaten et al., 2013). The rock is equigranular with grain sizes averaging 2–4 mm. Plagioclase is variably altered to albite-epidote-zoisite, and chlorite is reported to have altered from biotite and hornblende (Bysouth et al., 1995). Locally, the Mine phase tonalite contains a more leucocratic phase that contains less than 10–15% mafic minerals. The Granite Mountain phase trondhjemite to the northeast of the Mine phase tonalite comprises  $\geq 45\%$  quartz, 45% plagioclase and 10% chlorite, and is generally barren to weakly mineralized (van Straaten et al., 2013). Leucocratic quartz porphyry dikes intrude all mappable units (leucocratic phase of Bysouth et al., 1995). All phases, including the porphyry dikes, are variably deformed by  $S_1$ .

### Alteration, Veining and Mineralization

Van Straaten et al. (2013) describe vein types, alteration assemblages and mineralization distributions that are consistent with an origin as a calcalkaline porphyry. Hydrothermal alteration assemblages at the Gibraltar deposit can be used as ‘markers’ to define structures. There is a generally positive correlation between deformation intensity, alteration and mineralization (e.g., Oliver, 2007b; van Straaten et al., 2013). The vein descriptions in Table 1 provide temporal relationships between the veins and their associated alteration zone assemblages based on crosscutting relationships in the field and drillcore logging. This alteration scheme was used in the construction of the strip maps.

Hypogene mineralization, including chalcopyrite and to a lesser extent molybdenite, is predominantly vein hosted (van Straaten et al., 2013), occurring proximal to zones of

chloritization and sericitization (Bysouth et al., 1995) and is structurally controlled either during batholith emplacement or by post-emplacement modification (Drummond et al., 1973; Sutherland Brown, 1974; Bysouth et al., 1995; Ash and Riveros, 2001; Oliver et al., 2009; van Straaten et al., 2013).

## Structural Geology

Seven bench walls were mapped in Granite Lake, Pollyanna and Gibraltar West pits for lithology, alteration, structures and mineralization. A total of 50 hand samples and 30 drillcore samples were collected from selected structures and rock types for thin sections,  $^{40}\text{Ar}/^{39}\text{Ar}$  (illite) dates and U-Pb (zircon) dates (Figure 2). Below, the authors describe the structures recognized in the pits from the oldest to the youngest features; the description is focused on the Granite Lake pit and relationships are illustrated with a bench wall map from the pit (Figure 3).

The earliest fabric is a sporadically developed magmatic foliation ( $S_M$ ), defined by aligned but not strained chloritized hornblende and biotite; plagioclase is commonly saussuritized. Based on limited measurements,  $S_M$  dips gently to the northwest and southeast (Figure 4c).

The earliest tectonic fabric ( $S_1$ ) is well developed in deformation panels that are interspersed with panels of massive to poorly foliated rock. The  $S_1$  foliation is generally shallowly south dipping; however, the foliation is locally folded and poles to foliation define a weak girdle distribution (Figure 4c) with a shallowly southeast-plunging pole to the girdle. The  $S_1$  fabric is defined by elongate chloritized hornblende and elongate quartz, and ranges from weakly developed to schistose to gneissic in texture (Figures 3g, 5a–c). Increasing foliation intensity develops 1–3 mm wide subplanar chlorite ‘seams’ that are variably developed and interpreted to have formed from the accumulation, alignment and compositional zoning of chloritized primary mafic rocks. Deformation intensity is correlated with increased sericitic alteration, where  $S_1$  is defined by closely spaced sericite and chlorite lamellae. Locally, well-developed phyllonitic foliations are crenulated, with the crenulation lineations plunging shallowly to the southeast.

Early- to main-stage sheeted mineralized veins are oriented oblique and parallel to subparallel to the tectonic foliation (Figure 4; Sutherland Brown, 1974; Drummond et al., 1976; Ash and Riveros, 2001; Oliver et al., 2009) and in the field, aid in highlighting the foliation and folded foliation (Figure 5d). The sheeted veins can be folded. When present, the sheeted chlorite-epidote-quartz veins can also act as ‘C surfaces’ (in the S-C mylonite terminology): S surfaces are defined mostly by elongate quartz. This geometry gives the appearance of S-C mylonite in the field (Figure 5c) and consistently provides a top to the northeast

sense of shear. The sheeted veins clearly have slip along them, as illustrated by abundant lineated surfaces, thus, the S and C surfaces were likely kinematically linked during deformation.

It is difficult to uniquely determine if alteration and mineralization predate deformation or are syndeformational. In a weakly foliated tonalite, however, with  $S_1$  foliation defined by sericite and a weak chlorite alignment, the sericite foliation overprints previously saussuritized and veined Mine phase tonalite (Figure 5a, b). These crosscutting relationships imply that alteration and vein emplacement predate  $S_1$  formation. In highly strained rocks, foliation, veins and alteration patterns are transposed and crosscutting relationships are obliterated.

Subhorizontal, discontinuous high-strain zones (Figure 3a, b), described by Ash and Riveros (2001) as early subhorizontal shear zones, are subhorizontal to shallowly dipping toward the south-southwest and commonly contain boudinaged quartz veins with large chlorite knots and chalcopyrite±pyrite blebs (Figure 5d). Phyllonitic to schistose

$S_1$  foliation wraps around the boudinaged veins and form zones of localized high shear strain within the  $S_1$  foliation. The lineations associated with the necks of veins that are enclosed in the boudinage are shallowly plunging toward the southeast. The subhorizontal high-strain zones do not appear to be associated with any significant displacement and are interpreted to represent shearing caused by an instability related to deformation  $S_1$  fabric around the veins.

Oliver (2007a, 2008) mapped large, continuous, southeast-to east-trending, ductile, high-strain zones with reverse kinematics indicating a top to the northeast sense of movement. These high-strain zones are on the order of tens to hundreds of metres wide. In the Granite Lake pit, the high-strain zones (called Granite Lake faults; Oliver, 2007a, 2008) are bound or are spatially associated with ore mineralization (Figure 2); however, not all high-strain zones are mineralized (van Straaten et al., 2013). Drillcore intersects of these high-strain zones contain well-developed mylonite with extensive quartz grain elongation, solution transfer pressure shadows, limited dynamic recrystallization of

**Table 1.** Characteristics of the hydrothermal alteration assemblages and related vein-types at Gibraltar mine. Abbreviations: Ank, ankerite; Cb, carbonates; Chl, chlorite; Ccp, chalcopyrite; Ep, epidote; Fsp, feldspar; Hbl, hornblende; Mag, magnetite; Mol, molybdenite; Py, pyrite; Qz, quartz; QSP, quartz-sericite-pyrite; Ser, sericite; \*, data modified from van Straaten et al. (2013).

Hydrothermal alteration assemblage	Alteration characteristics	Vein assemblage	Vein shape and texture	Mineralization stage
Saussurite-chlorite (albite-epidote-zoisite)	No alteration to pale yellow-green saussuritization of feldspars, chloritized Hbl and presence of Ep veinlets	Ep	1 mm planar veinlets and 4–5 cm wide diffused flooding	Preminalization
Propylitic (chlorite-epidote)	Increase in pale yellow-green saussuritization of Fsp, chloritized Hbl, Ep grains and veinlets, and Chl-Ep veins*	Chl+Ep±Py±Cpy±Qz±Cb	1–15 mm wide Chl-Ep vein: a) thin, planar; b) wider, diffuse margins; c) wider, diffuse Qz envelope; d) Cb and cubic Py in the centre ±Ccp	Early
Chlorite-quartz	Alteration intensity characterized by vein density and ranges from no pervasive matrix alteration to prevalent Qz and Chl replacement of Fsp*	Qz±Chl±Mag±Py±Ccp±Mol	2–20 mm wide Qz vein with Chl halo; sometimes Mag-Chl-Mol-Ccp±Py aligned in centre: a) sharp boundaries; b) no margins, grey Qz; and c) disconnected, wavy veins with more diffuse Qz-Chl margins*	Main
Quartz-sericite	Qz-Ser flooding	Qz+Ser	Qz-Ser flooding and replacement of Chl-Qz-Fsp alteration	Late
Quartz-sericite-chlorite	Finely disseminated Ser±pale Chl±Qz alteration of matrix; euhedral grains of Py are sparse	~	No specific vein is closely associated with this alteration	Late
Phyllic (quartz-sericite-pyrite)	Occurs in varying intensities; weak QSP alteration is distinguished by 1–3 cm wide sheeted veins, while stronger QSP alteration is characterized by pervasive replacement of the matrix by Qz and Ser*	Qtz+Ser+Py±Ccp±Mol	a) 1–3 cm wide sheeted grey Qz veins, with Ser-Qz envelopes and cubic Py aligned in the centre; b) 1–200 cm wide milky-white veins, with parallel sheeted Mo veinlets, host bulk Mo mineralization (Harding, 2012)	Late
Ankerite-quartz	Pale Ank-Qz alteration commonly associated with high strain zones; sulphide mineralization may occur with Ser±Chl folia*	Ank whisps	2 mm in size, separated sinuous whisps; veins were either completely deformed or transposed as they are unidentifiable	Late
~	Not associated with any specific alteration assemblage	Qtz+Chl±Ccp±Py±Cb	0.1–1 m thick, boudinaged Qz veins with Chl knots ±Py±Ccp blebs, enveloped by Chl/Ser folia	Late or postmineralization

Granite Lake West:  
3770' - 3850'  
Ramp

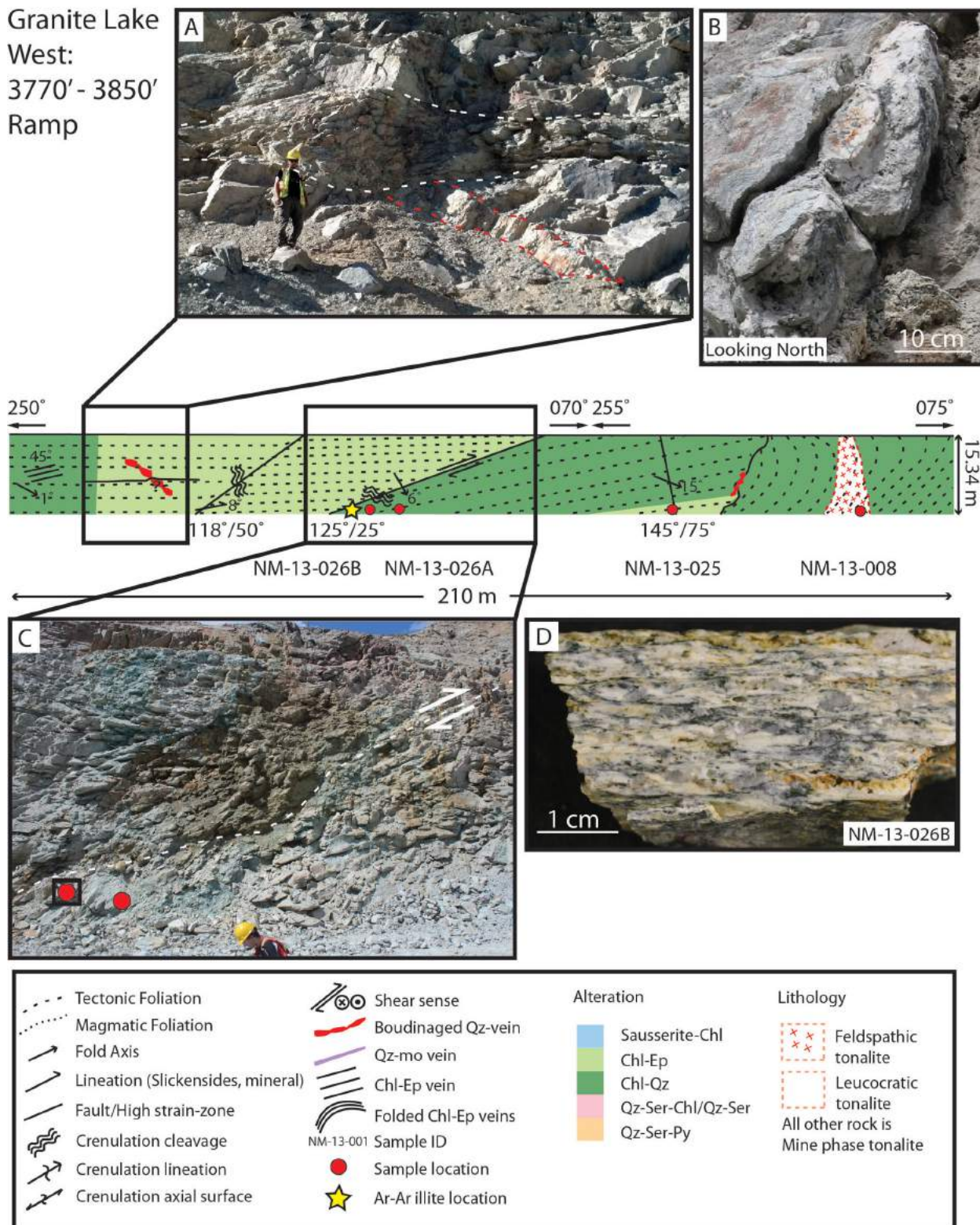


**Figure 3.** Bench-wall geological strip map from Granite Lake West, coloured according to the predominant (>50%) alteration assemblage. Figure 3a is the western end of the exposure; Figure 3e is the eastern end of the bench. Foliation intensity increases with decreasing space between form (strike) lines: **a**) subhorizontal, discontinuous, high-strain zone (outlined by white dashed lines) oblique to a boudinaged quartz vein; **b**) boudinaged quartz vein located in a high-angle fault from a different bench wall in Granite Lake West pit; similar boudinaged quartz veins are observed in subhorizontal discontinuous high-strain zones; lineations defined by the boudin neck plunging shallowly toward the southeast; **c**) imbricate thrust fault with a distributed zone of strain and a narrow (~30 cm thick) mylonitic fault core; **d**) sample from the core of the thrust fault, showing mylonitic fabric with fault zone-parallel chlorite layers and elongate quartz; sample collected from the red dot in the box of c).

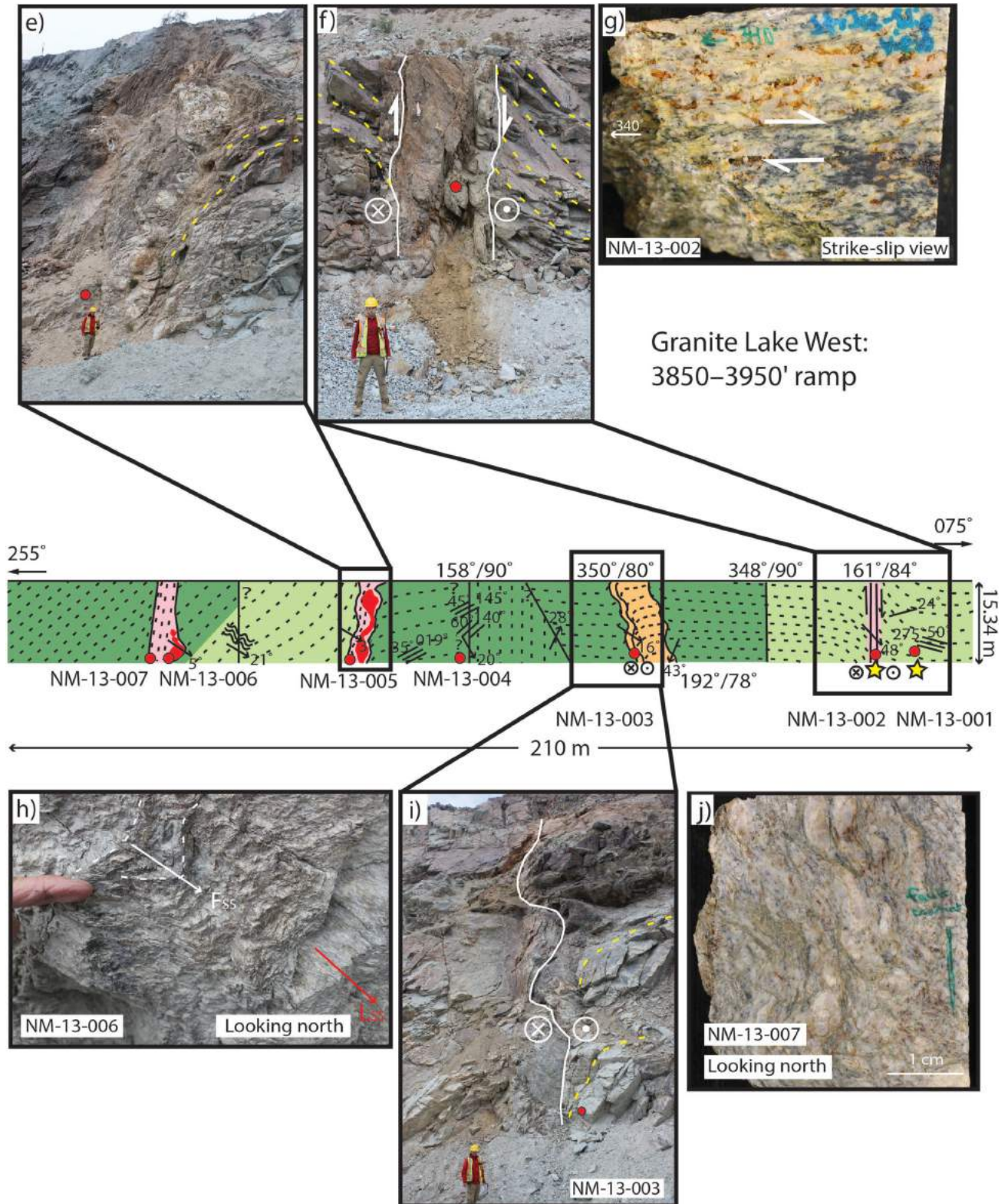


**Figure 3 (continued).** **e)** high-angle oblique-slip fault with boudinaged quartz-rich vein, boudins are elongated parallel to fault strike; **f)** high-angle dextral-normal fault zone;  $S_1$  foliation is dragged into the fault; **g)** dextral shear sense shown by the asymmetry of quartz pressure shadows; sample collected from the red dot in **f)**; **h)** parallel fold axes ( $F_{SS}$ ) and muscovite lineations ( $L_{SS}$ ) plunging  $5^\circ$  toward  $130^\circ$ ; sample collected from a high-angle fault; **i)** folded dextral, high-angle fault zone; fold axes plunge shallowly toward the southeast; **j)** highly strained fault rock with a crenulated fault fabric; sample taken from a high-angle oblique-slip fault.

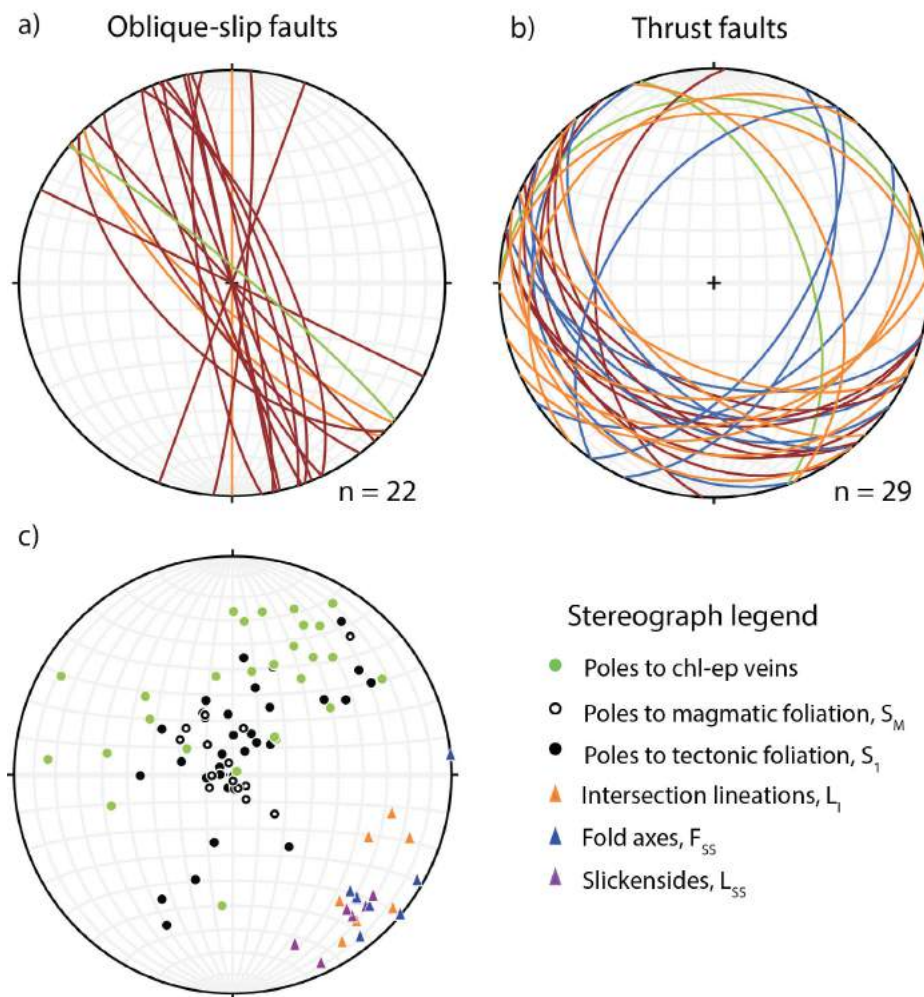


**Figure 4.** **a)** Stereographs of high-angle dextral-normal fault planes from Granite Lake West (in red), Pollyanna (in orange) and Gibraltar West (in green); **b)** stereographs of thrust faults, same colour scheme as in a) and Granite Lake East is in blue; **c)** stereograph of structural elements from the Granite Lake pit; poles to early mineralization-stage chlorite-epidote veins,  $n = 27$ ; poles to magmatic foliation,  $n = 20$ ; poles to tectonic foliation,  $n = 32$ ; intersection lineations between  $S_1$  and oblique-slip fault fabric ( $L_1$ ),  $n = 10$ ; fold axes within high-angle, oblique-slip faults ( $F_{SS}$ ),  $n = 9$ ; and slickensides and mineral lineations within high-angle, oblique-slip faults ( $L_{SS}$ ),  $n = 6$ .

quartz (Figure 5e, f) and higher degrees of alteration than less strained rock, suggesting that fluid flow assisted deformation. In the high-strain zones, veins are folded, sheared and transposed parallel to the main fabric. Large quartz clasts observed in mylonite are probably sheared and fragmented veins.

Smaller-scale thrust faults (Figure 3c) with the same attitude and shear sense as the Granite Lake faults are common in the Granite Lake, Pollyanna and Gibraltar West pits. They strike  $110\text{--}150^\circ$  and dip  $20\text{--}55^\circ$  toward the south-southwest (Figure 4b). These thrusts are imbricate in their spatial geometry, are more discrete than the larger Granite Lake faults and contain mylonitic zones up to 30 cm thick (Figure 3c, d). The presence of mylonite rather than brittle fault rocks implies that the physical conditions of deformation (e.g., temperature) were similar during the formation of both the Granite Lake faults and the imbricate thrust

faults. The imbricate thrusts are typically associated with high concentrations of copper oxides. In addition, boudinaged quartz veins enriched in chalcopyrite±pyrite are found within the thrust faults, indicating the remobilization of ore during thrust fault formation. Drag folds of  $S_1$  into the thrust faults provide reliable shear sense indicators and indicate that  $S_1$  existed prior to thrusting. Northeast-dipping thrust faults, with little to no mylonite developed, are spatially associated with the southwest-dipping thrusts, and are interpreted as conjugate faults. The strongly foliated rocks found in the Granite Lake faults, and in the more localized imbricate thrust faults, are crenulated (Figures 3h, 5f). The crenulation and intersection lineations plunge shallowly to the southeast.

The imbricate thrust faults offset and stack the ore body (Oliver, 2007a). Van Straaten et al. (2013) interpret the imbricate thrust faults as having formed during cooling and/or

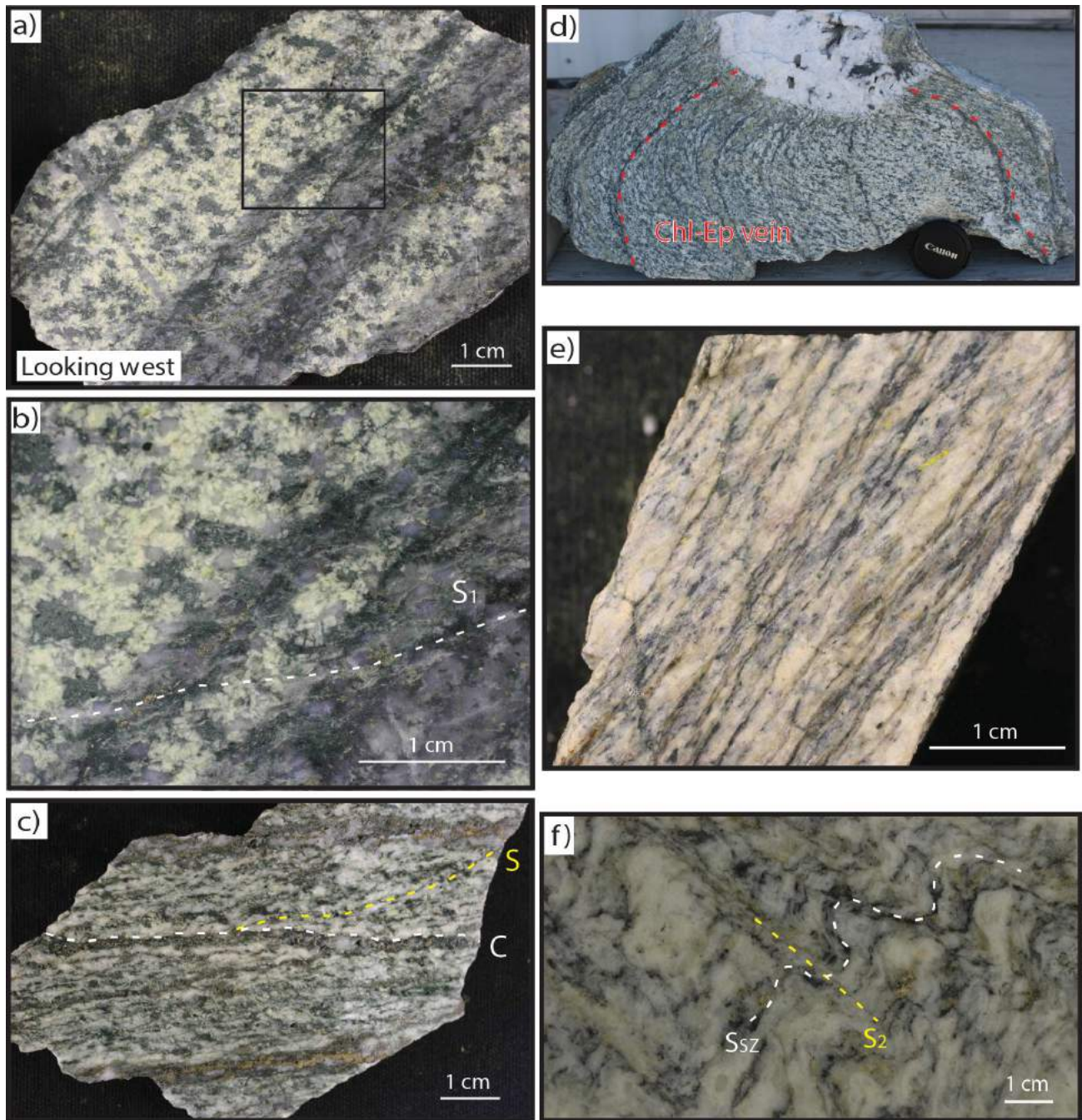


**Figure 5.** a) Mineralized chlorite-epidote-quartz-chalcopyrite vein overprinted by a weak  $S_1$  foliation defined by sericite and elongate quartz;  $S_1$  changes orientation from shallow in the chlorite-epidote-altered tonalite to more inclined in the vein due to rheological differences between the background rock and the vein; sample collected from Granite Lake East; box showing location of b); b) inset of a) illustrating the  $S_1$  foliation crosscutting the chlorite-epidote-quartz-chalcopyrite vein; c) S-C fabric in chlorite-quartz-altered Mine phase tonalite; the C surface is defined by mineralized chlorite-epidote-quartz-chalcopyrite veins, the S surface is defined by elongate quartz and inclined chlorite seams; sample collected from Granite Lake West; d) boudinaged late- or postmineralization-stage quartz vein with chlorite knots; dashed red lines highlight the folded mineralized chlorite-epidote-quartz-chalcopyrite veins in chlorite-epidote-altered Mine phase tonalite; sample collected from Granite Lake East; e) drillcore sample of a weakly mineralized ankerite-quartz-altered high-strain zone from a Granite Lake fault; f) drillcore sample of weakly mineralized, ankerite-quartz-altered leucocratic tonalite, with shear zone foliation ( $S_{sz}$ ) cut by  $S_2$  crenulation cleavage; sample taken from a Granite Lake fault.

exhumation after the ductile shearing. The authors of this paper suggest that large, ductile, high-strain zones and the imbricate thrust faults are kinematically linked during the same phase of deformation.

High-angle, oblique-slip fault zones strike northwest to northeast, are steeply dipping and crosscut all units and structures (Figure 4a; Oliver et al., 2009). Drag folds of  $S_1$  indicate a component of normal shear (Figure 3f) and shear-sense indicators from cataclasite (observed from the strike-slip kinematic plane) indicate dextral shear sense (Figure 3g). These fault zones have damage zones up to 5 m wide, and the fault zone cores have foliated cataclasite that can be up to 1 m thick. The foliation within the cataclasite is defined mostly by layers of quartz and illite (Figure 3g). Well-developed mineral lineations (illite and elongate quartz) and slickenlines plunge shallowly toward the southeast (Figures 3h, j, 4c). Folds are common in the fault zones and fold axes trend shallowly to the southeast (Figure 3h). Fault fabrics from all observed high-angle dextral-normal faults are crenulated, the intersection lineation and crenulation lineations plunge shallowly to the southeast (Figure 4c). The high-angle faults can be folded (Figure 3i) with fold axes subparallel to crenulation lineations (Figure 3h). When present in the high-angle dextral faults, late leucocratic dikes and thick, late quartz veins are folded and boudinaged (Figure 3e). Late-stage quartz-sericite-pyrite-molybdenite veins are tightly folded in these faults.

Large, brittle faults with thick gouge zones appear to be the latest brittle deformation feature. In the Granite Lake pit, these faults are exemplified by Fault 10 (Figure 2), which strikes  $200^\circ$ , dips  $44^\circ$  to the west and is marked by a 20 m thick zone of hematite staining Fault 10. Although the displacement is not known, this fault and others like it (or smaller in size) are generally geotechnical hazards causing slumping or pit wall failures within the pits.

## Conclusions

The authors propose that the formation of  $S_1$ , the formation of the subhorizontal high-strain zones, the large, ductile, compressive high-strain zones and the smaller scale thrust faults are all part of a progressive deformation that occurred under the same directed stress. Mineralized sheeted veins that occur parallel to subparallel to  $S_1$  act as pre-existing C surfaces and locally facilitate the formation of S-C mylonite. Subhorizontal, discontinuous high-strain zones are not well understood; however, they are interpreted to be caused by instabilities arising from the flattening of foliation around large veins. North-striking oblique-slip faults contain brittle fault rocks (foliated cataclasite) that suggest their formation in upper levels of the crust. These faults likely formed at higher levels in the crust than the main foliation and associated high-strain zones. Exhumation and uplift of the Granite Mountain batholith may be related to slip

along the oblique-slip faults and/or the late brittle faults. The shallowly southeast-plunging lineations, including intersections, fold axes and boudin necks, must represent the last stage deformation: the cause of this late-stage flattening resulting in boudinage and crenulations is not yet resolved.

## Future Work

Several cross sections of the Granite Lake pit will be constructed based on field observations, logged drillcore and fault offset information gleaned from using Leapfrog® Geo visualization with all drillcore data from Granite Lake. The main foliation ( $S_1$ ) and the different shear zones will be dated using Ar-Ar (illite) from fabrics with known kinematics. The Mine phase tonalite will be dated using U-Pb (zircon). Microstructural observations will allow constraints to be placed on the physical conditions (e.g., temperature) of deformation for each deformation structure. Ultimately, the goal is to constrain the absolute age of deformation and to determine the relative timing of intrusion, mineralization and deformation.

## Acknowledgments

The authors are grateful to Taseko Mines Ltd. for allowing access to the pits, the drillcore and their database. The authors thank L. Goodman for her assistance with the database and for assistance in the field. B. van Straaten is thanked for sharing his knowledge regarding the alteration and for beneficial discussions. Natural Resources Canada provided partial funding for this project. N. Mostaghimi is thankful for the generous financial support provided by Geoscience BC. The authors thank P. Schiarizza for his careful review of the manuscript.

## References

- Ash, C.H. and Riveros, C.P. (2001): Geology of the Gibraltar copper molybdenite deposit, east-central British Columbia (93B/9); *in* Geological Fieldwork 2000, BC Ministry of Energy and Mines, BC Geological Survey, Paper 2001-1, p. 119–133.
- Ash, C.H., Rydman, M.O., Payne, C.W. and Panteleyev, A. (1999a): Geological setting of the Gibraltar mine, south-central British Columbia (93B/8, 9); *in* Exploration and Mining in British Columbia 1998, BC Ministry of Energy and Mines, BC Geological Survey, p. A1–A15.
- Ash, C.H., Panteleyev, A., MacLennan, K.L., Payne, C.W. and Rydman, M.O. (1999b): Geology of the Gibraltar mine area, NTS 93B/8, 9; BC Ministry of Energy and Mines, BC Geological Survey, Open File 1999-7, scale 1:50 000.
- BC Geological Survey (2014): MINFILE BC mineral deposits database; BC Ministry of Energy and Mines, URL <<http://minfile.ca>> [November 2014].
- Bysouth, G.D., Campbell, K.V., Barker, G.E. and Gagnier, G.K. (1995): Tonalite-trondhjemite fractionation of peraluminous magma and the formation of syntectonic porphyry copper mineralization, Gibraltar mine, central British Co-

- lumbia; *in* Porphyry Deposits of the Northwestern Cordillera of North America, T.G. Schroeter (ed.), Canadian Institute of Mining and Metallurgy, v. 46, p. 201–213.
- Drummond, A.D., Tennant, S.J. and Young, R.J. (1973): The inter-relationship of regional metamorphism, hydrothermal alteration and mineralization at the Gibraltar Mines copper deposit in B.C.; Canadian Institute of Mining, Metallurgy and Petroleum, Bulletin, v. 66, p. 48–55.
- Drummond, A.D., Sutherland Brown, A., Young, R.J. and Tennant, S.J. (1976): Gibraltar – regional metamorphism, mineralization, hydrothermal alteration and structural development; *in* Porphyry Deposits of the Canadian Cordillera, A. Sutherland Brown (ed.), Canadian Institute of Mining and Metallurgy, Special Volume 15, p. 195–205.
- Harding, B. (2012): The characterization of molybdenum mineralization at the Gibraltar mines Cu-Mo porphyry, central British Columbia; B.Sc. thesis, Queen’s University, 52 p.
- Jones, S. (2011): Technical report on the 357 million ton increase in mineral reserves at the Gibraltar mine, British Columbia, Canada: NI 43-101 report by Taseko Mines Limited; URL <<http://www.sedar.com/>> [November 2014]
- Oliver, J. (2007a): Pollyanna – Granite Lake geological and structural domains; unpublished internal report for Gibraltar Mines, 8 p.
- Oliver, J. (2007b): Gibraltar mines GIB East pit field trip transect; unpublished internal report for Gibraltar Mines, 14 p.
- Oliver, J. (2008): Geological map of Granite Lake pit; unpublished internal map for Gibraltar Mines.
- Oliver, J., Crozier, J., Kamionko, M. and Fleming, J. (2009): The Gibraltar mine, British Columbia. A billion tonne deep copper-molybdenum porphyry system: structural style, patterns of mineralization and rock alteration; *in* Association for Mineral Exploration British Columbia, 2009 Mineral Exploration Roundup, program with abstracts, p. 35–36.
- Schiarizza, P. (2014): Geological setting of the Granite Mountain batholith, host to the Gibraltar porphyry Cu-Mo deposit, south-central British Columbia; *in* Geological Fieldwork 2013, British Columbia Ministry of Energy and Mines, British Columbia Geological Survey, Paper 2014-1, p. 95–110, URL <[http://www.empr.gov.bc.ca/Mining/Geoscience/PublicationsCatalogue/Fieldwork/Documents/2013/06\\_Schiarizza.pdf](http://www.empr.gov.bc.ca/Mining/Geoscience/PublicationsCatalogue/Fieldwork/Documents/2013/06_Schiarizza.pdf)> [November 2014]
- Sutherland Brown, A. (1974): Gibraltar mine (93B-12, 13); *in* Geology, Exploration and Mining in British Columbia 1973, BC Ministry of Energy and Mines, BC Geological Survey, p. 299–318.
- Tipper, H.W. (1978): Northeastern part of Quesnel (93B) map-area, British Columbia; *in* Current Research, Part A, Geological Survey of Canada, Paper 78-1A, p. 67–68.
- van Straaten, B.I., Oliver, J., Crozier, J. and Goodhue, L. (2013): A summary of the Gibraltar porphyry copper-molybdenum deposit, south-central British Columbia, Canada; *in* Porphyry systems of central and southern BC: Prince George to Princeton, J. Logan and T. G. Schroeter (ed.), Society of Economic Geologists Field Trip Guidebook, v. 43, p. 55–66.



# Magnetite as a Porphyry Copper Indicator Mineral in Till: a Test Using the Mount Polley Porphyry Copper-Gold Deposit, South-Central British Columbia (NTS 093A)

L.K. Pisiak, School of Earth and Ocean Sciences, University of Victoria, Victoria, BC, laurakay@mymts.net

D. Canil, School of Earth and Ocean Sciences, University of Victoria, Victoria, BC

C. Grondahl, School of Earth and Ocean Sciences, University of Victoria, Victoria, BC

A. Plouffe, Natural Resources Canada, Geological Survey of Canada, Ottawa, ON

T. Ferbey, British Columbia Geological Survey, British Columbia Ministry of Energy and Mines, Victoria, BC

R.G. Anderson, Natural Resources Canada, Geological Survey of Canada-Pacific, Vancouver, BC

---

Pisiak, L.K., Canil, D., Grondahl, C., Plouffe, A., Ferbey, T. and Anderson, R.G. (2015): Magnetite as a porphyry copper indicator mineral in till: a test using the Mount Polley porphyry copper-gold deposit, south-central British Columbia (NTS 093A); in Geoscience BC Summary of Activities 2014, Geoscience BC, Report 2015-1, p. 141–150.

## Introduction

Magnetite ( $\text{Fe}_3\text{O}_4$ ) is a common oxide mineral in a wide variety of igneous and metamorphic rocks, as well as in some ore-related hydrothermal systems. The composition of magnetite may be indicative of its environment including such factors as temperature, pressure, magma or fluid composition, and oxygen and sulphur fugacities (e.g., Buddington and Lindsley, 1964; Frost, 1991). Previous studies have demonstrated the utility of magnetite as a petrogenetic indicator because it can incorporate a wide variety of substituting cations such as Mn, Ni, Co, Zn, Al, Cr, Ti, V and Ga (e.g., Irvine, 1965, 1967; Dick and Bullen, 1984; Roeder, 1994; Barnes and Roeder, 2001). These studies predominantly focus on end-member compositions of spinel from igneous systems. More recent work has documented the variation in the trace-element composition of hydrothermal magnetite (Beaudoin and Dupuis, 2010; Nadoll et al., 2012, 2014; Dare et al., 2014).

In the Canadian Cordillera, Mesozoic calcalkaline and alkaline intrusive igneous rocks that are prospective for porphyry deposits may be overlain by a thick glacial sediment cover. Mineral exploration for porphyry deposits often utilizes bulk geochemical analysis of soil and stream sediments but results can be ambiguous due to the varied behaviour of ore-related elements during weathering and surface runoff. Therefore, a more robust geochemical indicator is required that would provide a direct vector to the actual bedrock source. Basal till represents a direct sample of the bedrock, which can be linked back to source via sediment

dispersal trains that are parallel to the ice-flow direction (Whiting and Faure, 1991; Levson, 2001).

The ubiquity of magnetite in porphyry systems and its resistance to weathering and glacial transport suggest that it may be a useful pathfinder mineral in basal till (Grigsby, 1990; Whiting and Faure, 1991). Ultimately, magnetite in till would provide a unique exploration vector for identifying mineralized porphyry systems up-ice and efficiently distinguish them from the vast number of barren felsic igneous intrusions in the Cordillera. To this end, a ground-truth test was performed using magnetite as an indicator mineral in till from the area surrounding the Mount Polley porphyry Cu-Au deposit. The purpose of the test was to determine if its geochemical signature can be applied to other locations in British Columbia without known porphyry deposits.

## Geological Setting

The Mount Polley porphyry Cu-Au deposit occurs in the Quesnel terrane of the Intermontane Belt, which comprises Late Triassic to Early Jurassic volcanic arc rocks, in south-central BC (Figure 1). The Mount Polley intrusive complex is described by Logan and Mihalynuk (2005) as a subvolcanic composite stock, 4 by 5.5 km in size, composed of fine-grained porphyritic diorite and monzonite with dikes of plagioclase porphyry and syenite. The Bootjack stock, a coarse-grained syenite pluton, also occurs in the area but is separated from the Mount Polley stock by a 1 km wide belt of metavolcanic rocks. Porphyry Cu-Au mineralization in Quesnellia arc rocks occurs in several of these high level alkalic intrusive complexes, such as Mount Polley where mineralization is concentrated in various types of hydrothermal breccias (Logan and Mihalynuk, 2005).

As part of the Natural Resources of Canada's Targeted Geoscience Initiative 4 (TGI-4) program, the Geological

---

**Keywords:** magnetite, mineral chemistry, exploration, indicator mineral, till provenance, hydrothermal, porphyry deposits

This publication is also available, free of charge, as colour digital files in Adobe Acrobat® PDF format from the Geoscience BC website: <http://www.geosciencebc.com/s/DataReleases.asp>.

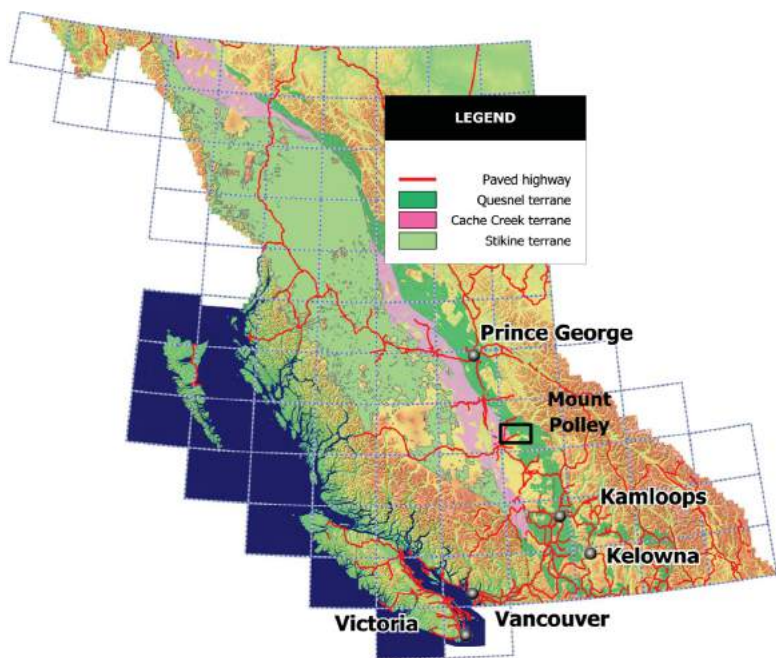


**Figure 1.** Location map of the Mount Polley study area in south-central British Columbia (courtesy of J.M. Logan).

Survey of Canada and the BC Geological Survey conducted a till sampling survey between 2011 and 2013 in the vicinity of the Mount Polley deposit, collecting 74 till samples covering an area of approximately 700 km<sup>2</sup> (Figure 2; Anderson et al., 2012; Plouffe et al., 2013b; Ferbey et al., 2014). Mineralized rocks were also sampled from bedrock exposed to recent glaciation and ice-flow indicators were measured from outcrop, allowing for reconstruction of the glacial history of the area. The dominant ice-flow direction in the Mount Polley area, which occurred at glacial maximum, was to the northwest and was preceded by ice flow to the west-southwest during an ice build-up stage (Hashmi et al., 2014).

## Methodology

### Sample Preparation

Large till samples (~10 kg) were submitted for heavy mineral separation. Bulk till samples were wet sieved to a <2 mm size fraction, which was first concentrated by density on a shaking table. The heavy minerals recovered on the shaking table were further concentrated in heavy liquids (methylene iodide) and sieved into three size fractions: 1–2 mm, 0.5–1 mm and 0.25–0.5 mm. Magnetite grains were separated from these heavy mineral concentrates by hand magnet and, for each sample, approximately 100 to 125 grains from the 0.25–0.5 mm fraction were randomly selected, mounted in epoxy and polished for analysis (Figure 3). Chips of bedrock samples from Mount Polley were also similarly prepared. Reflected-light microscopy was used to confirm mineral identification and visually assess

internal textures of individual grains prior to chemical analysis. Magnetite grains with appreciable alteration, fracturing or with a significant number of inclusions were excluded from analysis.

### Scanning Electron Microscope

A subset of magnetite grains were examined with a Hitachi S-4800 field emission scanning electron microscope (SEM) at the University of Victoria (Victoria, BC) using an accelerating voltage of 16 kV and emission current of 20 nA. This method allows the user to readily identify different exsolution and alteration phases, as well as mineral inclusions present in some grains.

### Electron Microprobe

Fifty magnetite grains per till sample were selected for elemental analysis. Concentrations of Al, Si, Ca, Ti, V, Cr, Mn, Fe and Ni were determined with a CAMECA SX 50 electron probe micro analyzer at the University of British Columbia (Vancouver, BC) using a 5 µm beam size, accelerating voltage of 25 kV and beam current of 20 nA. The Fe concentration in each magnetite grain is used as an internal standard for laser-ablation inductively coupled plasma–mass spectrometry (LA-ICP-MS) trace-element analysis (see below).

### Laser-Ablation Inductively Coupled Plasma–Mass Spectrometry

Analysis of Sc, Ti, V, Mn, Cr, Co, Ni, Cu, Zn, Ga, Nb, Mo, Sn, Ta and W in magnetite was performed by LA-ICP-MS at the University of Victoria using a 213 nm neodymium:yttrium-aluminum-garnet (Nd:YAG) ultraviolet laser operating at 50–55 Hz and interfaced to a Thermo Scientific XSERIES 2 Quadrupole ICP-MS. Spot and raster ablation methods were used with a beam size of 25–40 µm depending on grain size and the internal texture present. National Institute of Standards and Technology standard reference material glasses were used for standardization with <sup>57</sup>Fe selected as the internal standard. Analyses showing apparent contamination in their spectra (e.g., by inclusions) were edited to remove contaminated sections, or were discarded where editing was not feasible.

### Petrography

Petrographic analysis using reflected light microscopy identified a variety of habits, textures, inclusions and alteration types in magnetite from till (Figure 4). In general, magnetite grains vary from round, anhedral shapes to euhedral octahedrons and cubo-octahedrons, each reflecting the degree of sediment transport. Grain quality is also highly

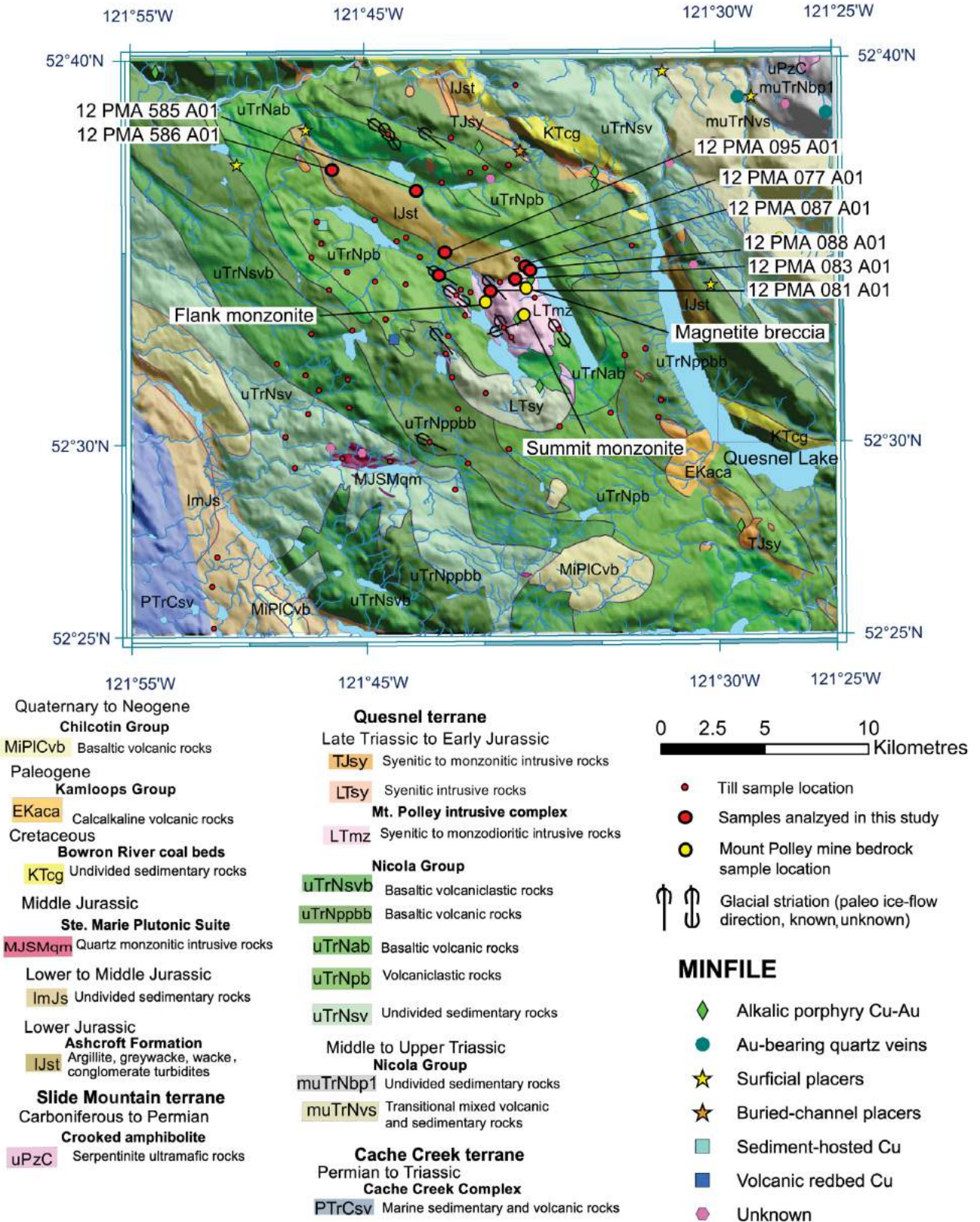
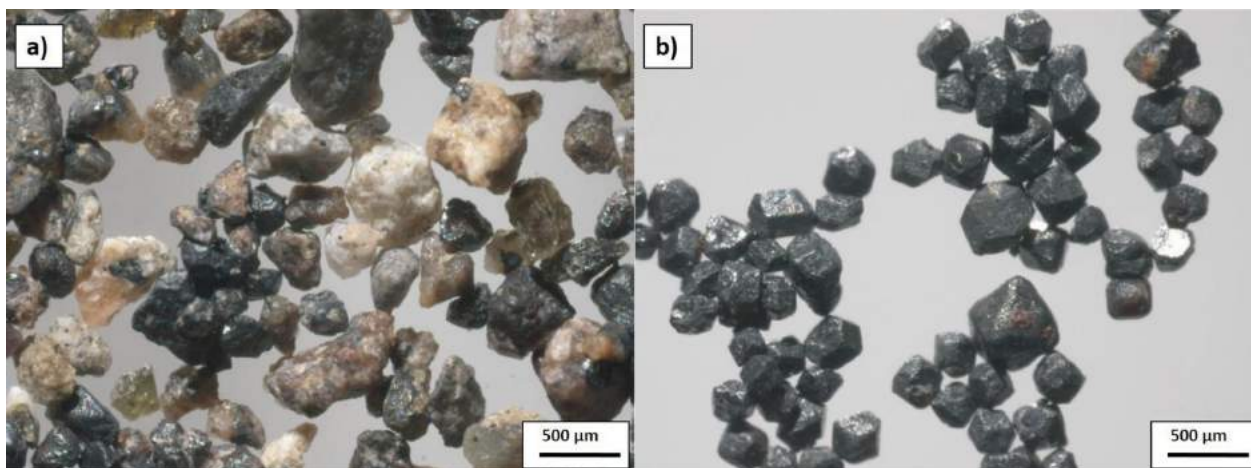
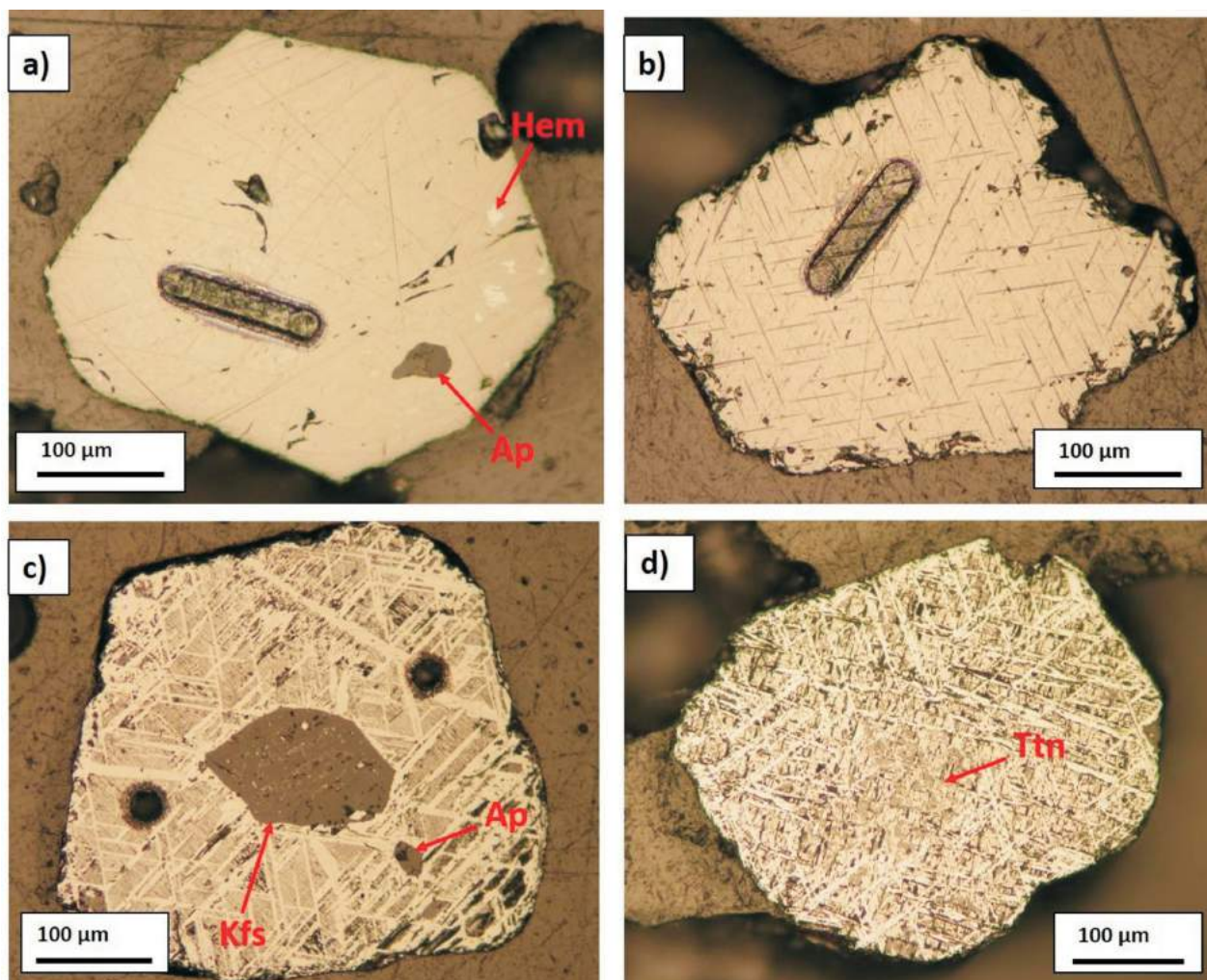


Figure 2. Geology of the Mount Polley area showing locations of till (red) and bedrock (yellow) samples used in this study (modified from Plouffe et al., 2013a), south-central British Columbia. MINFILE information from BC Geological Survey (2014).



**Figure 3.** a) Initial magnetic fraction of heavy mineral concentrates from till sample 12 PMA 586 A01, Mount Polley, south-central British Columbia; b) magnetite grain selection following sample picking.



**Figure 4.** Petrographic varieties of magnetite from till in reflected light at 20 times magnification (from Mount Polley, British Columbia). a) Euhedral, homogeneous grain, 385 µm across with 100 µm long laser-ablation raster, apatite (Ap) inclusion and minor hematite (Hem) alteration patches near rim (12 PMA 081 A01-C3). b) Subhedral, 520 µm grain with coarse trellis lamellae and 110 µm long laser-ablation raster (12 PMA 077 A01-D1). c) Subhedral, 425 µm grain with both coarse (white) and fine (grey) trellis lamellae, potassium feldspar (Kfs) and apatite (Ap) inclusions and two 30 µm laser-ablation spots (12 PMA 088 A01-D4). d) Subrounded, heterogeneous grain, 450 µm across with both coarse and fine trellis lamellae, as well as blebby titanite (Ttn) predominantly concentrated in the core (12 PMA 087 A01-G6).

variable as some magnetite grains are highly fractured or strongly pitted, whereas others are relatively free of pits and appear texturally homogeneous. Mineral inclusions occur in some magnetite grains—apatite is the most common, followed by quartz, potassium feldspar and chalcopyrite in decreasing abundance (Figure 4a, c).

Exsolution is a predominant textural feature commonly manifested as trellis-type lamellae (Figure 4b) or, to a much lesser degree, parallel or sandwich-type lamellae (Haggerty, 1991). These are observed at a variety of scales from submicroscopic to thick, dense lamellae that occur throughout the entire grain. Some magnetite contains more than one exsolution phase (e.g., Figure 4c, d). A significant example is in sample 12 PMA 095 A01-C11 where thick lamellae are composed of ulvöspinel ( $\text{Fe}_2\text{TiO}_4$ )  $\pm$  rutile ( $\text{TiO}_2$ ), whereas the interstitial thin trellis has been replaced by an unknown secondary Si-Al-Mg phase (Figure 5). The exsolution in magnetite occurs as a direct result of subsolidus oxidation during cooling, increasing in intensity as the degree of oxidation increases (Haggerty, 1991).

Alteration is not prevalent but can occur as hematite along magnetite grain boundaries, fractures and lamellae, as well as in discrete patches. Few grains are completely altered to hematite. A large proportion of magnetite also contains significant amounts of intergrown titanite, which occurs as blebs, irregular stringers and within lamellae (Figure 4d).

## Chemistry

Chemical analysis was completed for magnetites in eight till samples from various distances down-ice (northwest) from the Mount Polley deposit. Northwest also represents the dominant glacial transport direction of chalcopyrite grains in till from the Mount Polley mineralization (Hashmi

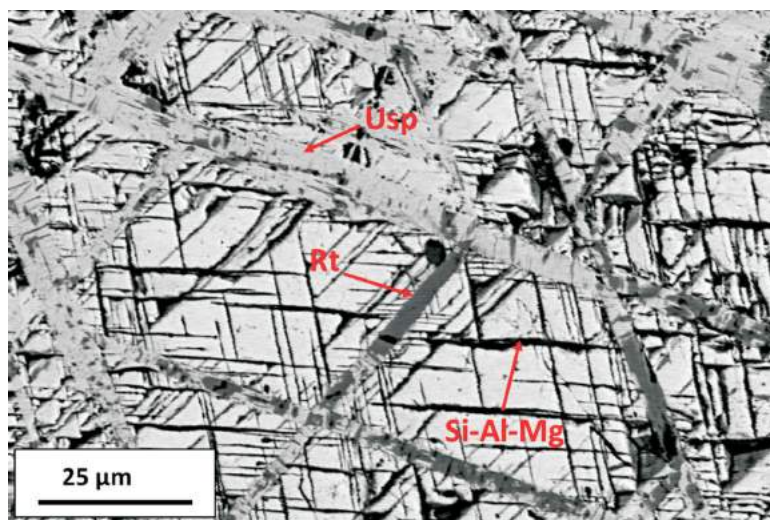


**Figure 5.** Back-scattered electron image of magnetite showing rutile (Rt) and coarse ulvöspinel (Usp) lamellae, and a Si-Al-Mg phase (possible alteration) along dark, fine trellis lamellae (12 PMA 095 A01-C11, Mount Polley, British Columbia).

et al., 2014). As expected, magnetite chemistry is highly variable reflecting the diverse bedrock sources of the till. In particular, titanium, which has strongly temperature-dependent substitution in magnetite (as a  $\text{Fe}_2\text{TiO}_4$  component), varies from 0.04 to 12 wt. % (Figure 6). The covariation of Ti with Ni/Cr was proposed by Dare et al. (2014) to discriminate between igneous and hydrothermal magnetite. In general, the proportion of magnetite grains in till with the hydrothermal signature increases with proximity to the deposit (Figure 6).

Cations that commonly substitute in magnetite, such as divalent Mg and Mn as well as trivalent Al and Cr, exhibit a wide range of values from a few hundred parts per million (ppm) to as much as 4 to 4.5 wt. % for Mg and Mn and up to 5 and 7.5 wt. % for Al and Cr, respectively. Other divalent cations vary from below detection limits to 2400 ppm for Ni, 1100 ppm for Cu and 500 ppm for Co; however, Zn can be concentrated up to 18 000 ppm. High valence elements (i.e., Sn, Mo, Nb, Ta), as well as Ga and Sc have low concentrations (<100 ppm).

A large proportion of grains have significantly high Si and Ca concentrations up to 4 and 5.5 wt. %, respectively. A positive correlation between Si and Ca is observed in a trend leading to uncommonly high cation sums in magnetite when calculated to three cation per four oxygen atoms stoichiometry (Figure 7).

## Discussion

### Distinguishing Hydrothermal Versus Igneous Magnetite

A fundamental goal of this study is to identify distinguishing characteristics of hydrothermal magnetite (associated to mineralization event) versus igneous magnetite (not associated to mineralization event) in till. Previous studies have shown the importance of integrating both petrography and chemical analysis in developing a general classification of magnetite provenance (e.g., Grigsby, 1990; Mücke, 2003; Bouzari et al., 2011). Those studies, however, focused on igneous magnetite with little or no data for magnetite precipitated directly from hydrothermal fluids.

Initial petrographic analysis of magnetite provides a preliminary evaluation of provenance prior to chemical analysis. For example, the presence of exsolution lamellae in magnetite can be interpreted as likely indicative of an igneous source, where any  $\text{Fe}_2\text{TiO}_4$  in solid solution with magnetite exsolves to ulvöspinel as a result of cooling and oxidation at magmatic temperatures (Buddington and Lindsley, 1964).

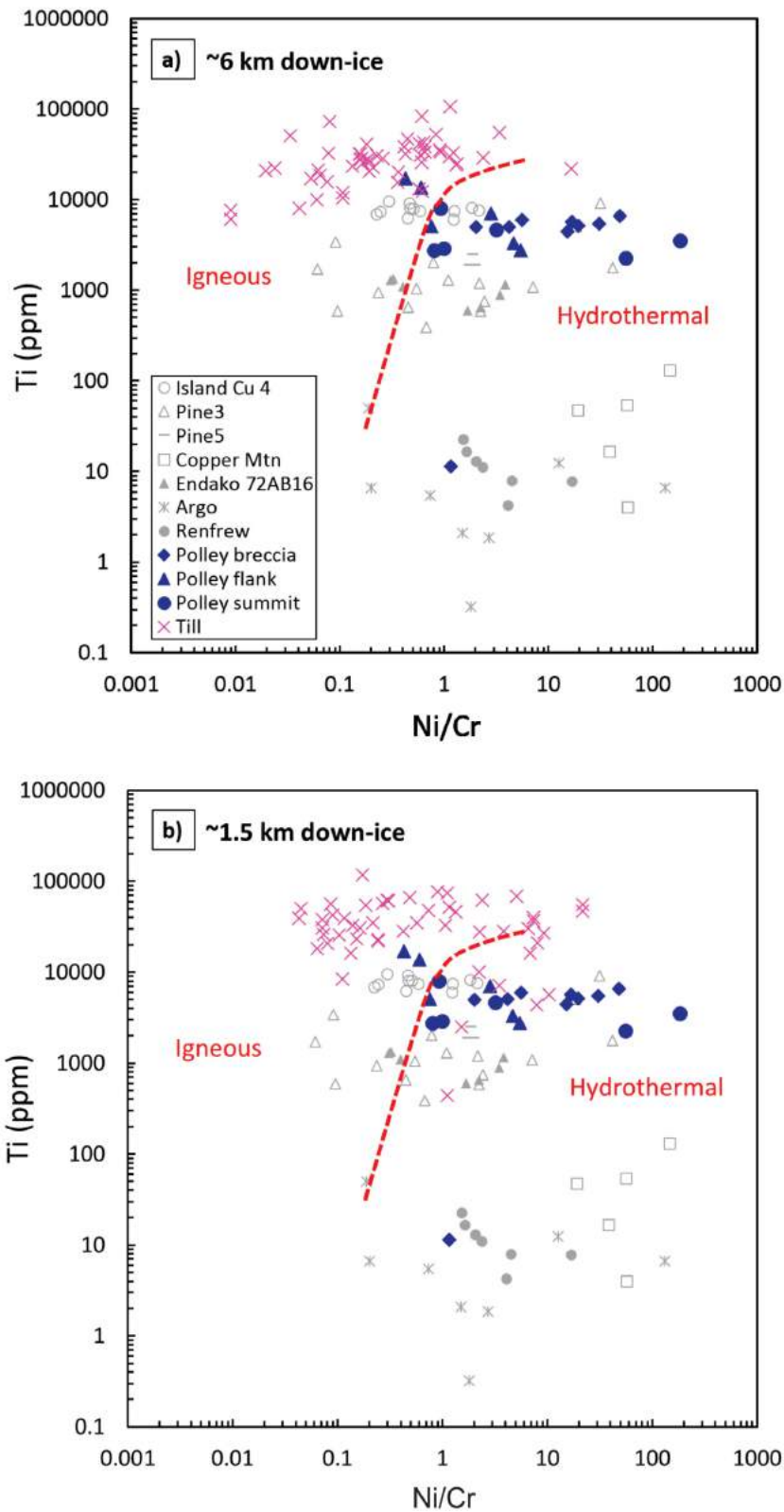


**Figure 6.** Concentrations of Ti (ppm) versus Ni/Cr in magnetite from till (pink X). Bedrock samples from Mount Polley (blue symbols) and various hydrothermal deposits in British Columbia (grey symbols) are also presented (Grondahl, 2014). **a)** Sample 12 PMA 585 A01 is located ~6 km down-ice from the Mount Polley deposit and **b)** sample 12 PMA 081 A01 is located ~1.5 km down-ice. Igneous and hydrothermal fields defined by Dare et al. (2014). Dashed line represents potential distinction of hydrothermal and igneous magnetite.

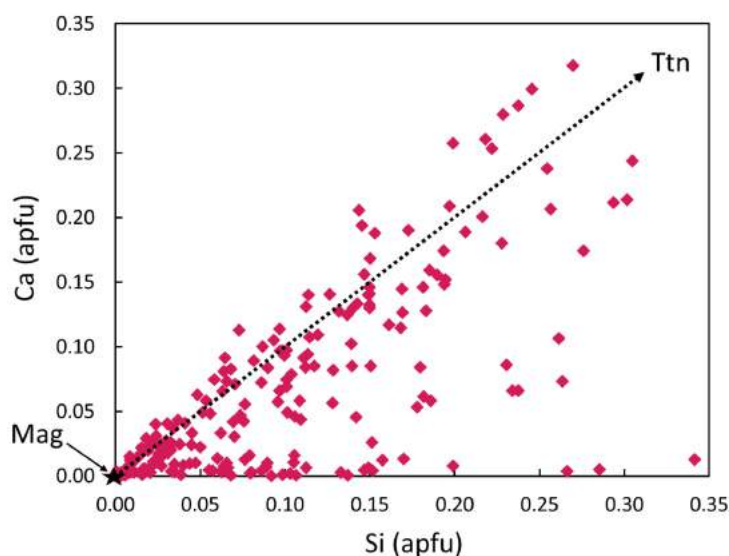


**Figure 7.** The Si and Ca contents in magnetite from till (Mount Polley, British Columbia) recalculated to atoms per formula unit (apfu), calculated assuming a three cation per four oxygen atoms stoichiometry. A positive correlation is consistent with mixing between magnetite (Mag) at the origin and titanite (Ttn), which contains one cation each Si and Ca (off axes). Several magnetite grains with high Si and low Ca may indicate some potential interference by quartz inclusions in these grains.

However, the absence of exsolution lamellae does not necessarily imply a non-igneous source since homogeneous magnetite can occur as phenocrysts in rapidly cooled volcanic rocks (Mücke, 2003) or as an accessory phase in felsic plutonic rocks, where the Ti content of magnetite is too low to exsolve (Grigsby, 1990). Thus, the integration of chemical analysis with petrography is essential.

A more recent chemical discrimination diagram suggested by Dare et al. (2014) provides a simple division of hydrothermal and igneous magnetite based on Ni/Cr and Ti concentrations. The general trend of increasing proportion of hydrothermal magnetite grains with decreasing distance from the deposit is favourable; however, the Ni/Cr versus Ti classification diagram fails to distinguish hydrothermal magnetite for various porphyry and skarn deposits in BC (Figure 6). Thus, consistent and accurate chemical discriminants for hydrothermal magnetite provenance have yet to be determined.

Anomalously high Si and Ca contents in some magnetite was also discovered by Dare et al. (2014), who attributed these values to substitution within the structure of hydrothermal magnetite. The results of this present study do not support this interpretation but instead suggest that high Si and Ca may be related to submicroscopic inclusions or reactions upon cooling to form titanite (Figure 4d). Such magnetites in this study appeared ‘clean’ in reflected light but show a submicroscopic turbid appearance in SEM images. This is consistent with the correlation of Si and Ca values along a mixing line between magnetite and titanite

(Figure 7) and is observed in a large proportion of magnetite grains. Further characterization by SEM of this phenomenon is required.

### Magnetite as an Indicator Mineral

The trace-element signature of ore-related magnetite has been determined in a parallel study by Grondahl (2014) for Mount Polley and other porphyry deposits in BC. Those results indicate that individual ore deposits have unique trace-element signatures in hydrothermal magnetite that differ from magnetite in igneous rocks. Figure 8, for example, illustrates the potential for Ti and Sn concentrations in ore-magnetite to discriminate between individual deposits and possibly define a hydrothermal magnetite field for porphyry deposits in BC.

As a ground-truth test, magnetite composition as a function of distance to the Mount Polley deposit was examined. It was found that the proportion of magnetite grains with the Mount Polley chemical signature increases with proximity to the deposit and that the ore deposit ‘signal’ is detectable only to a maximum distance of 6 km down-ice from Mount Polley (Figure 8). Magnetite in till from greater distances down-ice (northwest) show no overlap with the Mount Polley data (not shown). This relationship between chemistry and proximity to deposit is similar to the geochemical dispersal train typically found in glaciated terrain, and could potentially be a valuable tool in exploring for these deposits.

### Future Work

In principle, the method of using magnetite chemistry in till samples down-ice from the Mount Polley deposit as a pathfinder to the porphyry source is successful, however, this is complicated by the variety in composition of hydrothermal magnetite from several porphyry deposits in British Columbia. The implication of possible titanite exsolution on the chemistry of magnetite and its provenance also needs to be reconciled by further work. An empirical approach has been used to evaluate the similarity between Mount Polley ore magnetite and magnetite grains in till, but there also exists the potential to employ a more rigorous assessment of the magnetite trace-element concentrations (e.g., discriminant functions or multivariate analysis). Regardless, a method of more quantitative scoring needs to be developed in order to optimize the use of magnetite in basal till as an exploration tool.

### Acknowledgments

The authors would like to thank J. Spence at the University of Victoria and E. Czech at the University of British Colum-

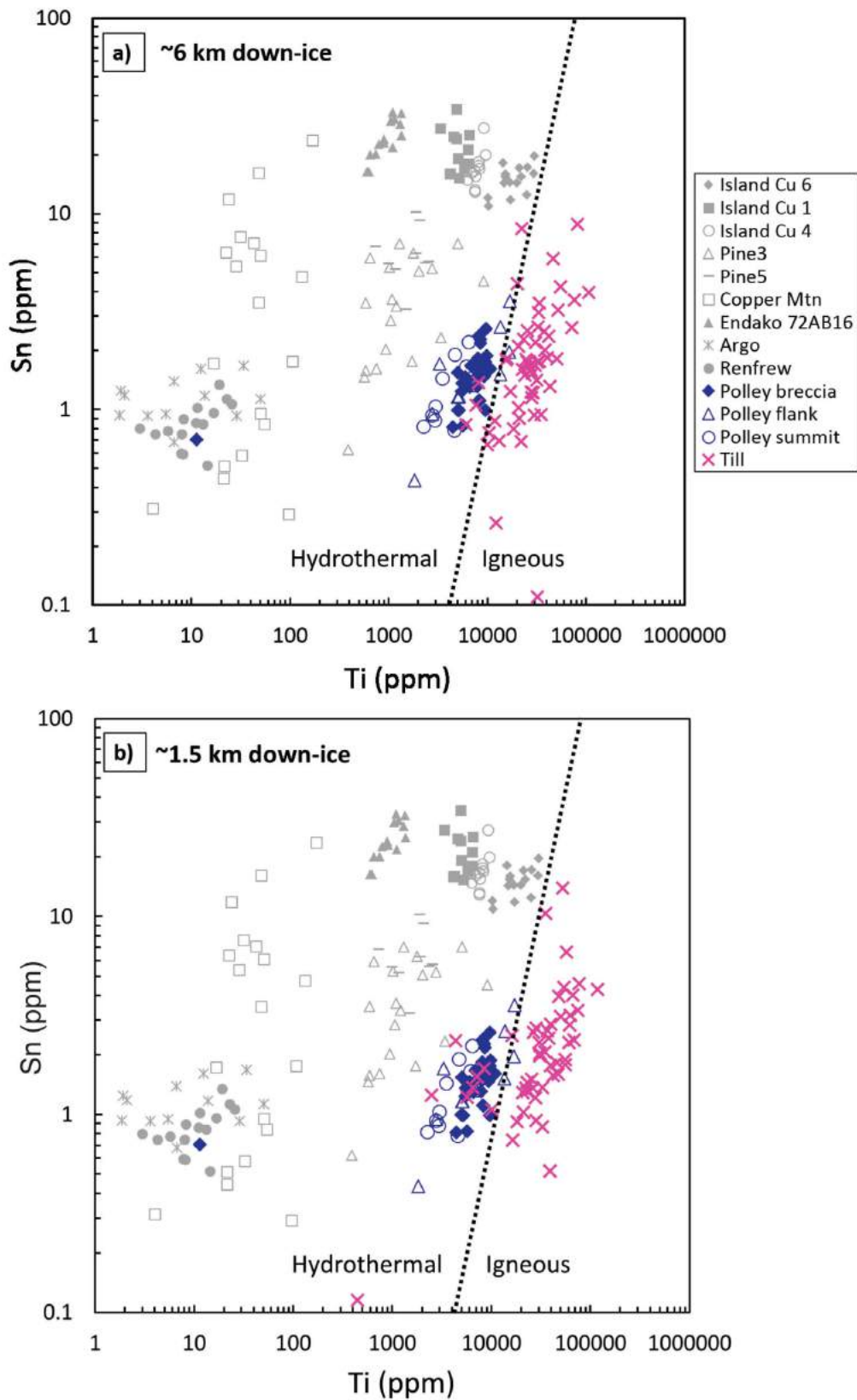


**Figure 8.** Concentrations of Sn versus Ti (ppm) in magnetite from till (pink X). Mount Polley ore magnetite (blue symbols) and various hydrothermal deposits in British Columbia (grey symbols) are also presented (Grondahl, 2014). **a)** Sample 12 PMA 585 A01 located ~6 km down-ice from the Mount Polley deposit and **b)** sample 12 PMA 081 A01 located ~1.5 km down-ice. Dashed line represents potential distinction of hydrothermal and igneous magnetite.

bia for analytical assistance, as well as R. D'Souza for his constructive review and comments on this paper. This research was funded by Society of Economic Geologists and Geoscience BC scholarships to L. Pisiak, and Natural Sciences and Engineering Research Council of Canada (NSERC) and BC Ministry of Energy and Mines grants to D. Canil. Till sampling was funded by Natural Resources Canada's Targeted Geoscience Initiative 4 program. Heavy mineral and magnetite separations from the till samples were completed by Overburden Drilling Limited (Nepean, Ontario).

Natural Resources Canada, Earth Sciences Sector contribution 20140335

## References

- Anderson, R.G., Plouffe, A., Ferbey, T. and Dunn, C.E. (2012): The search for surficial expressions of buried Cordilleran porphyry deposits: background and progress in a new TGI-4 activity in the southern Canadian Cordillera; Geological Survey of Canada, Current Research 2012-7, 15 p.
- Barnes, S.J. and Roeder, P.L. (2001): The range of spinel compositions in terrestrial mafic and ultramafic rocks; *Journal of Petrology*, v. 42, no. 12, p. 2279–2302.
- BC Geological Survey (2014): MINFILE BC mineral deposits database; BC Ministry of Energy and Mines, BC Geological Survey, URL <<http://minfile.ca/>> [October 2014].
- Beaudoin, G. and Dupuis, C. (2010): Iron-oxide trace element fingerprinting of mineral deposit types; *in* Exploring for Iron Oxide Copper-Gold Deposits: Canada and Global Analogues, L. Corriveau and H. Mumin (ed.), Geological Association of Canada, Short Course, v. 20, p. 111–126.
- Bouzari, F., Hart, C.J.R., Barker, S. and Bissig, T. (2011): Porphyry indicator minerals (PIMS): a new exploration tool for concealed deposits in south-central British Columbia; Geoscience BC, Report 2011-17, 31 p.
- Buddington, A.F. and Lindsley, D.H. (1964): Iron-titanium oxide minerals and synthetic equivalents; *Journal of Petrology*, v. 5, no. 2, p. 310–357.
- Dare, S.A.S., Barnes, S.-J., Beaudoin, G., Méric, J., Boutroy, E. and Potvin-Doucet, C. (2014): Trace elements in magnetite as petrogenetic indicators; *Mineralium Deposita*, v. 49, no. 7, p. 785–796.
- Dick, H.J.B. and Bullen, T. (1984): Chromian spinel as a petrogenetic indicator in abyssal and alpine-type peridotites and spatially associated lavas; *Contributions to Mineralogy and Petrology*, v. 86, p. 54–76.
- Ferbey, T., Plouffe, A. and Anderson, R.G. (2014): An integrated approach to search for buried porphyry-style mineralization in central British Columbia using geochemistry and mineralogy: a TGI-4 project; Geological Survey of Canada, Current Research 2014-2, 12 p.
- Frost, B.R. (1991): Magnetic petrology: factors that control the occurrence of magnetite in crustal rocks; *in* Oxide Minerals: Petrologic and Magnetic Significance, D.H. Lindsley (ed.), Mineralogical Society of America, Reviews in Mineralogy, v. 25, p. 489–509.
- Grigsby, J.D. (1990): Detrital magnetite as a provenance indicator; *Journal of Sedimentary Petrology*, v. 60, no. 6, p. 940–951.
- Grondahl, C. (2014): Trace elements in magnetite from porphyry deposits: applications in mineral exploration; B.Sc. thesis, University of Victoria, 83 p.
- Haggerty, S.E. (1991): Oxide textures – a mini-atlas; *in* Oxide Minerals: Petrologic and Magnetic Significance, D.H. Lindsley (ed.), Mineralogical Society of America, Reviews in Mineralogy, v. 25, p. 129–219.
- Hashmi, S., Ward, B.C., Plouffe, A., Ferbey, T. and Leybourne, M.I. (2014): Geochemical and mineralogical dispersal in till from the Mount Polley Cu-Au porphyry deposit, central British Columbia, Canada; Geological Survey of Canada, Open File 7589, 1 sheet.
- Irvine, T.N. (1965): Chromian spinel as a petrogenetic indicator – part 1: theory; *Canadian Journal of Earth Sciences*, v. 2, p. 648–672.
- Irvine, T.N. (1967): Chromian spinel as a petrogenetic indicator – part 2: petrologic application; *Canadian Journal of Earth Sciences*, v. 4, p. 71–103.
- Levson, V.M. (2001): Regional till geochemical surveys in the Canadian Cordillera: sample media, methods and anomaly evaluation; *in* Drift Exploration in Glaciated Terrain, M.B. McClenaghan, P.T. Bobrowsky, G.E.M. Hall and S.J. Cook (ed.), Geological Society, Special Publication, v. 85, p. 45–68.
- Logan, J.M. and Mihalynuk, M.G. (2005): Regional geology and setting of the Cariboo, Bell, Springer and Northeast porphyry Cu-Au zones at Mount Polley, south-central British Columbia; *in* Geological Fieldwork 2004, BC Ministry of Energy and Mines, BC Geological Survey, Paper 2005-1, p. 249–270.
- Mücke, A. (2003): Magnetite, ilmenite and ulvite in rocks and ore deposits: petrography, microprobe analyses and genetic implications; *Mineralogy and Petrology*, v. 77, p. 215–234.
- Nadoll, P., Angerer, T., Mauk, J.L., French, D. and Walshe, J. (2014): The chemistry of hydrothermal magnetite: a review; *Ore Geology Reviews*, v. 61, p. 1–32.
- Nadoll, P., Mauk, J.L., Hayes, T.S., Koenig, A.E. and Box, S.E. (2012): Geochemistry of magnetite from hydrothermal ore deposits and host rocks of the Mesoproterozoic Belt Supergroup, United States; *Economic Geology*, v. 107, p. 1275–1292.
- Plouffe, A., Ferbey, T., Anderson, R.G., Hashmi, S. and Ward, B.C. (2013a): New TGI-4 till geochemistry and mineralogy results near the Highland Valley, Gibraltar, and Mount Polley mines, and Woodjam District: an aid to search for buried porphyry deposits; Geological Survey of Canada, Open File 7473, 58 p.
- Plouffe, A., Ferbey, T., Anderson, R.G., Hashmi, S., Ward, B.C. and Sacco, D.A. (2013b): The use of till geochemistry and mineralogy to explore for buried porphyry deposits in the Cordillera – preliminary results from a TGI-4 intrusion-related ore systems project; Geological Survey of Canada, Open File 7367, 1 sheet.
- Roeder, P.L. (1994): Chromite: from the fiery rain of chondrules to the Kilauea Iki lava lake; *The Canadian Mineralogist*, v. 32, no. 4, p. 729–746.
- Whiting, K.S. and Faure, G. (1991): Transport of magnetite and ilmenite by glaciers in the Adirondack Mountains of New York; *Journal of Geology*, v. 99, p. 482–492.



# Uranium-Lead Age Constraints and Structural Analysis for the Ruddock Creek Zinc-Lead Deposit: Insight into the Tectonic Evolution of the Neoproterozoic Metalliferous Windermere Supergroup, Northern Monashee Mountains, Southern British Columbia (NTS 082M)

L.M. Theny, Simon Fraser University, Burnaby, BC, ltheny@sfu.ca

H.D. Gibson, Simon Fraser University, Burnaby, BC

J.L. Crowley, Boise State University, Boise, ID

---

Theny, L.M., Gibson, H.D. and Crowley, J.L. (2015): Uranium-lead age constraints and structural analysis for the Ruddock Creek zinc-lead deposit: insight into the tectonic evolution of the Neoproterozoic metalliferous Windermere Supergroup, northern Monashee Mountains, southern British Columbia (NTS 082M); *in* Geoscience BC Summary of Activities 2014, Geoscience BC, Report 2015-1, p. 151–164.

## Introduction

The Ruddock Creek property (Figure 1) is situated within the Windermere Supergroup of the northern Monashee Mountains of British Columbia. Structurally, the Ruddock Creek property is interpreted to reside within the base of the Selkirk allochthon, in the immediate hanging wall of the Monashee décollement, a crustal-scale, thrust-sense ductile shear zone. Crustal thickening associated with poly-phase deformation involved at least three episodes of superposed folding of rocks in the region and two prograde metamorphic events (Fyles, 1970; Scammell and Brown, 1990; Scammell, 1993; Höy, 2001). At Ruddock Creek, Fyles (1970) identified three phases of ductile deformation. The first phase of folding is interpreted to coincide with development of Early to Middle Jurassic southwest-vergent fold nappes that dominate the macroscopic structure of the southern Omineca Belt (Brown et al., 1986; Brown and Lane, 1988; Scammell, 1993; Figure 2a). At the property and outcrop scale, this first phase of folding is manifest as rootless isoclinal recumbent folds (Figure 2a). The second and third phase of folding are interpreted to have developed during Early Cretaceous northeast-vergent deformation (Scammell, 1993). Second phase folds ( $F_2$ ) are tight to isoclinal overturned toward the northeast (Figure 2b) and are refolded by coaxial third phase folds that are more open and upright (Figure 2c). The final phase of deformation is related to late brittle faulting (Figure 2d).

The lithological units that occur throughout the area include: quartzite, pelitic and semipelitic schist, quartz-feldspar psammite, calcsilicate gneiss and marble. Nepheline-

syenite gneiss and syenite gneiss occur as concordant layers within the calcsilicate gneiss. Pegmatite and granitoid intrusions account for approximately 50% of the overall outcrop (Fyles, 1970; Scammell, 1993; Höy, 2001). The metasedimentary rocks are thought to belong to the Windermere Supergroup (Scammell, 1993), which is an important stratigraphic succession in the North American Cordillera interpreted to have been originally deposited along the rifted western margin of Laurentia during Neoproterozoic time (Gabrielse, 1972; Stewart, 1972, 1976; Burchfield and Davis, 1975; Stewart and Suczek, 1977; Monger and Price, 1979; Eisbacher, 1981; Scammell and Brown, 1990; Ross, 1991). However, the age of the rocks that host the Ruddock Creek deposit and their stratigraphic position within the Windermere Supergroup are not well constrained. Estimates based mainly on lithological correlations within the Kootenay terrane and North American rocks to the east range from Mesoproterozoic to Paleozoic (Scammell, 1993).

During the Neoproterozoic, the horst and graben topography along the rifted western Laurentian margin controlled the sedimentary facies of the Windermere Supergroup and the potential formation of sedimentary exhalative (SEDEX) deposits (Goodfellow and Lydon, 2007; Lund, 2008). For instance, reactivation of faults along the irregular horst and graben topography may have provided a conduit system for the auriferous hydrothermal fluids driven by deeper seated magmatism, which is syngenetic with sedimentation (McMechan, 2012). The Ruddock Creek deposit is thought to represent one of these rift-related SEDEX deposits hosted within the Windermere Supergroup (Höy, 2001; Simpson and Miller-Tait, 2012).

Throughout the Canadian Cordillera, the temporal and spatial distribution of rift-related SEDEX deposits defines major metallogenic periods (MacIntyre, 1991). A major metallogenic event is associated with continued Early to Middle

---

**Keywords:** *U-Pb geochronology, Windermere Supergroup, SEDEX deposit, Cordilleran tectonics*

*This publication is also available, free of charge, as colour digital files in Adobe Acrobat® PDF format from the Geoscience BC website: <http://www.geosciencebc.com/s/DataReleases.asp>.*

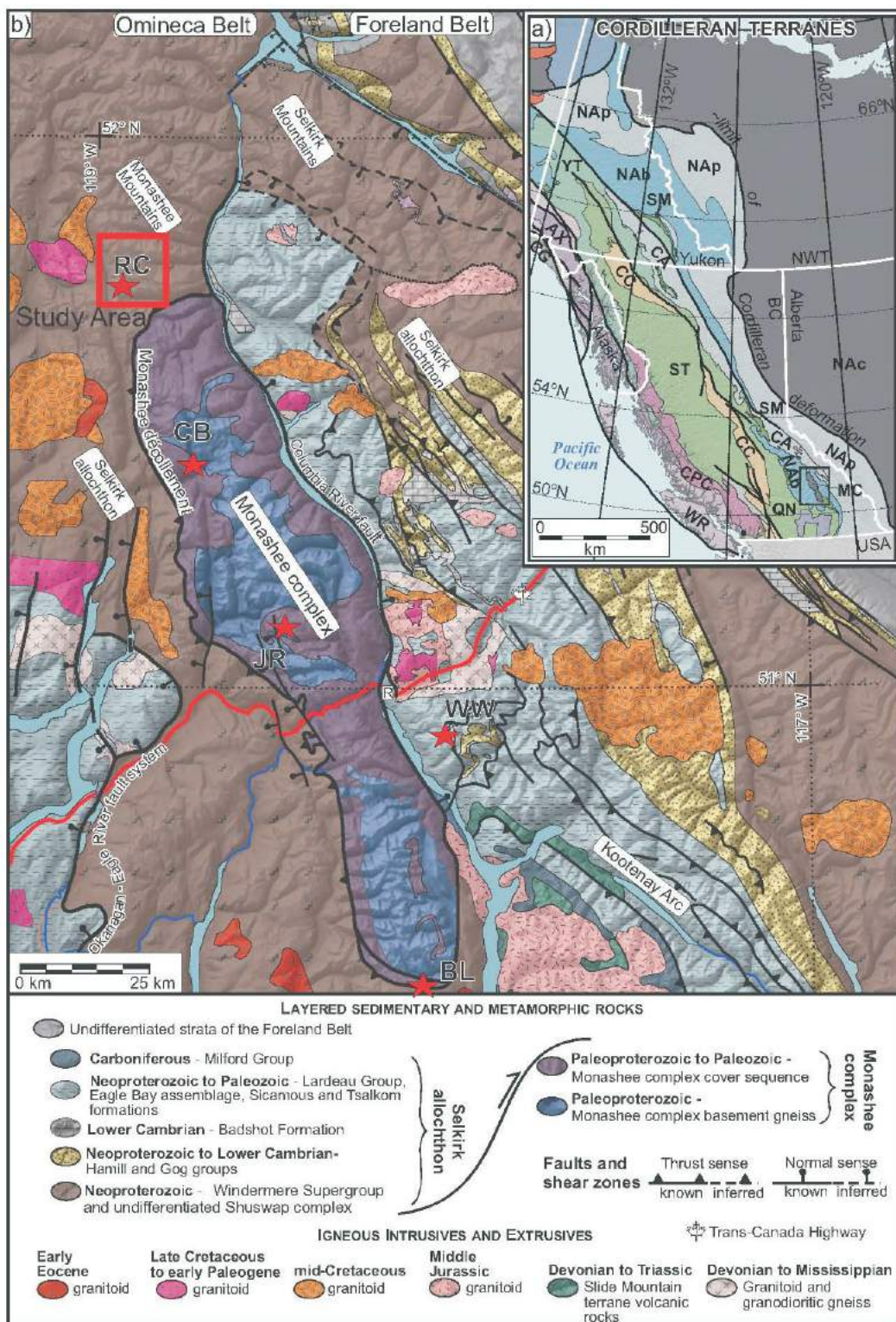


**Figure 1.** Regional geology of the southern Omineca Belt. **a)** Cordilleran terrane map (after Colpron and Nelson, 2011). Terranes: AX, Alexander; CA, Cassiar; CC, Cache Creek; CG, Chugach; CPC, Coast plutonic complex; MC, Monashee complex; NAb, North American basinal; NAc, North American craton and cover; NAP, North American platform; QN, Quesnellia; SM, Slide Mountain; ST, Stikinia; YT, Yukon-Tanana; WR, Wrangellia. Location of tectonic assemblage map indicated by the black box. **b)** Tectonic assemblage map, southeastern Omineca Belt, southern British Columbia (after Wheeler and McFeely, 1991; Gibson et al., 2008), showing lithological units of autochthonous Monashee complex (North American basement) and overlying Selkirk allochthon. Location of study area indicated by the red box. Red stars indicate location of major Pb-Zn deposits in the region: BL, Big Ledge; CB, Cottonbelt; JR, Jordan River; RC, Ruddock Creek (this study; see Figure 2); WW, Wigwam. Town: R, Revelstoke.

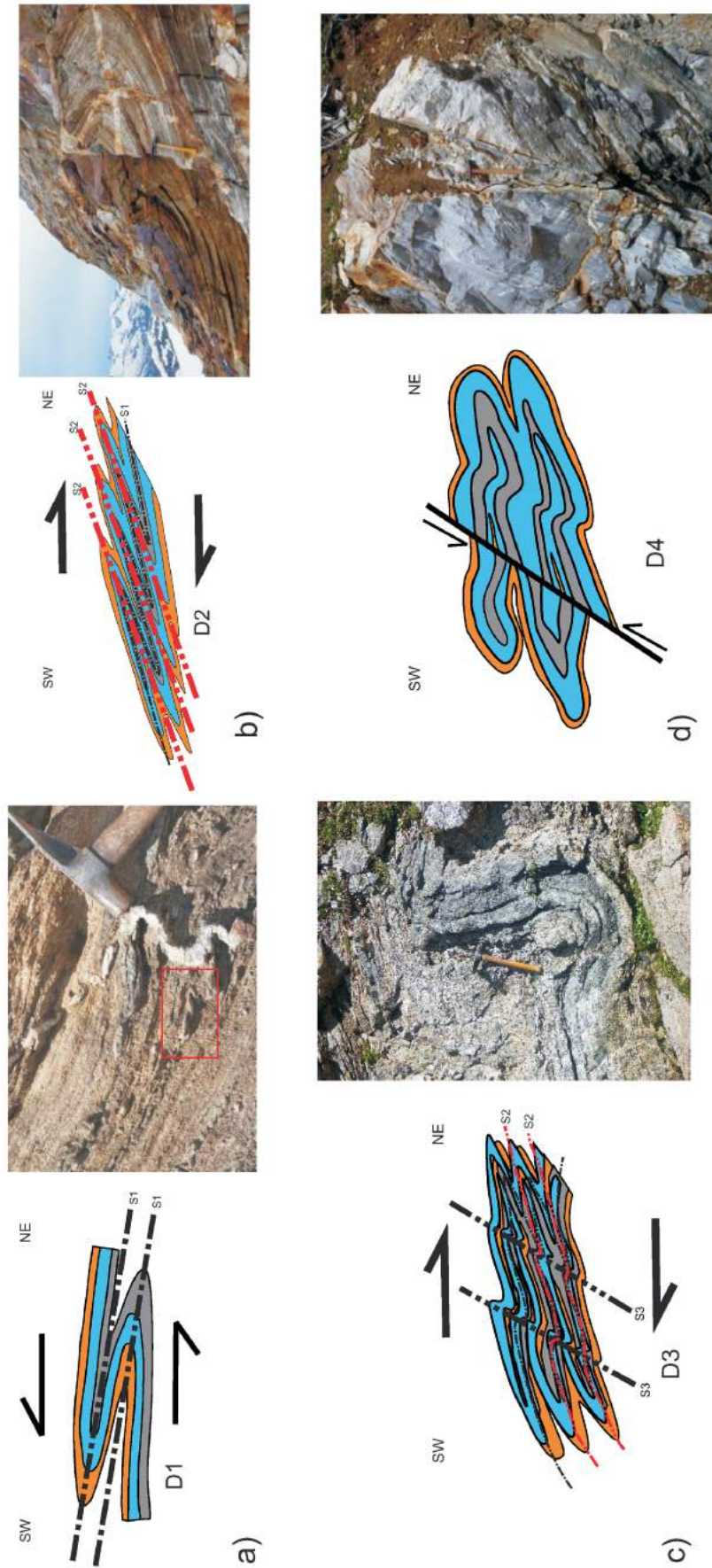


**Figure 2.** Schematic representation of deformation events that have affected the Ruddock Creek deposit, southern British Columbia. **a)** First phase of deformation ( $D_1$ ), include southwest-vergent kilometre-scale nappe folds ( $F_1$ ). The photo shows relict  $F_1$  folds observed at outcrop scale preserved as rootless folds in the penetrative  $S_2$  foliation. **b)** Second phase of deformation ( $D_2$ ), characterized by overturned northeast-vergent isoclinal folds (also shown in photo) that are axial planar to the  $S_2$  transposition foliation. **c)** The third phase of deformation ( $D_3$ ) refolds  $F_2$  folds and  $S_2$  foliation into more open, northeast-vergent folds as seen in the photo. **d)** The fourth phase of deformation ( $D_4$ ) consists of late brittle faults with minor observable offset (metres to tens of metres) and fault block rotation as shown in the photo.

Cambrian rifting of the margin that resulted in a series of uplifted and topographically higher sections that were capped by platformal sedimentary rocks. In the southern Canadian Cordillera, the Kootenay terrane and Monashee complex host shallow-water carbonate rocks and interbedded clastic rocks that underlie the strataform Pb-Zn deposits of the Kootenay Arc, and Shuswap and Adams plateaus (MacIntyre, 1991; Nelson, 1991).

The focus of this project is placed on 1) constraining the age of the Ruddock Creek deposit and evaluating the genetic relationship between several mineralized zones that comprise the deposit using detrital zircon U-Pb dating and Pb isotopic analysis, 2) refining the structural history through mapping at 1:10 000 scale, and 3) relating the deposit to the metallogenic evolution of the Canadian Cordillera.

### Regional Geology

The southern Omineca Belt (Figure 1) is the penetratively deformed metamorphic and plutonic hinterland to the Foreland (thrust-and-fold) Belt of the Canadian Cordillera, and is the result of long-lived convergence, primarily Mesozoic, between the North American craton and oceanic lithosphere, which resulted in collision between accreted terranes ferried in on the subducting oceanic crust and the westward underthrusting of the North American plate (Monger et al., 1982; Brown et al., 1992; Monger and Price, 2002; Gibson et al., 2008). The southern Omineca Belt includes North American basement and overlying strata and marks the transition between the ancient continental margin and accreted juvenile intra-oceanic rocks to the west (Monger et al., 1982). The study area lies within the parautochthonous Kootenay terrane of the southern Omineca Belt (Figure 1; Colpron and Price, 1995; Colpron et al., 2007), underlain by mainly clastic and carbonate rocks with lesser mafic volcanic rocks of the Neoproterozoic Windermere Supergroup (Scammell, 1993). In this region, the Kootenay terrane is situated within the Selkirk allochthon (Brown and Lane, 1988), which represents the hanging wall of the Monashee décollement, a crustal-scale northeast-vergent ductile shear zone (Read and Brown, 1981). The Monashee complex is the footwall of the Monashee décollement (Read and Brown, 1981), and is interpreted as a core complex that includes exposed Laurentian basement (Brown and Read, 1983; Journeay, 1986; Scammell and Brown, 1990; Armstrong et al., 1991; Crowley, 1999) in two tectonic windows, the Frenchman Cap dome and Thor Odin dome (Figure 1). The basement is mostly composed of granitic orthogneiss that ranges from 2270 to 1870 Ma (Armstrong et al., 1991; Crowley, 1997, 1999). The Monashee complex was tectonically exhumed during Eocene (55–45 Ma) extension, following a major orogenic episode of crustal thickening related to Mesozoic to earliest Paleogene (>60 Ma) compression (Monger et al., 1982; Brown et al., 1986; Parrish, 1995; Crowley, 1999;

Monger and Price, 2002; Gibson et al., 2008). The Monashee complex is bounded on the east by an early Paleogene (~55 Ma), east-dipping, normal fault referred to as the Columbia River fault (Read and Brown, 1981).

The regional geology of the Monashee Mountains, within which the Ruddock Creek deposit is found, has been divided into three crustal domains (Carr, 1991; Scammell, 1993) that are distinguished by distinct but associated tectonothermal histories. These domains were at different crustal levels within the Cordilleran orogen prior to Eocene extension (Carr and Brown, 1989; Carr, 1992). The domain that represents the deepest crustal level includes the Malton gneiss complex, Monashee complex and core of the Valhalla complex (Simony et al., 1980; Armstrong, 1982; Brown et al., 1986; Carr et al., 1987; Armstrong et al., 1991). The upper boundary is marked by crustal-scale thrust-sense shear zones, which include the Malton décollement, Monashee décollement and the Gwillim Creek shear zones (Simony et al., 1980; Read and Brown, 1981; Brown et al., 1986; Journeay, 1986; Carr et al., 1987).

The mid-crustal domain consists of the penetratively deformed amphibolite-facies rocks in the hanging wall of the aforementioned shear zones, and in the vicinity of the Monashee complex, the hanging wall rocks are part of the Selkirk allochthon within the Kootenay terrane (Read and Brown, 1981; Wheeler and McFeely, 1991; Scammell, 1993). The upper boundary of the mid-crustal domain is marked by east- and west-dipping crustal-scale normal faults (Read and Brown, 1981; Tempelman-Kluit and Parkinson, 1986; Parrish et al., 1988; Johnston and Brown, 1996; Brown et al., 2012). The upper crustal domain lies in the hanging wall of the normal faults and generally consists of lower metamorphic grade, polydeformed Upper Proterozoic to Jurassic sedimentary and mafic igneous rocks, and Eocene volcanic and sedimentary rocks (Carr, 1991).

### Previous Work and Geology of the Ruddock Creek Deposit

The earliest exploration and mapping of the Ruddock Creek property was done in the 1960s and 1970s by Cominco Ltd. (The Consolidated Mining and Smelting Company of Canada), Falconbridge Ltd. and Doublestar Resources Ltd. Regional-scale mapping in the 1970s was carried out by Fyles (1970) as part of a preliminary study of Pb-Zn deposits in the Shuswap metamorphic complex for BC's Department of Mines and Petroleum Resources. The purpose of his work was to describe the structure and lithology of the rocks associated with the conformable Pb-Zn deposits, which focused in part on the Ruddock Creek deposit. More recently, the Ruddock Creek property was acquired by Selkirk Metals Corp. in 2005. In 2010, Selkirk Metals Corp was sold to Imperial Metals Corporation and became Ruddock Creek Mining Company. Since those

early days, Ruddock has seen over 88 000 m of drilling, the development of an underground decline, support roadways and a substantial camp built onsite. In 2012, Ruddock Creek Mining Company invested in a bulk sample, which was taken from the deposit's main zone (the E zone), and metallurgical analysis of the sample. The current resource estimate at the Ruddock Creek deposit is 10 036 000 tonnes of 8.07% combined Zn and Pb (indicated and inferred resource at 4% cutoff).

Additional regional work was carried out by Scammell (1993) who examined the mid-Cretaceous to Paleogene thermotectonic history of former mid-crustal rocks within the northern Monashee Mountains of the southern Omineca Belt. Scammell's work included regional mapping and structural analysis, U-Pb geochronology, thermochronology and thermobarometry. The U-Pb dating of two-mica leucogranite suggested three periods of magmatism:  $135 \pm 2$  Ma, ca. 100 to 97 Ma and ca. 71 to 57 Ma. Scammell also suggested that the penetrative ductile strain in the Selkirk allochthon was heterogeneous and developed between ca. 135 and 97 Ma. In addition, he proposed that 'dynamic spreading' involving horizontal extension during constructive orogeny was accompanied by the removal of approximately 10 km of crust from 100 to 94 Ma.

As mentioned above, the host stratigraphy for the Ruddock Creek deposit is thought to belong to the Windermere Supergroup (Scammell, 1993). Although the Windermere Supergroup is arguably one of the most important stratigraphic successions in the Canadian Cordillera, there is a paucity of modern U-Pb dating of detrital zircon for the Windermere Supergroup in this part of the Canadian Cordillera. Past multigrain and single grain isotope dilution-thermal ionization mass spectrometry (ID-TIMS) dating of detrital zircon was undertaken by Ross and Bowring (1990), Ross and Parrish (1991), Smith and Gehrels (1991), Gehrels and Dickinson (1995) and Gehrels and Ross (1998). These studies returned Archean and Early Proterozoic ages that are the hallmarks of cratonic basement sources with Laurentian provenance, but left open the possibility for significant refinements to be made regarding the actual age of the Windermere Supergroup at any given interval and location. Hence, this was deemed to be one of the foci of the current study. With regard to the timing constraints for the various Zn-Pb deposits in the region, Höy (1987) produced a Cambrian Pb model age for the Cottonbelt deposit, 50 km to the south in the Monashee complex. Curiously, the mineralization occurs only a few hundred metres stratigraphically above the basal part of the Monashee complex cover sequence, which is interpreted to be Paleoproterozoic in age (Crowley, 1997; see also Scammell and Brown, 1990). Millonig et al. (2012) reported a U-Pb zircon age of ca. 360 Ma for the strataform Mount Grace carbonatite horizon, which underlies the Cottonbelt Pb-Zn deposit. The date suggests that the Cottonbelt deposit is either much

younger than the Cambrian Pb model age or the Mount Grace carbonatite represents a stratigraphically higher unit that is now found structurally beneath the Cottonbelt deposit due to folding and/or faulting.

## Methods

This study integrated a broad range of analytical techniques in the field and laboratory to obtain a robust constraint on the structural control of the mineralization and the maximum depositional age of the Ruddock Creek stratabound Zn-Pb deposit and its host stratigraphy, as well as determine the Pb isotopic signature of the deposit.

### Field Mapping

Fieldwork involved property mapping at a 1:10 000 scale and mapping of the mineralized horizons at a 1:5000 scale. Structural data, oriented samples for microstructural analysis, and geochronological and Pb isotope samples were collected. Mapping focused on the structural geometry of the deposit and the geological relationships of the mineralized horizon.

### Petrographic Analysis

Oriented hand samples from representative sites across the property have been cut into thin section and are being used for ongoing microstructural and petrographic analysis. Thin sections from all the geochronological and Pb isotope samples were also made in order to characterize the lithologies, contact relationships and mineral assemblages.

### U-Pb Geochronology

Zircon U-Pb data were obtained from 12 metasedimentary samples and 2 igneous samples from the Ruddock Creek property and nearby vicinity (see Figure 3 for sample locations). Zircon crystals were acquired using standard mineral separation techniques at Simon Fraser University (Burnaby, BC), which include jaw crushing, pulverizing in a disk mill, and density separation using a Wilfley table and heavy liquids (methylene iodide). The zircons from the igneous samples were also magnetically separated using an LB-1 Frantz<sup>®</sup> Magnetic Barrier Laboratory Separator (only for igneous zircon). At the Boise State University Isotope Geology Laboratory (Boise, Idaho) zircon crystals were hand-picked from the heavy mineral fraction and annealed at 900°C for 60 hours in a quartz vessel in a muffle furnace. Crystals were then mounted in epoxy, and polished stepwise using silicon carbide films of 30, 15, 9, 3 and 1 µm to expose a medial section of each crystal, followed by polishing with a 0.3 µm alumina slurry. Cathodoluminescence imaging was performed to characterize the internal zoning of the zircon. The grains were checked for zoning, inclusions and cracks, which could complicate the analyses. Zircon crystals were analyzed by laser-ablation inductively coupled plasma-mass spectrometry (LA-ICP-MS) using a

Thermo Scientific XSERIES 2 Quadrupole ICP-MS and New Wave Research laser ablation system. In-house analytical protocols, standard materials and data reduction software were used for acquisition and calibration of U-Pb dates and acquisition of a suite of high-field-strength elements (HFSE) and rare earth elements (REE). Zircon was ablated with a laser spot, 25 or 30  $\mu\text{m}$  wide, during a 45 second analysis consisting of 15 seconds of gas blank and 30 seconds of ablation, which quarried a pit  $\sim 25 \mu\text{m}$  deep. For U-Pb and  $^{207}\text{Pb}/^{206}\text{Pb}$  dates, instrumental fractionation of the background-subtracted ratios was corrected and dates were calibrated with respect to interspersed measurements of the zircon standard. For more complete details of the methodology, refer to Rivera et al. (2013). Future work will entail analyzing crystals requiring more precise ages (e.g., the youngest detrital zircon and igneous zircon); they will be plucked from the epoxy grain mounts and analyzed by chemical abrasion TIMS.

### Pb Isotopic Analysis

The Pb isotopic compositions of single grains of galena, pyrite and pyrrhotite were analyzed by TIMS at the Boise State University Isotope Geology Laboratory in an attempt to constrain the age of formation of the Ruddock Creek Zn-Pb deposit. Purified Pb and U from single dissolved grains of galena, pyrite and pyrrhotite were loaded together with a silica gel-phosphoric acid emitter solution on single Re filaments. The Pb and U isotopic compositions were measured sequentially as  $\text{Pb}^+$  ions or  $\text{UO}_2^+$  ions on a mass spectrometer.

## Preliminary Results

### Field Mapping

Mapping the property and undertaking a detailed structural analysis resulted in a more complete understanding of the mesoscale structures that control the map-scale pattern of lithologies and the geometry of the Zn-Pb deposit. The mineralized outcrop pattern displays a complicated outline that defines a type 3 fold interference pattern (Ramsay, 1962) created by superposed folding with significantly thickened hinges and attenuated and dismembered limbs (Figure 3). This led to the conclusion that the metasedimentary rocks present on the property have indeed been subjected to at least three phases of ductile deformation and that the main mineralized zone (the E zone) is hosted within the hinge (trending  $290^\circ$  and plunging  $\sim 30^\circ$ ) of a property-scale fold, as was previously suggested by Fyles (1970). It is clear that the E zone occurs within the hinge of the large fold and has been structurally thickened (Figure 3). Conversely, the mineralized horizon has been substantially attenuated and dismembered within the folds limbs, and as such had been historically mapped as separate mineralized zones. Based on these findings, it was possible to begin predicting where

the mineralized horizon would crop out in other parts of the property. Two new showings were identified during mapping. The S zone represents an extension of the upper limb of the overturned, recumbent  $D_2$  fold that controls the map-scale geometry and the K zone represents an extension of the lower limb. These two new showings have helped confirm the working hypothesis that the geometry of the mineralized horizon, which serves nicely as a marker unit, is controlled by a map-scale type 3 fold interference pattern (Figure 3). All the mineralized showings (E, F, G, T, Creek, Q, U, R, S and K; Figure 3) appear to be confined to a stratigraphic interval associated with the calcsilicate gneiss. These map patterns, confirmed by the two new showings, suggest that there are prospective targets yet to be found on the property within the tectonically thickened hinges of  $F_2$  folds to the west of the main E zone.

### U-Pb Geochronology

Geochronological analyses, including complete U-Pb and trace-element LA-ICP-MS analyses, were carried out on 2 granitoid (Table 1) samples and 12 detrital zircon samples from the host metasedimentary units. A total of 1571 spots on detrital and igneous zircon grains was acquired. The detrital samples are grouped together based on the similarity of their age probability distribution peaks (Figure 4).

- Samples LT13-255, LT13-245, LT13-242, LT13-007B and LT13-249 have peaks that are typical of zircon derived from the Laurentian craton with their largest peaks at ca. 1800 Ma. These samples also have minor peaks at ca. 2550 to 2500 Ma and a number of smaller peaks between ca. 3000 and 2550 Ma. Very small, almost indiscernible peaks also occur between ca. 1600 and 1150 Ma.
- Samples LT13-250 and LT13-017 have a broad distribution of ages, as young as ca. 1100 Ma, with the largest age peaks from ca. 1800 to 1550 Ma. Minor probability age peaks are again found at ca. 2550 Ma, with a number of smaller peaks between ca. 3000 and 2550 Ma.
- Sample LT13-254 includes the oldest grains of all the detrital zircon samples, with a peak at ca. 3350 Ma. The largest peaks range from ca. 2100 to 1600 Ma. The youngest grains are ca. 1450 Ma.
- Sample LT13-263 has a similar probability plot to sample LT13-254. Most peaks range between ca. 1850 and 1600 Ma, with a smaller peak at ca. 2550 Ma.
- Samples LT13-297 and LT13-246 are two of the four samples with small populations of ca. 650 Ma grains. Both samples have large peaks at ca. 1000 Ma grains and only a few analyses that fall between ca. 2650 and 2500 Ma.
- Samples LT13-276 and LT13-026 have the youngest of grains. A single grain dated at ca. 560 Ma was recovered from sample LT13-276 and five grains between ca. 591 and 574 Ma were found in sample LT13-026. Both sam-

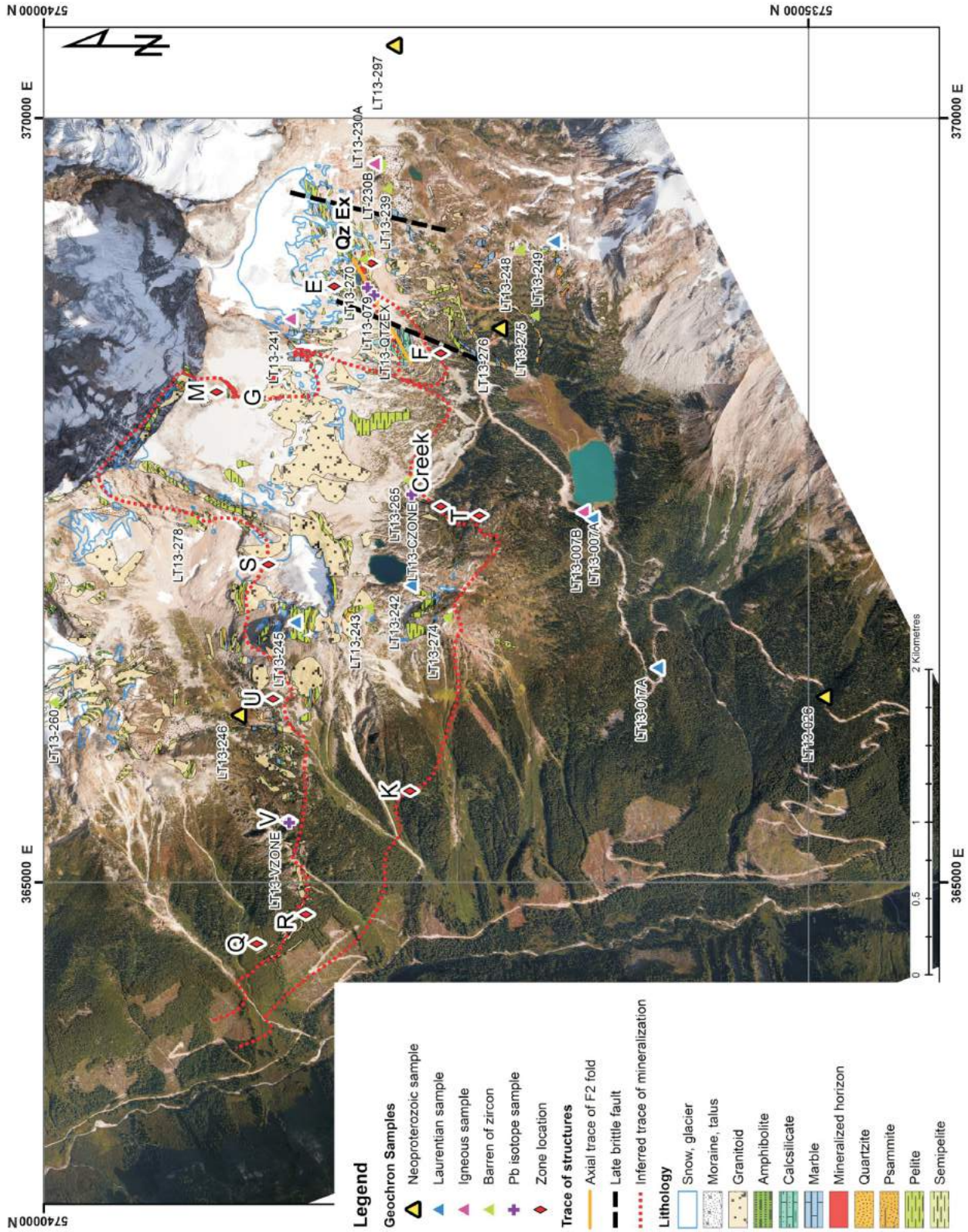


**Figure 3.** Geological map of the Ruddock Creek property (modified from Morris, 1965; Fyles, 1970), southern British Columbia, superimposed on a light detection and ranging (LIDAR) image (Eagle Mapping, 2012), including geochronology sample sites and lithology. Abbreviation: Qz Ex, quartz exhalite horizon.

ples have the largest peaks at ca. 650 Ma and do not contain zircon grains older than 1800 Ma.

The LA-ICP-MS data from the igneous lithologies, samples LT13-230 and LT13-241, suggest igneous crystallization occurred at ca. 103 and 63 Ma, respectively (Table 1).

### Pb Isotopic Analysis

Galena, pyrite and pyrrohotite from eight massive sulphide samples were analyzed for their common Pb isotopic signatures. Galena grains were picked from samples from the E zone, Creek zone, V zone and Quartz exhalite horizon (Figure 3). Pyrite was picked from the Quartz exhalite horizon and pyrrohotite was picked from the V zone. Galena duplicates were analyzed for the Quartz exhalite horizon and Creek zone. Isotopically, there was very little difference between galena-pyrite and galena-pyrrohotite pairs. Plotting the Pb isotopic data on the ‘shale curve’ (Godwin et al., 1988; Nelson, 1991; Mortensen et al., 2006; Figure 5) pro-

vides a model age of the mineralization of ca. 530 Ma. The values from the eight analyses show slight variation, with the E zone and V zone having similar  $^{207}\text{Pb}/^{204}\text{Pb}$  isotopic ratios and the Creek zone and Quartz exhalite horizon demonstrating similar  $^{207}\text{Pb}/^{204}\text{Pb}$  isotopic ratios (Table 2).

### Age Constraints for the Host Windermere Stratigraphy

The Ruddock Creek deposit has undergone a complex, penetrative deformation and polymetamorphic history, which relates to multiple tectonometamorphic events within the southern Canadian Cordillera. Ages of detrital zircon offer a geochronological fingerprint that reflects the age and distribution of continental basement from which the zircon was sourced (Ross and Parish, 1991). The age and chemistry of detrital zircon at the Ruddock Creek property can be used to infer the provenance of the grains, the majority of which are interpreted to be magmatic rocks with Laurentian heritage. The youngest ages of the detrital grains of zircon

**Table 1.** Summary of igneous samples’ location, geological relationships and age, Ruddock Creek property, southern British Columbia.

Sample	Easting <sup>1</sup>	Northing <sup>1</sup>	Elevation (m asl)	Description	Age (Ma)
LT13-230A	5737794	369694	2127	Medium-grained granitoid. Concordant with D2 and folded by F3.	103.2 ± 1.3
LT13-241	5738388	368685	2498	Crosscutting medium-grained granitoid, post-tectonic dike. Constrains the youngest age of deformation in the area.	62.93 ± 0.6

<sup>1</sup>NAD 83, UTM Zone 11

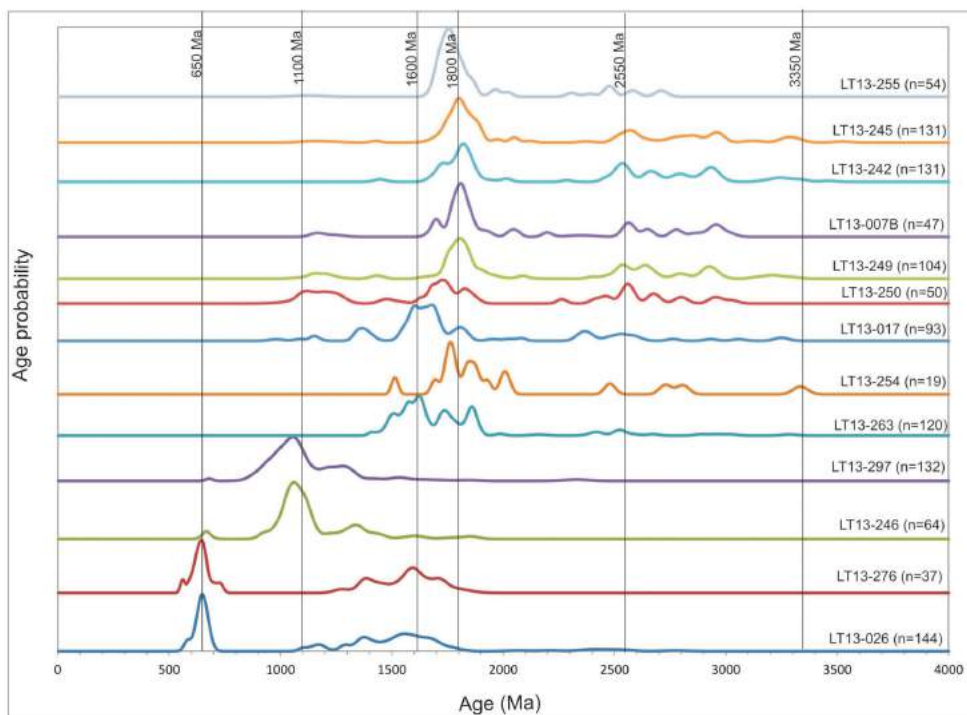


**Figure 4.** Normalized probability plot of 12 detrital zircon samples, Ruddock Creek property, southern British Columbia. Samples are grouped together based on similar probability peaks.

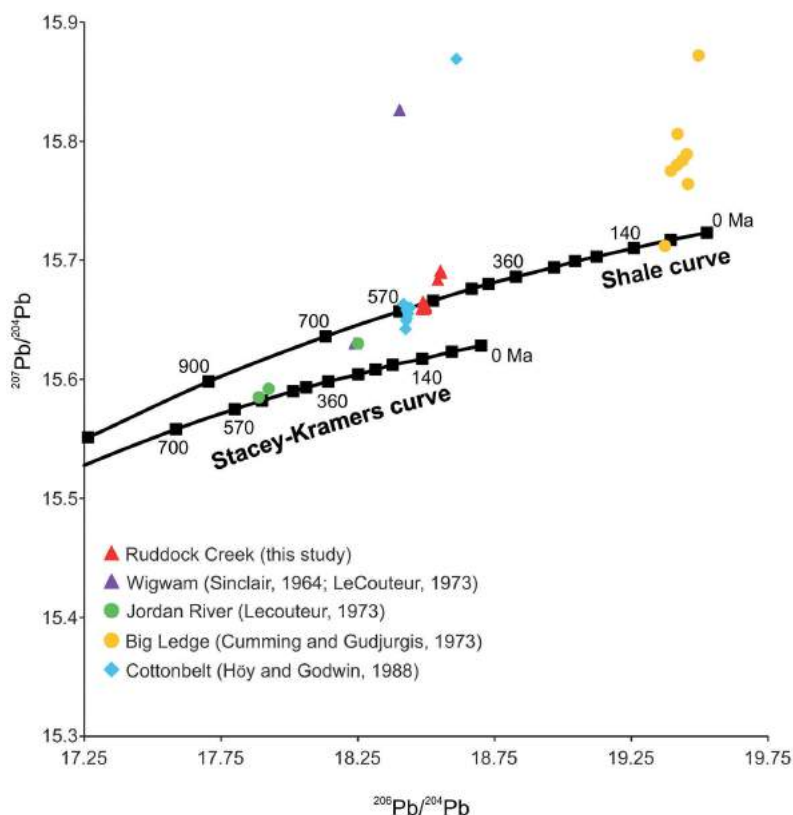


**Figure 5.** Lead isotopic data for sulphides from sedimentary exhalative (SEDEX)-type deposits (after Sinclair, 1964; Stacey and Kramers, 1975; Godwin et al., 1988; Nelson, 1991; Mortensen et al., 2006). The southern British Columbia Ruddock Creek deposit data (red triangles) plot on and just above the shale curve ca. 530 Ma.

**Table 2.** Lead isotopic data for the Zn-Pb horizon, Ruddock Creek property, southern British Columbia.

Sample	Pb ratios				
	208/206	207/206	208/204	207/204	206/204
Qtz ex galena 1	2.059968	0.846629	38.1063	15.6615	18.4986
Qtz ex galena 2	2.060209	0.846734	38.0994	15.6587	18.4932
Qtz ex pyrite	2.059462	0.846516	38.0981	15.6598	18.4992
V zone galena 2	2.058651	0.84577	38.1924	15.691	18.5523
V zone pyrrhotite	2.058658	0.84555	38.1983	15.6892	18.5551
Creek zone galena 1	2.060551	0.84729	38.0956	15.6649	18.4883
Creek zone galena 2	2.060024	0.847167	38.0771	15.6589	18.484
E zone galena 2	2.057998	0.845825	38.1598	15.6835	18.5423

Abbreviation: Qtz ex, Quartz exhalite

provide the maximum age of deposition for the individual sedimentary units.

The ages determined in this study carry with them important implications for the age of stratigraphy in the region, and allow for a comparison against stratigraphic ages previously determined for units within the Monashee complex to the south (Crowley, 1997; Millonig et al., 2012). The youngest detrital grains suggest that the maximum age of deposition in at least one sample at Ruddock Creek is ca. 560 Ma. Five grains in another sample have ages between ca. 591

and 574 Ma. Because it is possible that these young dates are inaccurate due to Pb loss or mixing with Cordilleran metamorphic rims, they should be considered suspect until more analyses can be carried out to confirm their legitimacy. Robust peaks from four samples occur at ca. 650 Ma. The youngest zircon in the other samples is >1000 Ma. The four youngest samples might suggest a stratigraphic facing toward the core of the fold with younger sedimentary rocks on the outside limbs of the fold and older rocks within the centre of the fold. If so, the detrital results suggest that the isoclinal, map-scale fold outlined by the Zn-Pb horizons, is an overturned, recumbent anticline as opposed to a syncline, as originally suggested by Fyles (1970).

### Age Constraints for Deformation at the Ruddock Creek Property

Igneous sample LT13-230A is a grey, medium-grained granitoid, which is concordant with the penetrative transposition foliation and has been folded by the third phase of deformation. The geological features of sample LT13-230A are interpreted to indicate that this body intruded syn-D<sub>2</sub>, and thus, its age of 103.2 ± 1.3 Ma is interpreted to constrain, in part, the age of D<sub>2</sub> and the development of the transposition foliation in this area. Sample LT13-241 is from a highly discordant medium-grained granitic dike. The sample occurs structurally above the E zone and crosscuts the penetrative foliation and is unaffected by F<sub>3</sub> folds. Thus, it is considered to be post-tectonic and its age of 62.93 ± 0.6 Ma is interpreted to constrain the end of the ductile deformation at the Ruddock Creek property.

### Age and Deposit Model for the Zn-Pb Horizon

One of the most difficult issues to address regarding the Ruddock Creek property is what model best fits the deposit. Traditionally, it has been interpreted to be a SEDEX-type deposit, and the deposit does fit the SEDEX model in many ways. The map patterns, consistency of stratigraphic position and similar Pb isotopic signatures are all consistent with the mineralized horizon having been originally deposited as a continuous horizon by subsurface dispersion of ore fluids along permeable strata within a single basin (Sangster, 2002). Furthermore, the principal ores are sphalerite and galena and there is evi-

dence of rifting, indicated by the presence of amphibolite interlayered with the metasedimentary units. However, because of the metamorphic grade and pervasive ductile deformation, there is no remaining primary evidence of submarine venting of hydrothermal fluids or a growth fault. The lack of an identifiable proximal growth fault brings into question whether or not the deposit might be characterized as Lydon's (1995) vent-distal model, when no growth fault is present in the immediate vicinity of the deposit. The amount of calcareous stratigraphy hosting the Zn-Pb horizon at the Ruddock Creek property reinforces Sangster's (2002) suggestion that it is unlikely that newly deposited sediments are absolutely impermeable and that auriferous seafloor brines most likely sink into the underlying sediments. The massive sulphide mineralization at the Ruddock Creek deposit locally displays a gradational contact with the host calcisilicate units; this implies that the deposit can still be characterized as a syngenetic SEDEX type, rather than an epigenetic carbonate-replacement-type deposit. Höy (2001) suggested that the deposit be classified as a Broken Hill-type deposit. Broken Hill-type deposits are interpreted to be metamorphosed equivalents of SEDEX deposits (Sangster, 1990; Höy, 2001). The high base metal/iron sulphide ratio, the presence of Fe-rich sphalerite and fluorite, and a calcareous host to the mineralization typifies Broken Hill-type deposits (Höy, 2001).

Another aspect of the project that could use refinement is directly dating the mineralized horizon. The Pb isotopic data for the Ruddock Creek deposit sits on and just above and to the right of the shale curve at ca. 530 Ma (Figure 5). This corroborates well with the maximum age of deposition provided from the detrital zircon dates (i.e., ca. 560 Ma); however, more work is necessary to confirm both the age of the deposit and the maximum age of the host stratigraphy. Regardless, the very close similarity in Pb isotopic compositions from the various mineralized zones is interpreted to indicate that the zones are genetically related, and may have originated as one lithostratigraphic horizon prior to dismemberment by isoclinal folding and transposition. The slight variability in the Pb isotopic compositions of the different parts of the deposit most likely reflects the inhomogeneity of the depositional environment. Some variability in the measured Pb isotopic compositions within a single deposit should be expected. For instance, on the continental slope, in the deep-water realm, there are many inherent facies changes due to the underwater geomorphology (Hubbard et al., 2012), which implies that there would never be complete homogenization of the isotopic compositions of the source rocks, even in SEDEX deposits. Due to the abundance of Pb in the initial mineralizing system of the Ruddock Creek deposit, all of the Pb in the immediate vicinity of the deposit would be overwhelmed by the initial Pb in the deposit (Mortensen et al., 2006), and therefore would reflect the original Pb concentrations of the deposit-

forming environment. There was very little variation in the Pb isotopic concentrations from the four mineralized zones, which suggests that all the zones were likely deposited at approximately the same time, all under the same environmental conditions.

### Regional Implications for Other Zn-Pb Deposits

There are a number of stratabound Pb-Zn deposits in the southern Canadian Cordillera that may be related to the Ruddock Creek deposit, including the Big Ledge deposit, 60 km south of Revelstoke, the Wigwam deposit, 20 km southeast of Revelstoke, the Jordan River, deposit 24 km northwest of Revelstoke, and the Cottonbelt deposit, 50 km northwest of Revelstoke. The Pb isotopic data for the Ruddock Creek and Cottonbelt deposits suggest they may have formed at the same time during the Cambrian metallogenic event that is well documented in the Canadian Cordillera (MacIntyre, 1991). However, the stark differences in the lithostratigraphy hosting the two deposits argue against their being genetically related. Furthermore, the ca. 360 Ma age for the extrusive Mount Grace carbonatite (Millonig et al., 2012) currently situated beneath the Cottonbelt deposit brings into question the Cottonbelt deposit's ca. 570 Ma Pb model age, this coupled with the absence of any detrital zircon <560 Ma at the Ruddock Creek property, makes any correlation between the two deposits all the more difficult. Further afield, the lack of recent age constraints on the Big Ledge and Wigwam deposits, situated to the south and east, respectively, of the Monashee complex, make it difficult to address their temporal relationship to the other SEDEX-type deposits of the area. Whether or not basin development, and therefore syngenetic SEDEX deposit formation, had a long and protracted history in this region is still debatable.

### Conclusions

The detrital zircon population from this study shows a temporal dichotomy. Four samples yielded a younger population of Neoproterozoic dates of ca. 650 Ma, with one analysis as young as ca. 560 Ma, and older grains include a peak at ca. 1100 Ma and reflect the typical Laurentian signatures that produce significant Meso- to Paleoproterozoic peaks at ca. 1500, 1700, 1800 and 2500 Ma. These data are consistent with the host lithologies of the Ruddock Creek deposit being part of the Windermere Supergroup, an interpretation previously made but never fully proven (Scammell, 1993). The  $^{207}\text{Pb}/^{204}\text{Pb}$  model age of ca. 530 Ma provided by plotting the Pb isotopic data on the shale curve supports the idea that the Ruddock Creek mineralized horizon was deposited syngenetically with the metasedimentary host rocks. Even if the Pb isotopic model age is brought into question, the maximum age determined for the metasedimentary units that bound the mineralized horizon at the Ruddock Creek

property has helped tighten the constraints on the age of deposition, which is no older than ca. 560 Ma.

The complicated structural history of the Ruddock Creek deposit makes detailed structural mapping essential for determining its geological history and evaluating its economic potential. Within the Selkirk allochthon, the first phase of deformation consisted of kilometre-scale south-west-vergent folds. The second phase of folding overturned the first phase and produced a penetrative transposition foliation and is characterized by northeast-vergent isoclinal folds. Development of the regional transposition foliation and subsequent overprint by D<sub>3</sub> deformation took place from ca. 136 to 57 Ma (Scammell, 1993), which correlates with the timing put forward in this research. Map patterns observed during this research have suggested that the mineralized horizon has been subject to all these phases of deformation. The fact that the deposit has been metamorphosed to upper amphibolite facies and polydeformed makes it very difficult to say with confidence what model the deposit would best fit. Based on the observations and data that were collected, the Ruddock Creek deposit seems to most closely fit that of a Broken Hill-type SEDEX deposit. Knowing what model can be applied to the deposit could help with future exploration for similar deposits, possibly even along the length of the Cordillera. The presence of the Ruddock Creek deposit within the Windermere Supergroup suggests that this succession of rocks is a viable exploration target.

Future work for the project includes the creation of a detailed geological map, possibly more detrital zircon analyses and Sm-Nd analyses of the mineralized horizon with hopes of directly dating the timing of ore genesis. Very few well defined ages have been produced for highly metamorphosed SEDEX-type deposits, provided that the Sm-Nd isotopic system has not been disrupted at the Ruddock Creek property, elucidating a Sm-Nd isochron. Testing both sphalerite and fluorite from the main mineralized zone, the E zone, could prove to be very instructive. Not only could this method of dating the mineralization help constrain the genetic model for ore deposition but it could also possibly provide a feasible method for dating highly metamorphosed SEDEX-type deposits.

The work included in this project is part of the senior author's master's thesis, which should be completed this summer.

### Acknowledgments

Geoscience BC is acknowledged and thanked for the funding provided for this project. Imperial Metals Corporation is thanked for their funding and field support. A. Wilkins, A. Schmaltz and R. Rollick are thanked for their field support. Natural Sciences and Engineering Research Council of Canada (NSERC) is thanked for their support by award-

ing H.D. Gibson with an Engage grant for this project. J.K. Mortensen is thanked for his insightful review of this document.

### References

- Armstrong, R.L. (1982): Cordilleran metamorphic core complexes—from Arizona to southern Canada; *Annual Review of Earth and Planetary Sciences*, v. 10, p. 129–254.
- Armstrong, R.L., Parrish, R.R., Scott, P., Runkle, D. and Brown, R.L. (1991): Early Proterozoic basement exposures in the southern Canadian Cordillera: core gneiss of Frenchman Cap, Unit 1 of the Grand Forks Gneiss, and the Vaseaux Formation; *Canadian Journal of Earth Sciences*, v. 28, no. 8, p. 1169–1201.
- Brown, R.L. and Lane, L.S. (1988): Tectonic interpretation of west-verging folds in the Selkirk Allochthon of the southern Canadian Cordillera; *Canadian Journal of Earth Sciences*, v. 25, p. 292–300.
- Brown, R.L. and Read, P.B. (1983): Shuswap terrane of British Columbia: a Mesozoic 'core complex'; *Geology*, v. 11, no. 3, p. 164–168.
- Brown, R.L., Carr, S.D., Johnson, B.J., Coleman, V.J., Cook, F.A. and Varsek, J.L. (1992): The Monashee décollement of the southern Canadian Cordillera: a crustal-scale shear zone linking the Rocky Mountain foreland belt to lower crust beneath accreted terranes; *in Thrust Tectonics*, K.R. McClay (ed.), Chapman & Hall, London, United Kingdom, p. 357–364.
- Brown, S.R., Gibson, H.D., Andrews, G.D.M., Thorkelson, D.J., Marshall, D.D., Vervoort, J.D. and Rayner, N. (2012): New constraints on Eocene extension within the Canadian Cordillera and identification of Phanerozoic protoliths for footwall gneisses of the Okanagan Valley shear zone; *Lithosphere*, v. 4, no. 4, p. 354–377.
- Brown, R.L., Journeay, J.M., Lane, L.S., Murphy, D.C. and Ree, C.J. (1986): Obduction, backfolding and piggyback thrusting in the metamorphic hinterland of the southeastern Canadian Cordillera; *Journal of Structural Geology*, v. 8, p. 255–268.
- Burchfield, B.C. and Davis, G.A. (1975): Nature and controls of Cordilleran orogenesis: extensions of an earlier synthesis; *American Journal of Science*, v. 275, series A, p. 363–396.
- Carr, S.D. (1991): Three crustal zones in the Thor-Odin-Pinnacles area, southern Omineca Belt, British Columbia; *Canadian Journal of Earth Sciences*, v. 28, p. 2003–2023.
- Carr, S.D. (1992): Tectonic setting and U-Pb geochronology of the early Tertiary Ladybird leucogranite suite, Thor-Odin – Pinnacles area, southern Omineca Belt, British Columbia; *Tectonics*, v. 11, p. 258–278.
- Carr, S.D. and Brown, R.L. (1989): Crustal structure and tectonic chronology near the LITHOPROBE line in the Thor/Odin-Pinnacles-Cherryville-Vernon area, southeastern British Columbia: a progress report; *in Southern Canadian Cordillera Transect Workshop*, February 25–26, 1989, Vancouver, BC, LITHOPROBE Secretariat, University of British Columbia, LITHOPROBE Report No. 7, p. 27–36.
- Carr, S.D., Parrish, R.R., Brown, R.L. (1987): Eocene structural development of the Valhalla Complex, southeastern British Columbia; *Tectonics*, v. 6, no. 2, p. 175–196.
- Colpron, M. and Nelson, J.L. (2011): A digital atlas of terranes for the Northern Cordillera; Yukon Geological Survey, URL

- [http://www.geology.gov.yk.ca/bedrock\\_terrane.html](http://www.geology.gov.yk.ca/bedrock_terrane.html) [December 2014] and BC Ministry of Energy and Mines, BC Geological Survey, GeoFile 2011-11.
- Colpron, M. and Price, R.A. (1995): Tectonic significance of the Kootenay terrane, southeastern Canadian Cordillera: an alternative model; *Geology*, v. 23, no. 1, p. 25–28.
- Colpron, M., Nelson, J.L. and Murphy, D.C. (2007): Northern Cordilleran terranes and their interactions through time; *GSA Today*, v. 17, no. 4–5, p. 4–10.
- Crowley, J.L. (1997): U-Pb geochronologic constraints on the cover sequence of the Monashee complex, Canadian Cordillera: Paleoproterozoic deposition on basement; *Canadian Journal of Earth Sciences*, v. 34, p. 1008–1022.
- Crowley, J.L. (1999): U-Pb geochronological constraints on Paleoproterozoic tectonism in the Monashee complex, Canadian Cordillera: elucidating an overprinted geologic history; *Geological Society of America Bulletin*, v. 111, p. 560–577.
- Cumming, G.L. and Gudjurgis, P.J. (1973): Alteration of trace lead isotopic ratios by postore metamorphic and hydrothermal activity; *Canadian Journal of Earth Sciences*, v. 10, p. 1782–1789.
- Eagle Mapping (2012): LiDAR image of Ruddock Creek; Eagle Mapping, acquired image.
- Eisbacher, G.H. (1981): Sedimentary tectonics and glacial record in the Windermere Supergroup, Mackenzie Mountains, northwestern Canada; *Geological Survey of Canada, Paper 80-27*, 40 p.
- Fyles, J.T. (1970): The Jordan River area near Revelstoke, British Columbia; BC Ministry of Energy and Mines, *Bulletin 57*, 64 p.
- Gabrielse, H. (1972): Younger Precambrian of the Canadian Cordillera; *American Journal of Science*, v. 272, p. 521–536.
- Gehrels, G.E. and Dickinson, W.R. (1995): Detrital zircon provenance of Cambrian to Triassic miogeoclinal and eugeoclinal strata in Nevada; *American Journal of Science*, v. 295, p. 18–48.
- Gehrels, G.E. and Ross, G.M. (1998): Detrital zircon geochronology of Neoproterozoic to Permian miogeoclinal and eugeoclinal strata in British Columbia and Alberta; *Canadian Journal of Earth Sciences*, v. 35, p. 1380–1401.
- Gibson, H.D., Brown, R.L. and Carr, S.D. (2008): Tectonic evolution of the Selkirk fan, southeastern Canadian Cordillera: a composite Middle Jurassic-Cretaceous orogenic structure; *Tectonics*, v. 27, p. 1–14.
- Godwin, C.I., Gabites, J.E. and Andrew, A. (1988): Leadtable: a galena lead isotope data base for the Canadian Cordillera, with a guide to its use by explorationists. Contribution to the Canada/British Columbia Mineral Development Agreement, 1985–1990; BC Ministry of Energy and Mines, BC Geological Survey, Paper 1988-4, 188 p.
- Goodfellow, W.D. and Lydon, J.W. (2007): Sedimentary exhalative (SEDEX) deposits; *in* *Mineral Deposits of Canada: a Synthesis of Major Deposit-Types, District Metallogeny, the Evolution of Geological Provinces, and Exploration Methods*, W.D. Goodfellow (ed.), Geological Association of Canada, Mineral Deposits Division, Special Publication no. 5, p. 163–184.
- Höy, T. (1987): Geology of the Cottonbelt lead-zinc-magnetite layer, carbonatites and alkalic rocks in the Mount Grace area, Frenchman cap dome, southeastern British Columbia; BC Ministry of Energy and Mines, *Bulletin 80*, 99 p.
- Höy, T. (2001): Sedex and Broken Hill-type deposits, northern Monashee Mountains, southern British Columbia; *in* *Geological Fieldwork 2000*, BC Ministry of Energy and Mines, BC Geological Survey, Paper 2001-1, p. 85–114.
- Hubbard, S.M., MacEachern, J.A. and Bann, K.L. (2012): Slopes; *in* *Trace Fossils as Indicators of Sedimentary Environments*, D. Knaust and R.G. Bromley (ed.), *Developments in Sedimentology*, v. 64, p. 607–642.
- Johnson, B.J. and Brown, R.L. (1996): Crustal structure and Early Tertiary extensional tectonics of the Omenica Belt at 51 N latitude, southern Canadian Cordillera; *Canadian Journal of Earth Sciences*, v. 33, p. 1596–1611.
- Journeay, J.M. (1986): Stratigraphy, internal strain, and thermotectonic evolution of northern Frenchman Cap dome, an exhumed basement duplex structure, Omineca hinterland, southeastern Canadian Cordillera; Ph.D. thesis, Queen's University, 404 p.
- LeCouteur, P.C. (1973): A study of lead isotopes from mineral deposits in the southeastern British Columbia and in the Anvil Range, Yukon Territory; Ph.D. thesis, University of British Columbia, 142 p.
- Lund, K. (2008): Geometry of the Neoproterozoic and Paleozoic rift margin of western Laurentia: implications for mineral deposit settings; *Geosphere*, v. 4, p. 429–444.
- Lydon, J.W. (1995): Sedimentary exhalative sulphides (SEDEX); *in* *Geology of Canadian Mineral Deposit Types*, O.R. Eckstrand, W.D. Sinclair and R.I. Thorpe (ed.), Geological Survey of Canada, *Geology of Canada Series no. 8*, p. 130–152.
- MacIntyre, D.G. (1991): SEDEX – sedimentary-exhalative deposits; *in* *Ore Deposits, Tectonics and Metallogeny in the Canadian Cordillera*, W.J. McMillan (co-ordinator), BC Ministry of Energy and Mines, Paper 1991-4, p. 25–69.
- McMechan, M.E. (2012): Deep transverse basement structural control of mineral systems in the southeastern Canadian Cordillera; *Canadian Journal of Earth Sciences*, v. 49, p. 693–708.
- Millonig, L.J., Gerdes, A. and Groat, L.A. (2012): U–Th–Pb geochronology of meta-carbonatites and meta-alkaline rocks in the southern Canadian Cordillera: a geodynamic perspective; *Lithos*, v. 152, p. 202–217.
- Monger, J.W.H. and Price, R.A. (1979): Geodynamic evolution of the Canadian Cordillera – progress and problems; *Canadian Journal of Earth Sciences*, v. 16, p. 770–791.
- Monger, J.W.H. and Price, R.A. (2002): The Canadian Cordillera: geology and tectonic evolution; *Canadian Society of Exploration Geophysicists Recorder*, v. 27, p. 17–36.
- Monger, J.W.H., Price, R.A. and Tempelman-Kluit, D.J. (1982): Tectonic accretion and the origin of the two major metamorphic and plutonic belts in the Canadian Cordillera; *Geology*, v. 10, p. 70–75.
- Morris, H.R. (1965): Report on Ruddock Creek lead-zinc property, 1961 to 1963; unpublished report prepared for Falconbridge Nickel Mines Ltd.
- Mortensen, J.K., Dusel-Bacon, C., Hunt, J.A. and Gabites, J. (2006): Lead isotopic constraints on the metallogeny of middle and late Paleozoic syngenetic base-metal occurrences in the Yukon-Tanana and Slide Mountain/Seventymile terranes and adjacent portions of the North American miogeocline; *in* *Paleozoic Evolution and Metallogeny of Pericratonic Terranes at the Ancient Pacific Margin of North America*, Canadian and Alaskan Cordillera, M. Colpron and

- J.L. Nelson (ed.), Geological Association of Canada, Special Paper 45, p. 261–279.
- Nelson, J.L. (1991): Carbonate-hosted lead-zinc ( $\pm$ silver, gold) deposits of British Columbia; *in* Ore Deposits, Tectonics and Metallogeny in the Canadian Cordillera, W.J. McMillan (co-ordinator), BC Ministry of Energy and Mines, Paper 1991-4, p. 71–88.
- Parrish, R.R. (1995): Thermal evolution of the southeastern Canadian Cordillera; *Canadian Journal of Earth Sciences*, v. 32, p. 1618–1642.
- Parrish, R.R., Carr, S.D. and Parkinson, D.L. (1988): Eocene extensional tectonics and geochronology of the southern Omineca Belt, British Columbia and Washington; *Tectonics*, v. 7, p. 181–212.
- Ramsay, J.G. (1962): Interference patterns produced by the superposition of folds of similar types; *The Journal of Geology*, v. 70, p. 466–481.
- Read, P.B. and Brown, R.L. (1981): Columbia River fault zone: southeastern margin of the Shuswap and Monashee complexes, southern British Columbia; *Canadian Journal of Earth Sciences*, v. 18, p. 1127–1145.
- Rivera, T.A., Storey, M., Schmitz, M.D. and Crowley, J.L. (2013): Age intercalibration of  $^{40}\text{Ar}/^{39}\text{Ar}$  sanidine and chemically distinct U/Pb zircon populations from the Alder Creek rhyolite Quaternary geochronology standard; *Chemical Geology*, v. 345, p. 87–98.
- Ross, G.M. (1991): Tectonic setting of the Windermere Supergroup revisited; *Geology*, v. 19, p. 1125–1128.
- Ross, G.M. and Bowring, S.A. (1990): Detrital zircon geochronology of the Windermere Supergroup and the tectonic assembly of the southern Canadian Cordillera; *The Journal of Geology*, v. 98, p. 879–893.
- Ross, G.M. and Parrish, R.R. (1991): Detrital zircon geochronology of metasedimentary rocks in the southern Omineca Belt; *Canadian Journal of Earth Sciences*, v. 28, p. 1254–1270.
- Sangster, D.F. (1990): Mississippi Valley-type and sedex lead-zinc deposits: a comparative examination; *Transactions of the Institution of Mining and Metallurgy, Section B*, v. 99, p. B21–B42.
- Sangster, D.F. (2002): The role of dense brines in the formation of vent-distal sedimentary-exhalative (SEDEX) lead-zinc deposits: field and laboratory evidence; *Mineralium Deposita*, v. 37, p. 149–157.
- Scammell, R.J. (1993): Mid-Cretaceous to Tertiary thermotectonic history of former mid-crustal rocks, southern Omineca Belt, Canadian Cordillera; Ph.D. thesis, Queen's University, 576 p.
- Scammell, R.J. and Brown, R.L. (1990): Cover gneisses of the Monashee terrane: a record of synsedimentary rifting in the North American Cordillera; *Canadian Journal of Earth Sciences*, v. 27, p. 712–726.
- Simony, P.S., Ghent, E.D., Craw, D., Mitchell, W. and Robbins, D.B. (1980): Structural and metamorphic evolution of the northeast flank of Shuswap complex, southern Canoe River area, British Columbia; *Geological Society of America Memoir*, v. 153, p. 445–461.
- Simpson, R.G. and Miller-Tait, J. (2012): Technical report Ruddock Creek Lead-Zinc Project, Kamloops Mining Division, British Columbia; unpublished report prepared for Selkirk Minerals Corp., 89 p., URL <[http://www.imperialmetals.com/i/pdf/Ruddock\\_Creek\\_Tech\\_Report-2012Final.pdf](http://www.imperialmetals.com/i/pdf/Ruddock_Creek_Tech_Report-2012Final.pdf)> [December 2014].
- Sinclair, A.J. (1964): A lead isotope study of mineral deposits in the Kootenay Arc; Ph.D. thesis, University of British Columbia, 257 p.
- Smith, M.T. and Gehrels, G.E. (1991): Detrital zircon geochronology of Upper Proterozoic to lower Paleozoic continental margin strata of the Kootenay Arc: implications for the early Paleozoic tectonic development of the eastern Canadian Cordillera; *Canadian Journal of Earth Sciences*, v. 28, p. 1271–1284.
- Stacey, J.S. and Kramers, J.D. (1975): Approximation of terrestrial lead isotope evolution by a two-stage model; *Earth and Planetary Science Letters*, v. 26, p. 207–221.
- Stewart, J.H. (1972): Initial deposits in the Cordilleran geosyncline: evidence of late Precambrian (<850 m.y.) continental separation; *Geological Society of America Bulletin*, v. 83, p. 1345–1360.
- Stewart, J.H. (1976): Late Precambrian evolution of North America: plate tectonics implication; *Geology*, v. 4, no. 1, p. 11–15.
- Stewart, J.H. and Suczek, C.A. (1977): Cambrian and latest Precambrian paleogeography and tectonics in the western United States; *in* Paleozoic Paleogeography of the Western United States, J.H. Stewart, C.H. Stevens and A.E. Fritsche (ed.), Society of Economic Paleontologists and Mineralogists, Pacific Section, Pacific Coast Paleogeography Symposium 1, p. 1–17.
- Tempelman-Kluit, D. J. and Parkinson, D. (1986): Extension across the Eocene Okanagan crustal shear in southern British Columbia; *Geology*, v. 14, p. 318–321.
- Wheeler, J.O. and McFeely, P., compilers (1991): Tectonic assemblage map of the Canadian Cordillera and adjacent parts of the United States of America; Geological Survey of Canada, Map 1712A, scale 1:2 000 000, 1 sheet.





## **VISION**

Our earth science builds the BC economy

## **MISSION**

We are a trusted partner providing earth science to encourage investment that benefits British Columbians

Suite 440 – 890 West Pender Street  
Vancouver BC V6C 1J9

[info@geosciencebc.com](mailto:info@geosciencebc.com)  
[www.geosciencebc.com](http://www.geosciencebc.com)